A STUDY OF TRANSPORT PROCESSES IN ION EXCHANGE MEMBRANES

A thesis presented for the degree of
Ph.D.
by

Colin R. Gardner.

Chemistry Department,
University of Glasgow.

30th March, 1970.

ProQuest LLC.
789 East Eisenhower Parkway
P.O. Box 1346
Ann Arbor, MI 48106 – 1346

SUMMARY.

The major part of this thesis is concerned with the study of transport and diffusion processes in ion-exchange membranes. The ion-exchanger chosen for study was the AMF C60 cation-exchange membrane. Previous studies (1) (2) had suggested that this membrane was more homogeneous than most commercially available exchangers and that it exhibited a high water content and high electrical conductivity, all of which made it a suitable subject for study. It had also been reported that heat treatment of this membrane led to an irreversible expansion of the membrane matrix, producing a membrane with a higher water content and lower flow resistance. (3) The normal and expanded forms of the exchanger were studied in the sodium form in sodium chloride solutions, so that a comparison of the results from the two exchangers might yield information about the effect of expansion on the exchanger properties. In addition to the determination of the basic properties of the exchangers, e.g. water content, physical dimensions, capacity etc., this study entailed the measurement of the following properties; (1) conductivity, (2) electro-osmotic flow, (3) diffusion of counter- and co-ions, (4) transport numbers of counter- and co-ions. These measurements were made for each membrane in 0.1M, 0.5M, 1.0M and 2.0M sodium chloride solutions. Three further experiments were conducted on/

on both membranes under the influence of an electrolyte concentration gradient: salt flow, osmosis and emf measurements were made with concentration gradients of 0.05/0.15 and 0.5/1.5. The results of these experiments have been discussed in terms of the current theories of membrane transport processes. It has been shown that the Nernst-Planck equation, modified to include the effects of convection, can adequately describe the variations in conductivity of the membranes with changing external concentration and the tortuosity factor, θ (= $1+v_w/1-v_w$), and absolute rate theory, (4) have been used to explain, satisfactorily, the dependence of the ionic diffusion coefficients on the concentration of the external solution.

Combining the results of all the transport experiments, it proved possible to carry out a complete analysis of the systems using the theory of non-equilibrium thermodynamics.(5) Examination of the results of this treatment reveals a number of important observations.

(1) Where a linear relationship exists between the counter-ion and water transference numbers, as it does for the C60 membranes, a complete analysis of the system can be achieved using the data mentioned above.

(2) For the counter-ions, isotope-isotope interaction is an important term and should not be omitted from the calculations as it has been frequently in previous studies. (5)

(3)/

(3) For the co-ions, the isotope term is not large enough to significantly affect the results, even when the electrolyte uptake is fairly great.

(4) Comparison of the results for the two membranes shows that, particularly at 0.1M, the variations in the fluxes of the species, through the membranes, can be almost wholly attributed to the difference in tortuosity of the exchangers.

In dilute solutions it has been possible to use some simplifying assumptions which have enabled accurate predictions of the salt flow through the membranes to be made.

Using the electrolyte uptake data required for the treatment described above, a structural analysis of the membranes has been obtained by employing the method of Glueckauf.[6] This analysis reveals that, although the membranes exhibit inhomogeneity, the degree of heterogeneity is considerably less than that observed in most commonly used ion-exchange membranes. The structural parameters have also been used in conjunction with the co-ion diffusion data, to show that the most continuous regions of the exchangers are those where the fixed charge concentration is very low.

The final chapter deals with a study of the inorganic ion-exchanger, hydrous zirconia, both in particle and membrane form. The main feature of this exchanger is the variation in ion-exchange capacity with pH of the external solution.[7] In the chloride form, the counter-ion diffusion coefficients have been determined as a function of the capacity. The results reveal that the/

the diffusion coefficients increase with decreasing capacity, i.e. with increasing distance between the sites of minimum energy, as predicted by the absolute rate theory. (4) Although the agreement is not quantitative owing to the assumptions made in the calculations, these results confirm the observations made for the C60 membranes, that absolute rate theory applied to diffusion processes can be used in the treatment of diffusion in ion-exchangers.

References.

(1) R. Arnold, Aust. J. Chem., 21, 521 (1968).

(2) J. M. Crabtree and E. Glueckauf, Trans. Faraday Soc., 59, 2639 (1963).

(3) R. Arnold and D.F.A. Koch, Aust. J. Chem., 19, 1299 (1966).

(4) B. J. Zwolinski, H. Eyring and C.E. Reese, J. Phys. Chem., 53, 1426 (1949).

(5) K. S. Spiegler, Trans. Faraday Soc., 54, 1408 (1958).

(6) E. Glueckauf, Proc. Roy. Soc. (London), A268, 350 (1962).

(7) F. Helfferich, "Ion Exchange", McGraw-Hill, New York, (1962) p.14.

Acknowledgements.

The author wishes to express his thanks to a number of people whose help has been invaluable in the execution of this project:

to Professor J. M. Robertson for assistance in obtaining financial support from the Science Research Council and the University of Glasgow,

to Dr. R. Paterson for his constant advice and encouragement,

to Dr. H. S. Dunsmore for advice on computer programming,

to D. Midgley and C. MacCallum for use of their linear titration plot method of chloride analysis.

to C. MacCallum for his computer program for calculating tracer diffusion coefficients,

to the members of the Electron Microscopy department who prepared the electron micrographs of the membranes and helped in the analysis of the photographs.

to the Physiology department for the use of the liquid scintillation counter, and

to the staff of the workshop and glass-blowing workshop for helpful advice and excellent service.

COLIN R. GARDNER.

Table of Contents.

Index of Figures.

Glossary of Symbols

Barred symbols refer to the exchanger phase unless otherwise stated.

A	lowest local counter-ion concentration in exchanger.
a_i	activity of species i.
$a_\pm$	mean activity of an electrolyte.
B	highest local counter-ion concentration in exchanger.
c_i	concentration of species i.
d	membrane thickness.
D_i	tracer diffusion coefficient of species i.
$\mathcal{D}_{ij}$	generalised Stefan-Maxwell diffusivity.
Ξ & E	electric potential.
E_m	diffusion potential through membrane.
f	parameter in structural analysis ($= \bar{m}/am$)
F	Faraday's constant.
H_i	hydration number of species i.
I	current density.
I_o	integral in structural analysis ($\int_0^\infty y\,(f + y)\,dy$)
J_i	flux of species i.
$(J_i)_{con}$	convective flux of species i.
$(J_i)_{diff}$	diffusion flux of species i.
$(J_i)_{el}$	electrical transference of species i.
$\bar{k}$	specific conductivity.
k_o	parameter in structural analysis.

l_{ij} phenomenological mobility coefficient.

M concentration of fixed charges.

m_i concentration of species i.

N_a Avogadro's number.

P chapter 2. Pressure.

P chapter 3. Permeability. ($= D\bar{c}/c$).

Q_i amount of species i in moles.

q_{ij} degree of coupling of species i and j.

q membrane cross section.

r_{ij} local phenomenological resistance coefficient.

R_{ij} integral phenomenological resistance coefficient.

R gas constant

r_o radius of ion-exchange particles.

t_i (i = 1, 2). transport number of species i.

t_3 transference number of water.

T absolute temperature.

t time.

u_i mobility of species i.

$\bar{u}_3$ mobility of pure liquid.

$\bar{v}_i$ partial molar volume of species i.

V volume.

v_w volume fraction of water in exchanger.

X_i generalised force on species i.

$\bar{X}_{ij}$ Friction coefficient between species i and j.

X concentration of fixed charges in equivalents per unit volume.

x length co-ordinate.

y parameter in structural analysis.

z heterogeneity parameter in structural analysis.

z_i electrochemical valence of species i.

Subscripts.

1 counter-ion.

2 co-ion.

3 water.

4 matrix.

o total test substance.

1' tracer isotopes of species 1

1" tracer isotopes of species 1

α chapter 2. parameter $(= \frac{\bar{k}}{F2})$

α chapter 3. constant in structural analysis.

β constant in structural analysis.

γ_i activity coefficient of species i.

δ thickness of unstirred layer.

θ tortuosity factor.

λ distance between positions of energy minima.

μ_i chemical potential of species i.

$\tilde{\mu}_i$ electrochemical potential of species i.

ν_i number of ions of species i formed by dissociation of an electrolyte.

ν_{12} number of ion formed by dissociation of an electrolyte, 12.

ν convection rate.

ρ_i parameter $(= c_i/c_o)$.

ρ_ω specific flow resistance of an ion exchanger.

ϕ electric potential.

ϕ^m volume fraction function in structural analysis.

ω sign of fixed charges.

σ entropy production.

Φ dissipation function.

CHAPTER ONE

Introduction

Introduction.

Ion-exchangers are usually considered to be insoluble liquids or solids which carry exchangeable ions called counter-ions. These ions may be exchanged for a stoichiometrically equivalent amount of other ions of the same sign if the exchanger is placed in contact with an electrolyte solution. Exchangers which carry positively charged counter-ions are called cation-exchangers while those carrying negatively charged ions are called anion-exchangers.

An ion-exchanger usually consists of a macromolecular structure which carries surplus positive or negative charges. Since electroneutrality must be preserved at all times, there must also be within the structure, an equivalent number of exchangeable counter-ions, their number depending on the number of fixed sites within the exchanger. This quantity is known as the capacity of the exchanger.

When an ion-exchanger is placed in an electrolyte solution, sorption of the electrolyte by the exchanger may occur. The sorbed counter-ions present in the exchanger in addition to those compensating the framework charge, are accompanied by an equivalent amount of so/

so called co-ions. These are the mobile ions with charges of the same sign as the framework charge.

There are many different kinds of exchanger, some of which are the naturally occurring inorganic exchangers such as the zeolites, the glauconites etc. but the greater proportion of them are man-made. Among the many synthetic inorganic exchangers are the hydrous oxide gels, including Fe_2O_3, Al_2O_3, Cr_2O_3, Bi_2O_3, TiO_2, ZrO_2, ThO_2, SnO_2, MoO_3, and WO_3. These oxides are pseudo-amphoteric and exhibit cation-exchange properties in solutions of pH above their isoelectric points and anion-exchange characteristics in solutions of pH below these values. However, only the oxides of zirconium and tin are sufficiently stable to warrant much study. (1)

The most commonly used exchangers are the synthetic organic ion-exchange resins. Most of these materials consist of three dimensional networks of hydrocarbon chains which carry ionic groups such as $-SO_3^-$, $-CO_2^-$, $-PO_3^{2-}$, $-AsO_3^{2-}$, in cation-exchangers and $-NH_3^+$, $>NH_2^+$, $>N^+<$, in anion-exchangers. The matrix itself is hydrophobic, but the incorporation of these ionogenic groupings introduces hydrophilic characteristics. Linear hydrocarbon macromolecules (or polyelectrolytes) of this type are water soluble, but the ion-exchange resins are rendered insoluble by the crosslinking introduced between adjacent chains./

chains. However the resulting matrix is elastic and can swell in the presence of a solvent.

The chemical and mechanical stability of the resins depends mainly on the structure and degree of cross-linking of the matrix and the nature of the fixed groups. Most studies have been carried out using polystyrene based materials, which, by careful selection of the degree of cross-linking and the nature of the ionogenic groups, can be made to yield exchangers with certain desired properties.

In recent years, ion-exchange resin membranes have become commercially available and have been the subjects of a considerable amount of work. Such membranes combine the ability to act as a separating wall between two solutions, with the chemical and electrochemical properties normally associated with ion-exchangers. They have not only facilitated the study of fundamental transport properties of ion-exchangers, but many of their properties, e.g. their permselectivity and high electrical conductivity, have made them extremely important in chemical technology: their relatively simple structure and well defined properties have also rendered them useful as simple model systems for the more complex biological membranes, many of whose properties remain as yet unexplained.

Ion-exchange membranes may be subdivided into two main classes, the so called "heterogeneous" and "homogeneous" membranes. "Heterogeneous" membranes consist of colloidal ion-exchange particles embedded in an inert binder such as polystyrene or polyethylene. "Homogeneous" membranes, on the other hand, are coherent gels in the shape of films or ribbons. Their structure is that of the normal ion-exchange resins. Practical difficulties in preparing membranes based purely on polystyrene has led to the production of graft co-polymer membranes of polystyrene and polyethylene, with improved properties.

Although many ion-exchange membranes have been considered to have an homogeneous structure, there is now a considerable amount of evidence which contradicts this view. Results of electrolyte uptake experiments and electron microscopy have shown that these materials may contain inhomogeneities of fairly large dimensions, (several thousand angstroms). (2) (3) (4) The conclusions of a number of investigations indicate that the graft co-polymer membranes AMF C 60 and C 100 exhibit a smaller degree of heterogeneity than is found in most of the commercially available ion-exchange membranes. (2) (3). Since all of the properties of the/

the membranes are affected to a lesser or greater extent, by any inhomogeneities in the system, it is important that experimental studies be carried out on membranes which are as homogeneous as possible. For this reason, the above mentioned membranes, AMF C60 and C100$_2$ were chosen for this study.

There are a number of variables which directly affect the transport properties of ion-exchange materials. These include, (a) the nature of the matrix, (b) the nature of the fixed groups, (c) the number of fixed groups per unit volume and (d) the geometrical properties of the aqueous channels in the exchanger. While a considerable amount of work has been done on exchangers with different types of hydrocarbon frameworks and with different kinds of fixed groups, there appears to be little information on the effect of variable capacity or variable 'pore' geometry on the transport properties of the exchanger.

The effect of capacity changes is a particularly interesting one. Absolute rate theory predicts that, if the capacity of an exchanger decreases, with a resultant increase in the distance between the exchange sites, then the diffusion rate of the counter-ions will increase accordingly. The verification of this prediction can only be made using an exchanger whose capacity can be altered/

altered while its other properties, in particular, its geometrical properties and water content, remain unchanged. Boyd, Soldano and Bonner [5] attempted to produce a series of exchangers of different capacity by desulphonating a polystyrene sulphonate exchanger. However, during this process, changes were observed to occur in the cross-linking and water content of the exchanger and hence, the conclusions drawn from the results of the diffusion experiments conducted on these exchangers, must remain in some doubt. In order to obtain unequivocal information on the effect of variation in capacity on the properties of an ion-exchanger, it is necessary to obtain an exchanger with variable capacity but otherwise constant properties. The organic ion-exchange resins are inadequate for this type of study and it is in the group of hydrous oxide exchangers mentioned previously, that a suitable material is to be found. By measuring the transport properties of the exchanger in a number of solutions of different pH, the effect of variable capacity on the properties of the exchanger can be isolated and studied. Such a study has been carried out using the anion exchange properties of hydrous zirconia in solutions of sodium chloride and hydrochloric acid, and the results are tabulated and discussed in Chapter 4 of this work.

Although/

Although a number of experimental studies have been conducted on series of exchangers of a similar type but with different degrees of cross-linking, no complete study has been made of the transport properties of exchangers with the same basic structure but with known differences in their geometric properties and water content. Such a comparison has now been made between the untreated and heat treated forms of the AMF C60 and C100 membranes prepared as described by Arnold and Koch.(104) In the heat treatment described by these authors, the membranes undergo an irreversible expansion with consequent increase in the fractional pore volume and water content of the exchangers. By examining these membranes in a variety of aqueous sodium chloride solutions of different concentrations, the effects of the expansion of the matrix on the membrane properties were determined under a variety of conditions. Such a comparison permits an accurate assessment of the effects of the changes introduced by the expansion into an otherwise identical system.

Since the introduction of ion-exchange membranes, a number of authors have determined some of the transport properties of a large selection of membrane systems under a/

a variety of external solution conditions. Many of these results have been analysed by use of the Nernst-Planck equations which gives the relation between the forces on and flow of any mobile species. The Nernst-Planck equation does not, however, include the effects of activity coefficients, convection or coupling of the flows of the mobile species and hence a number of extensions to the simple equation have been employed. Particularly important is the correction for the effect of convection and where appropriate, the results obtained using the AMF C60 membrane systems have been analysed using this extended form of the Nernst-Planck equation.

The Nernst-Planck equation does not, even in its extended form, include the effect of coupling between the flows of the various ionic species, and hence, cannot provide a complete picture of the situation in an ion-exchanger where coupling of this nature is very important. The application of the theory of thermodynamics of irreversible processes to ion-exchange membranes has allowed such interactions to be taken into account and has enabled a full analysis of the system to be under-taken. This treatment also has the advantage that it is not limited to electrochemical potential gradients only as is the case with the Nernst-Planck equation. It

is/

is possible, therefore, to employ a number of different forces such as chemical potential gradient, electrical potential gradient, and pressure gradient, either individually or in combination, and measure the flows of the various species in the system. From this information it is then possible to calculate the interaction coefficients of each species with every other species present in the system.

In this present work, the normal and expanded forms of the AMF C60 cation-exchange membrane referred to above, have been examined in a series of aqueous solutions of sodium chloride. Some transport and structural properties of these exchangers have been measured and correlations of the results have been found to be very good. The main aim of this work has been to obtain sufficient transport data on the systems studied to permit a full analysis of the systems using the theories of non-equilibrium thermodynamics, but where possible, parallel calculations have been carried out using the extended Nernst-Planck equation, and a limited structural analysis of the membranes has also been obtained using the electrolyte uptake/

uptake data.[2] These membranes provide two very similar systems which differ in certain well defined respects and can, therefore, provide a great deal of valuable information about the effects of these variables upon the properties of the ion-exchange membrane system as a whole.

Using the variable capacity exchanger hydrous zirconia, information has been obtained about the effects of capacity variation on the properties of the exchanger, and although the extent of the data is limited, some interesting correlations have been found.

Both of these studies provide information on systems which up till now have received little attention, but which can be made to yield a great deal of interesting information which may be extended to other similar systems.

CHAPTER TWO

Transport and diffusion through ion-exchange membranes.

2.1. Introduction.

There are three main theoretical approaches to the problem of analysing the transport processes occurring in ion-exchange membrane systems involving concentration and electrical potential gradients. These are:

(1) Simplified kinetic theory, e.g. the absolute rate theory of Eyring and co-workers. (100) (101) (102)

(2) The extension of the classical Nernst-Planck equation. (6)

(3) Application of the theory of non-equilibrium thermodynamics. (19) (21)

The absolute rate theory approach has not been widely used and it has been employed in this present study only to examine the effects of variation of the inter-site distances in the membranes on the tracer diffusion coefficients of the ions through the exchanger phase.

The extended forms of the Nernst-Planck equation have been fairly widely used in the analysis of membrane processes. (6) (7) (31) In this work, a simple extension of the Nernst-Planck equation allowing for the effect of convection has been used and is fully described in section 2.2.1.

In/

In recent years, considerable attention has been paid to the application of non-equilibrium thermodynamics to membrane processes and it is with this approach that this research program has been chiefly concerned. The aim has been to obtain sufficient data on a number of ion-exchange membrane/solution systems, to enable a complete analysis to be undertaken as described in section 2.2.2.

The accumulation of these data has also permitted a number of other studies of the systems to be carried out, and these approaches are described in section 2.5 and in chapter 3.

Where possible, correlations of the different approaches to transport processes have been given and comparisons drawn between the results of the different types of analysis used.

2.2. Theory.

2.2.1. The Nernst-Planck Equation.

Whenever an electric field is applied to an ion-exchange system, transference of ions occurs, and the flow of any ion, i, may be written in terms of its conjugate force as follows, (6)

$$(J_i)_{el} = -\bar{u}_i z_i \bar{c}_i \text{ grad } \emptyset \qquad (2.1)$$

where $(J_i)_{el}$ is the flow of species i under the electric potential gradient,

$\bar{u}_i$ is the mobility of species i,

z_i its electrochemical valence,

c_i its concentration,

and $\emptyset$ the electrical potential.

This expression is, however, only true if there is no coupling of the flows of the various species in the system and, therefore, must represent a considerable simplification of the real situation in the exchanger.

The above flux is independent of the nature of the electric potential, i.e. it is irrelevant whether the field is applied from an external source or is a result of diffusion within the system itself. Thus, in a system with a concentration gradient across an ion-exchange membrane, a diffusional potential is set up and electrical transference is superimposed on the purely diffusional flow,/

flow, $(J_i)_{diff}$, which is given by Fick's first law, as

$$(J_i)_{diff} = - \bar{D}_i \text{ grad } \bar{c}_i \qquad (2.2)$$

Where $\bar{D}_i$ is the self-diffusion coefficient of species i. Thus the resultant net flux of species i is given by

$$J_i = (J_i)diff + (J_i)_{el} = -\bar{D}_i \text{ grad } \bar{c}_i - \bar{u}_i z_i \bar{c}_i \text{ grad } \emptyset \qquad (2.3)$$

Using the Nernst-Einstein relation, $\bar{u}_i = \bar{D}_i F/RT$, this equation may be rewritten as

$$J_i = - \bar{D}_i \left(\text{grad } \bar{c}_i + z_i \bar{c}_i F/RT \text{ grad } \emptyset \right) \qquad (2.4)$$

This relation is known as the Nernst-Planck equation and is valid for all mobile species, when an electric field exists in the system. It does not, however, include the effects of pressure, activity coefficients, or of coupling. In ion-exchange systems, coupling between the flows of the counter-ions and the solvent is particularly important and cannot be neglected. The simple Nernst-Planck equation given above, must, therefore, be modified to include this term.

The Nernst-Planck equation was originally derived for ideal aqueous solutions where the flows of the individual species were measured relative to the fixed solvent. In ion-exchange systems, it is, in general, more convenient to consider the matrix as fixed, and hence the flows/

flows are measured relative to the exchanger itself. Owing to the coupling of the flows of counter-ions and solvent, there is a flow of solvent relative to the exchanger matrix. This flow is called convection. Since the solvent flow is usually in the same direction as the counter-ion flow, the value of the counter-ion flow measured on a matrix fixed frame of reference is greater than it would be on the corresponding solvent fixed reference frame, and the co-ion flow is similarly smaller. Thus, in the Nernst-Planck equation which was derived considering the solvent at rest, an additional term must be included to take account of this change of frame of reference. This so-called convective flow term is given by

$$(J_i)_{con} = \bar{c}_i v \qquad (2.5)$$

where v is the linear convection rate in the direction of the current. Thus, under the condition of an electric potential gradient only, the overall flux of species i is

$$J_i = (J_i)_{el} + (J_i)_{con}$$

$$\text{or} \quad J_i = -z_i \bar{c}_i \bar{u}_i \operatorname{grad} \phi + \bar{c}_i v \qquad (2.6)$$

$$\text{where} \quad v = (\omega FX/\rho_o v_w) \operatorname{grad} \phi$$

$$= \omega \bar{u}_3 \operatorname{grad} \phi$$

where $\bar{u}_3 = FX/\rho_o v_w$ is the mobility of the pore liquid,

X/

X is the concentration of the fixed charges, ω is the sign of the fixed charges, ρ_o the specific flow resistance of the exchanger, and v_w is the fractional pore volume of the exchanger.

2.2.1a. Convective Conductivity.

The electric current density is given by

$$I = F \sum_i z_i J_i \qquad (2.7)$$

Therefore, substituting for J_i from equation (2.6) gives

$$I = F \sum_i (-z_i^2 \bar{c}_i \bar{u}_i \text{ grad } \phi + z_i \nu \bar{c}_i)$$

$$= F \sum_i (-z_i^2 \bar{c}_i \bar{u}_i \text{ grad } \phi + z_i \omega \bar{u}_3 \bar{c}_i \text{ grad } \phi)$$

$$= F \sum_i (-z_i^2 \bar{c}_i \bar{u}_i \text{ grad } \phi) + F\omega\bar{u}_3 \sum_i (z_i \bar{c}_i \text{grad } \phi) \qquad (2.8)$$

But, for conservation of electroneutrality

$$\sum_i z_i \bar{c}_i + \omega X = 0 \qquad (2.9)$$

Therefore,

$$I = F \sum_i (-z_i^2 \bar{c}_i \bar{u}_i \text{ grad } \phi) - F\omega^2 \bar{u}_3 X \text{ grad } \phi$$

$$= -F\left(\sum_i (z_i^2 \bar{c}_i \bar{u}_i) + \bar{u}_3 X \right) \text{grad } \phi \qquad (2.10)$$

The specific conductivity $\bar{k}$ is

$$\bar{k} = -\frac{I}{\text{grad } \phi} = F\left(\sum_i (z_i \bar{c}_i \bar{u}_i) + \bar{u}_3 X \right) \qquad (2.11)$$

Using the Nernst-Einstein relation, this can be rewritten,

$$\bar{k} = F^2/RT \sum_i (z_i^2 \bar{c}_i \bar{D}_i) + F\bar{u}_3 X \qquad (2.12)$$

The second term in equation (2.12) is the contribution due to convection conductivity. In ion-exchangers with/

with high capacity and low flow resistance the convective conductivity can be a major part of the total conductivity.

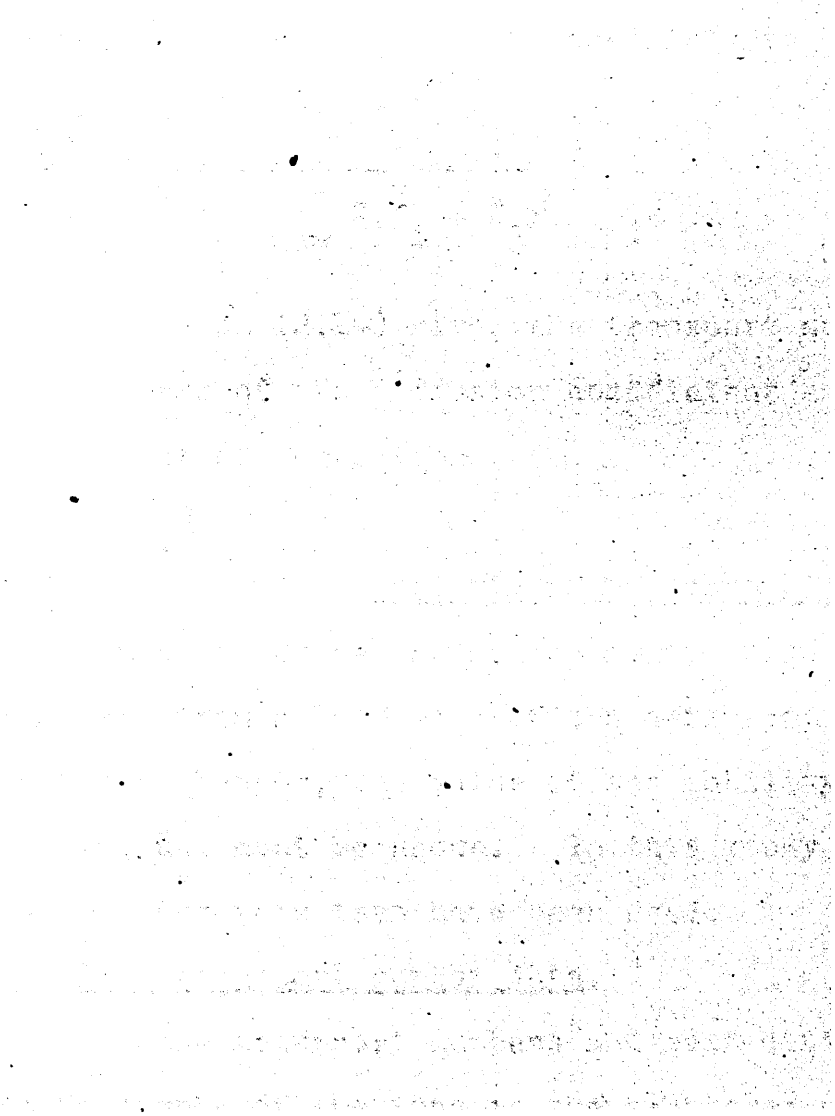

2.2.1.b. Effect of convection on transport numbers.

The transport number of an ion, i, is given by,

$$t_i = \frac{z_i F J_i}{I} \qquad (2.13a)$$

$$= \frac{z_i \bar{c}_i (z_i \bar{u}_i - \bar{u}_3)}{\sum_i z_i^2 \bar{u}_i \bar{c}_i + X \bar{u}_3} \qquad (2.13b)$$

or in terms of the diffusion coefficients,

$$t_i = \frac{z_i \bar{c}_i \left(\frac{z_i F}{RT} \bar{D}_i - \bar{u}_3\right)}{\sum_i \frac{z_i^2 F}{RT} \bar{c}_i \bar{D}_i + \bar{u}_3 X} \qquad (2.14)$$

Equation (2.14) gives the transport number of an ion, i, in terms of its diffusion coefficient and allows for the effect of convection.

2.2.1.c. Mobility of the pore liquid.

In calculating the conductivity of an ion-exchange membrane from a knowledge of the diffusion coefficients in the exchanger, the value of the mobility of the pore liquid, $\bar{u}_3$, must be known. In this study three methods of calculating this term have been used.

a) From transport number data.

If the transport numbers and self-diffusion coefficients of the ions in the exchanger are known, then substitution/

substitution in equation (2.14) gives the value of $\bar{u}_3$.

b). From electro-osmotic transport data.

This method has been used by Meares[7] to calculate the value of $\bar{u}_3$ from the experimentally determined electro-osmotic flow of solvent. The expression is

$$\sigma_3 = - \bar{u}_3 \text{ grad } \emptyset \qquad (2.15)$$

where σ_3 is the rate of electro-osmotic transport through the membrane divided by the porosity, v_w. In order to calculate the potential drop across the membrane, the value of the specific conductivity of the membrane must be known and this is the main drawback of this method.

c). From the electro-osmotic transport data using non-equilibrium thermodynamics.

By definition of $\bar{u}_3$,

$$(J_3)_{el} = - \bar{u}_3 \bar{c}_3 \text{ grad } \emptyset \qquad (2.16)$$

Anticipating the results obtained from the application of non-equilibrium thermodynamics to the system gives,

$$(J_3)_{el} = (z_1 l_{31} + z_2 l_{32}) \; F \; (- \text{grad } \emptyset) \qquad (2.17)$$

$$= \frac{t_3 \bar{k}}{F^2} \; F \; (- \text{grad } \emptyset) \qquad (2.18)$$

Since t_3 may be shown to be $(z_1 l_{31} + z_2 l_{32}) \cdot F^2/\bar{k}$.

Therefore/

Therefore, equating terms in equations (2.16) and (2.18) gives

$$\frac{t_3\bar{k}}{F} = \bar{u}_3\bar{c}_3$$

$$\bar{u}_3 = \frac{t_3\bar{k}}{\bar{c}_3 F}. \qquad (2.19)$$

Substituting this expression into equation (2.12) and rearranging, allows the specific conductivity of the exchanger to be calculated from the self diffusion coefficients of the ions and the water transference number without having to use the value of the specific conductivity in the calculation as has to be done in method (b) above. Carrying out this substitution and rearrangement gives

$$\bar{k} = \frac{F^2}{RT} \sum_i (z_i^2 \bar{c}_i \bar{D}_i) \cdot \frac{1}{(1 - \frac{Xt}{\bar{c}_3})} \qquad (2.20)$$

2.2.2. Application of Non-Equilibrium Thermodynamics.

The state of thermodynamic equilibrium is achieved when the internal parameters of the system under study are completely determined by the external parameters. Such a system is fairly simple and this is the reason why classical thermodynamics have been concerned mainly with the study of systems at equilibrium, where there are no variations of the state parameters either with time or distance. Many interesting phenomena occur in systems which are not in thermodynamic equilibrium and in which the forces on the species are non-zero. Such systems cannot fully be dealt with by the theories of classical thermodynamics and it is only the extension of thermodynamics to include irreversible processes which has allowed these systems to be studied and explained. Such a treatment requires the knowledge of the relation between the flows and forces which exist in the system and many attempts have been made to discover such correlations. In the early part of the nineteenth century a number of these relationships were discovered, notably those of Fourier (heat flow linearly related to temperature difference), Ohm (electric current proportional to electromotive/

electromotive force), and Fick (rate of diffusion of matter determined by the negative gradient of concentration). These phenomena were examples of a flow being dependent on its conjugate force. During this period, however, a number of workers found that application of a force could sometimes lead to a non-conjugated flow. Rouss (8) observed that application of an e.m.f. led to a flow of volume as well as a flow of charge, while it was shown that application of a pressure force could produce not only flow of matter, but also flow of electricity, and the findings of Liebeck and Peltier established the existence of the thermoelectric phenomena. All these discoveries suggested that there existed some form of coupling between a force of one type and flows of another type. In 1854, Kelvin published the first thermodynamic study of coupling phenomena in which he showed that for sufficiently slow processes any flow may depend in a direct and linear manner not only on the conjugate force but also on other non-conjugated forces. Kelvin's approach has since been modified but the study of coupling forms the basis of the application of non-equilibrium thermodynamics to irreversible processes.

As an example of how coupling between flows and forces/

forces may arise, consider the effect of concentration on the properties of aqueous electrolyte solutions.[9] In very dilute solutions the ions are sufficiently far apart that the coulombic interactions between them may be ignored, and consequently many of the ionic properties such as conductance, are additive. The flow of an ion will then be proportional to the gradients of its own properties and will not be influenced by the properties of the other ions. In more concentrated solutions, however, the ions must approach one another much more closely and hence influence one another's flows. The properties of one ion must, therefore, be influenced by those of other ions. This is manifest in the non-additivity of ionic conductances at other than infinite dilution, the specificity of activity coefficients, etc. It is this type of coupling of flows and forces which can be analysed by the application of non-equilibrium thermodynamics and with which this chapter will be chiefly concerned, but before going on to this discussion it is necessary to give a brief outline of the subject, to define its assumptions and its limitations.

The theory of non-equilibrium thermodynamics is based on the adaptation of the equation for the second law of/

of thermodynamics derived for equilibrium conditions, to the description of local processes in regions which may be considered to be at equilibrium even though irreversible processes are occurring in the system as a whole. Using this assumption and with the limiting condition of independent flows and forces, it is possible to calculate the entropy produced in the irreversible processes as [10]

$$\sigma = \sum_i J_i' X_i' \qquad (2.21)$$

where σ is the entropy production (always positive for an irreversible process),

J_i' is the flow of species i, X_i' its conjugate force, and the summation is carried out over all species. It is frequently more convenient to use another term, the dissipation function, Φ, defined as $\Phi = T\sigma$. Thus

$$\Phi = \sum_i J_i X_i \qquad (2.22)$$

where the new flows and forces J_i and X_i are usually in a more familiar form.[11]

In the thermodynamic analysis of the system, the flows and forces defined by equation (2.22) must be used. Thus, choice of the set of flows fixes the appropriate forces which have to be used in the thermodynamic treatment. The criteria used to obtain the flows and forces are that: [12] (a) the product of any flow and its conjugate/

conjugate force must have the same dimensions as the dissipation function, (b) for a given system, the sum of the products $J_i X_i$ must remain the same for any transformation of flows and forces and (c) the flows and forces are independent.

The manner in which these flows and forces may be used to give a thermodynamic treatment of any system was developed by Onsager [13] [14] using the principle of microscopic reversibility, and the resulting set of equations, called the phenomenological equations, may be written:

$$J_i = \sum_{k=1}^{n} l_{ik} X_k \qquad (i=1,2,3,\ldots.n) \qquad (2.23)$$

where l_{ik} are the phenomenological mobility coefficients, so called because they have the dimensions of reduced mobility or conductance.

The magnitude and direction of the flows are dependent on the reference frame from which the flows are measured. In aqueous solutions, it is usual to regard the solvent as fixed and calculate the other flows accordingly. In membrane systems, however, it is more convenient to regard the membrane as being fixed and measure the flows of the other species with reference to it. The choice of frame of reference is extremely important/

important since it directly affects the values of the l - coefficients.

Application of this theory to membrane processes also requires the assumption that there is equilibrium at the membrane solution-interface and that the chemical potential of any species in the solution at the interface is equal to the chemical potential of the same species in the membrane at the interface between the two phases.[15] The gradients of chemical potential of the same species in the two phases may, however, be quite different.

Provided no coupling occurs, i.e. if the cross-coefficients l_{ik} $(i \neq k)$ are zero, then each flow may be written as a linear function of its conjugate force in accordance with the discoveries of Fourier, Ohm and Fick. However, if the cross-coefficients are non-zero, then each flow is also linearly related to its non-conjugate forces. This linear dependence of flows and forces holds only when sufficiently slow processes are occurring in systems which are not too far from equilibrium. The applicability of linear non-equilibrium thermodynamics is, however, much wider than these limitations might suggest.[16]

The form of equation (2.23) allows an alternative set of equations to be presented which represent the forces as linear functions of the flows:

$$X_i = \sum R_{ik} J_k \quad (i=1,2,3,\ldots n) \qquad (2.24)$$

The/

The set of R-coefficients, which because of their form are often called phenomenological resistance coefficients, may be obtained from the corresponding l- or mobility coefficients by simple matrix inversion. Thus, (17)

$$R_{ik} = \frac{|l_{ik}|}{|L|} \qquad (2.25)$$

where $|L|$ is the determinant of the matrix of l-coefficients and $|l_{ik}|$ is the minor of the determinant corresponding to the term l_{ik}.

Although this formulation adequately describes the system, it can be seen that in order to obtain a complete analysis and determine the values of all the l- or R-coefficients, a large number of independent experiments are required, and this is frequently a difficult task. It is fortunate, therefore, that the matrices of l- and R-coefficients are symmetrical, thereby reducing considerably, the number of unknown terms. This symmetry was first proved by Onsager (13) and the symmetry properties i.e.

$$l_{ik} = l_{ki}, \text{ and } R_{ik} = R_{ki} \quad (i \neq k) \qquad (2.26)$$

are known as the Onsager Reciprocal Relations, or, as frequently abbreviated, O.R.R. These reciprocal relations apply only to systems which obey the limitations on the flows and forces discussed earlier, and under conditions which/

which are not far removed from equilibrium.

From the fact that the entropy production in an irreversible process must always be positive, it is possible to obtain a further inequality relating the phenomenological coefficients, [18] namely,

$$l_{ii}.l_{kk} \geqslant (l_{ik})^2 \qquad (2.27a)$$

and $$R_{ii}.R_{kk} \geqslant (R_{ik})^2 \qquad (i \neq k). \qquad (2.27b)$$

The theory of non-equilibrium thermodynamics as described above, is applicable to all irreversible processes in which there exists a linear relation between the flows and forces. The first applications of this theory to ion-exchange membrane processes were made by Staverman [19] and Lorenz.[20] Their calculations are very general but require a large number of independent experimental methods to enable a complete analysis to be undertaken. Spiegler [21] attempted to simplify the situation and reduce the number of independent transport data required, by making assumptions about the magnitude of some of the terms. Meares [46] applied this theory to the phenol-sulphonic cation-exchange membrane Zeocarb 315 and obtained the first set of frictional coefficients for an ion-exchanger. However, the assumptions used by/

by Spiegler have been frequently criticised [22] [23]. In particular it has been suggested that the frictional interactions between the cation and the anion and the isotope-isotope interactions in tracer experiments, are not zero as suggested by Spiegler and that these assumptions invalidate the results so obtained.

The next section deals with the theoretical approach used in this study and its relation to that used by other authors.

2.2.2a Theory.

The study of transport processes in ion-exchange membranes makes great use of isotopic tracers and hence it is important to establish, at the outset, the effect of isotope-isotope interactions on the calculation of the phenomenological coefficients in membranes. For this purpose, the excellent paper by Kedem and Essig [24] has been used as a basis and the following theory is taken mainly from this source.

This approach uses frictional coefficients and is concerned mainly with the local values of these coefficients, r_{ij}, which are then integrated through the entire thickness of the membrane to give the integral value, $R_{ij} = \int_o^{\Delta x} r_{ij}\, dx$. The subscript o refers to the total test substance, 1 to the abundant isotope, 1' and 1" to the tracer isotopes of test substance. The forces acting on the various species are taken as the negative gradients of their electrochemical potential, $-\frac{d\tilde{\mu}}{dx}$. Thus, using the formulation of flows and forces given in section (2.2.2), together with the limitations imposed by equation (2.22), the forces may be written:

$$X_i = -(d\tilde{\mu}_i/dx) = \sum_j r_{ij} J_j \qquad (2.28)$$

where i represents either an ion or an uncharged molecule.

Rewriting/

Rewriting equation (2.28) expressing the flows of the test species in terms of their driving forces and coupled flows gives for the total test substance;

$$-\frac{d\tilde{\mu}_o}{dx} = r_{oo}J_o + \sum_j r_{oj}J_j \qquad (2.29a)$$

and for the isotopic components,

$$-\frac{d\tilde{\mu}_1}{dx} = r_{11}J_1 + r_{11'}J_{1'} + r_{11''}J_{1''} + \sum r_{1j}J_j \qquad (2.29b)$$

$$-\frac{d\tilde{\mu}_{1'}}{dx} = r_{1'1}J_1 + r_{1'1'}J_{1'} + r_{1'1''}J_{1''} + \sum r_{1'j}J_j \qquad (2.29c)$$

$$-\frac{d\tilde{\mu}_{1''}}{dx} = r_{1''1}J_1 + r_{1''1'}J_{1'} + r_{1''1''}J_{1''} + \bar{\sum} r_{1''j}J_j \qquad (2.29d)$$

where the non-zero r_{ik}'s ($i \neq k$; $i,k = 1,1',1''$) allow specifically for the effect of isotope interaction.

Examination of equation (2.29b), and considering the assumed kinetic indistinguishability of $1,1'$ and $1''$, reveals that for a given value of $d\tilde{\mu}_1/dx$ and $\sum_j r_{1j}J_j$, J_1 must depend not on the individual values of $J_{1'}$ and $J_{1''}$ but only on their sum, $J_{1'} + J_{1''}$. Hence $r_{11'} = r_{11''}$, and must be independent of the ratios of the isotope concentrations $c_{1'}/c_{1''}$. Similarly, from equations (2.29c) and (2.29d), $r_{1'1} = r_{1'1''}$, and $r_{1''1'} = r_{1''1}$.

Further, since equations (2.29a) to (2.29c) relate conjugate forces and flows of the dissipation function of the process, the O.R.R. applies; i.e. $r_{ik} = r_{ki}$. Therefore, from/

from these two discussions it may be seen that all the r_{ik}'s are equal, ($i \neq k$: $i,k = 1,1',1''$).

Since $J_o = J_1 + J_{1'} + J_{1''}$, substituting for $J_{1'}$ and $J_{1''}$ in equations (2.29c) and (2.29d), gives

$$-\frac{d\tilde{\mu}_{1'}}{dx} = (r_{1'1'} - r_{ik})J_{1'} + r_{ik}J_o + \Sigma r_{1'j}J_j \qquad (2.30a)$$

$$-\frac{d\tilde{\mu}_{1''}}{dx} = (r_{1''1''} - r_{ik})J_{1''} + r_{ik}J_o + \Sigma r_{1''j}J_j \qquad (2.30b)$$

Since,

$$+(d\tilde{\mu}_o/dx) = RTd\ln c_o/dx + RTd\ln\gamma_o/dx + z_oFd\phi/dx + \bar{v}_o dp/dx \qquad (2.31a)$$

and $$+(d\tilde{\mu}_{1'}/dx) = RTd\ln c_{1'}/dx + RTd\ln\gamma_{1'}/dx + z_{1'}Fd\phi/dx + \bar{v}_{1'}dp/dx \qquad (2.31b)$$

then, since also $\gamma_o = \gamma_{1'}$, $z_o = z_{1'}$ and $\bar{v}_o = \bar{v}_{1'}$, and

$$\left(\frac{-d\tilde{\mu}_o}{dx}\right) - \left(\frac{-d\tilde{\mu}_{1'}}{dx}\right) = \frac{RT\ d\ln}{dx}\left(\frac{c_o}{c_{1'}}\right),$$

$$-(d\tilde{\mu}_o/dx) + (d\tilde{\mu}_{1'}/dxZ) = (r_{oo} - r_{ik})J_o - (r_{1'1'} - r_{ik})J_{1'}$$

$$= RT\ d\ln\rho_{1'}/dx$$

where $\rho_{1'} = c_{1'}/c_o$

Dividing by $r_{1'1'} - r_{ik}$ and introducing $\rho_{1'} = \frac{r_{oo} - r_{ik}}{r_{1'1'} - r_{ik}}$ (Appendix A.1)

gives:

$$J_{1'} - \rho_{1'}J_o = -\frac{RT}{r_{oo} - r_{ik}}\frac{d\rho_{1'}}{dx} \qquad (2.32a)$$

Similarly,

Similarly,

$$J_{1''} - \rho_{1''} J_0 = - \frac{RT}{r_{00} - r_{ik}} \frac{d\rho_{1''}}{dx} \qquad (2.32b)$$

Integrating in the steady state, yields,

$$\frac{J_0 \int_0^{\Delta x} (r_{00}' - r_{ik})\, dx}{RT} = \ln\left(\frac{J_{1'} - \rho^{I}_{1'} J_0}{J_{1'} - \rho^{o}_{1'} J_0} \right)$$

and similarly for species 1".

Denoting the term $\int_0^{\Delta x} (r_{00} - r_{ik})\, . \, dx$ by the quantity R^x, called the exchange resistance, then

$$\frac{JR^x}{RT} = \ln \left(\frac{J_{1'} - \rho^{I}_{1'} J_0}{J_{1'} - \rho^{o}_{1'} J_0} \right) \qquad (2.33a)$$

and $$\frac{JR^x}{RT} = \ln \left(\frac{J_{1''} - \rho^{I}_{1''} J_0}{J_{1''} - \rho^{o}_{1''} J_0} \right) \qquad (2.33b)$$

Therefore,

$$\frac{J_{1'} - \rho^{I}_{1'} J_0}{J_{1'} - \rho^{o}_{1'} J_0} = \frac{J_{1''} - \rho^{I}_{1''} J_0}{J_{1''} - \rho^{o}_{1''} J_0} \qquad (2.34)$$

If, for each tracer isotope, the tracer is added to one side only, then $\rho^{I}_{1'} = \rho^{o}_{1''} = 0$, and equation (2.34) reduces to

$$J_0 = (J_{1'} / \rho^{o}_{1'}) + (J_{1''} / \rho^{I}_{1''}). \qquad (2.35)$$

which is identical to the well used relation,

Net flux = influx - outflux.

Thus, this relation remains valid in the presence of isotope interaction.

The/

The treatment outlined above, demonstrates that, regardless of the interactions in the system, it is possible to obtain the net flux under any given force from two tracer fluxes, one with and one against the applied electrochemical potential gradient. This result is very important in determining the transport number of the ions in the membrane using tracer techniques, and in measuring the salt flow through the membrane when a salt concentration gradient is maintained across it.

It is also possible to show from this approach, the effect of isotope-isotope interaction on the tracer diffusion coefficient of the mobile species in the membrane. In an experiment of this nature, one of the species on one side of the membrane is tagged with an isotopic tracer and the flow of the tracer is monitored. Since only one tracer is used there are only two species of test substance namely 1 and 1'. Thus, since no current flows in the system and there are no salt concentration gradients, $J_o = J_1 + J_{1'} = 0$. Therefore,

$$J_1 = -J_{1'}. \qquad (2.36)$$

The forces acting on the species are

$$X_1 = -(d\tilde{\mu}_1/dx) = -RT d\ln c_1/dx - RT\, d\ln \gamma_1^{\pm}/dx - z_1 F\, d\phi/dx - \bar{v}_1\, dp_1/dx \qquad (2.37a)$$

and/

and $X_{1'} = -(d\tilde{\mu}_{1'}/dx) = -RTd\ln c_{1'}/dx - RT\, d\ln \gamma_{1'}/dx$

$$- z_{1'}F\, d\phi_{1'}/dx - \bar{v}_{1'}dp_{1'}/dx \qquad (2.37b)$$

Since the solutions on both sides of the membrane are identical apart from the presence of tracer on one side, then

$$\gamma_1 = \gamma_{1'}, \quad \phi_1 = \phi_{1'} \quad \text{and} \quad p_1 = p_{1'}.$$

Also $z_1 = z_{1'}$ and $\bar{v}_1 = \bar{v}_{1'}$.

Hence,

$$X_1 = (-RT/c_1)(dc_1/dx) \qquad (2.38a)$$

and $$X_{1'} = (-RT/c_{1'})(dc_{1'}/dx) \qquad (2.38b)$$

Since the flows of the other species 2 to n are zero, substitution of $J_2 = J_3 = \ldots J_n = 0$ into equation (2.29) gives

$$X_1 = (-RT/c_1)(dc_1/dx) = r_{11}J_1 - r_{11'}J_{1'} \qquad (2.39a)$$

and $$X_{1'} = (-RT/c_{1'})(dc_{1'}/dx) = r_{1'1}J_1 - r_{1'1'}J_{1'} \qquad (2.39b)$$

Now, since $J_1 = -J_{1'}$,

$$X_1 = (-RT/c_1)(dc_1/dx) = (r_{11} - r_{11'})J_1 \qquad (2.40)$$

therefore,

$$J_1 = -\left(\frac{RT}{c_1(r_{11} - r_{11'})}\right)\left(\frac{dc_1}{dx}\right) \qquad (2.41)$$

By Fick's first law of diffusion,

$$J_1 = -D_{11}\cdot\frac{dc_1}{dx}$$

so/

so that equating terms in equations (2.41) and (2.2), gives

$$D_{11} = \frac{RT}{c_1 (r_{11} - r_{11'})} \qquad (2.42)$$

This relation applies for each local region of the exchanger. Diffusion coefficients are usually obtained for the membrane as a whole, so that equation (2.42) must be integrated over the entire thickness of the membrane to give the integral diffusion coefficient. Integration of equation (2.42) yields

$$D_{11} = \frac{RT}{c_1 (R_{11} - R_{11'})} = \frac{RT}{c_1 R^{x}_{11}} \qquad (2.43)$$

where R^{x}_{11} is the exchange resistance and differs from the resistance to net flow, R_{11}, by the isotope interaction, $R_{11'}$. This result is of particular importance to the study of ion-exchange membranes, since if $R_{11'}$ is large, the assumption implicit in Spiegler's relation $D_{11} = RT/c_1 R_{11}$ is wrong and must lead to erroneous results. This point will be dealt with in greater detail in section 2.6.1.

Having shown the effect of isotope-isotope interaction on the theory of non-equilibrium thermodynamics, it is now possible to proceed and give the theory which may/

may be applied to ion-exchange membranes and which, under certain assumptions, can be made to yield a complete analysis of the system.

In the membrane system, there are four separate species, namely, the counter-ion, 1, the co-ion, 2, the water, 3, and the matrix (including the fixed charge), 4. Thus, the basic equations relating the flows and forces are

$$X_i = \sum_j R_{ij} J_j \qquad (i = 1,2,3,4) \tag{2.44a}$$

and

$$J_i = \sum_j l_{ij} X_j \qquad (i = 1,2,3,4), \tag{2.44b}$$

where the relation between the flows and forces is as given in section 2.2.2. ,

$$\Phi = T\sigma = \sum_i J_i X_i \tag{2.22}$$

Of the four forces, X_1 to X_4, only three are independent as may be seen from the Gibbs-Duhem equation

$$\sum_i c_i X_i = 0 \tag{2.45}$$

It is possible to carry out a transformation on the flows and forces and still preserve the yalue of the dissipation/

dissipation function, Φ. Thus eliminating X_4 from equation (2.45) and substituting in equation (2.22) gives

$$\Phi = T\sigma = \sum_{i=1}^{3} (J_i - (c_i/c_4)J_4)X_i$$

$$= \sum_{i=1}^{3} J_i^* X_i \qquad (2.46)$$

in which the flows are now considered on a membrane fixed frame of reference, which is the most convenient experimentally. Hereafter, the flows so defined will be denoted by J_i, the asterisk being dropped.

The phenomenological equations then become:

$$X_i = \sum R_{ij}J_j \qquad (i = 1,2,3) \qquad (2.47a)$$

and

$$J_i = \sum l_{ij}X_j \qquad (i = 1,2,3) \qquad (2.47b)$$

in which the O.R.R. holds i.e.

$$R_{ij} = R_{ji} \qquad (i \neq j)$$

and $$l_{ij} = l_{ji}$$

and where the l- and R-coefficients are related by

$$R_{ij} = \frac{|l_{ij}|}{|L|}$$

as discussed in section (2.2.2).

There has been considerable discussion as to whether a system is best represented by the l- or R-formalism. There/

There are advantages and disadvantages in both representations. The advantage of the l-coefficient approach is that these coefficients have the dimensions of mobility or conductance and tend to zero as the concentration tends towards zero. It is also possible to derive equations, from this approach, which will predict various properties of the system, e.g. the salt flow with a concentration gradient, or the e.m.f. of a concentration cell. The R-coefficients have an advantage over the l-coefficients in that they are frame of reference independent [25] which the l-coefficients are not. The use of the R-coefficients also allows the calculation of the interactions of all the other species with the membrane matrix, i.e. with species 4: This is not possible using the l-coefficients on a membrane fixed frame of reference. However, the cross-coefficients in the R-coefficient approach are frequently found to be negative and some authors have found the significance of negative friction somewhat difficult to explain.[9] [26] [27] It is now fairly generally accepted that the sign of the R-coefficients depends on the nature of the interaction which they measure. If the interaction is attractive, then the R-coefficients are negative, while repulsive interactions/

interactions give rise to positive R-coefficients.[28]

The work of Spiegler [21] has shown that resistance coefficients may be thought of as representing a frictional interaction between the various species. On this basis the term $c_i R_{ij}$ represents the friction of one mole of species i with those species j in unit volume around it: $c_i R_{ii}$ represents the frictional interaction of one mole of i with all other species except its own in unit volume, while $c_i(R_{ii} - R_{ii'})$ represents the frictional interaction of one mole of species i with all other species including its own, in unit volume around it.

Since the two approaches, using l- or R-coefficients, can equally well be applied to ion-exchange membrane systems, they have both been used where appropriate in the present study.

2.2.2.b. Mobility Coefficient Approach

The methods used are based on those given by Miller (9) for binary electrolytes, and in some cases the equations are identical in form to those obtained for aqueous solutions. (9)

Electric potential gradient only.

Conductivity.

When an electric potential is applied across the membrane the current flowing in the system is given by

$$I = (z_1 J_1 + z_2 J_2)F \qquad (2.48)$$

where J_1 and J_2 are the flows of the two mobile ionic species, and z_1 and z_2 are the signed valences of the ions. The forces acting on the various species are

$$X_i = -(d\tilde{\mu}_i/dx)$$

$$= -(d\mu_i/dx) + z_i F(-d\phi/dx) \qquad (2.49)$$

Since the concentration on either side of the membrane is the same, then

$$-(d\mu_i/dx) = 0 \qquad (2.50)$$

Therefore, for the ionic species the force is given by

$$X_i = z_i F(-d\phi/dx) \qquad (i = 1,2) \qquad (2.51)$$

and/

and for the water,

$$X_3 = 0. \qquad (2.52)$$

The phenomenological equation becomes,

$$J_1 = l_{11}X_1 + l_{12}X_2 \qquad (2.53a)$$

$$J_2 = l_{21}X_1 + l_{22}X_2 \qquad (2.53b)$$

$$J_3 = l_{31}X_1 + l_{32}X_2 \qquad (2.53c)$$

Substituting for the flows J_1 and J_2 in equation (2.48) gives for the current:

$$I = F^2 (-d\phi/dx).\ (z_1^2 l_{11} + z_1 z_2 (l_{12} + l_{21}) + z_2^2 l_{22}) \qquad (2.54)$$

However, by Ohm's law,

$$I = \bar{k}\ (-d\emptyset/dx) \qquad (2.55)$$

where $\bar{k}$ is the specific conductivity.

Therefore,

$$\bar{k} = F^2(z_1^2 l_{11} + z_1 z_2 (l_{12} + l_{21}) + z_2^2 l_{22}) \qquad (2.56)$$

$$= F^2 a$$

where $$a = (z_1^2 l_{11} + z_1 z_2 (l_{12} + l_{12}) + z_2^2 l_{22}) \qquad (2.57)$$

Equation (2.56) is identical to the one obtained by Miller for a binary electrolyte, since in both the solution and the membrane there are only two mobile charged species.

Transport Numbers./

Transport Numbers.

The transport number of an ion is defined by the relation:

$$t_i = \frac{z_i F J_i}{I} \qquad (2.58)$$

and the water transference number is given by,

$$t_3 = FJ_3/I \qquad (2.59)$$

Substituting for I using equation (2.48) in the expression for the counter-ion transport number gives

$$t_1 = \frac{z_1 F J_1}{F(z_1 J_1 + z_2 J_2)} \qquad (2.60)$$

which on substitution for J_1 and J_2 reduces to

$$t_1 = (1/a). \ (z_1^2 l_{11} + z_1 z_2 l_{12}) \qquad (2.61a)$$

A similar calculation for the co-ion and for the water yields

$$t_2 = (1/a). \ (z_2^2 l_{22} + z_1 z_2 l_{21}) \qquad (2.61b)$$

and

$$t_3 = (1/a). \ (z_1 l_{13} + z_2 l_{23}) \qquad (2.61c)$$

Chemical Potential gradient.

When the membrane is placed between two solutions of the same electrolyte but of different concentrations, a potential difference is developed across the membrane, but/

but no current flows in the system.

i.e. $I = (z_1 J_1 + z_2 J_2) = 0$

In this case the forces acting on the species are given by the negative gradients of their electrochemical potential, i.e.

$$X_i = (-d\tilde{\mu}_i/dx)$$
$$= (-d\mu_i/dx) + z_i F(-d\phi/dx) \quad (i=1,2) \tag{2.62}$$

and $$X_3 = (-d\mu_3/dx) \tag{2.63}$$

Substituting,

$$J_1 = l_{11}X_1 + l_{12}X_2 + l_{13}X_3$$

and $$J_2 + l_{21}X_1 + l_{22}X_2 + l_{23}X_3$$

into equation (2.62) and rearranging, gives

$$(z_1 l_{11} + z_2 l_{21})X_1 + (z_1 l_{12} + z_2 l_{22})X_2 + (z_1 l_{13} + z_2 l_{23})X_3 = 0. \tag{2.64}$$

Comparison of the bracketed terms with equations (2.61a) (2.61b) and (2.61c) shows that equation (2.64) may be rewritten

$$\frac{t_1}{z_1} X_1 + \frac{t_2}{z_2} X_2 + \frac{t_3}{} X_3 = 0 \tag{2.65}$$

or $$(t_1/z_1).(-d\tilde{\mu}_1/dx) + (t_2/z_2).(-d\tilde{\mu}_2/dx) + (t_3).(-d\mu_3/dx) = 0. \tag{2.66}$$

Expanding $(-d\tilde{\mu}_i/dx)$ and collecting terms yields

$$(t_1/z_1)(d\mu_1/dx) + (t_2/z_2)(d\mu_2/dx) + (t_3).(d\mu_3/dx) = F(-d\phi/dx) \tag{2.67}$$

Integration of this expression gives the diffusion potential set up across the membrane. If electrodes reversible to the anion are used for measuring the cell potential, and if a Donnan equilibrium is assumed at the membrane/solution interfaces, then for a 1:1 electrolyte, the measured e.m.f. is given by

$$E = -2\bar{t}_1 \left(\frac{RT}{F}\right) \ln \left(\frac{\bar{a}_{\pm}'}{\bar{a}_{\pm}''}\right) - \bar{t}_3 \left(\frac{RT}{F}\right) \ln \left(\frac{\bar{a}_3'}{\bar{a}_3''}\right) \qquad (2.68)$$

(See appendix A.2.)

Salt flow.

It is possible to obtain a relation which expresses the salt flow through the membrane under the influence of a concentration gradient, in terms of the l-coefficients, some of the transport properties of the system, and the activity gradients of the salt and the water.

The salt flow, in the absence of current, is given by

$$J_s = (J_1/\nu_1) = (J_2/\nu_2) \qquad (2.69)$$

where ν_1 and ν_2 are the number of counter- and co-ions obtained from one molecule of salt and where $\nu_{12} = \nu_1 + \nu_2$.

Expanding J_1 in terms of $(d\tilde{\mu}_1/dx)$ and $(d\tilde{\mu}_2/dx)$, and substituting for the term $(F(-d\phi/dx))$ using equation/

equation (2.67), yields for a 1:1 electrolyte, after rearranging, (see appendix A.3.)

$$J_s = (1/a)(l_{11}\, l_{22} - l_{21} l_{12})(-d\mu_{12}/dx) + (l_{13} - \frac{a t_1 t_3}{z_1})(-d\mu_3/dx) \qquad (2.70)$$

This is equivalent to treating the system as comprising only two mobile species, namely the salt(s) or (12) and the water (3). The term $(1/a)(l_{11}l_{22} - l_{12}\, l_{21})$ represents an l_{ss} coefficient while the term $(l - \frac{a t_1 t_3}{z_1})$ is an l_{s3} coefficient. Since the forces $(-d\mu_{12}/dx)$ and $(-d\mu_3/dx)$ act in opposite directions, the coupling of the salt and water flows as represented by the term $l_{s3} X_3$ tends to reduce the salt flow through the membrane, unless l_{13} is less than $(a t_1 t_3/z_1)$.

Osmotic flow.

Using a method similar to that used for obtaining the salt flow, the osmotic flow J_3 under a salt concentration gradient may be shown to be, (see appendix A.4)

$$J_3 = (l_{13} - \frac{a t_1 t_3}{z_1})(-d\mu_{12}/dx) + (l_{33} - t_3^2 a)(-d\mu_3/dx) \qquad (2.71)$$

where/

where again $(l_{13} - \frac{a t_1 t_3}{z_1})$ can be taken as l_{3s} and $(l_{33} - t_3^2 a)$ as l'_{33}. As for the salt flow, the effect of coupling is to reduce the water flow produced by the direct coefficient l'_{33} unless l_{13} is less than $(a t_1 t_3 / z_1)$. Comparison of equations (2.70) and (2.71) shows that $l_{s3} = l_{3s}$ and thus the transformation has preserved the O.R.R.

The five independent equations (2.56) (2.61b) (2.61c) (2.70) and (2.71) contain six unknown l-coefficients and so a complete analysis of the system using only this information is impossible, although section 2.6.2. shows that by making some assumptions about the system, a reasonably precise analysis can be achieved, for dilute solutions.

There are of course other ways of representing the system using the l-coefficient formulation. Writing the phenomenological equations for applied electric potential and concentration gradients, six equations relating the flows and forces of the mobile species are obtained:

$$J_1^{el} = l_{11} X_1^{el} + l_{12} X_2^{el} + l_{13} X_3^{el} \qquad (2.72a)$$

$$J_2^{el} = l_{21}X_1^{el} + l_{22}X_1^{el} + l_{23}X_3^{el} \qquad (2.72b)$$

$$J_3^{el} = l_{31}X_1^{el} + l_{32}X_2^{el} + l_{33}X_3^{el} \qquad (2.72c)$$

$$J_1^{c} = l_{11}X_1^{c} + l_{12}X_2^{c} + l_{13}X_3^{c} \qquad (2.72d)$$

$$J_2^{c} = l_{21}X_1^{c} + l_{22}X_2^{c} + l_{23}X_3^{c} \qquad (2.72e)$$

$$J_3^{c} = l_{31}X_1^{c} + l_{32}X_2^{c} + l_{33}X_3^{c} \qquad (2.72f)$$

where the superscripts el and c refer to the electric potential and electrochemical potential gradients respectively.

However, only two of the last three equations (2.72 (d - f)) are independent, since the forces are related by the equation (2.65) proved in the preceding section. Therefore, the situation is again one of five independent equations and six unknowns. It is only possible to solve for the l-coefficients if the value of one of the coefficients is estimated. This approach is discussed further in section 2.6.2.

2.2.2.c. Frictional Coefficient Representation.

As discussed in section 2.2.2, the flows and forces may also be related by use of the resistance or frictional coefficients, R_{ij}. Given applied electric potential and concentration gradients, six equations analogous to equations (2.72) may be used to represent the system:

$$X_1^{el} = R_{11}J_1^{el} + R_{12}J_2^{el} + R_{13}J_3^{el} \qquad (2.73a)$$

$$X_2^{el} = R_{21}J_1^{el} + R_{22}J_2^{el} + R_{23}J_3^{el} \qquad (2.73b)$$

$$X_3^{el} = R_{31}J_1^{el} + R_{32}J_2^{el} + R_{33}J_3^{el} \qquad (2.73c)$$

$$X_1^{c} = R_{11}J_1^{c} + R_{12}J_2^{c} + R_{13}J_3^{c} \qquad (2.73d)$$

$$X_2^{c} = R_{21}J_1^{c} + R_{22}J_2^{c} + R_{23}J_3^{c} \qquad (2.73e)$$

$$X_3^{c} = R_{31}J_1^{c} + R_{32}J_2^{c} + R_{33}J_3^{c} \qquad (2.73f)$$

As for the mobility coefficients, however, only five of the six forces are independent, and so there remains one more unknown than there are independent equations. A number of authors have used tracer diffusion experiments to supply further relations involving the R-coefficients, but it has been shown in section 2.6.1. that this introduces further unknown frictional interactions between/

between the isotopes and hence, this method cannot be used to produce a complete analysis of the system unless proof can be obtained that the values of R_{11}, and R_{22}, are so small that they may be ignored. There are, however, a number of other reasonable assumptions which may be made in order to reduce the number of unknown R-coefficients to the same as the number of independent equations.

Fixed charge interactions.

As mentioned in section 22.2, one of the advantages of using the R-coefficient approach is that the interactions between the mobile species and the matrix can also be obtained. The R_{4i} coefficients are obtained from a relation which is one of the requirements of this representation, namely, (29)

$$\sum_{j=1}^{n} c_j R_{ij} = 0 \qquad (i = 1,2,3,4) \qquad (2.74)$$

This equation provides four further relations from which the values of R_{14}, R_{24}, R_{34}, and R_{44} may be obtained.

Second frictional coefficient representation.

Another representation of the phenomenological equations which was used by Spiegler (21) involves the use/

use of the friction coefficient $\bar{X}_{ij}$, defined as

$$F_{ij} = -\bar{X}_{ij} (u_i - u_j) \qquad (2.75)$$

where F_{ij} is the frictional force between species i and j moving with respective velocities u_i and u_j. $\bar{X}_{ij}$ is, therefore, the frictional coefficient between one mole of i and the existing concentration of j around it in the membrane phase. Spiegler's assumption is that, under steady state conditions, the directly applied thermodynamic force, X_i, is balanced by the frictional interaction of species i with all the other species. Thus,

$$X_1 = -F_{12} - F_{13} - F_{14} \qquad (2.76a)$$

$$X_2 = -F_{21} - F_{23} - F_{24} \qquad (2.76b)$$

$$X_3 = -F_{31} - F_{32} - F_{34} \qquad (2.76c)$$

Expanding in terms of equation (2.75) and rearranging,

$$X_1 = (\bar{X}_{12} + \bar{X}_{13} + \bar{X}_{14})u_1 - \bar{X}_{12}u_2 - \bar{X}_{13}u_3 \qquad (2.77a)$$

$$X_2 = -\bar{X}_{21}u_1 + (\bar{X}_{21} + \bar{X}_{23} + \bar{X}_{24})u_2 - \bar{X}_{23}u_3 \qquad (2.77b)$$

$$X_3 = -\bar{X}_{31}u_1 - \bar{X}_{32}u_2 + (\bar{X}_{31} + \bar{X}_{32} + \bar{X}_{34})u_3 \qquad (2.77c)$$

Since $u_i = J_i/c_i$, equation (2.77) becomes

$$X_1 = \frac{(\bar{X}_{12} + \bar{X}_{13} + \bar{X}_{14})}{c_1} J_1 - \frac{\bar{X}_{12}}{c_2} J_2 - \frac{\bar{X}_{13}}{c_3} J_3 \qquad (2.78a)$$

$$X_2 = \frac{-\bar{X}_{21}}{c_1} J_1 + \frac{(\bar{X}_{21} + \bar{X}_{23} + \bar{X}_{24})}{c_2} J_2 - \frac{\bar{X}_{23}}{c_3} J_3 \qquad (2.78b)$$

$$X_3 = -\frac{\bar{X}_{31}}{c_1} J_1 - \frac{\bar{X}_{32}}{c_2} J_2 + \frac{(\bar{X}_{31} + \bar{X}_{32} + \bar{X}_{34})}{c_3} J_3 \qquad (2.78c)$$

This equation is identical in form with equations (2.47a) so that equating the corresponding coefficients gives,

$$R_{ii} = \sum_j \frac{\bar{X}_{ij}}{c_i} \qquad (2.79)$$

and

$$R_{ij} = R_{ji} = -\frac{\bar{X}_{ij}}{cj} = -\frac{\bar{X}_{ji}}{c_i} \qquad (2.80)$$

Substiution for $\bar{X}_{ij}$ in equation (2.79) gives

$$c_i R_{ii} = \sum_i c_j R_{ij}$$

which is the requirement referred to above, equation (2.74).

The matrix of $\bar{X}_{ij}$ coefficients is not symmetrical and does not lend itself to such simple manipulation as does the R-coefficient formulation. Therefore, the R-coefficient approach has been preferred in this work.

2.2.3. Correlation of Simple flux equations with the Non-equilibrium thermodynamic treatment.

Since the transport properties of ion-exchangers can be treated either by the use of the extended Nernst-Planck equation or by non-equilibrium thermodynamics, correlations must exist between the two approaches. In this section, some of these correlations are discussed, and the validity of the Nernst-Planck approach evaluated by comparing it with the rigorous treatment of irreversible thermodynamics.

For an electrical force only, the extended Nernst-Planck equation may be written, for species 1, as

$$J_1 = - \bar{u}_1 z_1 \bar{c}_1 (\text{grad } \emptyset) + \bar{c}_1 \omega \bar{u}_3 (\text{grad } \emptyset) \qquad (2.6)$$

For a cation exchanger, $\omega = -1$: therefore,

$$J_1 = - \bar{u}_1 z_1 \bar{c}_1 (\text{grad } \emptyset) - \bar{c}_1 \bar{u}_3 (\text{grad} \emptyset)$$

$$= z_1 \bar{c}_1 (\bar{u}_1 + \bar{u}_3/z_1) (-\text{grad} \emptyset) \qquad (2.81)$$

Considering the non-equilibrium thermodynamic approach, the proportionality constant between the flow of a species i and its conjugate force is given by l_{ii}. Therefore, equation (2.81) may be written as

$$J_1 = l_{11} z_1 F (-\text{grad } \emptyset) \qquad (2.82)$$

where,/

where,

$$l_{11} = \bar{c}_1/F\ (\bar{u}_1 + \bar{u}_3/z_1) \qquad (2.83)$$

Using the Nernst-Einstein relation, this becomes,

$$l_{11} = \bar{c}_1/F\ (\bar{D}_{11}F/RT + \bar{u}_3/z_1)$$

or $$l_{11} = \bar{c}_1\bar{D}_{11}/RT + \bar{c}_1\bar{u}_3/z_1F \qquad (2.84)$$

Therefore,

$$\bar{c}_1\bar{D}_{11} = RT(l_{11} - \bar{c}_1\bar{u}_3/z_1F) \qquad (2.85a)$$

Likewise, it may be shown that,

$$\bar{c}_2\bar{D}_{22} = RT(l_{22} - \bar{c}_2\bar{u}_3/z_2F) \qquad (2.85b)$$

For a cation-exchanger and a 1:1 electrolyte, $z_1 = +1$ and $z_2 = -1$.

Therefore,

$$\bar{c}_1\bar{D}_{11} = RT(l_{11} - \bar{c}_1\bar{u}_3/F) \qquad (2.86a)$$

$$\bar{c}_2\bar{D}_{22} = RT(l_{22} + \bar{c}_2\bar{u}_3/F) \qquad (2.86b)$$

From equation (2.12),

$$\bar{k} = F^2/RT(\bar{c}_1\bar{D}_{11} + \bar{c}_2\bar{D}_{22}) + F\bar{u}_3X$$

Substituting for $\bar{c}_1\bar{D}_{11}$ and $\bar{c}_2\bar{D}_{22}$ from equations (2.86a) and (2.86b) gives,

$$\bar{k} = RT.F^2/RT(l_{11} - \bar{c}_1\bar{u}_3/F + l_{22} + \bar{c}_2\bar{u}_3/F) + F\bar{u}_3X$$

$$\bar{k} = F^2(l_{11} + l_{22} - \bar{u}_3/F(\bar{c}_1 - \bar{c}_2) + F\bar{u}_3X$$

$$\bar{k} = F^2(l_{11} + l_{22}) - F\bar{u}_3X + F\bar{u}_3X$$

$$\bar{k} = F^2(l_{11} + l_{22})$$

Comparison/

Comparison with the rigorous non-equilibrium thermodynamic equation for the specific conductivity of the exchanger, shows that the Nernst-Planck treatment neglects the term in l_{12}. The error so introduced is negligible in dilute solutions where l_{12} is very small, and even in concentrated solutions, the contribution of l_{12} is small as may be seen by use of the equations derived by Miller for ternary mixtures [30]. Even in binary mixtures at high concentrations, l_{12} is only some 10% of $(l_{11} + l_{22})$ and so this term does not significantly affect the results.

Thus, in highly permselective exchangers where the concentration of the co-ion is small, the term l_{12} will also usually be small and the Nernst-Planck equation may be used to obtain a good estimate of the specific conductivity and ionic transport numbers in the exchanger.

2.2.4. Tortuosity.

In considering the diffusion of mobile species in ion-exchangers, Meares has calculated an expression which corrects the diffusion coefficients of the species for the effect of obstruction of the diffusion paths by the exchanger matrix.[31] This calculation gives θ, the ratio of the true diffusion path length in the exchanger to the geometric thickness of the resin, as

$$\theta = (2-v_w) / v_w \qquad (2.87)$$

where v_w is the fractional pore volume in the exchanger. Meares then suggests that this correction should also be applied to the force producing the diffusion of the species and hence arrives at the expression,

$$D_{corr} = D_{meas}.\theta^2 \qquad (2.88)$$

where D_{corr} and D_{meas} are the corrected and measured diffusion coefficients respectively.

When applied to the diffusion of counter- and co-ions and water in Zeocarb 315, PSA membranes, this relation gives values of D_{corr} which agree fairly well with the corresponding values of the diffusion coefficients of these ions in aqueous solutions of the same concentration. However, many other authors have found that, in/

in a number of other membranes, the agreement is far from satisfactory. [32] [33] [34] It would appear, therefore, that the nature of the membrane contributes to the effect of tortuosity on the diffusion coefficients in a manner which is not wholly accounted for by the relation (2.88). The values of θ for the Zeocarb 315 membranes are very low (approx. 1.5-2.0) whereas in many of the other systems studied the values of θ have been much larger, and the use of equation (2.88) for these systems has produced values of D_{corr} which are much larger than the corresponding solution values. This suggests that the expression (2.88) is overcorrecting the experimental data.

Consider a membrane as shown in figure 2.1 . Then making the same assumptions as Meares [31] regarding the structure, i.e. assuming the exchange sites lie at the corners of a cubic lattice, then the ratio of the true path length to the geometric thickness is as before,

$$\theta = (2-v_w) / v_w$$

If the true diffusion path is represented by the route abcde...z, then, when an ion situated at f, say, moves to position/

position g, the condition of electroneutrality requires that another ion must move to fill the vacant position f. Because of this coupling of the movement of the ions, the flow along the section ef must, on average, equal that along the section fg, and the force experienced by an ion is the same no matter the direction of the next step. There is, therefore, no need to resolve the force along the direction of motion as has been done in Meares' approach. The correction to the diffusion coefficient becomes simply θ, and the relation between the corrected and measured diffusion coefficients is

$$D_{corr} = D_{meas}.\theta \qquad (2.89)$$

It is this expression which has been used to give the corrected ionic tracer diffusion coefficients in the C60N and C60E membranes used in this study.

2.3. Experimental

2.3.1. Preparation of Solutions.

With the exception of those used for the conductivity measurements, all the solutions used throughout this work were prepared from AnalaR sodium chloride which had been dried at 120°C for several days and stored in a desiccator over phosphorus pentoxide. The solutions were made up in Grade A volumetric flasks at 25°C using distilled water. For the conductivity measurements, the solutions were prepared from AnalaR sodium chloride which had been twice recrystallised from a water/ethanol mixture [35].

Radioactive isotopes, Na^{22} and Cl^{36}, were obtained from the Radiochemical Centre, Amersham, as aqueous solutions of sodium chloride. These solutions were made up to the appropriate concentrations in graduated flasks using AnalaR sodium chloride and distilled water.

2.3.2. Counting Methods.

All radioactivity measurements were made using a Packard Tricarb Liquid Scintillation Spectrometer, model 3003,/

3003, fitted with an automatic sample changer and print out device, model 527. The phosphor used was dioxan based and was suitable for aqueous samples [36]. Small samples, usually 0.08 ml. but occasionally 0.45 ml., of the aqueous sodium chloride solutions were added to 10 ml. of the phosphor solution contained in special low-potassium content glass vials. When solutions of concentration higher than 0.5M were used, precipitation of the sodium chloride occurred. Samples counted with a precipitate showed that, owing to variations in the distribution of the precipitate on the bottom of the vial, the error in the count was increased by a factor of 2-3. In all cases in which precipitation occurred, therefore, a small volume of water, usually 1 ml., was added to each vial to dissolve the precipitate and restore 4π counting geometry. It was found that this volume of water did not have any significant quenching effect.

The background count of each vial was determined before the samples were added and any vials with high counts due to adsorption of radioactive isotopes from previous samples, were rejected. The average background count was approx. 25 cpm.

The conditions of the experiments were so arranged that/

that no activities of less than 100 cpm above background were measured. Samples were counted for at least 20 minutes, during which time sufficient counts were recorded to give a statistical error of 2% on the lower counts and 1% on the higher ones. The efficiency of counting, as, measured by counting a standard radioactive solution, was greater than 90%.

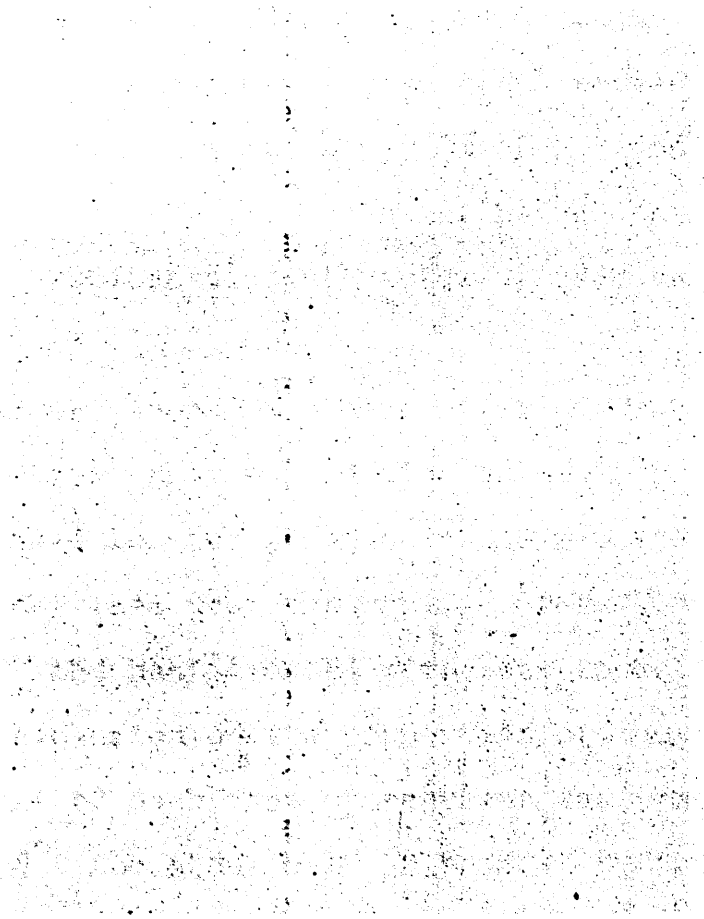

2.3.3. Ion-Exchange Membranes.

The membranes used in this work were the AMF C60 and C100 polyethylene/polystyrene sulphonic acid cation exchangers, manufactured by the American Machine and Foundry Company. The C60 membranes were made from low density polythylene containing 35% of styrene and up to 2% divinyl benzene. 40% of the styrene was grafted using free radical initiators, the rest polymerised in the bulk of the polyethylene. Oleum was used as the sulphonating agent. The C100 membranes were manufactured from high density polythylene containing 23% of styrene and no divinyl benzene, the cross-linking being done by Co^{60} radiation. Chlorosulphonic acid was used as the sulphonating agent.

Arnold and Koch (104) have reported that C60 membranes undergo an irreversible expansion on heating. Therefore, it was decided to study, not only the C60 and C100 membranes as obtained from the manufacturers, but to include samples of the heat treated membranes to determine the effect of expansion on the properties of the exchanger.

A sheet of each type of membrane was immersed in water at 95°C for about half an hour. During this treatment the C60 membrane became slightly opaque and expanded/

expanded both in thickness and length. Close examination with a microscope failed to reveal any visible damage to the membrane. The C100 membrane, on the other hand showed considerable damage. Large regions of damage were visible on the surface. These regions can best be described as blisters. They were fairly wide-spread, and were considered to be unsuitable for further investigation. There were however, some areas where expansion had occurred without the attendant blistering. These areas were selected for further study.

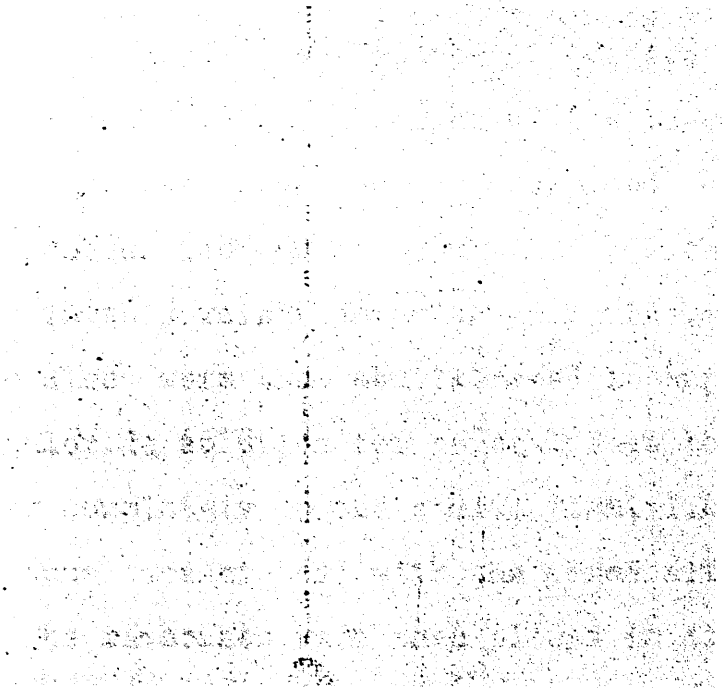

2.3.4. Conditioning Process.

The sheets of ion-exchange membranes were cut into circular discs approx. 3.8 centimeters in diameter using a machined brass dye. These discs were treated in turn with methanol, 1M hydrochloric acid, distilled water, 1M sodium hydroxide and distilled water again, each treatment lasting several hours. This cycle of treatments was repeated a number of times. Any monomer or other organic solvent soluble materials remaining in the membranes were dissolved out by the methanol, while the hydrochloric acid and sodium hydroxide removed any acid or base soluble impurities, e.g. iron or other heavy metal ions, accummulated in the course of preparation.

After each cycle the weight of the leached sodium form membrane was determined as described below. The cycling process was continued until no further changes occurred in this weight after several treatments.

The discs were then equilibrated in approx. 1M sodium chloride solution for several days to ensure that they were completely in the sodium form, i.e. that all the counter-ions 'associated' with the fixed sites were sodium ions. The membranes were then placed in distilled water for/

for several days to leach out any sorbed electrolyte.

During the succeeding experiments, the membranes were required in equilibrium with a number of sodium chloride solutions of different concentration. It was found that several days were required for the completion of the equilibration process. In all cases the equilibration time was at least three days, and frequently one week. During this time the equilibrating solutions were frequently changed.

2.3.5. Dry Weights.

Each leached membrane, in the sodium form, was placed in a petri dish in a desiccator over phosphorus pentoxide and the desiccator evacuated using a water pump. The desiccator was then sealed and placed in an oven at $40^{\circ}C$ for several days. The membranes were then removed and weighed to determine their dry weights. This process was repeated several times until constant weight was obtained. At no time in the course of subsequent experiments was any of the membranes allowed to dry out again.

2.3.6./

2.3.6. Wet Weights.

The following method, referred to as a kinetic method of weighing, was used to determine the wet weights of each membrane after equilibration with water or sodium chloride solutions.

The membrane was removed from the solution with which it had been equilibrated and its surface quickly blotted dry between two hardened filter papers. At the instant when all the moisture had been removed from the surface, a stop-clock was started. The membrane was then carefully examined to see if any traces of solution remained on its surface. If any moisture was observed on the surface, the membrane was replaced in the equilibrating solution and the process restarted. If there was no moisture on the surface the membrane was placed on a small wire rack suspended from a balance pan. The weight of the rack was already known. The rack plus membrane were then weighed, the weight being noted every fifteen seconds for the next minute and a half. The total time taken for this procedure was about two minutes. The weights were plotted against time and extrapolated back to zero time to determine the true wet weight of the membrane. The weight loss was about 0.001 gm. every 15 seconds.

This/

This procedure was carried out about ten times per membrane per equilibrating solution. The average of these determinations was taken as the wet weight of the membrane in that solution. The weights were reproducible to ±0.0003 gm.

This process was carried out for each membrane at each of the required sodium chloride concentrations. The complete process was then repeated to determine if any weight changes had occurred during this cycle. No such changes were observed.

Each membrane disc was then examined under a light microscope to ensure that the membranes chosen for further study had no visible inhomogeneities or surface damage which might invalidate the results of succeeding experiments.

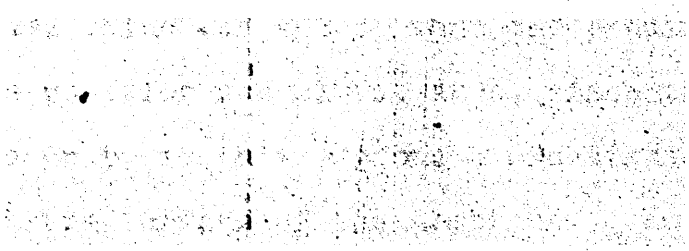

2.3.7. Physical dimensions.

Diameter

The membrane was removed from its equilibrating solution and placed, still wet, between two thin glass plates. The membrane was positioned over a fixed sheet of graph paper in such a way that its diameter could be determined by use of a travelling microscope. The average of eight such determinations was taken as the diameter. The error on the measurement was ± 0.03 cm.

Thickness.

The apparatus used was a Mitronic guage and is shown in figure 2.2. A small volume of solution was placed in the membrane container and the membrane placed in position so that it was completely immersed in the solution. The membrane was slipped below the tip of the measuring device which had previously been adjusted to read a predetermined value. The new reading was taken and the membrane thickness obtained by difference. The predetermined value was set so that the reading with the membrane in position was almost zero, since the instrument was most accurate in this region. Readings were taken over the entire surface of the membrane. No deviation

from/

from the average thickness, of greater than the experimental error was observed. The error on the measurements was ± 0.0003 cm.

An attempt was also made to determine the membrane thickness using a micrometer screw gauge. Here the membrane was clamped between two thin flat glass plates and the thickness measured. The membrane was removed and the new thickness measured. The membrane thickness was then easily calculated. This method was, however, less accurate than the first owing to slight deviations in the thickness of the plates.

2.3.8. Ion-Exchange Capacity Determinations.

The scientific capacity of each membrane was determined by an isotopic dilution method. The membrane in the leached sodium form was surface dried and placed in a known volume of 0.005M sodium chloride solution containing Na^{22}, the specific activity of this solution also being known. The membrane was allowed to equilibrate overnight in order that an equilibrium distribution of the Na^{22} should occur. Samples were then removed from the solution and their specific activities determined.

From/

From these results it was possible to calculate the capacity of the membrane as shown in Appendix A.5. Three such determinations were carried out for each membrane, the reproducibility being about ± 1.5%.

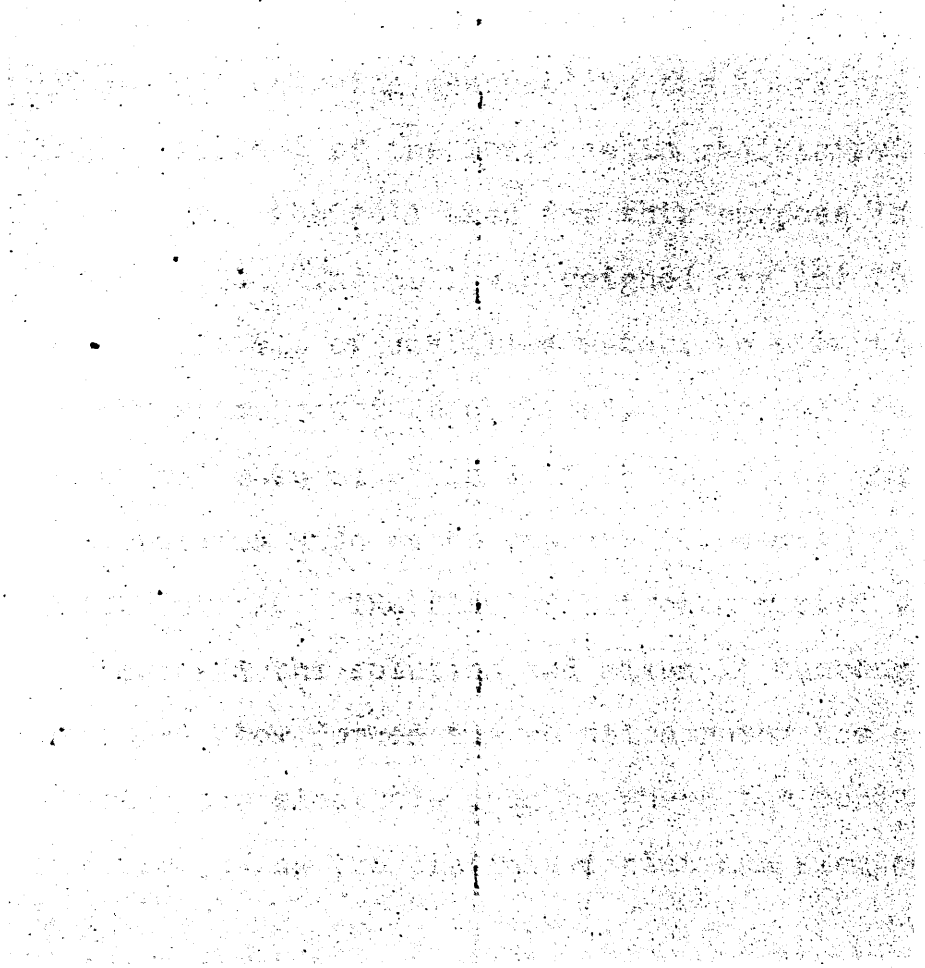

2.3.9. Electrolyte Uptake.

Two methods of determining the electrolyte uptake were tried. (i) Leaching out the sorbed salt and measuring the conductivity of the resultant solution. (ii) Leaching out the sorbed electrolyte and titrating with silver nitrate.

(i) Conductivity method.

The principle of this method was similar to that of the method described by Glueckauf and Watts,[38] the rate of desorption being measured by the increase in conductivity instead of the increase in radioactivity in the solution. The cell used for this purpose is shown in figure 2.3. The cell was weighed dry and then containing approx. 80 ml. of distilled water, so that the volume of the water could be obtained. The cell was then placed in an oil bath maintained at 25± 0.005°C, and nitrogen, presaturated with water vapour, allowed to flow in through inlet tube A. The flow of nitrogen served two purposes; it degassed the solution and mixed it thoroughly. The nitrogen flow forced the solution round the circuit through the electrode chamber where the conductivity was measured using two platinised platinum electrodes connected to/

to a Wayne Kerr B331 conductivity bridge. The nitrogen flow was continued until the conductivity of the water had reached a steady value. The membrane was then removed from the equilibrating solution, its surface carefully dried with filter paper, and placed on the glass rack above the water level in the cell. Since the execution of this step required the cap of the cell to be removed, with a resultant inflow of air, the conductivity of the water increased. The cap was replaced and the membrane allowed to remain suspended above the water level while degassing of the water continued. The nitrogen atmosphere of the upper cell was saturated with water vapour so that the membrane did not loose water by evaporation. When the conductivity of the water reached its previous steady value the membrane was quickly lowered into the water and a stop-clock started. Conductivity measurements were taken at half minute or minute intervals for ten to fifteen minutes and at longer intervals for several hours.

A conductivity - sodium chloride concentration curve had previously been determined by making additions of a standard sodium chloride solution to the cell from a weight burette, and measuring the conductivity. It was, therefore, possible to relate the conductivity measured in the electrolyte desorption experiment to the concentration/

concentration of sodium chloride in the solution.

Unfortunately, this method proved unsatisfactory. Instead of reaching a steady value after a few hours, the conductivity of the desorption solution continued to increase indefinitely. Various attempts were made to explain this phenomenon and these are discussed in the discussion sections.

(ii) Titration method.

This method was based on the fact that even very dilute solutions of sodium chloride, i.e. 10^{-4}M, can be titrated accurately by a potentiometric method.

The method of carrying out these titrations is as follows. The solution to be titrated was placed in a small beaker containing a small magnetic stirrer and a silver electrode.

The beaker was covered with parafilm, to prevent evaporation, and placed in a small water bath on top of a magnetic stirring block. All the experiments were carried out with the water bath at $25 \pm 0.1^{\circ}C$. The silver nitrate used for the titration was placed in a 10 ml. calibrated burette which could be read accurately to 0.02 ml. Into the nozzle of the burette was sealed a silver/

silver electrode and the tip of the nozzle was drawn out to a fine point. The tip of the burette was immersed in the solution which was to be titrated so that the solution in the nozzle acted as a liquid junction. The finely drawn out tip served to minimise diffusion of the silver nitrate solution into the beaker while e.m.f. measurements were being taken. The two electrodes were connected through a Solartron digital voltmeter, model LM 1867, capable of measuring to 0.01 mV. The ionic strength of the titrant and the electrolyte desorption solution was approx. 0.1, sodium nitrate being used as the supporting electrolyte. This helped to minimise the liquid junction potential.

Titrations were carried out with standard sodium chloride solutions and even at 10^{-4}M the error was only 2-3%. The electrolyte desorption solutions usually had sodium chloride concentrations much greater than 10^{-4}M.

The membrane was removed from the equilibrating solution, its surface thoroughly dried with filter paper, and placed in a small beaker to which were added 5 ml. of 0.1M sodium nitrate solution. The top of the beaker was covered with parafilm and the membrane allowed to

equilibrate/

equilibrate for several hours. The membrane was then removed from this solution, its surface washed with 2ml. of sodium nitrate solution, the washings being collected in the beaker in which the equilibration had been carried out, and the membrane placed in a second beaker with 2 ml. of sodium nitrate solution and again left to equilibrate for several hours. The membrane was then removed from this solution and equilibrated with the next sodium chloride solution. The 7 ml. and 2 ml. portions of solution now containing the leached sodium chloride were titrated potentiometrically as described above.

Besides reducing the liquid junction potential in the titration, the sodium nitrate served a purpose in the leaching process. After leaching, the membrane was in equilibrium with a solution in which the nitrate concentration was many times greater than the chloride concentration. Electrolyte uptake from this solution was, therefore, mainly sodium nitrate. This was reflected in the fact that greater than 95% and frequently as high as 99% of the sodium chloride leached out of the membrane was to be found in the first beaker. At no time were more than two equilibrations required to remove all the sodium chloride from the membrane.

The/

The concentration of the solution was calculated from the e.m.f. data using a linear titration plot method.[39] The error on the determination was about 1% for the membranes equilibrated in 0.5M, 1.0M, and 2.0M sodium chloride solutions. For the equilibration with 0.1M sodium chloride solution, the error was approx. 3%.

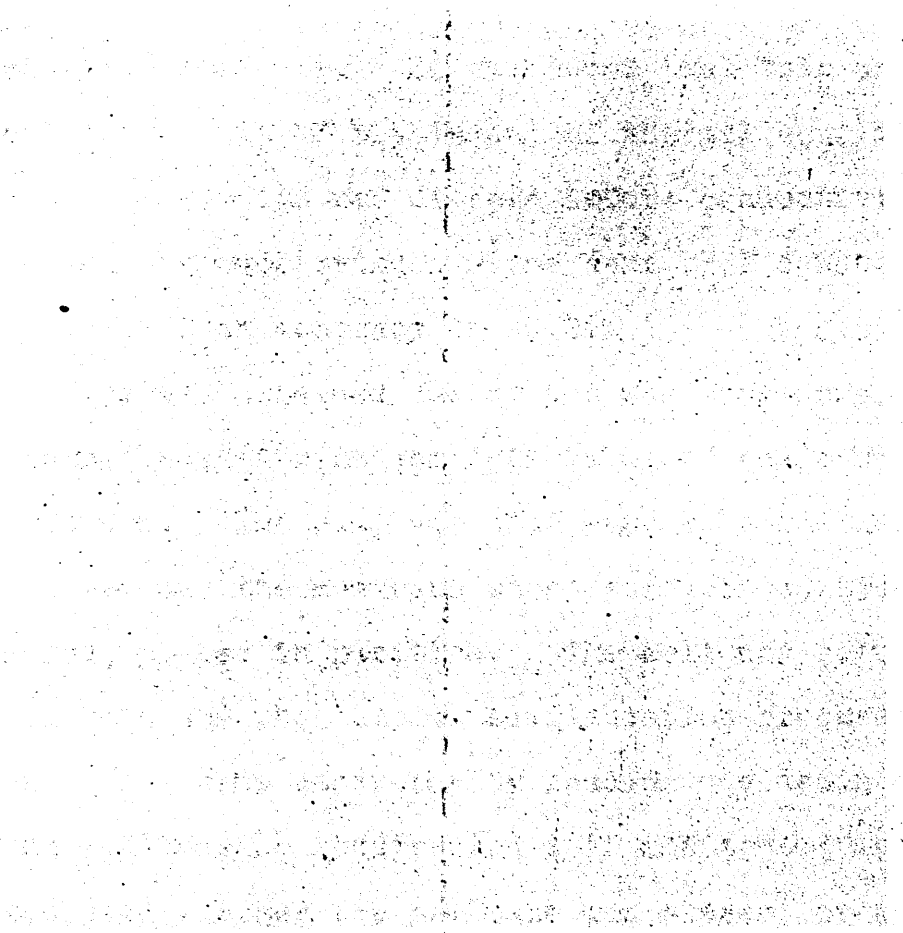

2.3.10. Membrane conductivity.

Membrane conductivities were measured using a high precision conductivity cell described in the U.S. Manual for Testing Permselective Membranes [40], and shown in figure 2.4. The cell was filled with the appropriate solution, placed in a polythene bag, and positioned in an oil bath whose temperature was maintained at 25±0.005°C. Solution stored in a reservoir which was also in the oil bath, was then forced through the cell under a pressure of compressed air. It was found that this process accelerated the rate of attainment of thermal equilibrium. The flow of solution was stopped before conductivity measurements were made using a Wayne Kerr B331 conductivity bridge capable of an accuracy of ±0.01% [58]. When a steady reading was obtained the system was considered to be at thermal equilibrium and this value of the conductivity recorded. The cell was then removed from the bath, dismantled and the membrane whose surface had been thoroughly dried, placed in position. The cell was returned to the oil bath and the thermal equilibration process repeated until a steady conductivity reading was again obtained. The cell was so constructed that the same volume of solution was used whether the membrane was present or not. Thus from the two values of the conductivity recorded as above,

it was possible to calculate the resistance of the solution and of the solution plus membrane. The resistance, and hence the conductivity, of the membrane was then easily calculated. The measured value of the membrane resistance was corrected for edge effects using the equation derived by Barrer [41]. This equation is given in Appendix A.6. In the measurements described above the radius of the membrane was many times that of the area exposed in the conductivity cell. The edge effect correction was therefore, fairly large, being about 4% of the measured value. The membrane conductivities recorded in the results section were the averages of 8-10 values obtained for each membrane in each solution. The reproducibility of the values was ±1%.

In this method the resistance of the membrane was obtained indirectly, but it has several advantages over the other direct methods described in the literature. [42] [43] [44] These direct methods involve clamping an electrode to the surface of the membrane and hence include the difficulty of circumventing the effect of interfacial resistances. Although this problem has been alleviated by measuring the resistance at various points along the membrane length and calculating the true resistance by difference/

difference, the indirect method described here requires no such modifications. The direct methods also measure the resistance of the membrane strip along its length whereas most other transport measurements are made in the direction normal to the membrane surface. If the membrane is anisotropic then the results obtained by the direct method may be in error if they are used in conjunction with other properties which have been measured along different directions.

In many of the cells used to determine membrane resistances, there is the problem of the membrane drying out during the measurement, or of conduction along a liquid film on the membrane surface if the membrane is immersed in a shallow bed of solution. The indirect method used here does not suffer from any of these problems. However, there is one limitation on the use of this method. In dilute solutions, the conductivity of the membrane is much greater than that of the solution, and hence the difference in resistance between the two measurements is small. To overcome this problem a very small area of the membrane was used so that its resistance was of the same order as that of the solution. In the cell used here, the area of/

of exposed membrane was approx, 0.1 cm^2., and even using this area, the lower limit of accurate resistance measurement was 0.1M. The disadvantage of using such a small area is one of reproducibility. Gregor, Kramer, Lalik, Holmstom and Saber [45] have found differences of 300% in the resistances of pieces of membrane cut from the same sheet. Therefore, a number of samples of membrane were examined and one disc of C60N and one of C60E were cut up into smaller areas and their resistances determined. The results of these measurements were all within 1% of the mean. The small area of membrane was therefore taken as representative of the entire disc.

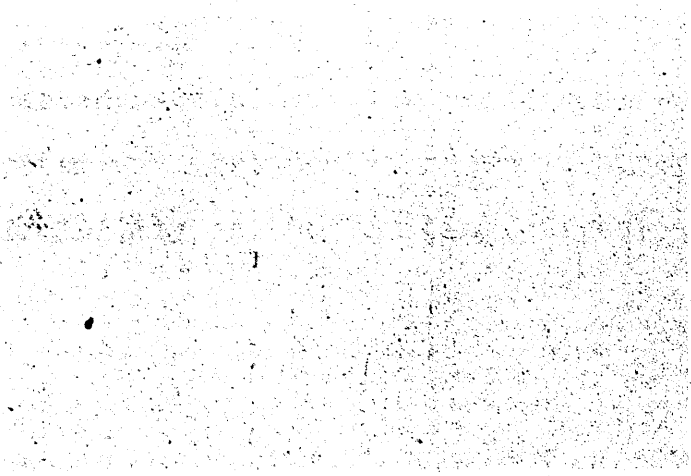

2.3.11. Calibration of diffusion cell.

The cell was set up as shown in figure 2.5, except that the membrane was replaced by a sheet of silver foil and the solution was 0.0005M silver nitrate in 1.0M sodium nitrate. In the experiment the silver foil acted as the cathode in the circuit and a piece of silver wire placed in one of the sample portals was the anode. Current was supplied from a variable voltage supply, the rate of voltage change being kept constant. The current flowing in the system was monitored by measuring the potential difference across a standard 20 ohm resistor in the circuit, using a Servoscribe (Goerz electro potentiometer screiber RES11) chart recorder. Curves similar to the one shown in figure 2.6, were obtained. The experiment was repeated several times for each of a number of stirring speeds in the range 250 to 550 rpm., and from the values of the limiting currents obtained, the mass transfer coefficient for the system was obtained as shown in appendix A.7. The reproducibility of the limiting current was ± 2-3%.

2.3.12. Tracer Diffusion Coefficients.

The most accurate method of determining individual ionic diffusion coefficients in ion exchange membranes is to use steady state radio-isotope diffusion across the membrane between two solutions of identical chemical composition, but to one of which has been added a quantity of isotopic tracer of the ion under study. There is an initial time lag while a steady state or quasi-steady state, is set up in the membrane. Thereafter, the flux of tracer through the membrane is constant so long as the difference between the tracer concentrations in the two bathing solutions is not allowed to diminish significantly. In the steady state, the tracer concentration in the initially inactive solution increases linearly with time and from this increase, the tracer diffusion coefficient may be calculated as follows [47]

The steady state isotopic flux is given by

$$J = \frac{\bar{c}'\bar{D}}{d} \qquad (2.90)$$

where J is the isotopic flux in moles $cm^{-2}sec^{-1}$,

$\bar{c}'$ is the concentration of tracer in the membrane on the high activity side,

$\bar{D}$ is/

$\bar{D}$ is the tracer diffusion coefficient in the membrane and d is the membrane thickness.

The indices ' and " refer to the high and low activity sides resp.

For mass balance in the system,

$$qJ = V''.dC''/dt. \qquad (2.91)$$

where q is the area of the membrane through which diffusion occurs and V" is the volume of solution on the initially inactive side.

Since a steady state has been attained, each side of the membrane is in equilibrium with the adjacent solution, provided that there is no interfacial resistance. Therefore,

$$\frac{\bar{c}'}{\bar{c}} = \frac{c'}{c} \quad \text{and} \quad \frac{\bar{c}''}{\bar{c}} = \frac{c''}{c} \qquad (2.92)$$

Substituting for J from equation (2.90) and $\bar{c}$ from equation (2.92) into equation (2.91) gives, on rearranging,

$$\bar{D} = \frac{dc''/dt.V''.c.d.}{c'.\bar{c}.q} \qquad (2.93)$$

This equation is valid provided c', the tracer concentration in the active solution, remains virtually unchanged throughout the duration of the experiment. This is the situation in most diffusion experiments where the concentration of tracer in the initially inactive side is/

is monitored until only some 1-2% of the total activity has passed through the membrane. If, however, c' is allowed to change significantly during the experiment, then equation (2.93) may be modified and the tracer diffusion coefficient given by [48],

$$\bar{D} = d(c''/c')/dt. \frac{V''.c.d}{\bar{c}.a} \qquad (2.93a)$$

The above derivation implies steady state conditions and ideal membrane diffusion control. However, at the membrane-solution interfaces, there will be a region of liquid which will remain unstirred no matter how efficient is the stirring in the bulk solution. This liquid film has a very important influence on the nature of the diffusion characteristics of the system. If the diffusion rate in the film is lower than that in the membrane then the diffusion through this film will very quickly become the rate determining step of the complete diffusion process. If, however, the rate of diffusion in the membrane is the slow step then this process becomes rate determining. The exact nature of the dependence of the diffusion characteristics on the other properties of the system can be determined as shown below.

In the tracer diffusion experiment, the system is in overall/

overall equilibrium and there are, therefore no bulk gradients of activity coefficients, of electric potential and of pressure and no convection occurs. Therefore, applying Fick's First law for the species i, the flux becomes [49]:

$$J_i = -D_i dc_i/dx \qquad (2.94)$$

This relation holds both in the membrane and in the unstirred liquid films adjacent to the membrane surface. Furthermore, the flux of species i in the membrane and in the films must be equal. Therefore, examination of figure 2.7 shows that the flux of species i is given by:

$$J_i = D_i \frac{c_i - c_{i'}}{\delta} = \bar{D}_i \frac{\bar{c}_{i'} - \bar{c}_{i''}}{d} = D_i \frac{c_{i''}}{\delta} \qquad (2.95)$$

where D_i is the diffusion coefficient of the species i, c_i is its concentration, d and δ are the membrane and film thicknesses resp. The barred species refer to the membrane phase and the indices ' and " refer to the high and low activity sides resp.

Also, under the equilibrium conditions existing at both solution-membrane interfaces,

$$\frac{c_{i'}}{c} = \frac{\bar{c}_{i'}}{\bar{c}} \quad \text{and} \quad \frac{c''_i}{c} = \frac{\bar{c}''_i}{\bar{c}} \qquad (2.96)$$

where/.

where c is the total bulk concentration of the species of which i represents the tracer isotope.

From equations (2.94) (2.95) and (2.96), the tracer flux is given by,

$$J = - \frac{\bar{D}_i \bar{c}_i}{d\left(1 + \frac{2\bar{D}_i \bar{c}_i \delta}{D_i c_i d}\right)} \qquad (2.97)$$

The criterion for determining whether the diffusion processes will be membrane or film diffusion controlled can be readily obtained from equation (2.97). (50)

If $\frac{D_i c_i d}{\bar{D}_i \bar{c}_i \delta} \gg 2$ then $J_i = \frac{\bar{D}_i \bar{c}_i}{d}$ and the process is membrane diffusion controlled. Similarly, for film diffusion control the relation $\frac{D_i c_i d}{\bar{D}_i \bar{c}_i \delta} \ll 2$ must hold.

The nature of the diffusion process is therefore governed by the dimensionless factor $D_i c_i d \,/\, \bar{D}_i \bar{c}_i \delta$. By substitution of typical values into this quotient it is possible to show (50) that for co-ions, film diffusion control can only operate under extremely unfavourable conditions, whereas for counter-ions, film diffusion control may be quite common. For a given system, the only variable in the quotient $D_i c_i d \,/\, \bar{D}_i \bar{c}_i \delta$ is the film thickness, δ. It is, therefore, important to keep the/

the film thickness as small as possible in order to obtain membrane diffusion control. This is done by efficient stirring as close to the membrane surface as possible. In practice, counter-ion diffusion usually has some measure of film diffusion control and corrections must be applied to the observed values in order to obtain the true membrane diffusion coefficients. A number of attempts have been made to calculate this correction. [51] [52] [53] There have also been a number of attempts to calculate the film thickness, δ, all of which give values of the order of 10 - 100 microns depending on the stirring speed or efficiency of mixing. [51] [54] [55] [56] In this present study the correction used is that given by Scatter-good and Lightfoot, [57] and the theoretical basis of this treatment is to be found in Appendix A.7.

Tracer diffusion was measured in a cell similar to one described by Meares [7], and is shown in figure 2.5. Small magnets were sealed into the rear paddles of the teflon stirrers and these were driven by master magnets connected to a train of gear wheels powered by an electric motor./

motor. The motor was connected to the power supply through a voltage stabiliser to ensure that the speed of rotation of the stirrers would not be affected by voltage fluctuations, and would remain constant throughout the experiment. The stirrer speed was measured directly using a stroboscope, (Dawe 1200E). The volume of each half of the cell was approx. 60 ml.

The membrane was removed from the solution, its surface dried, and placed between two perspex discs. These discs could be so positioned that exactly the same area of membrane was exposed on either side. The disc and membrane were then mounted in the cell, which was then filled with the appropriate solution from two burettes in such a way that both sides were filled simultaneously, so preventing bulging of the membrane. The complete assembly process was carried out as rapidly as possible to prevent the membrane drying out. This would have contributed to buckling when it reswelled. A thin layer of paraffin wax was then put round the outside of the seal to prevent any leak of water from the water tank into the cell. The cell was immersed in a water bath at $25 \pm 0.1^{\circ}C$ so that only the sample portals remained

above/

above the surface, and left to equilibrate for at least half an hour. A known volume of solution was then removed from one side of the cell and replaced by an equal volume of solution of the same concentration containing radioactive tracer ions, Na^{22} or Cl^{36} as required by the nature of the experiment. The stirrers were switched on, a few seconds allowed for mixing then a stop-clock was started, and samples were withdrawn from the initially inactive side at noted times. This procedure was continued until approx. 2% of the added radioactive isotope had passed through the membrane. The time required for a counter-ion diffusion experiment was 1-2 hours, whereas a co-ion experiment required up to 12 hours. Samples were also taken from the active side near the start and end of the experiment. The samples were withdrawn using Hamilton microlitre syringes which were fitted with Chaney adapters to ensure that the same volume of solution was removed in each sample. The volume of the samples was approx. 0.08 ml. and was reproducible to 0.1%. The radioactive samples were counted as described in section 2.3.2. The activity on the receiving side was corrected for the volume of the samples removed, (see Appendix A.8).

A/

A plot of activity against time gave a straight line whose gradient was used in calculating the diffusion coefficient. The error in the gradient was never greater than 1.5%. In calculating the diffusion coefficient, a correction was applied for film diffusion effects as described in Appendix A.7. (57)

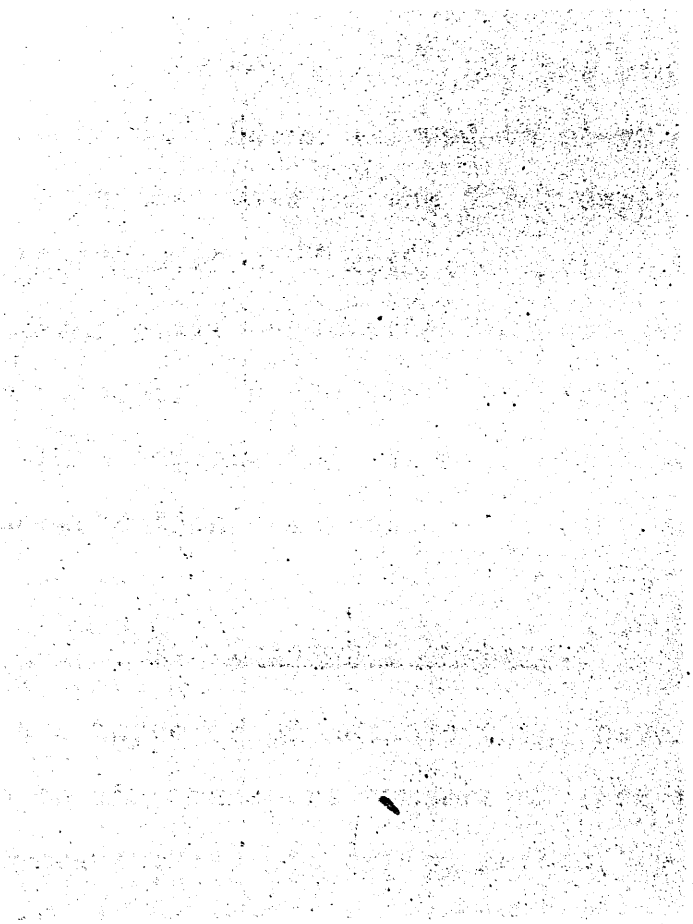

2.3.13. Diffusion with a Concentration Gradient - Salt Diffusion.

The method was similar to that used for tracer diffusion. The membrane was equilibrated for three days between two solutions of the same concentration as those to be used in the salt diffusion experiment, during which time the solutions were frequently renewed. A diffusion experiment was then carried out, the co-ion, chloride, being labelled with Cl^{36}. The membrane was then re-equilibrated to remove any sorbed Cl^{36} and the process repeated, the diffusion of Cl^{36} being allowed to occur in the direction opposite to that used in the first experiment. Therefore, the flow of Cl^{36} with and against the concentration gradient could be obtained and the net flow of chloride calculated. Since electroneutrality must be maintained, this represented the flow of sodium chloride with the concentration gradient.

2.3.14. Transport Numbers.

There are three chief methods which have been employed to obtain transport numbers of ions in ion-exchange membranes: (a) Hittorf's method, (b) modified Hittorf's method and (c) membrane potential method. In the/

the following sections the advantages and disadvantages of each method will be discussed.

(a) Most transport number measurements have been made using the Hittorf method. (59) (60) (61) (62) (63) (64) (65) (66) (67) (68). In this type of experiment, the same electrolyte solution is placed on either side of the membrane and an electric current passed through the system for a given time, using either reversible Ag/AgCl electrodes or irreversible platinum electrodes. During the experiment, concentration changes of 10-15% in the cell solutions are common. While these changes do not appear to affect the transport number significantly in dilute solutions, (69) where the co-ion uptake is small, Kressman and Tye (70) and Lewis and Tye (71) showed that at higher concentrations the transport number could be dependent on the concentration of either the donating or the receiving sides, both of which were changing during the experiment. A further disadvantage of this method is the dependence of the transport numbers on the current density used. (72) (73) (74) With dilute solutions, the effect is one of polarisation (75) while in concentrated solutions the dependence on current density has been attributed to/

to the effect of back diffusion caused by the concentration gradient produced during the experiment. [72] [73] [74] [76], Although a number of experimental methods have been devised to overcome these problems, the availability of radio-isotopic tracers has led to improved methods of transport number determination.

(b) The use of radioactive tracers means that the transport number may be obtained from the net flow of tracer ion added to one side of the transport number cell. Since small concentrations of tracer can easily be detected radiochemically, this removes the need to produce large changes in the concentrations of the bathing solutions during the experiment. There is, however, a need to determine the tracer flow with and against the electric potential gradient, in order to obtain the net flow of isotope due solely to the electric current. Recently Meares [77] has shown how the transport number may be obtained from flow with or against the electric potential gradient and the self diffusion flow.

Using the net flow of isotope, the net flow of the traced ion can be obtained and the transport number calculated from the equation,

$$t_i = z_i F J_i / I \qquad (2.13a)$$

where/

where z_i is the electrochemical valence of species i, J_i its net flow and I is the current density. F is Faraday's constant.

The transport number may also be calculated from the ratio of the fluxes with and against the current using the following equation, (24) (78)

$$\ln(J_i/J_{i'}) = \frac{t_i I d}{z_i F \bar{c}_i \bar{D}_{ii}} \qquad (2.98)$$

where J_i and $J_{i'}$ are the fluxes with and against the current, $\bar{c}_i$ is the concentration of species i in the membrane, $\bar{D}_{ii}$ is its membrane self diffusion coefficient and d is the membrane thickness.

(c) Membrane potentials in concentration cells containing an ion-exchange membrane, have been used as another method of calculting the average transport number of the exchanger. If electrodes reversible to the anion are used then the e.m.f. of the cell is given by the expression (67) (79) (76)

$$E = 2\bar{t}_+^a \frac{RT}{F} \ln\left(\frac{a'}{a''}\right) \qquad (2.99)$$

where $\bar{t}_+^a$ is the apparent transport number which has been derived ignoring the effect of water transference. In dilute solutions this equation gives a good estimate of the true transport number. The true value for any concentration/

concentration may be calculated from the membrane potential if the water transference at that concentration number is known, by use of the equation, [64] given in section (2.2.2b)

$$E = -2\bar{t}_{+}\frac{RT}{F}\ln\frac{a_{\pm}'}{a_{\pm}''} - \bar{t}_{3}\frac{RT}{F}\ln\frac{a_{3}'}{a''_{3}} \qquad (2.68)$$

The value derived from this equation is an average value since the concentration of the solution is not the same on both sides of the membrane. If the concentration difference is small, then the transport number calculated in this way should be a good estimate of the value corresponding to the mean of the two concentrations. However, the lower the concentration difference, the smaller the e.m.f. and hence the greater the error in measuring it. Also, the accuracy of the values of activities $a_{\pm}'$ and $a_{\pm}''$ becomes extremely important. Therefore, the best values of $\bar{t}_{+}$ are obtained by a compromise between the accuracy of the e.m.f. measurement and the magnitude of the concentration difference between the two solutions.

Transport numbers were determined by a co-ion flux-ratio method. The cell used was similar to the one used for diffusion, but fitted with circular electrodes situated approx. three centimeters from the membrane, on either side of it, and parallel to it. The electrodes were made of coarse platinum mesh plated with silver and silver chloride.

A/

A fine coating of silver was plated on to the platinum using potassium argentocyanide [80]. A thicker coating was added by electrolysing in 0.1M silver nitrate solution using a silver anode. One of the electrodes was given a fine coating of silver chloride while most of the silver on the other electrode was converted to silver chloride by anodising in 0.1M hydrochloric acid solution using a platinum cathode. During the transport number determination, this last mentioned electrode was made the cathode and released chloride ions into the solution while the other electrode removed chloride from the other side of the cell.

The procedure used to determine the transport number of the ions through the membrane was similar to that used for determining diffusion coefficients. The radioactive solution was added to the anode compartment and the experiment allowed to run until sufficient activity had passed through the membrane to allow an accurate determination of its value. In practice, the time required was usually about one hour, although longer periods were necessary when low current densities were used. 0.45 ml. samples were removed with Hamilton syringes as before. The larger samples were used in order/

order to reduce the duration of the experiment. In order to prevent entraining of air bubbles in the paddles, the samples removed for counting had to be replaced by an equal volume of inactive solution of the same concentration. In calculating the flow of the isotope, a correction was applied for this procedure, and is described in Appendix A.8.

After the prescribed time the direction of the current was reversed and the flow of radioactive isotope again similarly determined. During this period Cl^{36} ions were being removed from the receiving side by the electrode reaction. A correction for this dilution of the tracer concentration was applied as described in Appendix A.9.

The current was supplied from a constant current supply source - Solartron P.S.U. AS.1413. The current flowing was monitored throughout the experiment by measuring the potential drop across a standard resistor, using a digital voltmeter.

After use the cell was thoroughly cleaned and the silver chloride electrodes reconverted to silver electrodes so that all traces of Cl^{36} were removed. The electrodes were then replated before re-use.

The/

The current density was never allowed to exceed 4 mamps per cm^2. in order to avoid polarisation. The membrane properties were such that at this current density the flux ratio was of the order of 1.1-1.2. Therefore, the co-ion transport numbers were obtainable to an accuracy of only ± 10%.

2.3.15 Electro-osmosis and Water Transference Numbers.

These measurements were made in the cell used for transport number measurements. A horizontal calibrated capillary was attached to each side of the cell so that the changes in volume of the solution on either side of the membrane could be determined. (7) The stoppers and cones of the capillaries were lightly greased with apieson to prevent leaks from the cell. The solution used was de-gassed before use by placing it in a flask under reduced pressure and shaking vigorously for a few minutes. In this way most of the dissolved gasses were removed. Care was taken when filling the cell, to ensure that no bubbles collected on the teflon stirrers. The level of the solution in the capillaries was read using a clip-on magnifying glass, and the current was supplied and measured/

measured as in the transport number experiments.

Corrections for the electrode reactions were applied to the volume changes in the usual way [7]. The average of six or more such experiments was used in calculating the electro-osmotic transport, and the water transference number for each external solution concentration. The reproducibility of the measurements was ± 2%.

2.3.16. Water Flow with a Salt Concentration Gradient - Osmosis.

The method used was similar to the determination of electro-osmotic transport, except that instead of applying a potential between solutions of the same concentration, the concentrations on either side of the membrane were different and no electric potential was applied. As in the case of the salt diffusion experiments, the membrane was equilibrated between the appropriate solutions for three days before the osmotic flows were determined. The reproducibility was ± 3%.

2.3.17. E.M.F. of a concentration cell.

The cell was set up in a manner similar to that for the determination of osmotic flow except that the two capillaries were replaced by a matched pair of Ag/AgCl electrodes, one being placed on each side of the membrane. After allowing a period of time for thermal equilibration to be completed, the e.m.f. of the cell was determined using the digital voltmeter described previously. The e.m.f. was monitored over a period of several hours to determine how rapidly it decreased from the true equilibrium value. This rate of decrease was never so large that significant error was introduced by failure to record the value during the period of thermal equilibration. The error on each e.m.f. measurement was approximately ± 1%.

2.4. Results.

Table 2.1

Membrane C60N

Dry weight of leached membrane disc in Na form = 0.2345 gm.
Ion-exchange capacity = 1.57 meqs/gm dry membrane.

Ext soln. concn.	Wet wt.	% water w.r.t. dry wt.	Diameter	Thickness	Volume	c_1	c_2	c_3
(molar)	(gm.)		(cm.)	(cm.)	(cm^3.)		(meqs/cm^3.)	
0.1	0.3579	52.6	3.698	0.0335	0.360	0.980	0.0024	19.03
0.5	0.3449	46.7	3.655	0.0314	0.329	1.104	0.0360	18.48
1.0	0.3320	40.8	3.611	0.0308	0.315	1.209	0.0946	16.86
2.0	0.3176	33.7	3.551	0.0299	0.296	1.419	0.2312	14.89

Table 2.2.

Membrane C60E

Dry weight of leached membrane disc in Na form = 0.2249 gm.
Ion-exchange capacity = 1.70 meqs/gm. dry membrane.

Ext soln. concn. (molar)	Wet wt. (gm.)	% water w.r.t. dry wt.	Diameter (cm.)	Thickness (cm.)	Volume (cm^3.)	c_1	c_2	c_3 (megs/cm^3.)
0.1	0.3998	77.7	3.847	0.0333	0.387	0.960	0.0052	25.07
0.5	0.3807	68.6	3.754	0.0321	0.355	1,112	0.0717	24.11
1.0	0.3629	59.8	3.697	0.0317	0.340	1.270	0.1832	21.94
2.0	0.3470	50.5	3.616	0.0308	0.316	1.621	0.4533	19.95

Table 2.3.

Membrane CLOON.

Dry weight of leached membrane disc in Na form = 0.1348 gm.
Ion-exchange capacity = 1.23 meqs/gm. dry membrane matrix.

Ext soln. concn. (molar)	Wet wt. (gm.)	% water w.r.t. dry wt.	Diameter (cm.)	Thickness (cm.)	Volume ($cm.^3$)	c_1	c_2 ($meqs/cm.^3$)	c_3 ($meqs/cm.^3$)
0.10	0.1640	22.2	3.80	0.0142	0.161	1.005	0.0010	10.05
0.50	0.1619	20.6	3.75	0.0142	0.157	1.04	0.0126	9.55
1.00	0.1609	19.7	3.74	0.0141	0.154	1.09	0.0350	9.30
2.00	0.1589	17.8	3.70	0.0140	0.149	1.19	0.0954	8.66

Table 2.4.

Membrane C100E.

Dry weight of leached membrane disc in Na form = 0.1317 gm.
Ion-exchange capacity = 1.26 meqs/gm. of dry membrane matrix.

Ext soln. concn. (Molar)	Wet wt. (gm.)	% water w.r.t. dry wt.	Diameter (cm.)	Thickness (cm.)	Volume (cm^3.)	c_1	c_2	c_3 ($meqs/cm.^3$)
0.10	0.1659	26.7	3.80	0.0147	0.167	0.966	0.0017	11.38
0.50	0.1635	24.7	3.76	0.0147	0.163	1.005	0.0178	10.77
1.00	0.1619	23.2	3.74	0.0144	0.158	1.062	0.0512	10.43
2.00	0.1587	20.2	3.71	0.0143	0.155	1.172	0.1310	9.22

Table 2.5. Ratio of water contents of normal and expanded membranes.

$\bar{c}_3(N)/\bar{c}_3(E)$

concentration.	C60N	C60E	C100N	C100E
0.1	0.76		0.88	
0.5	0.77		0.89	
1.0	0.77		0.89	
2.0	0.75		0.93	

Table 2.6.

External solution concentration (molar)	D_{Na} $cm^2 sec^{-1} \times 10^6$		$\bar{D}_{Cl}$ $cm^2 sec^{-1} \times 10^6$	
	C60N	C60E	C60N	C60E
0.1	1.76	2.26	3.38	4.62
0.5	1.49	2.11	2.53	3.94
1.0	1.36	2.03	2.09	3.56
2.0	1.03	1.68	1.46	2.59

Table 2.7.

Tortuosity Factor θ.

Ext. solution concentration (molar)	C60N	C60E
0.1	4.81	3.45
0.5	4.99	3.61
1.0	5.60	4.07
2.0	6.46	4.58

Table 2.8a.

Tortuosity scaled diffusion coefficients.

Ext. solution concentration (molar)	C60N			C60E		
	Internal molality	$\bar{D}_{Na}.\theta$ $\times 10^5$ $cm^2 sec^{-1}$	D_{Na} in corr. aq. solution $\times 10^5$ $cm^2 sec^{-1}$	Internal molality	$\bar{D}_{Na}\theta$ $\times 10^5$ $cm^2 sec^{-1}$	$\bar{D}_{Na}$ in corr. aq. sol. $\times 10^5$ $cm^2 sec^{-1}$
0.1	2.87	0.85	1.04	2.13	0.78	1.12
0.5	3.33	0.74	0.99	2.56	0.76	1.08
1.0	4.00	0.76	0.90	3.21	0.83	1.00
2.0	5.31	0.67	0.76	4.50	0.77	0.85

Table 2.8b.

Ext. solution concentration (molar)	C6ON			C6OE		
	Internal molality	$\bar{D}_{Cl^-}$ $\times 10^5$ $cm^2 sec^{-1}$	D_{Cl^-} in corr. aq. sol. $\times 10^5$ $cm^2 sec^{-1}$	Internal molality	$\bar{D}_{Cl^-}$ $\times 10^5$ $cm^2 sec^{-1}$	D_{Cl^-} in corr. aq. sol. $\times 10^5$ $cm^2 sec^{-1}$
0.10	2.87	1.63	1.46	2.13	1.59	1.59
0.50	3.33	1.26	1.37	2.56	1.42	1.52
1.00	4.00	1.17	1.24	3.21	1.45	1.40
2.00	5.31	0.94	1.01	4.50	1.19	1.15

Table 2.9.

D_{Na}/λ^2 using λ calculated from the relation

$$\lambda = 9.4c^{-\frac{1}{3}} \quad (159)$$

ext. soln. concentration (molar)	λ(Å)	λ^2(Å)^2	$\bar{D}_{Na}$ x10^6 cm^{2}sec^{-1}	D/λ^2 sec^{-1} (x10^8)
(a) C60N				
0.10	13.3	174.4	1.76	1.01
0.50	12.6	158.8	1.49	0.94
1.00	11.8	139.8	1.36	0.98
2.00	10.8	114.8	1.03	0.92
(b) C60E				
0.10	14.4	208.0	2.26	1.09
0.50	13.7	178.4	2.11	1.12
1.00	12.7	161.6	2.03	1.26
2.00	11.4	129.6	1.68	1.29

Table 2.10.

Simple prediction of co-ion transport numbers.

Ext. soln. concentration (molar)	$t_2 = \frac{\bar{c}_2 \bar{D}_2}{\sum_i \bar{c}_i \bar{D}_i}$	
	C60N	C60E
0.10	0.0057	0.011
0.50	0.052	0.107
1.00	0.107	0.196
2.00	0.188	0.302

Table 2.11.

Transport with an electric potential gradient.

Ext. soln. concentration (molar)	C60N			C60E		
	t_1	t_2	t_3	t_1	t_2	t_3
0.10	0.998	0.002	10.75	0.995	0.005	15.77
0.50	0.986	0.014	9.04	0.967	0.033	12.24
1.00	0.951	0.049	7.75	0.921	0.079	9.70
2.00	0.916	0.084	5.48	0.892	0.108	6.05

Table 2.12.

Predicted and observed specific conductivity of C60N and C60E.

$\bar{K} \times 10^2$ ($ohm^{-1}cm^{-1}$)

Ext. soln. concentration (molar)	C60N				C60E			
	Predicted			Observed	Predicted			Observed
	1	2	3		1	2	3	
0.10		1.40	1.45	1.37		1.98	2.06	1.92
0.50	1.18	1.24	1.36	1.12	1.71	1.88	2.09	1.70
1.00	0.99	1.27	1.41	1.12	1.81	2.12	2.32	1.90
2.00	0.93	1.15	1.20	1.09	2.03	2.25	2.27	2.21

1. Using u_3 calculated from transport number data: section (2.2.1c(a)).
2. Using u_3 calculated from water transference number data: section (2.2.1c(b)).
3. Using method described in section (2.2.1c(c)).

Table 2.13.

Water mobility.

Ext. soln. concentration (molar)	$\bar{u}_3 \times 10^5$					
	C60N			C60E		
	1	2	3	1	2	3
0.10	-	7.95	7.97	-	12.5	13.0
0.50	5.08	5.68	5.75	7.16	8.95	9.06
1.00	2.81	5.32	5.48	5.73	8.65	8.87
2.00	2.19	4.14	4.33	5.06	6.95	7.27

1. $\bar{u}_3$ calculated from transport number data: section (2.2.1c(a)).
2. $\bar{u}_3$ calculated from electro-osmotic transference data: section (2.2.1c(b)).
3. $\bar{u}_3$ calculated using equation (2.19).

Table 2.14.

Observed specific conductivity of C100N and C100E.

Ext. soln. concentration (molar)	$\bar{K}$ ($ohm^{-1}cm^{-1}$) x 10^3	
	C100N	C100E
0.10	3.84	4.89
0.50	3.55	4.35
1.00	3.31	4.27
2.00	3.05	3.97

Table 2.15.

Predicted and observed e.m.f. of concentration cells.

Ext. soln. concentrations (molar)	observed e.m.f. (mV)		predicted e.m.f.* (mV)	
	C60N	C60E	C60N	C60E
0.05/0.15	50.6	49.7	50.6	48.9
0.5/1.50	45.6	41.8	44.5	41.4

* From equation (2.68).

Table 2.16.

Salt and water flows with a salt concentration gradient.

Ext. soln. concentrations (molal)	J_s (moles $cm^{-2}sec^{-1}$) $x10^{10}$		J_3 (moles $cm^{-2}sec^{-1}$) $x10^{7}$	
	C60N	C60E	C60N	C60E
0.05/0.15	3.90	12.22	0.65	1.65
0.05/1.50	89.6	272.3	1.42	4.06

Table 2.17.

Ext. soln. concentrations (molal)	C60N		C60E	
	X_{12}	X_3	X_{12}	X_3
0.05/0.15	1.50×10^5	2.44×10^2	1.51×10^5	2.46×10^2
0.50/1.50	1.71×10^5	2.90×10^3	1.66×10^5	2.80×10^3

Table 2.18.

Water transference number as a function of current density.

External solution: 0.1M sodium chloride.

Current density mamps/cm^2	t_3 C60N	C60E
1.06	10.8_2	-
3.04	10.7_5	15.7_5
8.33	10.6_8	15.6_5

Table 2.19.

Comparison of predicted [21] and observed water transference numbers.

Ext. solution concn. (molar)	C60N t_3 predicted *	C60N t_3 observed	C60E t_3 predicted *	C60E t_3 observed
0.10	10.9	10.75	16.4	15.7
0.50	-	-	-	-
1.00	15.3	7.90	25.95	9.70
2.00	-	-	-	-

* Using the equation

$$\frac{1}{t_3} = \frac{\bar{c}_1}{\bar{c}_3} + \frac{\bar{c}_4 R_{34}}{\bar{c}_3 R_{13}}$$

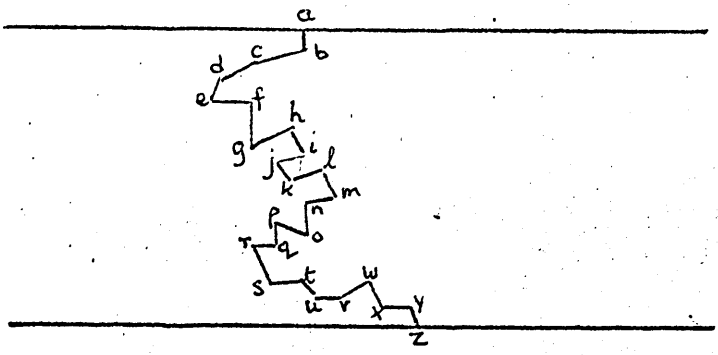

Figure 2.1. Schematic representation of tortuosity.

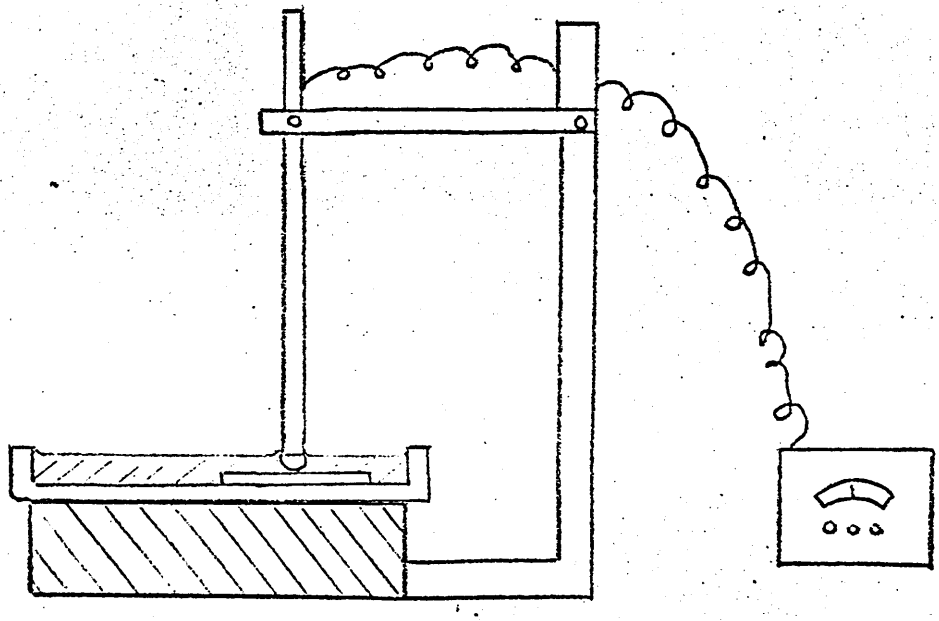

Figure 2.2. Apparatus for determining membrane thickness.

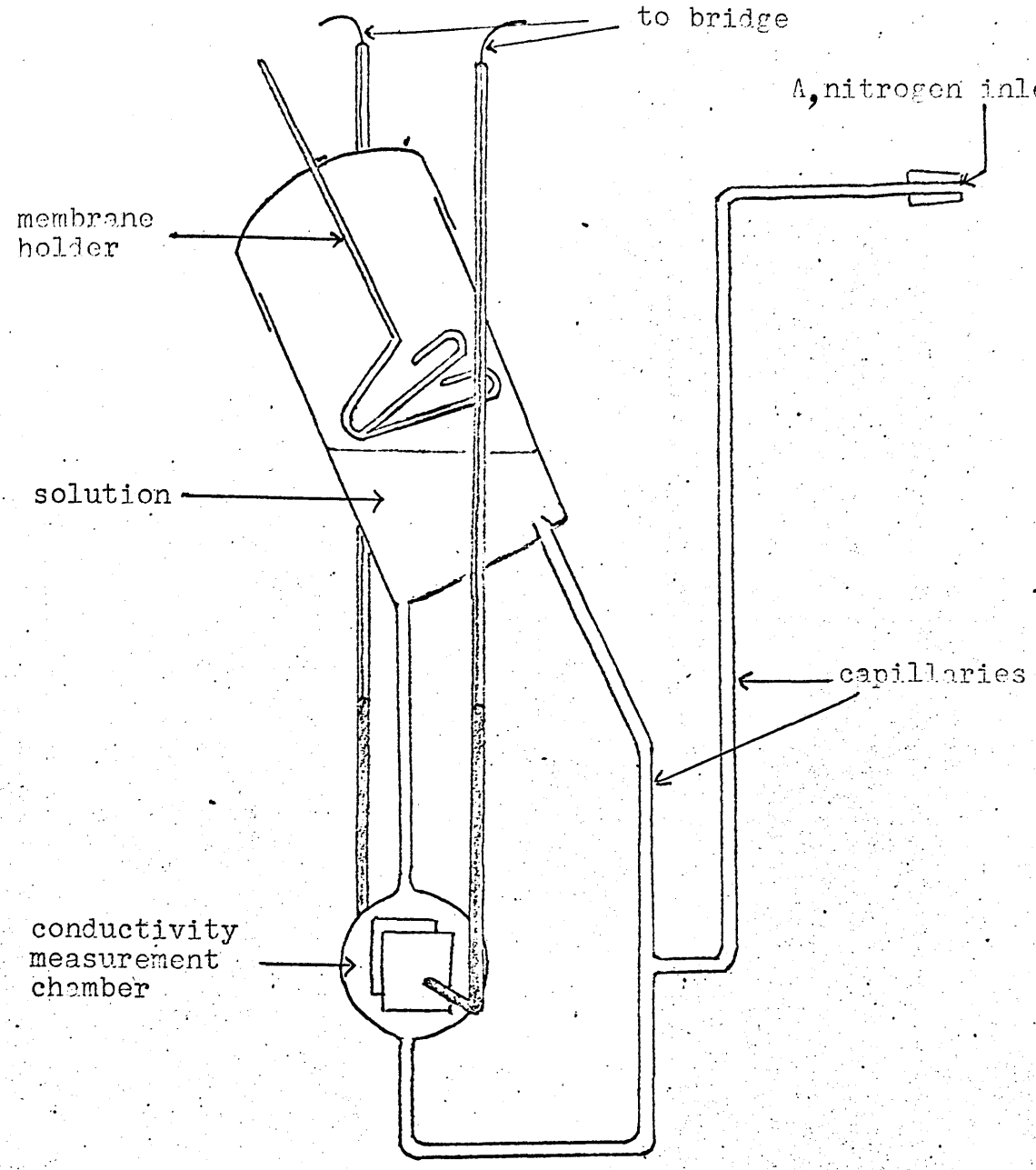

Figure 2.3. Apparatus for determining electrolyte uptake by conductivity.

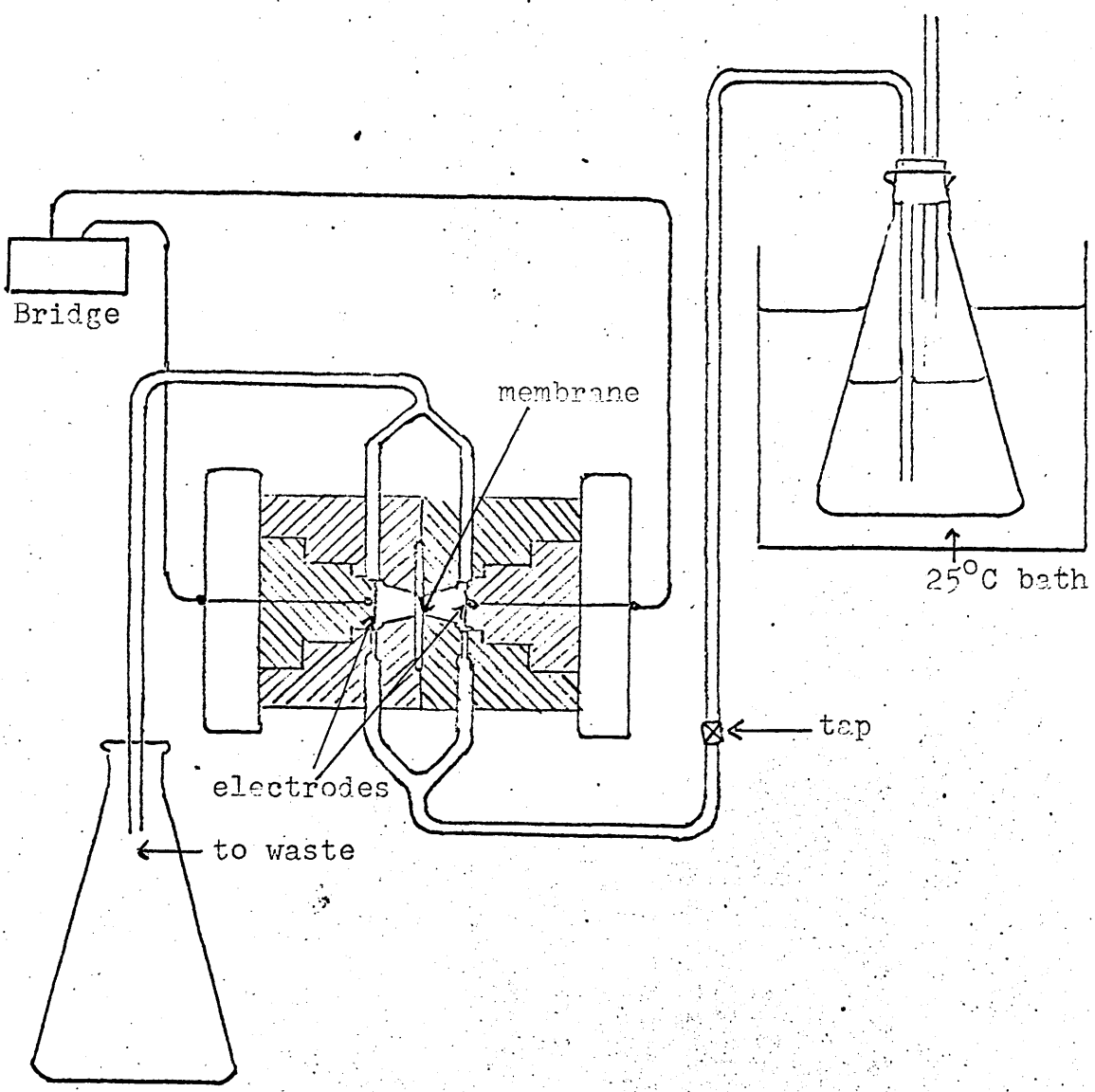

Figure 2.4. Membrane conductivity cell.

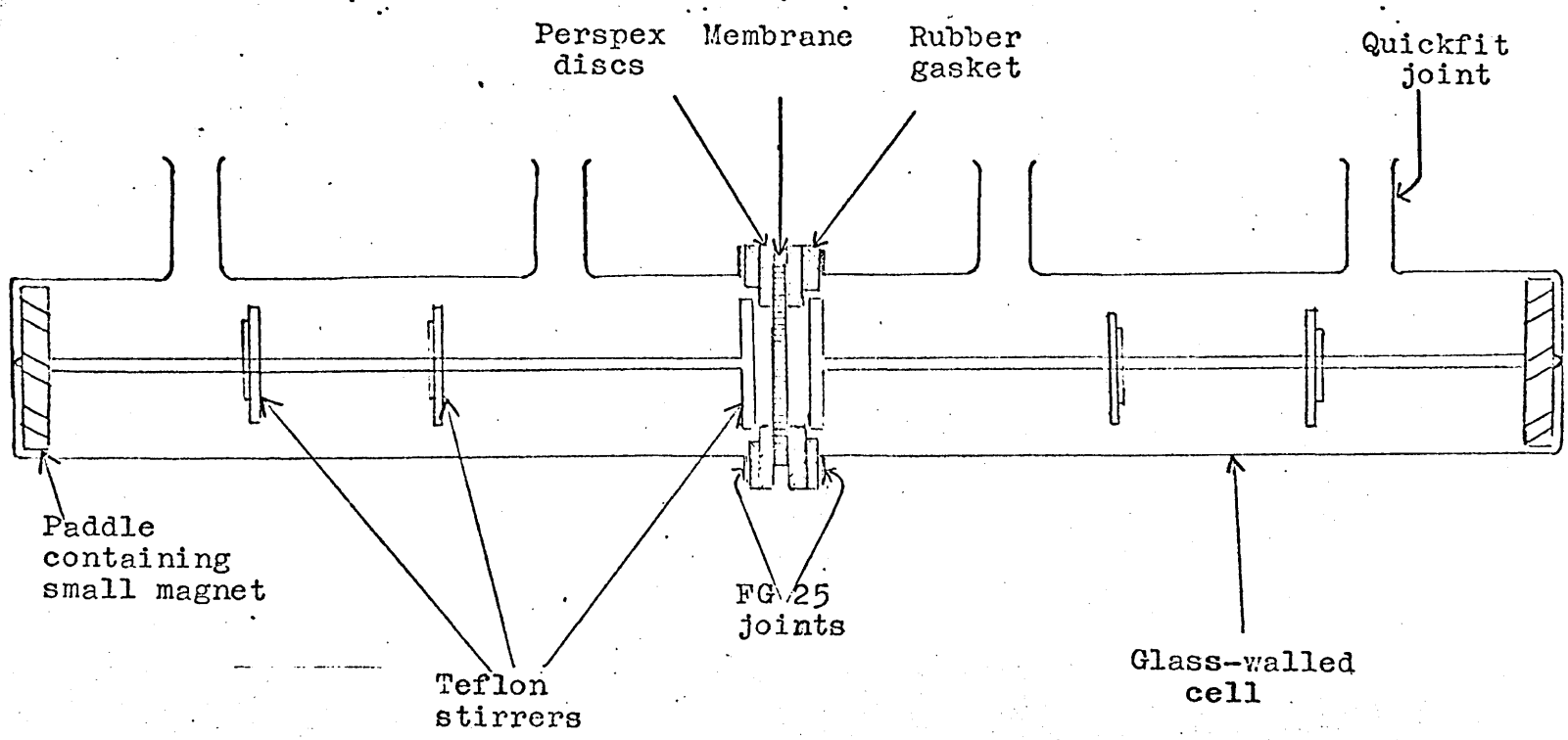

Figure 2.5. Membrane diffusion cell.

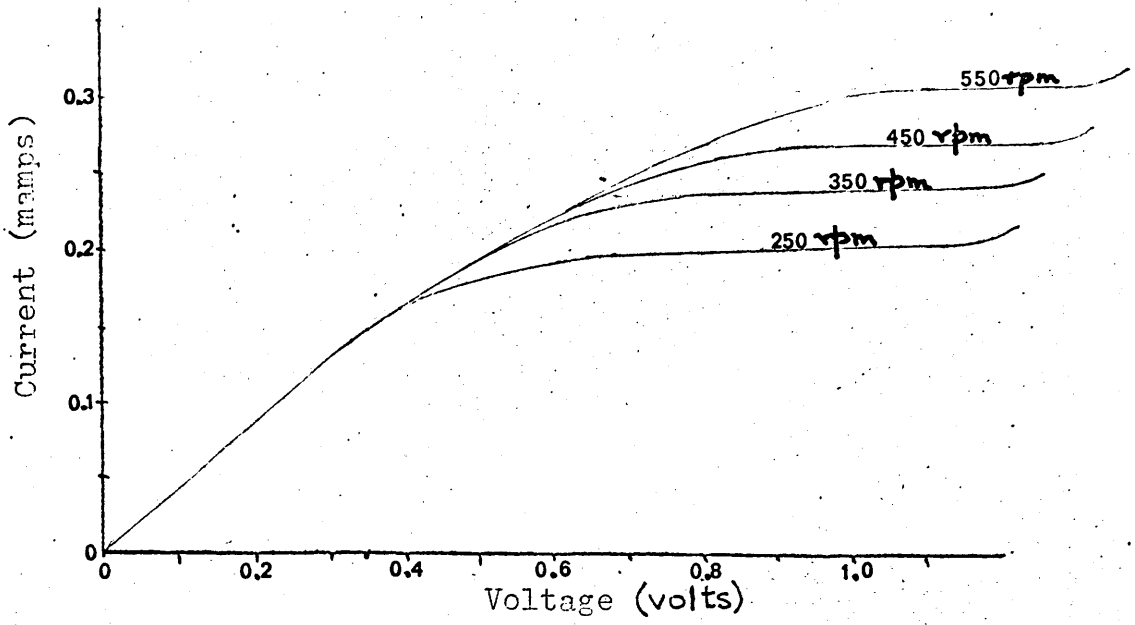

Figure 2.6. Typical limiting current measurements.

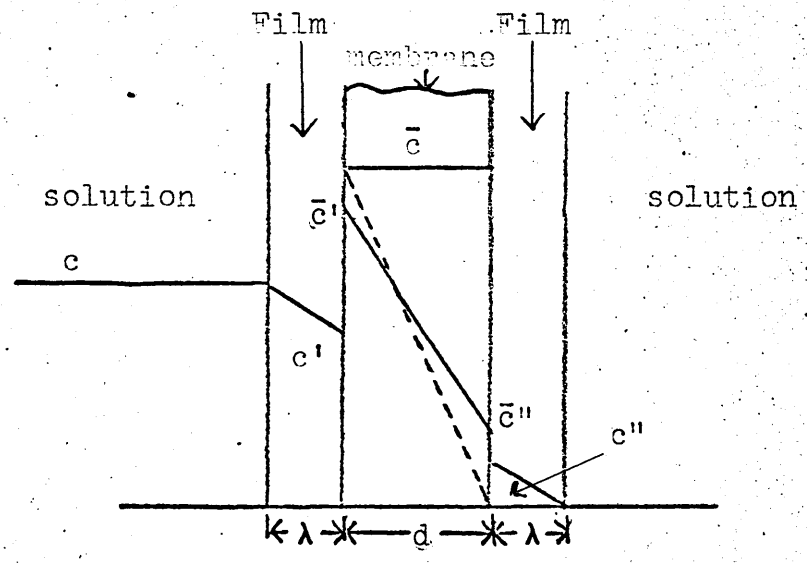

Figure 2.7. Concentration profile in diffusion through ion exchange membranes (schematic).

_____ Partial film diffusion control.

----- Ideal membrane diffusion control.

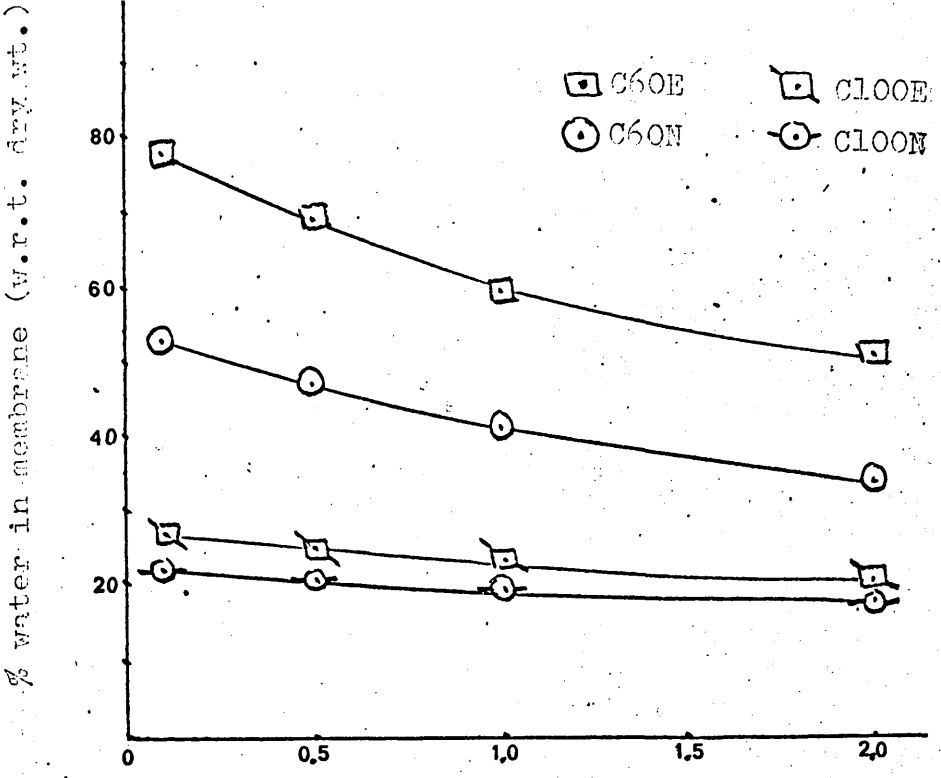

Figure 2.8. Water content of membranes versus concentration of external solution.

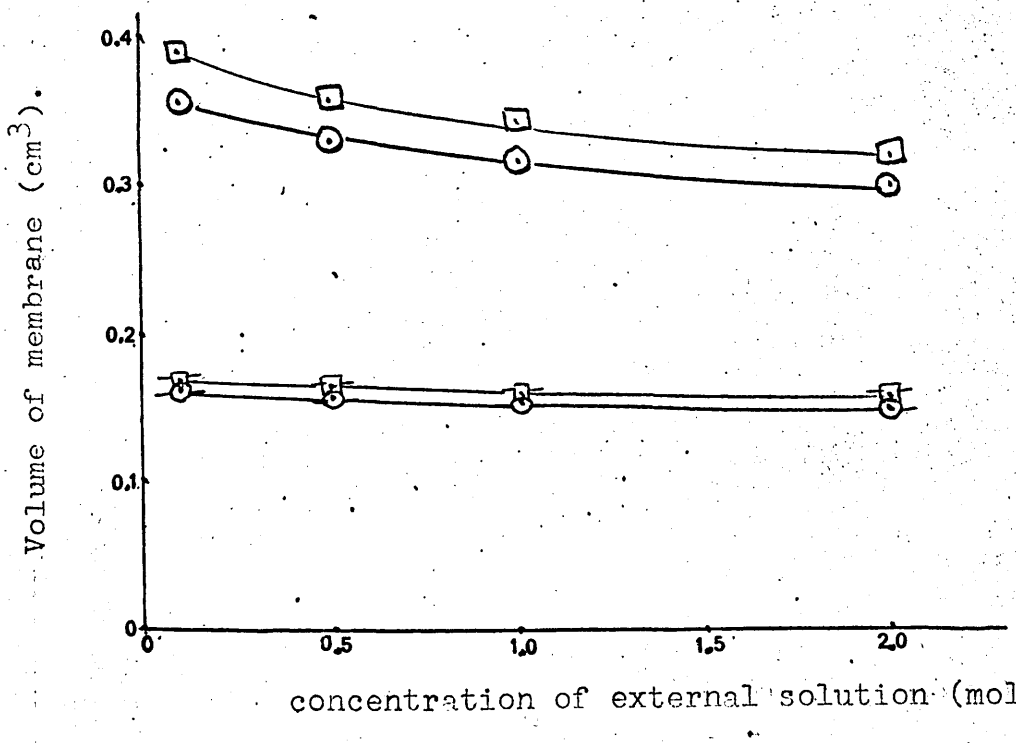

Figure 2.9. Volume of membranes versus concentration of external solution.

C60E C60N C100E C100N

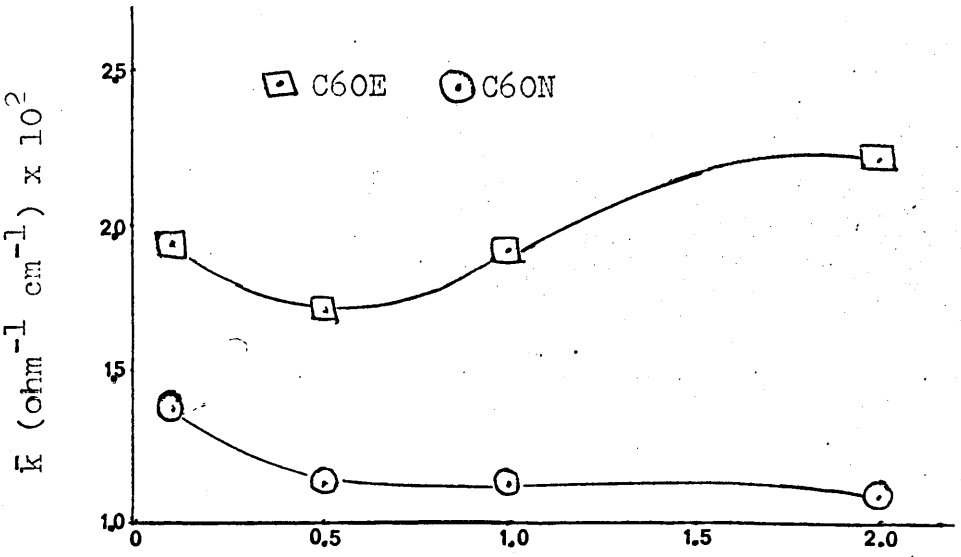

Concentration of external solution (molar)

Figure 2.10a. Conductivity of C60 membranes versus concentration of external solution.

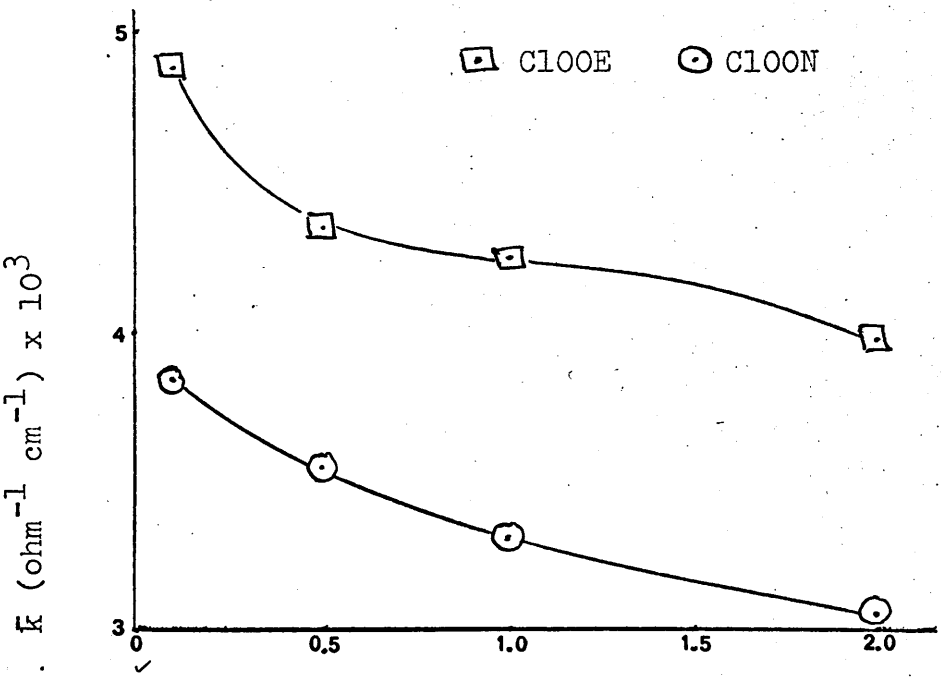

Concentration of external solution (molar)

Figure 2.10b. Conductivity of C100 membranes versus concentration of external solution.

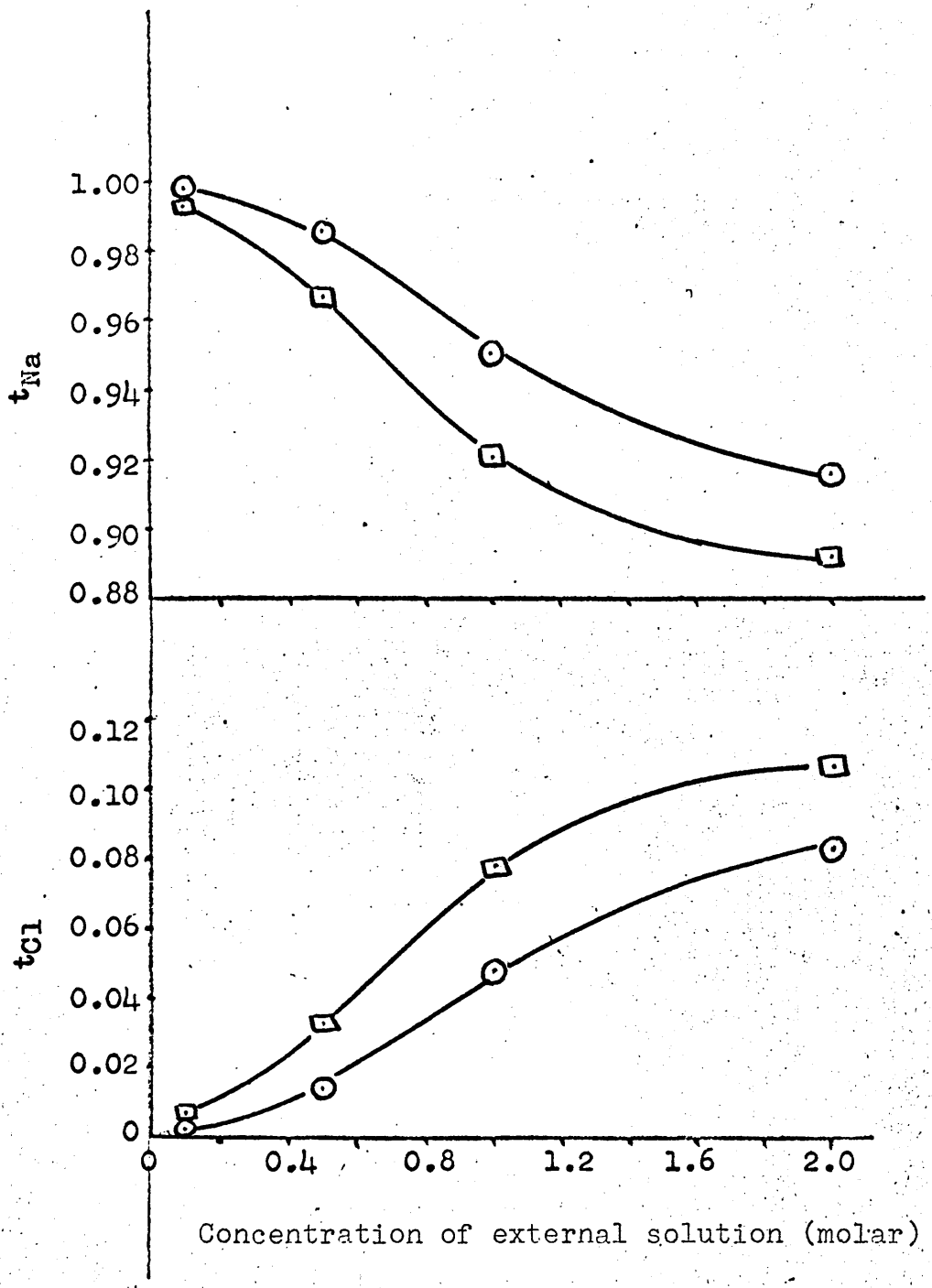

Figure 2.11. Transport numbers of counter- and co-ions in membranes versus concentration of external solution.

⊡ C60E ⊙ C60N

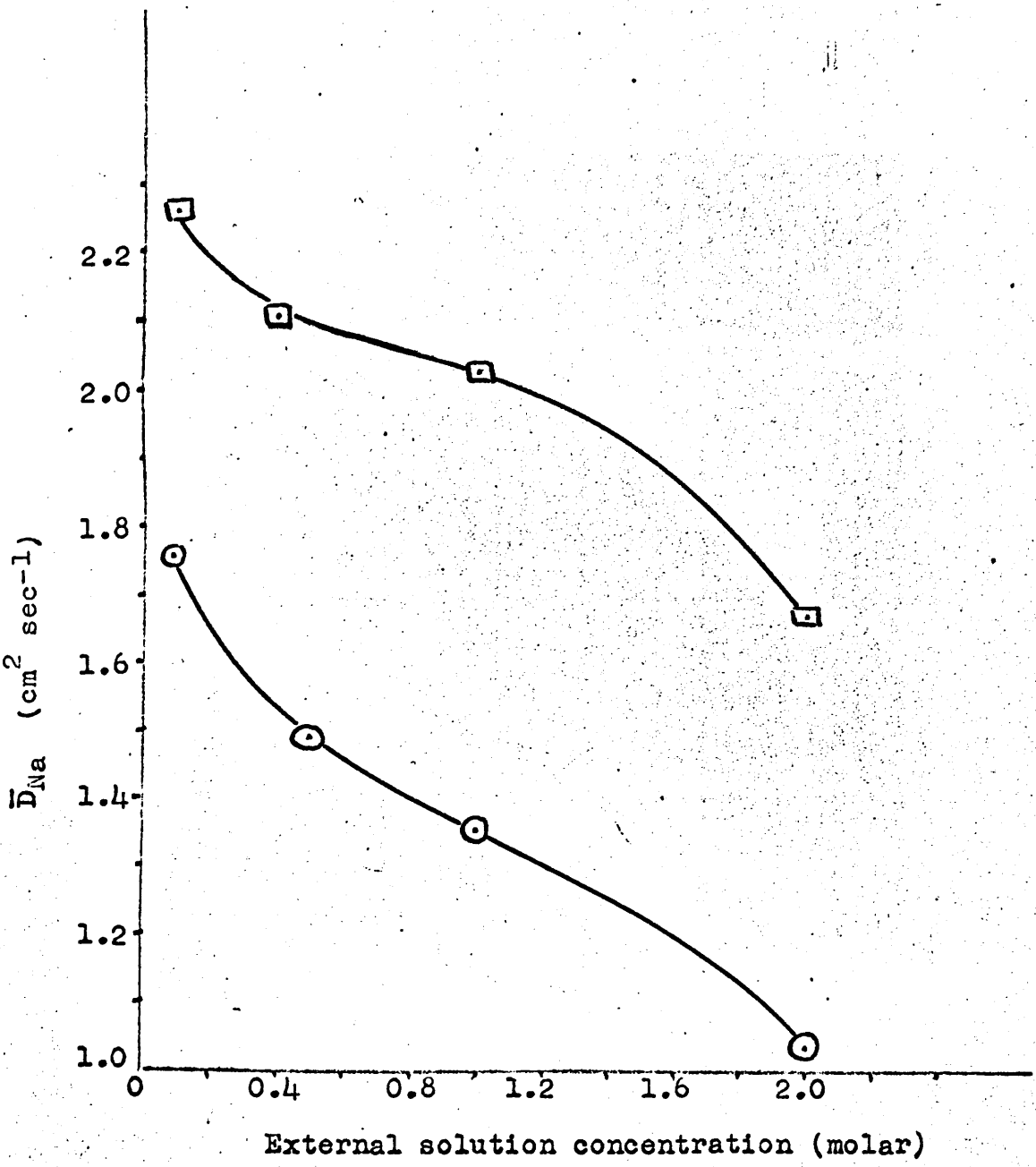

Figure 2.12. Sodium ion diffusion coefficients in membranes versus concentration of external solution.

⊡ C60E ⊙ C60N

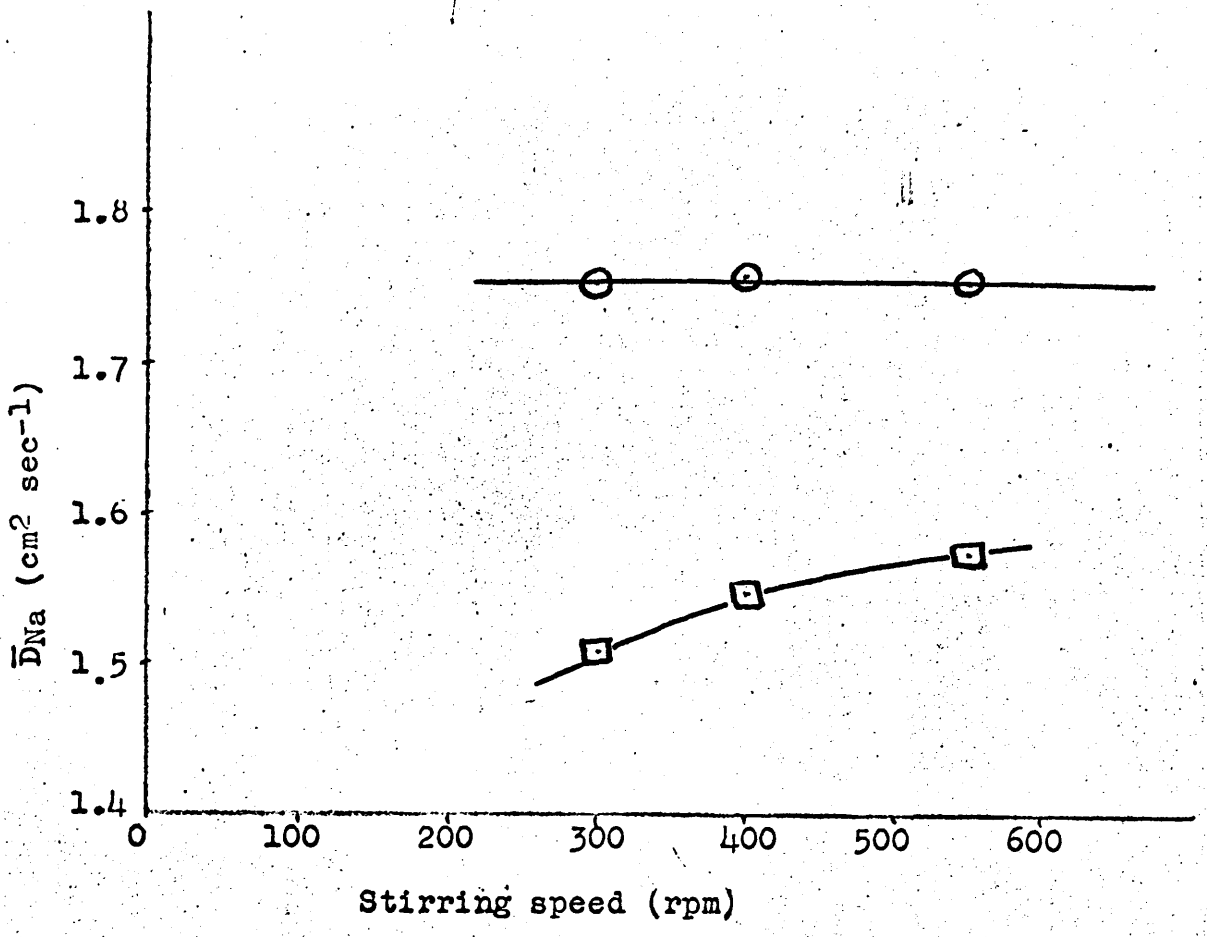

Figure 2.13. Sodium ion diffusion coefficients in membranes versus stirrer speed.

⊡ uncorrected ⊙ corrected

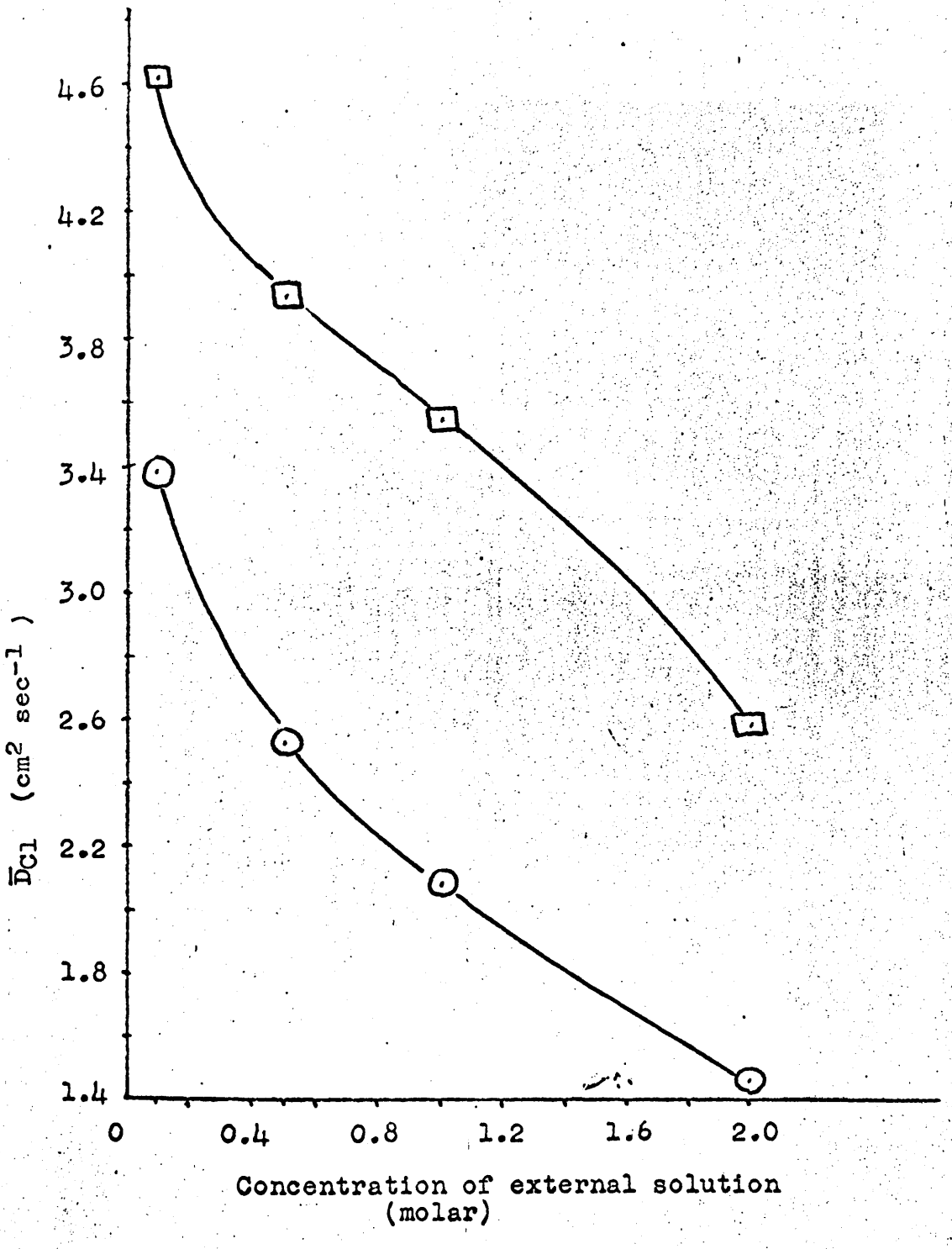

Figure 2.14. Chloride ion diffusion coefficients in membranes versus concentration of external solution.

⊡ C60E ⊙ C60N

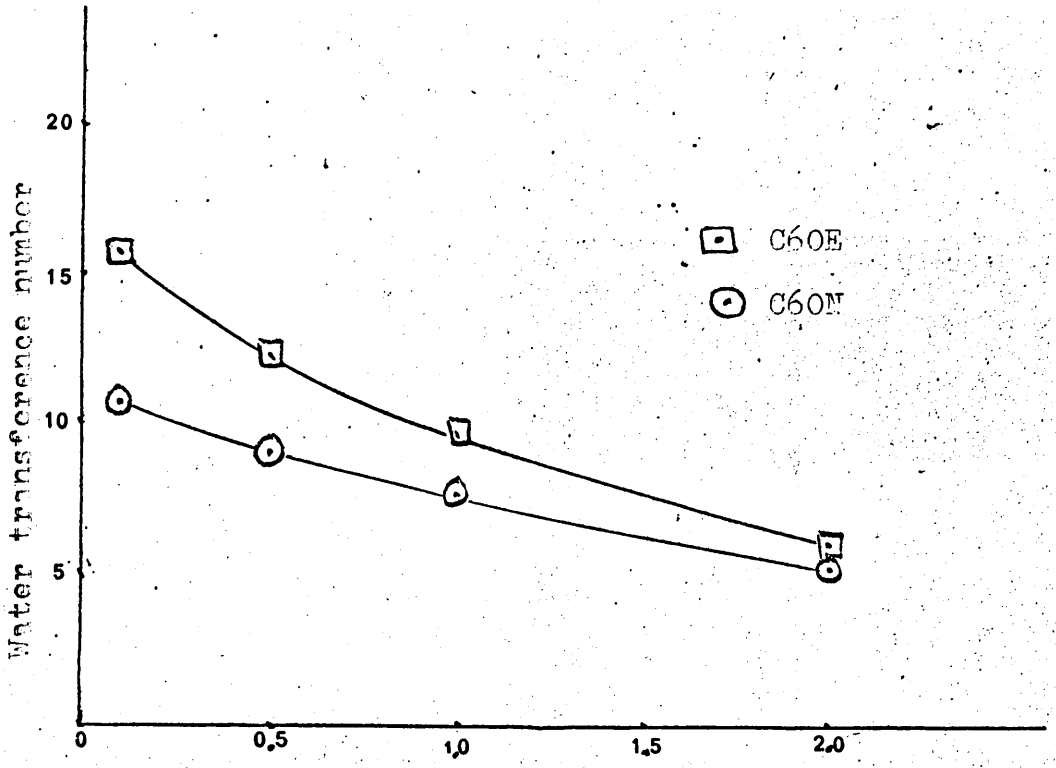

Figure 2.15. Water transference number versus concentration of external solution.

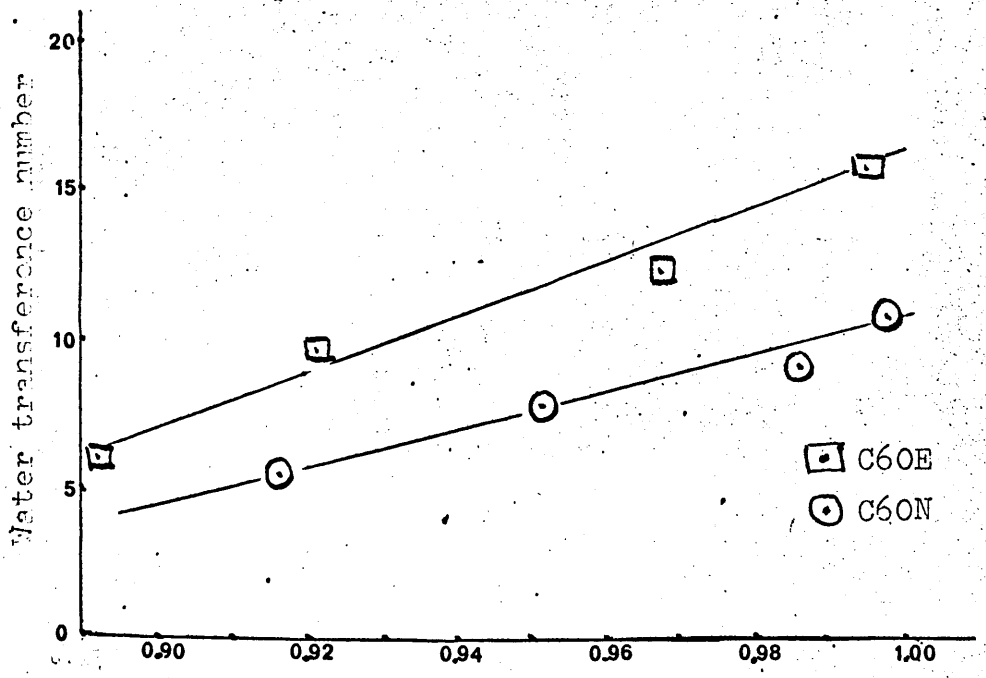

Figure 2.16. Water transference number versus counter-ion transport number.

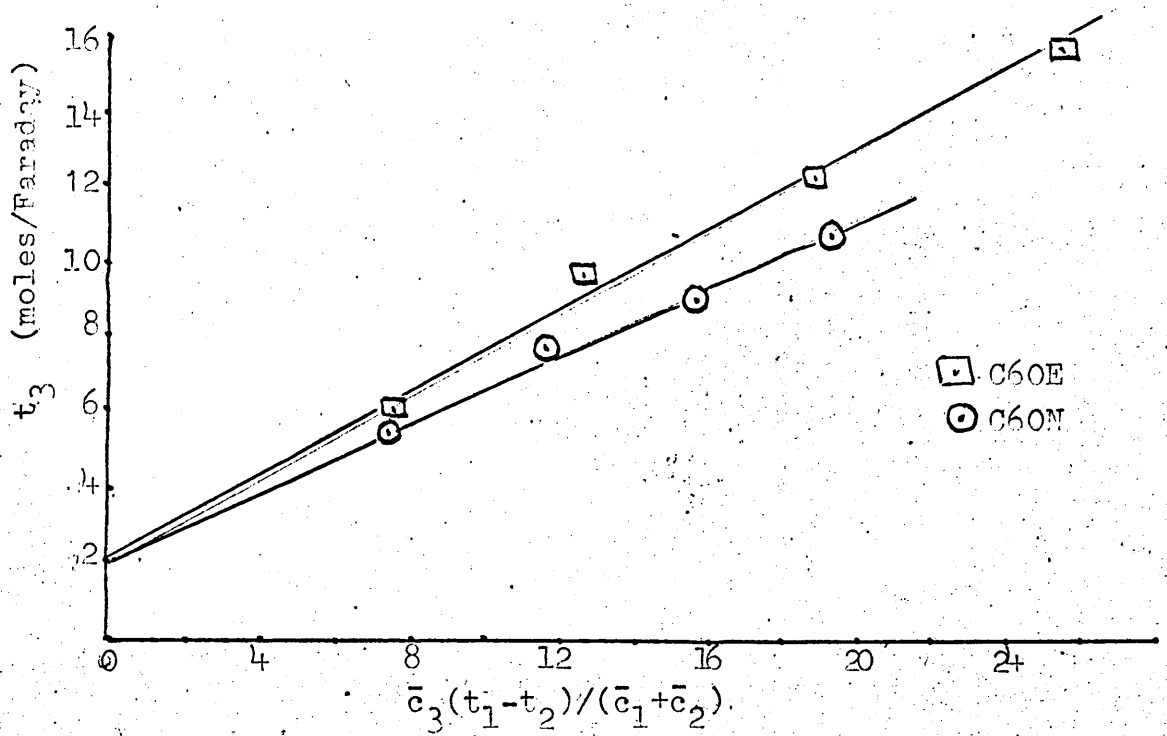

Figure 2.17. Water transference number, t_3, versus the function $\bar{c}_3(t_1-t_2)/(\bar{c}_1+\bar{c}_2)$.

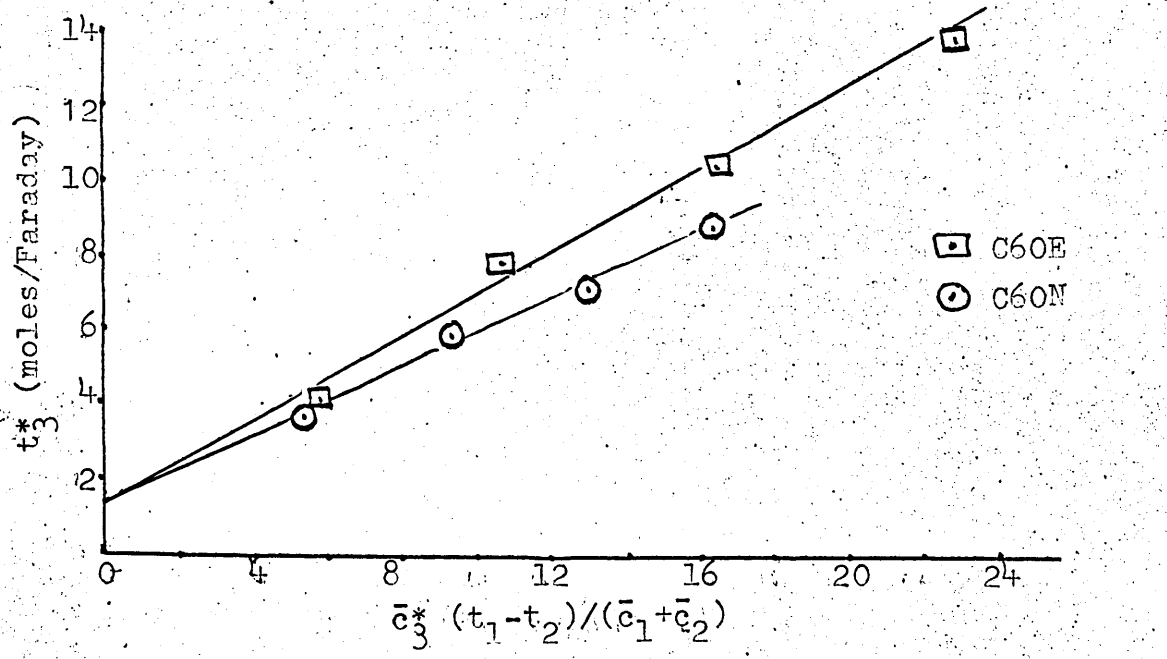

Figure 2.18. Water transference number, t_3^*, versus the function $\bar{c}_3^*\ (t_1-t_2)/(\bar{c}_1+\bar{c}_2)$.

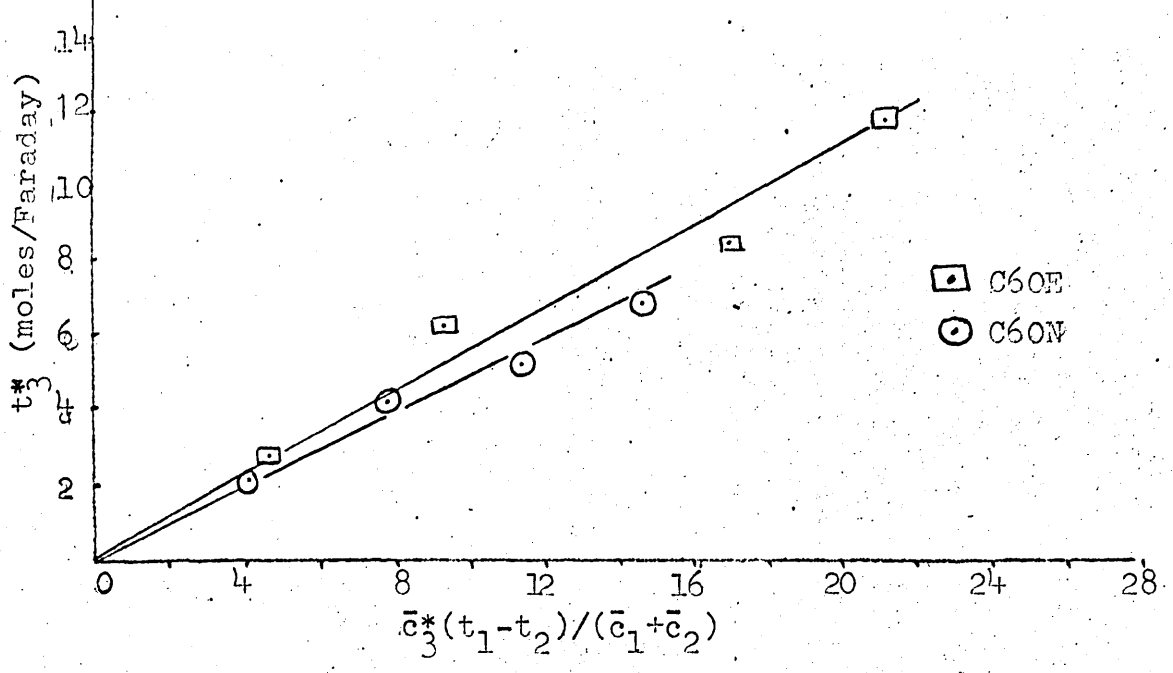

Figure 2.19. Water transference number, t_3^*, versus the function $\bar{c}_3^*(t_1-t_2)/(\bar{c}_1+\bar{c}_2)$ (values of H_1, H_2 and H_4 chosen so that plot passes through the origin).

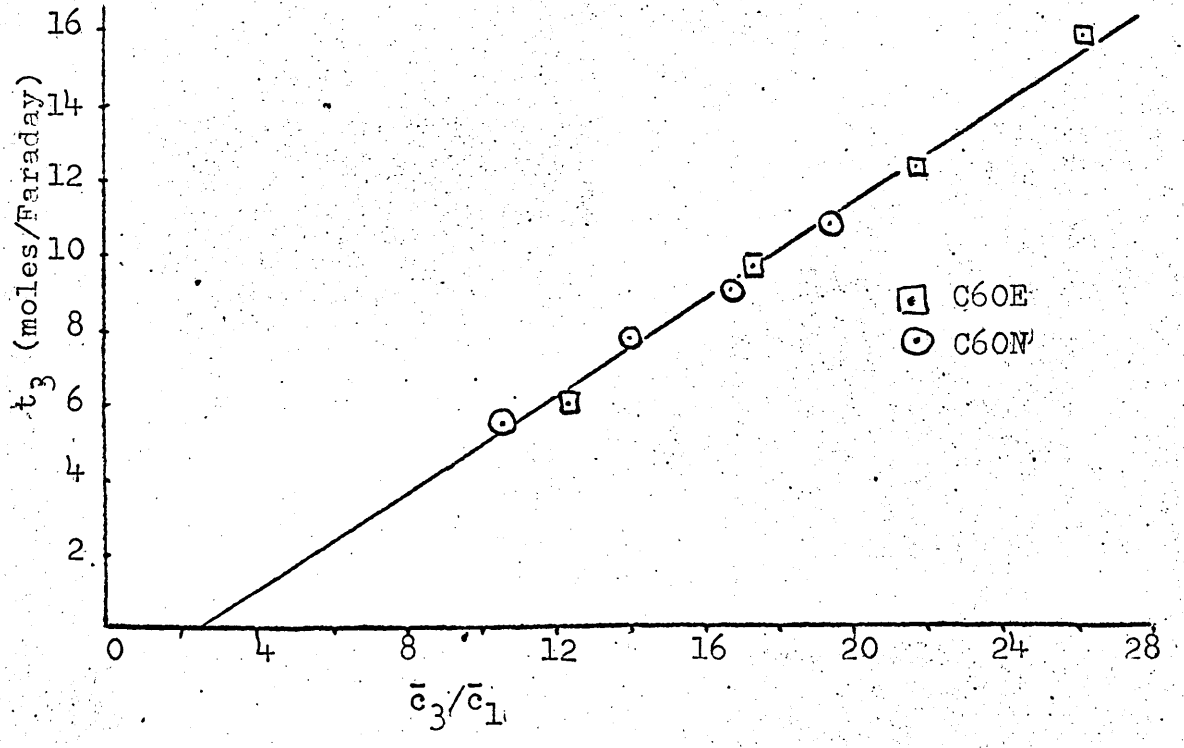

Figure 2.20. Water transference number, t_3, versus the function $\bar{c}_3/\bar{c}_1$.

2.5. Discussion.

The results shown in Tables 2.1 - 2.4 show the general properties of the ion-exchange membranes studied in this work, and demonstrate the effect of the external solution concentration on these properties. Comparisons can be made of the various membrane systems studied, the effect of the thermal expansion of the exchanger being particularly interesting.

2.5.1. Water Content.

The water content of an ion-exchanger depends on the 'tightness' of the resin structure and on its ability to swell and hence accommodate the solvent. This, in turn, depends on the degree of cross-linking of the hydrocarbon matrix. The water content also depends on the concentration and nature of the fixed and mobile ions, but where these are similar, as they are in the membranes studied here, the main factor influencing the water content is the structure of the membrane itself. Bearing this fact in mind, examination of figure 2.8 yields information about the structures of the membranes relative to one another. The C100 membranes have a fairly low water content suggesting/

suggesting that the structure of these membranes is fairly tight whereas the C60 series exhibit a high water content corresponding to their more open structure. In both cases, the effect of the thermal treatment is to expand the structure of the membranes and enable them to absorb more water from the external solution.

The effect of membrane expansion on the water content of the membranes is constant over the entire range of concentration studied, as is demonstrated by the constancy of the ratio, $\bar{c}_3(N)/\bar{c}_3(E)$, shown in table 2.5.

When an exchanger is in equilibrium with the external solution, the chemical potential of the water in the exchanger is equal to that of the water in the external solution,

$$\text{i.e.} \quad \bar{\mu}_3 = \mu_3 \qquad (2.100)$$

Expanding this equation and choosing the standard states so that $\bar{\mu}_3^{\circ} = \mu_3^{\circ}$, this equation may be rewritten, (178)

$$RT\ln a_3 = RT\ln \bar{a}_3 + (\bar{P} - P)\ \bar{v}_3 \qquad (2.101)$$

where P and $\bar{P}$ are the pressures in the external solution and in the exchanger resp., a_3 and $\bar{a}_3$ are the water activities in the external solution and in the membrane resp., and $\bar{v}_3$ is the p.m.v. of water.

As the concentration of the external electrolyte solution/

solution increases, so the activity of the water in the solution decreases. Since the concentration changes in the exchanger are small compared to those in the external solution, the water activity in the exchanger changes by a smaller amount than does the external water activity. Reference to equation (2.101), therefore, shows that a drop in the water activity in the external solution is reflected by a drop in the swelling pressure term $(\bar{P} - P)\,\bar{v}_3$. Thus as the external concentration increases, the swelling pressure decreases and consequently, the exchanger swells less and absorbs less water from the solution. Since the water content and degree of swelling of the exchangers are so closely related, the similarity of the shapes of the curves in figures 2.8 and 2.9 is not unexpected.

2.5.2. Electrolyte Uptake.

In principle, the most accurate method of determining electrolyte uptake, especially at low external solution concentrations, should be by measuring the conductivity of the solution containing the salt leached out of the membrane which had been previously equilibrated with an electrolyte solution. This method has been used by Meares [81] to determine/

determine the sodium chloride uptake by Zeocarb 315 membranes. In this present study further modifications to the technique were attempted as described in section 2.3.9, in an effort to obtain, not only the absolute value of the co-ion uptake, but also the rate of effusion of the electrolyte from the membrane. These efforts were, however, frustrated by failure of the conductivity of the leaching solution to reach a steady value. It was concluded that in the leaching process, not only was sorbed electrolyte being released into the external solution but some other process was occurring which also contributed to the rise in conductivity of the solution. This hypothesis was supported by the fact that a membrane previously leached for several weeks in distilled water, showed similar behaviour.

When a membrane which had been equilibrated with a concentrated electrolyte solution (1.0M) was used, the conductivity due to the large amount of salt released was sufficient to swamp this anomolous increase and the preliminary results obtained from such experiments agreed very well with those obtained from the potentiometric titration method. When the equilibrating solution was dilute, however,/

however, the conductivity of the leaching solution was low and the constant increase in conductivity due to the secondary process was sufficient to render this method unusable.

Therefore, the values of the electrolyte uptake recorded in this study were obtained using the potentiometric titration method described in section 2.3.9.

The uptake of electrolyte by the resin is governed by the magnitude of the Donnan potential which tends to exclude the co-ions. The efficiency of this exclusion is greatest at low solution concentrations and reference to Tables 2.1 - 2.4 shows that even at 0.1M, the co-ion concentration in the exchanger, c_2, is less than 1% of that of the counter-ions, c_1. Expansion of the membrane matrix leads to a reduction in the value of the Donnan potential and hence to an increase in the electrolyte uptake. The results show that the co-ion concentration in the expanded membranes is considerably greater than in their normal counterparts. As the external concentration increases, the electrolyte uptake increases ever more rapidly until at 2M the electrolyte uptake for the C60E membrane represents some 30% of the total exchangeable ion concentration.

The electrolyte uptake data will be fully treated in Chapter 3, but where this increase in concentration of the mobile ions in the pores of the exchanger has considerable effect on the properties of the resin this effect will be noted.

2.5.3. Diffusion.

As described in section 2.3.12 and Appendix A.7. a correction for film diffusion effects has been applied to all the tracer diffusion coefficients. The magnitude of this correction is fairly large, 10-15% for the counter-ion in the membranes in equilibrium with 0.1M solution, the correction for the other concentrations being considerably smaller, approx. 2-3% or less. The correction to the co-ion diffusion coefficient is also small never exceeding 1%. The magnitude of the correction is dependent on the stirring speed employed in the experiment. One test of the validity of the correction is, therefore, to examine the corrected values for a given membrane and given solution concentration but at different stirring speeds. A valid correction should, under these circumstances, produce identical results for all the stirring speeds. The results of such a series of experiments are shown in figure 2.13, where it may be seen that the correction for film diffusion effects has produced the same values for the diffusion coefficient over a wide range of stirring speeds, although the uncorrected values differ widely. All the diffusion coefficients in the succeeding tables have been determined at a stirring/

stirring speed of 550 rpm. and have been corrected as above.

From the film diffusion correction, the value of the film thickness can also be obtained. The values are in the range 15-25 microns for stirring speeds of 550 to 250 rpm. These values, which are of course dependent on the efficiency of the particular stirrer, are of the same order as other values of the film thickness calculated by other authors, often using different techniques. (54) (55)(56) (57).

The variations of the tracer diffusion coefficients of the ions in an ion-exchanger with changing external concentration have been the subject of much work and discussion. (82) (83) (84) (32) (33) (38) (85) From the results of these investigations no clear general pattern emerges, the nature of the variations depending greatly on the type of exchanger used. Because of the differences in counter- and co-ion diffusion behaviour which have been observed by most workers, it is best to treat the two types of diffusion separately before drawing any general conclusions about the behaviour of the ions in the exchanger phase.

(a) Counter-ion diffusion.

In comparison with most other cation-exchangers (82) (83) (86) (87) (88) (89) the sodium tracer diffusion coefficient in/

in the C60N and C60E membranes is fairly large, as shown in table 2.6 and figure 2.12. This is due to the relatively high water contents and open structures of these exchangers. The values for the expanded membrane are considerably greater than those for the normal one, again demonstrating the effect of increased water content and openness of structure. It is, however, the variation of these diffusion coefficients with the concentration of the external solution which demands considerable attention. In contrast to the increasing resin diffusion coefficients which have been observed by many workers, the trend of the sodium ion diffusion coefficients in the C60N and C60E membranes, with increasing solution concentration, is downwards.

This difference in the trend of the diffusion coefficients is not simply due to the corrections which have been applied for film diffusion. Even the uncorrected values show a general downward trend, although the difference between the successive values are smaller than for the corrected results. Also Meares has applied a correction for film diffusion to his results [84] and yet has found that the counter-ion diffusion coefficients increase with increasing concentration.

There/

There still remains a considerable number of counter-ion diffusion phenomena which are not quantitatively explained. The difficulties of determining the potential energy profiles, the effect of electrolyte uptake and of tortuosity on the diffusion process are extremely large: nevertheless, it is possible to present an argument which can fit the observed facts, qualitatively at least.

The tracer diffusion coefficients of sodium ions in aqueous sodium chloride solutions exhibit a decrease with increasing solution concentration [90] [91] and this tendency is displayed by all cations in aqueous solutions. Although the concentration changes occurring in the ion-exchanger are not so large as those in the external aqueous solution, it seems not unlikely that a similar decrease in diffusion coefficients would be observed in the exchanger phase. In addition to the normal factors tending to reduce solution diffusion coefficients (e.g. increased numbers of collisions and increased electro-static drag), there is the increased totuosity in the exchanger which also produces a decrease in the observed mobility of the ions in the resin, (Sect. 2.2.4).

In the treatment of aqueous solutions, another cause of decreasing diffusion coefficients with increasing concentration/

concentration is ion-association. It is, therefore, important to consider the probability of such an interaction in the exchanger. P.M.R. and Raman studies [92] [93] [94] [95] [96] [97] have shown the complete absence of covalent bonding but this does not exclude the possibility of other forms of association which would not be detected by these methods. Strauss and Leung [98] have shown that site binding of alkali and alkaline earth ions occurs with many polyelectrolytes, but the effect observed with sulphonate groups is small, and in a recent study using sodium counter-ions and a PSA membrane, Meares [84] has shown that there is no evidence of specific association.

In the absence of further information, therefore, it may be assumed that although ion association cannot be ruled out completely, it is improbable that the degree of association is large enough to significantly affect the counter-ion diffusion coefficients.

It has been suggested by Spiegler, [99] that the exchanger diffusion coefficients should in fact decrease with increasing concentration, and that the increasing trend observed in so many exchangers is due to the inhomogeneity of the resin structure. At low external concentration when there is little or no electrolyte uptake the/

the counter-ions will be concentrated in the regions of high fixed charge density, where the cross-linking is probably greatest, and hence, the diffusion is slowest. As the external concentration increases, so the electrolyte uptake will increase. The counter-ions present in the exchanger due to salt uptake will tend to be in regions of lower charge density and lower cross-linking i.e. in the regions known as voids. The diffusion coefficients of these ions will be greater than those of the original counter-ions, and hence the average counter-ion diffusion coefficient will be increased. As the salt uptake increases and accounts for a significant proportion of the total counter-ion concentration, so this effect will be enhanced and may be sufficient to offset the general decrease in diffusion coefficient resulting from the increased concentration and tortuosity. If this explanation is valid, then the C60N and C60E membranes must be considered to have more homogeneous structures than most other membranes previously examined. This proposal is borne out by the results of the structural analysis, based on electrolyte uptake, which is given in Chapter 3.

Jakubovic, Hills and Kitchener [32] [33] have suggested that if the counter-ions are held fairly tightly in the electrical/

electrical double layer associated with the charged polymer, then the counter-ion mobility would depend on the distance between the potential energy minima corresponding to the fixed sites, the diffusion rate being lower if the site to site distances were large enough to prevent the ions from jumping easily from one polymer chain to another or indeed from one segment to another segment of the same chain. This type of "chain diffusion" would be facilitated by the reduction of the distances between the sites and between adjacent chains which would occur in solutions of higher concentration. Therefore on this model the diffusion coefficient would be expected to increase with increasing external solution concentration. Schlogl [85] has suggested that if the counter-ions are pictured as moving from one fixed charge to another across a potential energy barrier, then the invading co-ions present at higher concentrations would provide troughs of high mobility and thus facilitate the migration of the counter-ions. In the absence of other effects, both these theories would predict an increasing counter-ion diffusion coefficient with increasing external concentration, the opposite of what is observed in the C60N and C60E membranes. It seems, therefore, that this type of 'chain diffusion' is unlikely/

unlikely to occur in these systems.

On the other hand, absolute rate theory applied to diffusion processes [100] [101] [102] predicts that the diffusion coefficient of a species is proportional to the square of the distance between potential energy minima, (see Section 4.6). For the counter-ions the positions of energy minima in an ion-exchanger, are the fixed sites and the mobile co-ions. As the concentration of both these species increases with increased electrolyte uptake and reduced swelling experienced by the exchanger in more concentrated solutions, so the distance between adjacent energy minima decreases. It is to be expected, therefore, that the diffusion coefficient of the counter-ions will also decrease.

Assuming that the fixed charges and the co-ions occupy only the volume fraction of the exchanger which contains aqueous solution, the average concentration of the positions of potential energy minima can be obtained by dividing the total concentration of these sites expressed on the basis of the whole membrane, by the volume fraction of water in the exchanger. From this value, and assuming that the sites are distributed at the corners of a cubic lattice, the value of λ, the inter-site distance, can be calculated/

calculated. If the diffusion process is to be explained by absolute rate theory then D/λ^2 must be a constant. The results of this calculation for both membranes are shown in table 2.9. For both membranes the quotient, D/λ^2, is reasonably constant, particularly so for the C60N membrane. Considering the nature of the assumptions made in this calculation it appears that the absolute rate theory approach satisfactorily explains the trend in the diffusion coefficients observed in these membranes.

(b) Co-ion diffusion.

As with the counter-ions, there appears to be no general pattern for co-ion diffusion coefficients, some exchangers exhibiting a decrease with increasing concentration, [38] [85] others an increase [84]. As shown in table 2.6 and figure 2.14, the chloride co-ion diffusion coefficients in the C60N and C60E membranes decrease with increasing concentration of the external solution. Owing to the high water contents of the exchangers, the co-ion diffusion coefficients are large, the expanded membrane having values greater than the normal one, as expected. The variation of the diffusion coefficients with concentration can be explained by arguments similar to those employed/

for the counter-ions. Whether or not the exchanger has inhomogeneities, the effect of increased co-ion uptake would be expected to produce a decrease in the co-ion diffusion coefficients in a manner analagous to that observed in aqueous solutions [91], and the effect of the tortuosity increase is to further reduce the observed mobility of the ions.

Comparison of the values of the counter-ion and co-ion diffusion coefficients given in table 2.6, reveals that the co-ion mobility is the greater. In aqueous solutions, chloride ions have an intrinsically higher mobility than sodium ions and the values of the diffusion coefficients in the exchanger phase may be simply a reflection of this fact; or it may be that in the membrane there is a further factor which tends to enhance the co-ion diffusion coefficients with respect to those of the sodium ions. Wyllie [103] has proposed that the difference between counter-ion and co-ion mobilities in the resin can be partly attributed to the influence of the matrix and the fixed sites. The species which has the greater affinity for the fixed ionic groups will experience a greater retardation from the presence/

presence of the matrix than that species which can move through the resin unhindered by interaction with the exchange sites. Thus the co-ions would be expected to have a higher mobility than the counter-ions. Section 2.8 will deal with the relationship between the interaction of species and the effect on their mobilities, using the theories of non-equilibrium thermodynamics.

(c) The effect of tortuosity.

If the analogy between aqueous solutions and ion-exchangers is to hold, then a correction to the exchanger diffusion coefficients which allows for the increase in tortuosity of the aqueous paths along which the ions are constrained to move, should give the values of the diffusion coefficients of the ions in the corresponding aqueous solution of the same concentration, provided that the other factors which can affect the ionic diffusion, and which have been mentioned above, are not dominant. The calculation of this tortuosity factor has already been discussed in section 2.2.4, and the values of θ are given in table 2.7. As expected, the tortuosity factor is lower for the expanded membrane, and for both membranes, it increases with increasing solution concentration. Since the tortuosity/

tortuosity factor corrects for the effect of the polymer chains on the diffusion paths of the ions, the corrected exchanger diffusion coefficients must be compared with those of the same ions in aqueous solutions of the same molal concentration as that in the exchanger pores. Since the diffusion coefficients of sodium and chloride ions in solutions of sodium polystyrenesulphonate or even sodium toluene sulphonate, at high polyelectrolyte concentrations, are not recorded in the literature, comparisons have been made with their values in aqueous solutions of sodium chloride. (90) (91) The exchanger diffusion coefficients corrected for tortuosity, $D\theta$, are shown in table 2.8, together with the literature values for the diffusion coefficients in sodium chloride solutions of the same concentration. In view of the assumptions made in calculating the tortuosity factor and the neglect of other factors such as the interaction of the ions with the matrix, the agreement between the observed and predicted values is fairly good. The fact that even after correction, the counter-ion values are somewhat lower in the exchanger than in the aqueous solution, whereas the co-ions values are in very good agreement, is interesting. Two possible explanations of this behaviour can be suggested. First, there may be retardation/

retardation of the counter ions by the matrix and the fixed charges, and second, the tortuosity factor may be greater for the regions of high counter-ion concentration than for the exchanger as a whole. This latter suggestion would imply that the counter-ion regions were more highly cross-linked and less continuous than the regions of lower fixed charge density. This proposal gains support from the results of the structural analysis, the results of which are given in Chapter 3. In the comparison given in table 2.8, it must be remembered that the solution results are for sodium chloride solutions where the ionic interactions may be quite considerably different from those in the membrane.

The results in table 2.8 also show that the correction factor is much closer to θ than to the θ^2 proposed by Meares, [31] and found by a number of workers to give good agreement. [82] [84] This is in accordance with the theory proposed in section 2.2.4.

2.5.4. Transport Numbers.

The transport number of an ion in an exchanger represents the fraction of the current carried by that species of ion when a potential difference is applied across the exchanger and a current allowed to pass. Like the conductivity of the exchanger, the transport numbers of the ions depend on their concentrations and mobilities in the resin phase and on the influence of the solvent motion on the mobilities of the ions. Neglecting this last factor for the present, then the transport number of an ion may be written as

$$t_i = \frac{\bar{C}_i \bar{D}_i}{\sum_j \bar{C}_j \bar{D}_j} \qquad (2.102)$$

the summation in the denominator being carried out over all ionic species. The co-ion values calculated from this expression are shown in Table 2.10, and are, in all cases, greater than the experimental values shown in Table 2.11, and figure 2.11. There are two main causes of this difference: the interactions of the counter- and co-ions with one another, and the effect of the solvent motion on the mobilities of the ions.

The/

The diffusion coefficients of each ionic species in the exchanger are measured while the other species of ions are statistically at rest. In determining the transport numbers of the ions by passing a current through the exchanger, the counter- and co-ions are forced to move in opposite directions. There will, therefore, be an extra drag exerted by the counter-ions on the co-ions and vice versa. Owing to the difference in concentration of the ionic species, this effect will be much larger on the co-ions and so will tend to reduce their mobility by an amount greater than the corresponding reduction of the counter-ion mobility.

When a current is passed through two solutions separated by an ion-exchange membrane flow of solvent also occurs. This flow is usually in the same direction as the counter-ion flow and, therefore, enhances the mobility of these ions, while it tends to reduce the mobility and hence the transport number of the co-ions. The difference between the measured transport number and that calculated from equation (2.102) becomes greater as the external concentration increases. Since the mobility of the solvent decreases with increasing external concentration (see Table 2.13), the increased reduction of the transport number/

number must indicate that the co-ions are in regions in the exchanger where the effect of solvent transport is small in dilute solutions but becomes increasingly more important in more concentrated solutions. From this it may be deduced that initially the co-ions are in regions of low counter-ion concentration where any electro-osmotic transport due to the movement of sorbed counter-ions is small in comparison to the total water transport. As the electrolyte uptake increases the solvent transport associated with the sorbed counter-ions will become an ever increasing fraction of the total solvent flow, and hence the effect on the co-ion mobility will be increased. This hypothesis is in agreement with that proposed in section 2.55 on conductivity and in Chapter 3 on the structural analysis of the membranes.

2.5.5. Conductivity.

The specific conductivity of an aqueous solution of an electrolyte is governed by the concentrations and mobilities of the ions. The mobilities of the ions are themselves, influenced by the concentration, decreasing as the concentration of the solution increases. However, this decrease is fairly small, and is far outweighed by the effect of the increased number of current carrying ions, on the conductivity of the solution. For this reason, the specific conductivity of an aqueous electrolyte solution increases with increasing solution concentration. In ion-exchange resins the factors affecting the conductivity are similar in nature but the magnitudes of the changes in concentration and mobility of the ions in the exchanger phase, are somewhat different from those observed in free aqueous solutions. As shown in Tables 2.1 - 2.4, the total ionic concentration in the exchanger increases with increasing external solution concentration, the rate of increase, however, being much smaller in the exchanger. The mobilities of the ions in the resin are also functions of the external solution concentration but in this case their dependence on this factor is much more marked than in free solution. Due to the reduced swelling of exchangers in/

in concentrated solutions, the mobilities of the ions are greatly reduced as a result of the increased tortuosity of the paths along which the ions are forced to travel. As a result of the reduced water content of the exchanger in the more concentrated solutions, the convective contribution to the total conductivity is also reduced and this, along with the aforementioned factors, plays an important part in determining the variation of the conductivity of ion-exchangers with external solution concentration.

Several workers (28) (104) (105) (106) have observed that the conductivity of ion-exchangers increases with increasing solution concentration although the increase is by no means as great as for aqueous solutions. This means that, as the solution concentration increases, the effect of increasing ionic concentration in the exchanger is sufficient to overcome the decrease in conductivity due to increased tortuosity and the reduction of the convective contribution. Both sets of membranes studied in this work show interesting deviations from this pattern of behaviour.

C60N and C60E membranes.

As shown in table 2.12 the electric conductivities of both these membranes are quite large, a consequence of their/

their open structure and low tortuosity. The effect of expansion is to produce conductivity-concentration characteristics which are quite different from the normal form of the exchanger. Figure 2.10a shows that after an initial drop in conductivity, which is displayed by both membranes in the 0.1 to 0.5 molar range, the C60N membrane thereafter exhibits an almost constant conductivity, whereas the conductivity of the C60E membrane rises rapidly. Between 0.1M and 0.5M, the effect of increased tortuosity and reduced convective conductivity is dominant and leads to a decease in the membrane conductance. Thereafter, for the C60N membrane, the effect of increased ionic contration is large enough to cancel this effect, leaving the conductivity virtually unaffected by the increase in solution concentration. For the expanded membrane, the tortuosity increase is less and the increase in ionic concentration within the membrane is greater and hence an increase in the conductance of the membrane is observed.

As discussed in section (2.2.1a) the conductivity of an ion-exchanger is related to the concentrations and diffussion coefficients of the ions in the resin phase and to the magnitude of the convective conductivity. It is, therefore, possible to calculate the conductivity of the exchanger, if the values of these terms are known. The concentrations/

concentrations and diffusion coefficients of the ions are given in tables 2.1, 2.2., and 2.6 resp. The contribution of the convective conductivity can only be calculated if the mobility of the solvent is known. This term may be calculated in a number of ways, as described in section (2.2.1c), and the values of the water mobility calculated by a number of methods are given in Table 2.13. It is interesting to note that the value calculated using the transport number data is smaller than that calculated from the electro-osmotic flow data. This would suggest that the co-ions suffer less retardation from the flow of solvent than might be expected, a fact which in turn suggests that the co-ions are moving in regions where the solvent flow is smaller i.e. in regions of low counter-ion concentration. This deduction is in agreement with those obtained from the structural analysis of the membranes which is given in Chapter 3. The values of $\bar{u}_3$ calculated from equation (2.16) are, in every case, almost identical to those obtained from equation (2.15). This proves that the electro-osmotic flow of water must be directly proportional to the total water content of the membrane a point which will be discussed in more detail in section 2.5.7.
The values of the conductivity calculated using the above mentioned terms are shown in Table 2.12. Given that the membrane/

membrane is not as homogeneous as is assumed in the calculation of these results, the agreement between predicted and observed values of the conductivity is fairly good, the results obtained using the value of the water mobility calculated from the electro-osmotic data being in closer agreement with the observed values than those obtained using the transport number data. It is particularly satisfying to see that the calculated values show the same trends as the observed results, the conductivity of the C60N membrane falling while that of the C60E membrane falls initially then rises steeply.

The conductivity-concentration curves obtained in this work are quite different from those obtained by other workers using the same membranes but in the hydrogen form, Arnold and Koch [104] and Zapior, Leszko and Klinowski, [106] found that the conductivity of these membranes in sulphuric and hydrochloric acids resp., showed an increase in the concentration range studied at this present work. This may be due to a type of Grotthius chain conductance mechanism normally associated with hydrogen ion transport in aqueous solutions and to the much higher water content and hence lower tortuosity, of the hydrogen form of the membranes.

The/

The agreement of the predicted and observed specific conductivities of the membranes found in this study, is confirmation of the fact that the modified Nernst-Planck equation is a good approximation for these systems.

C100 and C100E membranes.

As shown in table 2.14 and figure 2.10b, the conductivities of the C100N and C100E membranes decrease with increasing external solution concentration over the whole range studied. This suggests that the increase in the ionic concentrations in these membranes is insufficient to compensate for the reduction in the mobilities of the ions produced by increased tortuosity. The conductivities of the C100 membranes are much lower than those of the C60 membranes, probably due to the tighter structure and greater tortuosity of the former. The effect of expansion is also quite different for the C100 membrane. Figure 2.10b shows that for the C100 membrane expansion produces a vertical displacement of the conductivity-concentration curve, a result which differs greatly from the effect of expansion of the C60 membrane, (figure 2.10a).

Since/

Since the diffusion coefficients of the ions in the C100 membranes have not been determined in this study, it is not possible to predict the conductivity of these membranes as it was for the C60N and C60E membranes.

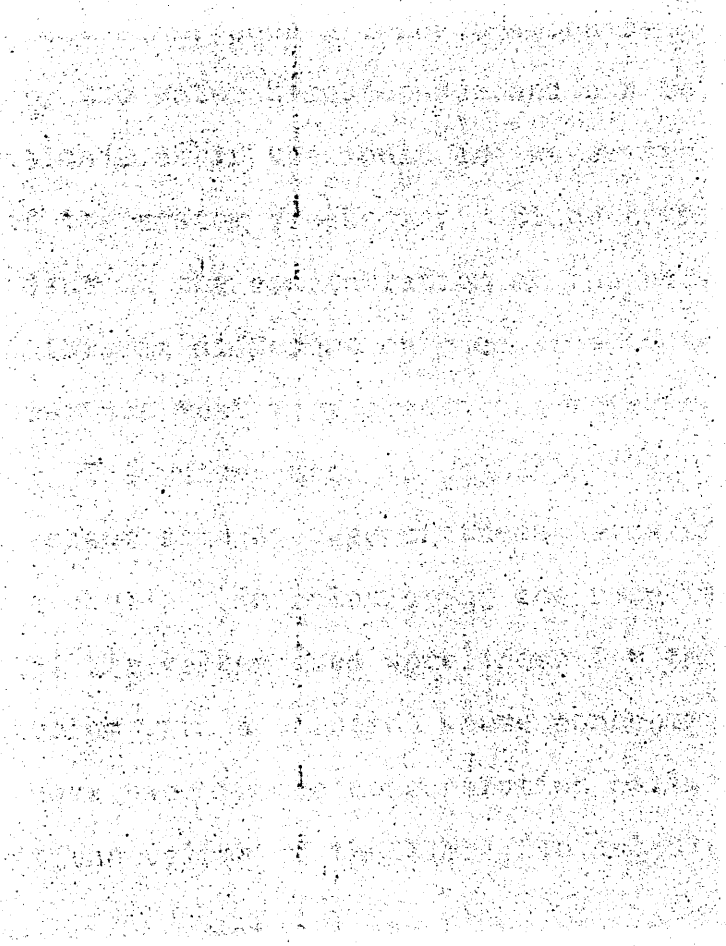

2.5.6. Membrane potentials.

The e.m.f. developed across a cation-exchange membrane separating two solutions of the same electrolyte of different concentration, and determined using electrodes reversible to the anion of the system, gives a measure of the ease with which the salt can diffuse through the membrane and, as such, is a measure of the counter-ion transport number of the membrane. As described in section 2.2.2b, the e.m.f. of such a concentration cell is also affected by the water transference and can be calculated from equation (2.68) if the ionic and water transference numbers of the system are known. Since both these factors are dependent on the concentration of the external solution and since this is different on each side of the membrane, these properties must vary across the thickness of the membrane. The values used in equation (2.68) must, therefore, represent some average of these terms for the membrane as a whole. In calculating the results shown in table 2.15, the values used were those for the membrane in equilibrium with a solution whose concentration was the mean of those used in the concentration cell. Table 2.15 shows that the values of the e.m.f. so calculated are in good/

good agreement with the observed values, thereby, not only confirming equation (2.68) but proving that the values used in this equation represent a very good estimate of the mean properties of the membrane. This is particularly interesting in the 0.5/1.5 molal cells, since at these two concentrations the membrane properties are quite markedly different.

Molal concentration units were used in the concentration cell experiments since the water and salt activities are given in the literature at integer molalities. The error resulting from use of the values of the membrane properties associated with the corresponding molar concentrations is negligible. Even at 1 molal the difference between the molal and molar concentrations is only approx. 2% which would give an error of less than 1% on any of the membrane properties, i.e. an error less than the uncertainty associated with each e.m.f. measurement.

2.5.7. Electro-osmosis and Water Transference numbers.

The concentration dependence of the electro-osmotic transport of both membranes is quite normal, showing behaviour similar to that observed with a number of other membranes. (84) (107) (108) The water transference number for both membranes is fairly high at a solution concentration of 0.1M, and falls, with increasing concentration, as shown in table 2.11 and figure 2.15. At low concentrations, the value for the expanded membrane is some 50% greater than that for the normal one, but at 2.0M, the difference is only approximately 10%. This demonstrates the effects of the two main factors affecting water transport - water content and ionic concentration in the membrane. The increased water content of the expanded exchanger allows a higher electro-osmotic transport, thus at low external concentration the water transference number of the expanded membrane is much greater than that for the normal one. As the external concentration increases, so the water content of both membranes decreases, reducing the electro-osmotic flow. As shown in section 2.5.1, the ratio of the water contents of the two exchangers at any given concentration is constant over the whole range studied; the lowering of the C60E water transference number relative to that of the C.60N membrane,/

membrane, must therefore, be a result of the increased salt uptake of the expanded exchanger. The electrolyte uptake of the C60E membrane is greater than that for the C60N membrane (tables 2.1 and 2.2). Thus, while at 0.1M there are approx. the same number of mobile ions in both membranes, as the external concentration increases, the C60E membrane has an ever increasing excess of mobile counter- and co-ions relative to the C60N exchanger. The number of moles of water associated with each ion will therefore fall more rapidly for the expanded membrane, and hence the electro-osmotic transport will also be reduced by a greater amount.

A number of authors have found that the electro-osmotic transport of water in ion-exchange membranes is dependent on the current density employed in the measurements. (73) (107) (108) (109) (110) (111) (112) Lakshminarayanaiah (107) reports that at concentrations of 0.1M and below the water transference number increase with decreasing current density. Others (7) (105) (108) (179) have found no evidence of this phenomenon. The effect of the current density on the t_3 value in the C60N and C60E membranes was examined in this study in particular at the lowest concentration studied, 0.1M, and the results are shown for this concentration in table 2.18. There is no dependence of t_3 on/

on current density for either membrane and this observation was confirmed at the higher concentrations.

The electro-osmotic transport in ion-exchangers is a very important property, having many far reaching ramifications. The effect of the water flow on the membrane transport number and conductivity has already been discussed in terms of electro-convectivity and it was seen that this phenomenon contributed largely to the excellent permselectivity and to the high conductivity exhibited by both membranes. There remain two further interesting features of the water transference number - its linear relationships to the counter-ion transference number and to the $\bar{C}_3/\bar{C}_1$ ratio.

Winger Ferguson and Kunin [68] and Stewart and Graydon [54] noted that in their studies, there was a linear relationship between the counter-ion and the water transference numbers. This linearity is also found in the C60N and C60E membranes used in this present study, as shown in figure 2.16. The error in t_3 required to fit the straight line is approx. 2% i.e. within the experimental error. This linear relationship between t_1 and t_3 has been/

been used to great advantage in calculating the frictional coefficients of all the species in the membrane, and hence will be dealt with more fully in section 2.6.4.

Kressman, [114] working on the cation-exchange membrane TNO 60 which is almost identical to the C60 membrane used here, found that with the lithium form of the exchanger in lithium hydroxide solution, the relationship between t_1 and t_3 was linear until t_1 fell below 0.8 when the curve deviated markedly from linearity. The counter-ion transport numbers for this sytem fell rapidly as the external concentration increased, probably as a result of the high mobility of the hydroxide co-ion. It may be that investigation of the t_3 - t_1 relationship in the C60 membranes in sodium chloride solution of much higher concentration would also reveal a similar deviation from linearity, but over the range studied, the linear relationship was maintained.

Spiegler [21] has proposed that for very porous membranes studied in the leached condition, a large part of the water molecules can remain at a distance from the matrix. This reduces the frictional interaction between the water and the solid matrix. With this assumption he then proposes/

proposes that his equation (43) would reduce to,

$$t_3 - H = \bar{c}_3^*/\bar{c}_1 \qquad (2.103)$$

where H represents the hydration number of the counter-ion and $\bar{c}_3^*$ is the concentration of free water in the membrane. For a membrane which contains sorbed electrolyte, the above equation has to be somewhat modified, as shown in Appendix A.10.

If no assumptions are made concerning the state of hydration of the ions, then the expression (A.10.7) becomes

$$t_3 = P.\ \bar{c}_3(t_1 - t_2)/(\bar{c}_1 + \bar{c}_2) \qquad (A.10.8)$$

A plot of t_3 against $\bar{c}_3(t_1 - t_2)/(\bar{c}_1 + \bar{c}_2)$ should then be a straight line. The plots for the C60N and C60E membranes are shown in figure 2.17. The relationship is linear for both membranes and the value of P is 0.45 for the normal membrane and 0.54 for the expanded form. The two plots intersect on the t_3-axis where t_3 is 2.0. The concurrence of the two plots at this point suggests that the finite intercept on the t_3-axis is due to the hydration of the ions and is not a function of the membranes.

If the effects of hydration are specifically included in the calculation using equation (A.10.2), then the plots obtained are shown in figure 2.18. The relationship

between/ ·

between t_3^* and $\bar{c}_3^*(t_1-t_2)/(\bar{c}_1+\bar{c}_2)$ is also linear for both membranes the values of P* being 0.50 and 0.58 for the normal and expanded membranes resp., and the two plots again intersect on the t_3-axis. The point of intersection with the axis is dependent on the values of the hydration numbers used for the ions, although the slopes of the lines are unaffected.

There are two ways in which the term $\bar{c}_3^*(t_1-t_2)/(\bar{c}_1+\bar{c}_2)$ may take a zero value:

(a) If $\bar{c}_3^* = 0$, then the free water concentration in the membrane is zero and the only flow of water is that of hydration water. Since t_3^* neglects hydration water flow, then t_3^* must also take the value zero.

(b) If $t_1 = t_2$, then the transport numbers of the counter- and co-ions are equal and the free water transported in each direction must be equal. Therefore, no net flux of free water occurs, and again t_3^* must be zero.

These considerations imply that the t_3^* against $\bar{c}_3^*(t_1-t_2)/(\bar{c}_1+\bar{c}_2)$ plots should pass through the origin of the co-ordinate system. Using $H_2=H_4 = 0.9$, [38] the value of H_1 which fits this requirement is 3.6 as shown in figure 2.19./

2.19. This value for the hydration number of sodium, although larger than that obtained by Glueckauf [38] is not at all unreasonable when compared with some of the values obtained in aqueous solutions. This value of H_1 depends on the values taken for H_2 and H_4, particularly that for H_4. The greater the value of H_4, the smaller the value of H_1 required to fit the above conditions.

A plot of t_3 against $\bar{c}_3/\bar{c}_1$ is also linear, the points for both membranes falling on one line, as shown in figure 2.20. By neglecting the effect of the co-ion in transporting water, this relationship attributes to the counter-ion a degree of hydration which is far in excess of its true value, and hence, the intercept on the t_3-axis is negative. The interest in this equation is the co-incidence of the plots for the two membranes. The explanation of this phenomenon may be seen by considering the form of the expression for t_3. The water transference number may be written

$$t_3 = J_3F/I = J_3F/(z_1J_1 + z_2J_2)F \qquad (2.60)$$
$$= J_3/(z_1J_1 + z_2J_2)$$

If/

If J_2 is small compared to J_1 as it is in the exchangers studied here, then,

$$t_3 = J_3/z_1J_1 \qquad (2.104)$$

$$= J_3/J_1 \quad (\text{since } z_1 = +1 \text{ for a cation-exchanger})$$

$$= \bar{c}_3v_3/\bar{c}_1v_1 \qquad (2.105)$$

Thus if v_3/v_1 is a constant, then t_3 is proportional to $\bar{c}_3/\bar{c}_1$. Calculations for both membranes show that within experimental error the value of v_3/v_1 is indeed constant and equal to 0.59. This means that in the electrical potential gradient experiments, the linear velocity of the counter-ions is 1.7 times that of the water, and explains why the plot of t_3 against $\bar{c}_3/\bar{c}_1$ is linear and coincident for both membranes.

The t_3 against $\bar{c}_3/\bar{c}_1$ plot does not pass through the origin as might be expected from the above calculation. However, the values of $\bar{c}_3$ used to obtain the plot are the total water concentrations in the membrane. Since some of the water is present as water of hydration of the ionic species, the value of $\bar{c}_3$ which should be used is less than the total water concentration.

A number of workers have observed that the water transference number is approximately half the ratio $(\bar{c}_3/\bar{c}_1)$. The value of 0.59 found in this study (54) (68) (177) (178)

falls/

falls within the range of values exhibited by the other membranes studied in this way. The explanation of this recurring factor may be found by considering the frame of reference used in membrane studies, namely the membrane itself. Under an applied electric potential gradient and on a solvent fixed frame of reference, the counter-ions and fixed charges would move in opposite directions with velocities of v_1' and v_4' respectively. Changing to a membrane fixed frame of reference, the counter ions now have a velocity of $v_1=v_1' + v_4'$ and the solvent a velocity of $v_3=v_4'$. Therefore, the ratio v_3/v_1 is equal to $v_4'/(v_1' + v_4')$. Since 1 and 4 are both ionic species, their velocities might be expected to be similar, so that the ratio v_3/v_1 takes a value of approximately 0.5 as observed.

Spiegler's[21] equation (43) may be written in terms of the frictional coefficients, R_{13} and R_{34} which will be used in chapter 4, and the relation then becomes

$$J_3/J_1 = \bar{c}_3/(\bar{c}_1 + \bar{c}_3(\bar{c}_4 R_{34}/\bar{c}_3 R_{13})) \qquad (2.106)$$

Anticipating the values of R_{13} and R_{34} calculated in chapter 4 using a completely different method, the values of t_3 for both membranes in 0.1M sodium chloride solution may be obtained. In table 2.19 these values and the measured values are shown, and the agreement is fairly good showing that/

that Spiegler's pore model is useful for predicting electro-osmotic transport in dilute solutions.

2.5.8. Osmosis.

When two aqueous solutions of the same electrolyte, but of different concentrations, are separated by an ion-exchange membrane, a chemical potential gradient is set up, not only for the electrolyte but also for the water. This water activity gradient is, of course, in the opposite sense to that for the salt, and hence it might be expected that salt and water flow would occur in opposite directions, the water flow being from the more dilute to the more concentrated solution. This phenomenon is known as normal osmosis. Normal osmosis is found to occur in the case of both the C60N and the C60E membranes, the water flow rate being shown in table 2.16. For both concentration gradients studied, the flow rate for the expanded membrane was found to be 2-3 times that for the normal one, an observation which is consistent with the higher water content and more open structure of the C60E membrane.

A comparison of the forces acting on the water shows that in the 0.5/1.5 molal concentration cell, the force is some ten times greater than that in the 0.05/0.15 cell (table 2.17), while the water flow rate is only increased by a factor of approximately 2.5. The two main factors producing this effect are the much reduced water contents of/

of the membranes at the higher external solution concentrations and the increased salt flow occurring in the opposite direction to the water flow, and producing a coupled flow of water counter to the main osmotic flow. This latter effect is shown explicitly in the non-equilibrium thermodynamic treatment given in section (2.2.2b).

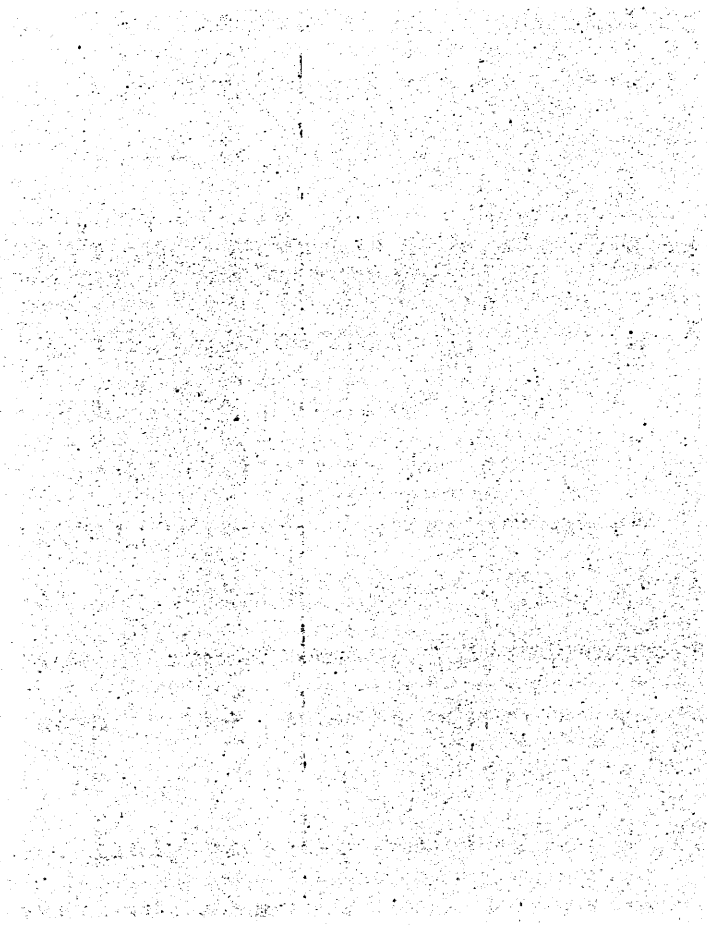

2.5.9. Salt flow.

Table 2.16 shows that, as with the osmotic flow, the salt flow for the C60E membrane is greater than that for the C60N membrane, the factor in this case being approximately three. The effect of using solutions of higher concentration is much more marked, however, in the case of the electrolyte flow than it is for the osmotic flow. The forces acting on the salt in both cells are very similar (table 2.17) yet the salt flow is some thirty times greater in the more concentrated solutions, a direct result of the increased electrolyte uptake of the membranes. The salt flow is governed mainly by the concentration and mobility of the co-ions in the membrane.[115] [116] [117] At low external solution concentrations, where the electrolyte uptake is small, the co-ion content of the exchanger is low and hence the salt flow rate is also small. At higher concentrations, however, the co-ion concentration increases rapidly and the membrane becomes a less efficient barrier to salt flow. The effect of this enhanced salt diffusion is to be seen in the membrane potential measurements where the e.m.f. of the cell falls off from its initial value much more rapidly when external solutions of high concentration are used.

2.5.10. Conclusions.

The results and discussion above show quite clearly the effect of the matrix expansion on some of the transport and equilibrium properties of the cation exchange membrane AMF C60. As shown by the water content results, the effect of expansion is constant throughout the range of concentration studied. The increased water content of the expanded form results in a lower tortuosity for this membrane with a consequent increase in the flow rate of the mobile species through the membrane. The tortuosity factor, θ, gives a very good fit over the entire range, the agreement being better for the co-ion than for the counter-ion, probably for the reasons already discussed. Other work on the same two membranes by Paterson and Ferguson [118] has shown that for water diffusion, this tortuosity factor gives an excellent correspondence with the results from aqueous solutions of the same concentration, supplying further evidence for this choice of correction.

The extended form of the Nernst-Planck equation, which includes the effects of convection but not of ionic interactions, has been shown to work very well in predicting the nature of the variation in conductivity of the ion-exchange membranes./

membranes. The explanation of this good agreement is to be found by considering the comparison of the Nernst-Planck equation with the more rigorous non-equilibrium thermodynamic treatment as shown in section (2.2.3). The difference between the two approaches is due to the term l_{12} which has been shown to be very small, even when the exchanger is in equilibrium with concentrated electrolyte solutions.

The effects of convection are very important in both exchangers, especially in the more concentrated solutions. At 0.1M, the convective conductivity contribution is more than 50% of the total conductivity, while, the relatively high counter-ion transport numbers obtained for both membranes even at the higher concentrations, is due largely to the effect of convection.

The C60N membrane displays properties which are very desirable in an ion-exchange membrane, namely, high electric conductivity and low co-ion transport number. The expanded form has a higher conductivity but at the expense of a slightly reduced counter-ion transport number. Even so, the transport properties of this exchanger, in concentrated solutions, are extremely good for many of the practical applications of ion-exchange membranes.

The conclusions to be drawn from the transport data

on/

on the two membranes studied, support the hypothesis that, in many respects, ion-exchangers can be regarded as concentrated electrolyte solutions and that many of the relations used for these solutions can be suitably modified by considering tortuosity and convection, to apply to ion-exchange systems.

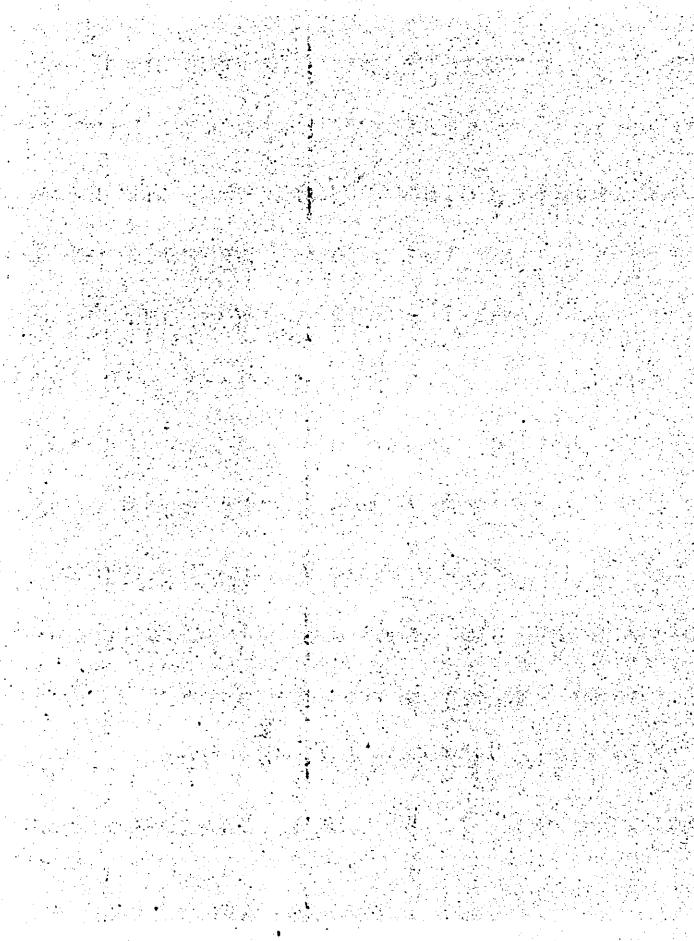

2.6. Non-Equilibrium Thermodynamic Approach Methods of Calculation of Results.

A number of methods of calculation have been employed in determining the frictional and mobility coefficients from the transport and diffusion data given in section 2.4. Using only the data given in section 2.4, there is, unfortunately, one more unknown than there are independent phenomenological equations and hence some assumptions about the system have to be made in order to obtain an estimate of all the phenomenological coefficients. A number of assumptions have been proposed by other authors, and each of these, together with any new relations suggested by this present study will be treated in the following sections.

In all of the succeeding calculations it has been assumed that the average frictional and mobility coefficients R^*_{ij} and l^*_{ij}, used to describe the systems with salt concentration gradients, are identical to those which apply to the membrane in equilibrium with an electrolyte solution whose concentration is the mean of those used in the concentration cell. There are no a priori reasons for accepting this assumption but the reasonable agreement between the observed and predicted e.m.f's of the concentration cells (see/

(see section 2.5.6. and table 2.15) suggests that this assumption is acceptable.

2.6.1. Neglecting isotope - isotope interactions.

This assumption was implicit in the theory presented by Spiegler, [21] and first tested experimentally by Meares, [46] in which it was suggested that only five transport and diffusional experiments were sufficient to give the values of the major frictional interactions in the membrane. Spiegler's equation (24) is equivalent to equation (2.43) of this treatment, except that R_{11}' and R_{12}' have been omitted from Spiegler's considerations. Similarly in Spiegler's calculation based on the co-ion diffusion coefficient, R_{22}' was ignored. While neglecting the isotope-isotope interactions, whether by accident or design, Spiegler chose also to set R_{12} equal to zero. This assumption has been challenged by Spiegler himself [21] and by a number of other authors. [22] [23] It seems likely that this assumption is not a good one and has not been used in this present work. A number of questions have also been raised concerning the validity of assuming that isotope-isotope interaction is zero, [24] [57] and it is one of the aims of this study to ascertain whether or not this assumption applies to the membrane systems studied here.

Since only one assumption is required to enable a complete/

complete calculation of phenomenological coefficients to be undertaken, each of the assumptions, $R_{11'} = 0$ and $R_{22'} = 0$, have been made in turn and the values of the resulting coefficients compared, not only with one another, but with the results calculated from other, perhaps better estimates.

2.6.2. Using Mobility coefficients and assuming $l_{12} = 0$.

This is equivalent to using the five equations (2.72a - e) and assuming $l_{12} = 0$ in order to calculate the remaining five unknown l-coefficients. These five l-coefficients may then be obtained and from them, by matrix inversion, the frictional coefficients may be calculated. As shown by Miller [9] for aqueous electrolyte solutions, l_{12} is concentration dependent, tending to zero as c tends to zero. It seems probable then, that l_{12} in the exchanger will tend to zero when the co-ion uptake is small, as is the case for both the C60N and C60E membranes in equilibrium with 0.1M sodium chloride solutions; the ratio $\bar{c}_2/\bar{c}_1$ is 2.48×10^{-3} for the normal membrane and 5.42×10^{-3} for the expanded one.

A method very similar to the one just described is to use equations (2.56), (2.61b) (2.61c), (2.70), and (2.71), which were developed for the completely general case, and then, in the light of the above discussion, to assume that l_{12} and l_{23} are both zero.

Both of these methods are applicable only to systems where the co-ion concentration is low, i.e. in this case to the/

the membranes equilibrated with 0.1M sodium chloride solutions.

2.6.3. Assuming concentration dependence of l_{13} and l_{23}.

In the preceding section it was assumed that l_{12} was concentration dependent. If this assumption is extended to include all the interactions of the ions with the water, then this provides yet another method of obtaining a complete analysis of the membrane system. The interactions of counter- and co-ions with the water molecules are ion-dipole interactions and must therefore, be of the same order of magnitude. Therefore, assuming the concentration dependence of the l-coefficients, the following relation may be written:

$$l_{13}/l_{23} = \bar{c}_1/\bar{c}_2. \qquad (2.107)$$

This relation can, at best, be regarded as an estimate of l_{23}, but where $\bar{c}_2 > \bar{c}_1$, the value of l_{23} will be small and will not affect the values of the other coefficients significantly. In these circumstances, any reasonable estimate of l_{23} will be sufficient to allow a complete analysis of the system. This assumption will work best where $\bar{c}_2$ is small compared to $\bar{c}_1$ but it may also be used at higher $\bar{c}_2$ values to provide estimates of the phenomenological coefficients.

Some/

Some direct support for this type of relation comes from Miller's treatment of ternary systems [30], where he used the mole fractions of the various species and the values of the l-coefficients in binary systems to predict, fairly accurately, the values of the l-coefficients in the ternary systems.

2.6.4. Using the linearity of the t_3 versus t_1 plot.

The fact that t_3 is linearly related to t_1 (figure 2.16) may be used to give a further relation between the frictional coefficients of the system. Using equation (2.73c) for the case of an applied electric potential, where $X_3 = 0$, it may be shown, on substituting $t_2 = 1 - t_1$ and rearranging, that

$$t_3 = -\left(\frac{R_{13} + R_{23}}{R_{33}}\right). t_1 + \frac{R_{23}}{R_{33}} \qquad (2.108)$$

Thus, if as in the present case, a linear relationship between t_3 and t_1 is observed, the gradient and/or intercept of the t_3-t_1 plot may be used to give a further equation involving the frictional coefficients. Using this relation, it is, therefore, possible to give a complete analysis of the system without making any assumptions concerning the values of the frictional coefficients involved. This method may be used equally well over the entire concentration range for which the linear $t_3 - t_1$ relation is valid.

This method of calculation is superior to the others listed above since no specific assumptions concerning the system are required and all the relationships are experimentally determined. It is, nevertheless, interesting to compare the results so calculated with those obtained from the above/

above assumptions and hence determine which assumptions best fit the experimental data.

2.7. Results.

Estimated error in major I- and R-coefficients is ± 5%.

Units R-coefficients : $mole^{-2}$. joule. cm. sec.

I-coefficients : $mole^{2}$. $joule^{-1}$. cm^{-1}. sec^{-1}.

Table 2.20.

C60N External solution: 0.1M sodium chloride at 25°c. Frictional coefficients.

Method of calculation	R_{11} x10^{-12}	R_{12} x10^{-12}	R_{13} x10^{-10}	R_{14} x10^{-11}	R_{22} x10^{-14}	R_{23} x10^{-11}	R_{24} x10^{-11}	R_{33} x10^{-9}	R_{34} x10^{-10}
1	+1.44	-2.72	-7.07	-0.58	+4.20	+2.68	-35.0	+6.61	-5.84
2	+1.01	+4.37	-2.99	-4.42	+3.02	-4.13	+29.1	+2.70	-2.15
3	+1.01	+1.57	-3.00	-4.28	+3.49	-1.44	+3.77	+2.76	-2.32
4	+1.01	+1.62	-2.99	-4.34	+3.49	-1.49	+4.09	+2.75	-2.32
5	+1.07	+0.51	-3.58	-3.77	+3.64	-0.47	-4.95	+3.31	-2.84

Methods.

1. Using $R_{11}' = 0$.
2. Using $R_{22}' = 0$.
3. Using $R_{13}/R_{23} = 0.208$ (from $t_3 = t_1$ relation)
4. Using $l_{12} = 0$, and matrix inversion.
5. Using $l_{13}/l_{23} = c_1/c_2$, and matrix inversion.

Table 2.21.

C60E. External solution: 0.1M sodium chloride at 25°c. Frictional coefficients

Method of calculation	R_{11} x10	R_{12} $x10^{-12}$	R_{13} $x10^{-10}$	R_{14} $x10^{-11}$	R_{22} $x10^{-14}$	R_{23} $x10^{-11}$	R_{24} $x10^{-11}$	R_{33} $x10^{-9}$	R_{34} $x10^{-10}$
1	+1.14	-1.35	-4.18	-0.45	+1.32	+0.96	+6.13	+2.67	-2.85
2	+0.85	+1.56	-2.24	-2.75	+1.03	-0.96	-21.0	+1.38	-1.32
3	+0.84	+1.65	-2.18	-2.83	+1.02	-1.02	-21.9	+1.34	-1.28
4	+0.70	+1.34	-1.29	-3.71	+1.06	-0.82	+2.26	+0.79	-0.73
5	+0.78	+0.37	-1.84	-3.05	+1.14	-0.23	-3.84	+1.16	-1.18

1. Using R_{11}, = 0.
2. Using R_{22}, = 0.
3. Using R_{13}/R_{23} = 0.213, (from $t_3 - t_1$ relation)
4. Using l_{12} = 0, and matrix inversion.
5. Using $l_{13}/l_{23} = c_1/c_2$, and matrix inversion.

Table 2.22

C60N External solution: 0.1M sodium chloride at 25°c. Mobility coefficients.

Method of Calculation	l_{11} x10^{12}	l_{12} x10^{16}	l_{13} x10^{11}	l_{22} x10^{15}	l_{23} x10^{13}	l_{33} x10^{10}
1	+1.47	0.0	+1.60	+2.94	+1.59	+5.47
2	+1.47	-1.96	+1.59	+2.75	+0.39	+4.74
3	+1.47	0.0	+1.58	+2.94	0.0	+4.56

Methods:
1. Using $l_{12} = 0$.
2. Using $l_{13}/l_{23} = c_1/c_2$.
3. Using $l_{12} = l_{23} = 0$.

Table 2.23.

C60E External solution: 0.1M sodium chloride at 25°c. Mobility coefficients.

Method of Calculation	l_{11} x10^{12}	l_{12} x10^{15}	l_{13} x10^{11}	l_{22} x10^{14}	l_{23} x10^{12}	l_{33} x10^{9}
1	+2.05	0.0	+3.36	+1.03	+1.07	+1.93
2	+2.05	-1.48	+3.27	+0.88	+1.18	+1.39
3	+2.05	0.0	+3.25	+1.03	0.0	+1.29

Methods: Using $l_{12} = 0$.
Using $l_{13}/l_{23} = c_1/c_2$.
Using $l_{12} = l_{23} = 0$.

Table 2.24a

External solution: 0.1M sodium chloride at 25°c.

$c_i R_{ii}$ x 10^{-11}	C60N	C60E	1.0M NaCl
$c_1 R_{11}$	9.9	8.2	2.4
$c_2 R_{22}$	8.5	5.3	1.5
$c_3 R_{33}$	5.3×10^{-1}	3.4×10^{-1}	0.61×10^{-1}

Table 2.24b

External solution: 0.1M sodium chloride at 25°c.

$\frac{c_i R_{ii}\text{ (membrane)}}{c_i R_{ii}\text{ (soln)}}$	C60N	C60E
i = 1	4.1	3.4
i = 2	5.6	3.5
i = 3	8.6	5.5
average (1,2)	4.8	3.5

NOTE: C60N. $\theta = 4.8$ C60E. $\theta = 3.5$

Table 2.25.

External solution: 0.1M sodium chloride at 25°C.

Membrane	l_{11}/c_1 x10^{12}	l_{22}/c_2 x10^{12}	l_{33}/c_3 x10^{11}
C60N	1.50	1.21	2.88
C60E	2.14	1.98	7.7

l-coefficients calculated assuming $l_{12} = 0$.

Table 2.26.

External solution: 0.1M sodium chloride at 25°c $l_{12} \times 10^{15}$

Method of calculation	C6ON observed	C6ON from Staverman	C6ON from Spiegler	C6OE observed	C6OE from Staverman	C6OE from Spiegler
1	0.0	14.6	4.65	0.0	65.4	18.6
2	-0.19	3.63	1.32	-1.48	11.1	4.16

Methods

1. Using $l_{12} = 0$.
2. Using $l_{13}/l_{23} = c_1/c_2$.

Table 2.27.

External solution: 0.1M sodium chloride at 25°c.
Observed and predicted salt flows.

C6ON J_s obs.	C6ON J_s calc.	C6OE J_s obs.	C6OE J_s calc.
3.90×10^{-10}	4.32×10^{-10}	1.22×10^{-9}	1.51×10^{-9}

Table 2.28.

External solution: 1.0M sodium chloride at 25°c. Frictional coefficients.

C6ON

Method of calculation.	R_{11} x10^{-12}	R_{12} x10^{-12}	R_{13} x10^{-10}	R_{14} x10^{-11}	R_{22} x10^{-13}	R_{23} x10^{-11}	R_{24} x10^{-11}	R_{33} x10^{-9}	R_{34} x10^{-10}
1	+1.52	+0.39	-7.66	-5.20	+1.45	-0.63	-6.99	+9.00	-4.75
2	+1.33	+1.01	-4.97	-7.74	-1.25	-1.51	+1.35	+5.14	-1.10
3	+1.26	+1.25	-3.89	-8.77	+1.17	-1.87	+4.70	+3.59	+0.37
4	+1.59	+0.54	-8.41	-4.98	+1.41	-0.85	+2.59	+9.79	+1.50

Method.

1. Using R_{11} = 0.
2. Using R_{22} = 0.
3. Using R_{13}/R_{23} = 0.208 (from t_3-t_1 relation).
4. Using $l_{13}/l_{23} = c_1/c_2$, and matrix inversion.

Table 2.29.

External Solution: 1.0M sodium chloride at 25°c. Frictional coefficients.

C6OE

Method of calculation.	R_{11} $\times 10^{-11}$	R_{12} $\times 10^{-12}$	R_{13} $\times 10^{-10}$	R_{14} $\times 10^{-11}$	R_{22} $\times 10^{-13}$	R_{23} $\times 10^{-11}$	R_{24} $\times 10^{-11}$	R_{33} $\times 10^{-9}$	R_{34} $\times 10^{-10}$
1	+0.96	-0.16	-4.21	-2.45	+0.49	+0.05	-7.40	+4.04	-3.33
2	+0.81	+0.24	-2.48	-4.91	+0.38	-0.42	-0.66	+2.01	-0.45
* 3	+0.73	+0.47	-1.49	-6.32	+0.32	-0.70	+3.22	+0.84	+1.21
4	+0.89	+0.10	-3.32	-3.86	+0.42	-0.26	-3.01	+2.94	-1.62

Methods

1. Using $R_{11} = 0$.
2. Using $R_{22} = 0$.
3. Using $R_{13}/R_{23} = 0.213$ (from t_3-t_1 relation).
4. Using $l_{13}/l_{23} = c_1/c_2$ and matrix inversion.

*NOTE: $R_{22}.R_{33} \leqslant R_{23}^2$: violation of basic theory of irreversible thermodynamics. (in method 3).

Table 2.30a

External solution: 1.0M sodium chloride at 25°c. $c_1R_{11} \times 10^{-12}$

Method of calculation.	C60N	Corresponding NaCl solution value X θ	C60E	Corresponding NaCl solution value X θ
1	1.52	1.38	0.93	1.00
2	1.68		1.03	

Table 2.30b

External solution: 1.0M sodium chloride at 25°c. $c_2R_{22} \times 10^{-12}$

Method of calculation.	C60N	Corresponding NaCl solution value X θ	C60E	Corresponding NaCl solution value X θ
1	1.11	0.89	0.58	0.64
2	1.21		0.68	

Table 2.30c.

External solution: 1.0M sodium chloride at 25°c. $c_3R_{33} \times 10^{-10}$

Method of calculation.	C60N	Corresponding NaCl solution value X θ	C60E	Corresponding NaCl solution value X θ
1	6.10	4,25	1.80	3.10
2	10.7		4.20	

Methods for Tables 2.30a-c.

1. Using R_{13}/R_{23} from t_1-t_3 relationship.
2. Using average value for all assumptions, except R_{11}, = 0.

Table 2.31

External solution: 1.0M sodium chloride at 25°c. $l_{12} \times 10^{14}$

Method of calculation	C6ON		C6OE	
	Present Study	from Staverman *	Present Study	from Staverman
1	1.63	9.1	9.58	27.4

1. Using $l_{13}/l_{23} = c_1/c_2$

* Reference: (22)

Table 2.32. External solution: 0.1M sodium chloride at 25°c

Method of calculation	C6ON $c_3R_{13} \times 10^{12}$	C6ON $c_4R_{14} \times 10^{11}$	C6OE $c_3R_{13} \times 10^{12}$	C6OE $c_4R_{14} \times 10^{11}$
1	-0.57	-4.32	-0.56	-2.63
2	-0.57	-4.18	-0.55	-2.70
3	-0.57	-4.24	-0.32	-3.54
4	-0.68	-3.69	-0.46	-2.91

1. Using $R_{11}' = 0$.
2. Using $R_{22}' = 0$.
3. Using R_{13}/R_{23} from t_1-t_3 relationships.
4. Using $l_{13}/l_{23} = c_1/c_2$.

Table 2.33

External solution: 1.0M sodium chloride at 25°c. Mobility Coefficients.

Membrane	l_{11} x10^{12}	l_{12} x10^{14}	l_{13} x10^{11}	l_{22} x10^{14}	l_{23} x10^{13}	l_{33} x10^{10}
C60N	+1.16	+1.63	+1.01	+7.52	+7.91	+1.96
C60E	+1.97	+9.58	+2.31	+25.7	+33.4	+6.31

l-coefficients obtained using $l_{13}/l_{23} = c_1/c_2$.

Table 2.34.

External solution: 1.0M sodium chloride at 25°c.

Membrane	l_{11}/c_1 x10^{12}	l_{22}/c_2 x10^{12}	l_{33}/c_3 x10^{11}
C60N	0.96	0.80	1.16
C60E	1.55	1.40	2.88

l-coefficients obtained using $l_{13}/l_{23} = c_1/c_2$.

Table 2.35.

External solution: 1.0M Sodium chloride at 25°c.

Method of calculation	C60N c_3R_{13} x10^{-12}	C60N c_4R_{14} x10^{-11}	C60E c_3R_{13} x10^{-12}	C60E c_4R_{14} x10^{-11}
1	-0.84	-8.63	-0.54	-5.34
2	-0.66	-9.77	-0.33	-6.87
3	-1.42	-5.55	-0.73	-4.20

1. Using $R_{22} = 0$.
2. Using R_{13}/R_{23} from t_1-t_3 relationship.
3. Using $l_{13}/l_{23} = c_1/c_2$.

Table 2.36.

i	C60N $\frac{l_{ii}/c_i\ (0.1)}{l_{ii}/c_i\ (1.0)}$	C60N $\frac{\theta(1.0)}{\theta(0.1)}$	C60E $\frac{l_{ii}/c_i\ (0.1)}{l_{ii}/c_i\ (1.0)}$	C60E $\frac{\theta\ (1.0)}{\theta\ (0.1)}$
i = 1	1.56	1.17	1.38	1.18
i = 2	1.52	1.17	1.41	1.18
i = 3	2.55	1.17	2.67	1.18

2.8. Discussion.

The discussion consists of comments on, and comparisons of, the values of the frictional and mobility coefficients calculated for both membranes as described above, considering the 0.1M and 1.0M cases separately, followed by general discussion of the trends exhibited by the results.

2.8.1. C60N and C60E. 0.1M sodium chloride solutions.

Tables 2.20 and 2.21 show the values of all the frictional coefficients R_{ij}, calculated by a number of different methods, while tables 2.22 and 2.23 show the mobility coefficients, l_{ij}, from which some of the R-coefficients have been obtained. The most interesting observation to be made from tables 2.20 and 2.21 is the remarkable agreement between the R-coefficients calculated using assumptions 2, 3, 4 and 5. As already discussed, in section 2.6.4, the values calculated using the $t_3 - t_1$ relationship are considered to represent the best analysis of the system. The fact that three other assumptions give almost identical results is indeed surprising and lends credence to the validity of these assumptions for this system.

It may be seen that the results obtained using assumption/

assumption 1, ($R_{11'} = 0$), differ considerably from those obtained from the other assumptions. This suggests that the isotope-isotope interaction of the counter-ions is not zero. The ratios $R^{x}_{11}/R_{11'}$ are 1.42 and 1.36 for the normal and expanded membranes respectively, values which, allowing for the errors involved, must be considered to be very similar, if not identical. The values of $R_{11'}$ are -4.3×10^{11} and -3.0×10^{11} for the C60N and C60E membranes respectively. Since $R_{11'}$ represents a frictional interaction between two species of the same sign it might be expected that the sign of $R_{11'}$ would be positive. (28) (113) There seems little doubt from the above calculations that $R_{11'}$ is negative but no explanation of this anomaly is suggested at this time. The magnitude of $R_{11'}$ is fairly large, - almost of the same order as R_{11}, and, therefore, it has a considerable influence on the calculation of the other R-coefficient values. This does not appear to be the case with $R_{22'}$, since the analysis carried out neglecting this term -assumption 2- gives results very similar to those obtained using the other assumptions 3, 4, and 5.

The explanation of this can be seen by examining the two following equations,

$\bar{c}_2/$

$$\bar{c}_2 R_{22} = \bar{c}_1 R_{21} + \bar{c}_3 R_{23} + \bar{c}_4 R_{24} \qquad (2.109)$$

$$\bar{c}_2 R_{22}^{x} = \bar{c}_2 (R_{22} - R_{22'})$$

$$= \bar{c}_2 R_{22} - \bar{c}_2 R_{22'}. \qquad (2.110)$$

In (2.110), $c_2 R_{22'}$ represents the frictional interaction of one mole of species 2' with those species 2 in unit volume in the vicinity. Since $R_{22'}$ measures an ion-ion interaction its value should be of the same order of magnitude as the other ion-ion interactions particularly R_{21} and R_{24}. Therefore, since species 2 is a minor component of the system, $\bar{c}_2$ is very small and $\bar{c}_2 R_{22'}$ is small compared to $\bar{c}_1 R_{21}$ and $\bar{c}_4 R_{24}$, i.e. the terms of $\bar{c}_2 R_{22}$. Therefore, the difference between $\bar{c}_2 R_{22}$ and $\bar{c}_2 R_{22}^{x}$ is negligible and the assumption that these terms are equal is fairly satisfactory. A similar argument for species 1 and 1' shows why $\bar{c}_1 R_{11'}$ is a fairly major term of $\bar{c}_1 R_{11}^{x}$ and explains why the assumption that $c_1 R_{11'} = 0$ does not yield good results.

The difference between R_{22}^{x} and R_{22} is only approx. 14%, and since the error on the R-coefficients is considered to be of this order of magnitude, no good estimate of $R_{22'}$ is possible.

No great reliance can be placed on the values of R_{12}, R_{23}/

R_{23} and R_{24} since their magnitudes and indeed, their signs are dependent on the input data. Fairly large variations in the values of these coefficients can be achieved by using different t_2 values which fall within the experimental error on this measurement. Much greater accuracy in the determination of transport numbers would be required in order to obtain precise values of the co-ion frictional coefficients. One exception to the above is the value of R_{23} which is calculated using the t_3-t_1 relationship. Here, R_{23} is obtained directly from the value of R_{13} one of the more precisely defined terms.

Since R_{12} like R_{14} measures the interaction of positively and negatively charged species it would be expected that the sign of these terms would be negative,[28] whereas the calculated value of R_{12} is positive. No explanation can be offered for this apparent anomaly except to suggest that since the value of R_{12} is one of the least accurate results, no conclusions should be drawn from this discrepancy. The sign of R_{24} is subject to some variation depending on the assumptions made in the calculation. According to convention, R_{24} should be positive since it measures the interaction of two negatively charged species, but like

R_{12}/

R_{12} the value of R_{24} must be in some doubt and therefore, no great importance can be attached to the variations observed. The other ion-ion interaction, measured by R_{14}, is precisely defined and in all cases is of the expected sign.

The frictional interactions of all the ionic species with water, R_{13}, R_{23} and R_{34}, are all of the same order of magnitude, suggesting that the type of interaction is similar in all three cases. Since species 1 and 4 must occupy similar regions of the exchanger, it is interesting to compare their values. In all cases, the value of R_{34} is lower than R_{13}, the ratio R_{34}/R_{13} having a value of 0.78 for the C60N membrane and 0.61 for the C60E membrane. For sodium chloride at 3.0 molal, the ratio of R_{23}/R_{13} has a value of 0.55. These results are not strictly comparable since in the solution case, the ratio is a measure of the relative interactions of chloride and sodium ions with water, whereas, in the membrane it is a measure of the interactions of sulphonate ions and polymer matrix relative to the interaction of sodium ions with water. The above result, nevertheless, indicates that the sulphonate and sodium ions in the membrane interact with the water molecules in a manner which is analogous to the type of interaction/

interaction encountered in aqueous solutions. This analogy is not maintained when the ratio R_{23}/R_{13} is considered. The value of this term is largely dependent on the assumptions made but in all cases it is greater than unity, (values in the range 4.5-10). This is not simply a consequence of the inaccuracy of R_{23} since the t_3-t_1 relationship gives R_{23}/R_{13} as 4.8 for the normal membrane and 4.7 for the expanded one. All normal cation-solvent interactions are greater than the corresponding anion-solvent interactions,[9] hence it is difficult to account for this anomalous behaviour observed in the membrane systems. The explanation may lie in the fact that the counter- and co-ions occupy different regions of the membrane, the counter-ions being concentrated in regions of high charge density and probably low water content, whereas the co-ions will tend to be found in regions of low cross-linking and high water content. The results in chapter 3 show that most of the counter-ions are in regions where the ratio $\bar{c}_3/\bar{c}_1$ is considerably less than the average value for the membrane as a whole. The co-ions, on the other hand, are to be found in the regions where the $\bar{c}_3/\bar{c}_1$ ratio is probably far in excess of the average value. It may be, therefore, that when the values of R_{13} and R_{23} are calculated using/

using the average value $\bar{c}_3/\bar{c}_1$, R_{13} is diminished and R_{23} enhanced.

It can easily be shown that $\bar{c}_3 R_{33}$ which is the sum of the frictional coefficients between one mole of water and all other species per litre in the surrounding membrane system, is less than either $\bar{c}_1 R_{11}$ or $\bar{c}_2 R_{22}$, thereby explaining the relative ease with which the water is transferred through the membrane under an applied water chemical potential gradient.

Comparison of the values of the frictional coefficients for the two membrane systems reveals that without exception the interactions in the expanded membrane are less than in the unexpanded form. This result is in agreement with the theory that the heat treatment expands the membrane, reduces the drag exerted by the membrane on the various species, and hence increases the permeability of all the mobile components of the system. The ratios of the corresponding R_{ij}'s for the two membranes are in the range 1.5 to 3 and most of the flows in the expanded membrane are larger by factors of the same order.

Table 2.24a shows the values of the terms $\bar{c}_i R_{ii}$ ($i = 1, 2$ or 3), for both membranes and for an aqueous sodium chloride solution of the same molar concentration. The/

The ratio $\bar{c}_i\bar{R}_{ii}/c_iR_{ii}$ for each membrane is shown in table 2.24b. The average value of this ratio for the normal membrane is 4.8 while the value for the expanded exchanger is 3.3. In both cases these values are very close to the values of the tortuosity factor. It would appear, therefore, that the total frictional interaction of one mole of any species in the membrane with those other species in one litre of the surrounding system can be calculated from the corresponding value in aqueous solution provided the tortuosity of the membrane is known. This suggests that the increased interaction experienced by any species in the membrane phase is produced only by the increased contact of the species due to the longer diffusion paths within the polymer matrix, and that the type of interaction in the exchanger pores is very similar to that which occurs between these species in aqueous solutions.

The ratio R_{13}/R_{23} obtained from the t_3-t_1 relationship is very similar for both membranes indicating that the counter- and co-ion water interactions have decreased by relatively similar amounts, upon expansion of the polymer matrix. This is in sharp contrast to the difference in the ratio R_{34}/R_{13} for the two membranes already discussed in/

in this section. R_{34} must decrease more rapidly on expansion than does R_{13}. This is not really unexpected, since as the matrix expands and allows entry to more water, a greater proportion of the water will be at some distance from the polymer chains and so the interaction R_{34} will be decreased. The interaction of the counter-ions with the water molecules can occur at any point within the pores and so the effect of expansion on R_{13} will be less than on R_{34}.

l-coefficients.

The l-coefficients calculated by the assumptions 1 and 3 (see tables 2.22 and 2.23) are almost identical, as would be expected from the similarity of the assumptions. The mobility coefficients calculated assuming $l_{13}/l_{23} = \bar{c}_1/\bar{c}_2$, are, for the most part, very similar to those calculated using the above assumptions. Significant deviations occur only in the values of l_{12} and l_{23}, and these coefficients are so small in comparison with the others that it is difficult to determine them accurately.

The terms $l_{ii}/\bar{c}_i$ represent an intrinsic mobility of the species i and hence it is interesting to compare these values for the different mobile components in the membrane, as shown in table 2.25. The intrinsic mobility of the water is much greater than that of either of the two ionic species, which explains the much greater flow of water per unit applied force, (see table 2.16). The effect of expansion of the membrane matrix, is to increase the intrinsic mobilities of all the mobile species, the effect being greater with the water than with the ions.

Using the l_{13}/l_{23} assumption the value of l_{12} is found/

found to be very small and negative for both membrane systems. Since it is difficult to obtain the exact value of this term, its value in succeeding calculations was taken as zero. The negative value is obtained as a consequence of obtaining the small term l_{12} by subtraction of two large terms. Any small errors in these terms lead to large errors in l_{12}. Fortunately the values of l_{12} and l_{23} are relatively unimportant in the matrix inversion process to give the corresponding R-coefficients.

Two equations relating the value of l_{12} to the values of other l-coefficients have been given by Spiegler [21] and by Staverman, [22] and these relations have been used to estimate the magnitude of this term. The Spiegler equation, which arises as a consequence of the model of the system which he uses, is $l_{12}l_{33} = l_{13}l_{23}$. The values so calculated are given in table 2.26 together with those calculated from the Staverman equation, $l_{12}l_{13} = l_{23}l_{11}$. These values can be little more than order of magnitude estimates of l_{12}, but they show that this term is small and of the same order as l_{22}, thus confirming that it may be taken as zero without significantly affecting the other l- and R-coefficients.

Using/

Using the l-coefficients calculated by use of assumption 3, (tables 2.22 and 2.23), it is possible to predict the salt flow across the membrane for a given chemical potential gradient. This may be done using equation (2.70) which has not been used in determining the mobility coefficients. The predicted and observed values of the salt flow are shown in table 2.27. In both cases, the predicted values are somewhat higher (by approximately 10% for the C60N membrane and 20% for the C60E membrane) than the observed values, - a consequence of ignoring l_{12}. The agreement is considered very good indeed in the light of the error on t_2, and hence l_{22}, and this constitutes a valid method for predicting salt flows from electrical transference data alone ($t_1, t_2, t_3, \bar{k}$) for membranes with low electrolyte uptake where l_{12} and l_{23} are negligible.

All the l-coefficients are larger in the case of the expanded membrane, indicating not only increased permeability of the mobile species under the applied forces, but also the increases in the coupling between the flows of the species, as measured by the cross-coefficients. A quantitative measure of the degree of coupling is given by q_{ij} defined by, (121)

$$q_{ij} = \sqrt{\left(\frac{l_{ij}}{l_{ii} \cdot l_{jj}}\right)} \qquad (2.111)$$

In/

In this sytem where $\bar{c}_2$ is small, the most interesting coupling is between the counter-ions and the water. The degree of coupling for this interaction q_{13}, is 0.59 for the normal membrane and 0.61 for the expanded form. These values must be considered identical within the experimental error. The much larger water transference number of the expanded membrane therefore is not a result of the greater coupling between counter-ions and water but is a consequence of the greater value of l_{13} for this membrane, as can be seen from equation (2.71).

2.8.2. C60N and C60E. 1.0M sodium chloride solutions.

The frictional coefficients for these systems are given in tables 2.28 and 2.29. Owing to the much larger value of $\bar{c}_2$ observed at this higher external concentration, it is no longer possible to assume that l_{12} is zero. Examination of the results reveals that there is not the great measure of agreement between the different assumptions as was observed at 0.1M. For the reasons discussed in section 2.8.1, the values calculated assuming R_{11}, to be zero must be considered unreliable and they will be excluded from the succeeding discussion. The assumption that R_{22}, is zero fails to produce such good agreement with the R_{13}/R_{23} assumption, a fact which suggests that R_{22}, now represents a significant fraction of R_{22} so that the R^x_{22} begins to differ from R_{22}. The l_{13}/l_{23} assumption produces results which are closer to those from the R_{11}, = 0 assumption, and so they must be in some doubt. l_{23} is now fairly large, and hence a more accurate assessment of its value is required than is given by the relation $l_{23} = (\bar{c}_2/\bar{c}_1)\, l_{13}$.

Since the values of R_{13}/R_{23} has been obtained from experimental data, the frictional coefficients calculated from/

this relation should represent the best estimates which can be achieved from the existing data. Nevertheless, these values, like those obtained from other assumptions, must suffer from inaccuracies resulting from the assumption that the R^{*}_{ij}'s used in the concentration gradient experiments are identical to the R_{ij}'s which apply to the systems without concentration gradients. This assumption is probably less accurate than for the 0.1M situation.

Assuming the R_{13}/R_{23} treatment gives the true value of R_{11} then the values of $R_{11'}$ are found to be $-2.6\text{x}10^{11}$ and $-2.3\text{x}10^{11}$ for the normal and expanded membranes respectively, values which are slightly lower than those obtained at 0.1M but probably not significantly different. Similar calculation for $R_{22'}$ gives values of $-8.0\text{x}10^{11}$ for the C60N membrane and $-6.4\text{x}10^{11}$ for the expanded form. The accuracy of these estimates is probably not very high since they are obtained from the difference of two large numbers, whose magnitudes are considerably greater than $R_{22'}$.

The values of $\bar{c}_i R_{ii}$ (i = 1, 2 and 3) shown, for both membranes, in table 2.30, do not exhibit such good agreement with the tortuosity scaled solution values, as was observed for the more dilute solutions. For both membranes, the value/

value of $\bar{c}_i R_{ii}$ calculated from assumption 3 of tables 2.28 and 2.29 are lower than the average values which include the other assumptions. Although the agreement with the solution values is poor, these results show that the frictional interactions within the membrane are greatly increased over those in free aqueous solution, by a factor of the same order as the tortuosity factor.

Since the co-ion is no longer a minor component of the system, the values of the frictional coefficients involving this species, become more accurately defined and are, therefore, more worthy of comment. The values of R_{12} for both membranes are again positive as was found for the 0.1M solutions. In this case there seems little doubt that this is a real effect and not simply a consequence of the method of calculation. The phenomenon of a net repulsion between two ions of opposite sign is difficult to understand. The explanation may lie in the heterogeneity of the membrane and the fact that the co-ion inhabits regions of the exchanger where the mean counter-ion concentration is low. Treatment of such a system as homogeneous may lead to cross-coefficients of the "wrong" sign. Certainly, in truly homogeneous aqueous solutions, the cross-coefficients between/

between ions of opposite sign are negative.[9]

In most cases the value of R_{24} is positive, indicating a repulsive interaction between the co-ion and the matrix as might be expected, while all the values of R_{14} are negative, in accordance with the attractive interaction which this coefficient measures.

The ratio R_{13}/R_{23} obtained from each set of R-coefficients is of interest. From the t_3-t_1 relationship this ratio has the value of approximately 0.21 for both membranes. Assuming R_{22}, equals zero, gives the values 0.3 and 0.5, while assuming that $l_{13}/l_{23} = \bar{c}_1/\bar{c}_2$, the ratio becomes 1.0 and 1.3 for the normal and expanded membranes respectively. This last result indicates the similarity of frictional interaction between the counter- and co-ions and the water, which is implicit in the $l_{13}/l_{23} = \bar{c}_1/\bar{c}_2$ relation. The values obtained from the two other assumptions give ratios which show the interaction of the co-ion with water to be greater than that of the counter-ion with water, a surprising result which has already been discussed at some length in the section sealing with the 0.1M solutions.

The values of R_{34} are somewhat unusual, (tables 2.28 and 2.29), taking positive and negative values, depending on the assumption used in the calculation. Positive values of R_{34} would indicate that the polymer matrix was exerting/

exerting a greater hydrophobic influence than the hydrophilic effect of the fixed charges, thereby producing a net repulsion between the matrix and the water. It is possible that such a situation could arise, although much more information about the mechanism of the shrinking process would be required in order to discuss this phenomenon even in qualitative terms. However, it is possible that the sign variation in this term is simply due to the method of calculation. R_{34} is obtained using equation (2.74) and, therefore, must contain the errors accummulated in the calculation of the other frictional coefficients. These errors may be large enough to produce the observed effects.

As for the 0.1M case, the effect of membrane expansion is to reduce the frictional interactions of all the species. The ratios of the corresponding frictional coefficients for the two membranes are mostly in the range 1.5 to 3.0, showing similar values to those obtained in the more dilute solutions and comparing favourably with the ratio of the permeabilities of the various species through the system.

l-coefficients.

The increased uptake of co-ions at the higher external concentration allows calculation of values of l_{12}. These values cannot be compared with those predicted from the equation of Spiegler (section 2.8.1), since, of course, this relation was derived assuming $\bar{c}_2$ as zero. Staverman,[22] however, has applied his relation at higher concentrations, and a comparison of those values predicted by this relation and the observed results are given in table 2.31. For both membranes, the agreement is poor, although it is slightly better for the expanded form. It appears that this relation can be used to give only an order of magnitude for l_{12}, although it must be remembered that the value of l_{23} required by the equation is also in some doubt.

Comparison of the values of the l-coefficients for the normal and expanded membranes, - table 2. 33, - shows that they are all increased as a result of the expansion. This fact not only explains the greater permeabilities associated with the C60E membrane, but also why the water transference numbers of the two membranes have smaller and more similar values at high external concentrations. Examination of equation (2.61c) reveals that as the value of the ratio l_{23}/l_{13} increases, so the value of t_3 will decrease. Also since/

since the value of l_{23}/l_{13} increases faster for the expanded membrane as the concentration increases, so the water transference number will decrease more rapidly than for the normal form.

The intrinsic mobilities of the species in the membrane as defined by the relation $l_{ii}/\bar{c}_i$ are shown in table 2.34. As for the dilute solutions, the value for the water is much greater than for either of the mobile ionic species. The counter-ion mobility is greater than that of the co-ion, - a result of the choice of reference frame, - and, of course, the values for the C60E membrane are greater than for the normal form.

The degree of coupling between the counter-ion and water q_{13}, is 0.63 for the normal membrane and 0.64 for the expanded form, these values being identical within the experimental error.

2.8.3. Concentration dependence of frictional and mobility coefficients.

(a) Frictional coefficients.

The normalised frictional coefficients $c_i R_{ii}$ show considerable variation as a result of varying the external solution concentration. In all cases except one, the frictional interactions are greater when the membrane is in equilibrium with a solution of higher concentration. This is reasonable, since, on increasing the solution concentration, the membrane shrinks thus bringing the various species into closer proximity within the pores and hence increasing their interactions with one another, whether this interaction be electrostatic in nature or a result of collisions between the molecules or ions. The increased tortuosity of the paths along which the mobile species are forced to diffuse also tends to increase the total interaction of each species. In view of these changes the value of $\bar{c}_3 R_{33}$ for the C60E membrane in 1.0M solution, as calculated by assumption 3, (tables 2.29 and 2.30), seems anomalously low and there must be some doubt about the validity of this result, especially as the other assumptions give results which fit better into the trends observed for the other coefficients and/

and for the other membrane.

Since the diffusion coefficients of the mobile species, in the membrane can be predicted fairly accurately by applying a tortuosity factor to the corresponding solution values, and since

$$D_{ii} = \frac{RT}{\bar{c}_i R^x_{ii}} , \qquad (2.43)$$

it would be expected that $\bar{c}_i R^x_{ii}$, suitably scaled for tortuosity, would also agree with the solution values of this term. If $\bar{c}_i R_{ii}$ is not the dominant term in $\bar{c}_i R^x_{ii}$ then, the values of $\bar{c}_i R_{ii}$ might also be expected to show a similar relation to the solution values. Although the agreement is not completely quantitative the results in tables 2.24 and 2.30 show that this type of relation does in fact exist.

It is difficult to assess accurately the effect of concentration change on the cross coefficients R_{13} and R_{14}. The general trend appears to be an increase in the frictional interaction with increasing concentration, although in many cases the increases are insignificant and in one or two cases, decreases are observed. As shown in tables 2.32 and 2.35, the values of $c_3 R_{13}$, which measures the total interaction of one mole of counter-ion with those water molecules in unit volume of the surrounding membrane, show, in general,/

general, only slight increases with concentration, whereas $\bar{c}_4 R_{14}$ increases by a factor of approximately two, going from 0.1M to 1.0M. This suggests that, whereas the total interaction of one mole of counter-ions with water increases only slightly, the interaction of the counter-ions with the fixed charges is doubled, a fact which may account for the reduced diffusion coefficients of the counter-ions at the higher concentrations. There is no evidence that there is covalent bond formation between the fixed charges and the sodium counter-ions in a polystyrene sulphonate exchanger, [92] [93] but there remains the possibility of some form of ion-association which would remain undetected by the methods used so far, for studies of this nature. It is possible, therefore, that at higher concentrations, there is some form of association between the counter-ions and the exchanger sites which would explain the fairly large increase in $\bar{c}_4 R_{14}$ observed for both membranes. Indeed in solutions of higher concentration the contraction of the diffuse double layers towards the 'pore' walls may be sufficient to produce this effect.

As the concentration increases, R_{12} becomes less positive i.e. it tends towards a negative value as might be expected for an attractive interaction. At the higher concentration/

concentration, a greater proportion of the counter- and co-ions must occupy the same regions of the exchanger and hence interact with one another, whereas, at low concentration the co-ions probably only encounter a small fraction of the total number of counter-ions. Calculations of the total interactions on the basis of a completely homogeneous mixture of counter- and co-ions may be the explanation of the unusual behaviour of R_{12}.

R_{24} is the least well defined of the frictional coefficients at all concentrations and this is shown by the variations in magnitude and sign of this term under different assumptions, and it, therefore, merits no further discussion.

The results show that the effect of increasing concentration on the interaction between the matrix and the solvent, R_{34}, is to reduce the attraction between them and even, under some assumptions, to produce a net repulsion. This effect has already been discussed in section 2.8.2.

(b) Mobility coefficients.

Increasing the concentration of the external solution reduces the values of l_{11} and l_{33} for both membranes, the effect being greater for l_{33}, but the effect on l_{22} is to produce a very large increase in this term owing to the vastly increased concentration of co-ion in the exchanger phase, and consequent higher permeability of this species. It is easier to examine the effect of concentration on these terms if the intrinsic mobilities, $l_{ii}/\bar{c}_i$, are used. Comparison of the results for the C60N and C60E membranes (table 2.25 and 2.34) shows that the mobilities of all the species are reduced at the higher concentration as expected. The ratios of the intrinsic mobilities at 0.1M to those at 1.0M are given in table 2.36. The effect of increasing concentration is very similar for the counter- and co-ions in both membranes, the effect being slightly greater in the C60N membrane. The water mobility is, however, affected to a considerably greater extent in both cases. None of these increases is wholly attributable to the increased tortuosity since the value of the ratio $\theta_{1.0}/\theta_{0.1}$ is only 1.17 for both membranes. The decrease in intrinsic mobilities must, therefore, in part be due to increased interactions of the species within the membrane itself.

This/

This may explain why the $\bar{c}_i R_{ii}$ values at 1.0M are greater than the corresponding solution values corrected for tortuosity, whereas, at 0.1M the agreement between these terms is fairly good.

Like l_{11} and l_{33}, l_{13} also decreases as the membrane shrinks, but l_{23} increases due to the greatly increased salt uptake at the higher external concentrations. The effect of these changes on the water transference number has already been mentioned in section 2.8.2.

Since l_{12} is not well defined at 0.1M, it is not possible to determine its dependence on concentration, although it seems likely that it will increase with increasing concentration of the co-ion in the exchanger pores.

The values of q_{13} are not particularly sensitive to the effects of concentration changes. The values of this term at the two concentrations studied are, within the limits of experimental error, identical.

2.8.4. Conclusions.

The preceding sections have shown how frictional and mobility coefficients in membrane systems, may be calculated from diffusion and transport data, and there are a number of conclusions and generalisations which may be drawn from the results.

It seems fairly certain that the isotope-isotope frictional interaction for the counter-ions, R_{11}' is non-zero, and is of the same order as R_{11} itself. The neglect of this term in many membrane studies must have considerable effects on the results obtained. On the other hand, although R_{22}' may be of the same order of R_{11}' it is small in comparison to R_{22} and, therefore, its omission only begins to have any significant effect on the results when the co-ion uptake is large and R_{22} is reduced. These conclusions confirm those of Scattergood and Lightfoot, [57] who found that, in a system similar to the one studied here, isotope-isotope interaction was a major term. The value of R_{11}' for sodium counter-ions calculated from their results is -6.2×10^{11}, a value which agrees well with the values obtained in the C60 membranes, not only in magnitude but/

but in sign. The values of R^{x}_{11}/R_{11} for the C60N and C60E membranes fall in the range 1.2 - 1.4. In aqueous solutions of sodium chloride of comparable concentration this ratio has the value of approx. 0.80. Thus in aqueous solutions R_{11}, is positive in contrast to the negative values obtained in membrane systems. This discrepancy is as yet unexplained.

It appears that when the co-ion uptake is low, there are a number of assumptions which may be made in order to reduce the number of independent transport properties required for a satisfactory analysis of the system. These include: (a) setting l_{12} equal to zero, (b) obtaining l_{23} from the relation $l_{23} = l_{13}.(\bar{c}_2/\bar{c}_1)$, and (c) setting R_{22}, equal to zero. However, the most reliable results appear to be those obtained from the ratio R_{13}/R_{23} calculated from the t_3-t_1 relation. Since all the data used in such a treatment is experimental and no assumptions are required, this method must yield results as accurate as the data allows. The only doubt concerning this approach is the violation of the $R_{23}^2 \ll R_{22} . R_{33}$ requirement, obtained in the C60E membrane in 1.0M sodium chloride solution. Like all other treatments of membrane systems, this method of calculation of frictional interactions must ultimately rely on the validity/

validity of treating the membrane as a homogeneous phase which is sometimes a doubtful premise. The degree of heterogeneity of the system may well be the explanation of a number of anomalies which have appeared in the calculations. The low value of the R_{13}/R_{23} ratio and the positive values obtained for R_{12} may be a result of inhomogeneity of the membranes which allows the sorption of salt in regions where the fixed charge and hence the counter-ion concentration is low. In the absence of a suitable t_3-t_1 relation, the assumption that R_{22}, is zero, gives the best estimate of the frictional coefficients in the system.

The use of two membranes which differ only in their degree of expansion, has allowed an examination of the effect of such treatment on the properties of the exchanger. The interesting feature is not the greater permeability of all the mobile species in the expanded membrane, but the fact that, on expansion, most of the interactions between the species have been affected in very similar ways. This suggests that the expansion process has been uniform and that it has not led to changes in the basic structure of the membrane. This proposal finds support in the results of the next chapter where it is shown that the expanded membrane/

membrane has a degree of heterogeneity only slightly greater than that of its normal counterpart.

When the sorbed electrolyte concentration is low, it is possible to use the specific conductivity and co-ion and water transference numbers to predict, accurately, the salt flow through the membranes under an applied salt concontration gradient. Indeed, it is this ability to predict the properties of such a system which makes the application of irreversible thermodynamics such a useful tool in the analysis of membrane processes. Knowledge of all the frictional coefficients in the system allows the calculation of the flows of any species under any forces applied to the system, at or around the external concentration for which these coefficients are valid, and provided that the flows and forces fall within the region of application of the linear relationships between them. Measurement of flows under, say a pressure gradient or a combination of applied electric potential and pressure gradients would test the validity of the frictional coefficients determined as described in this chapter, and might help to explain the anomalies which have been observed.

CHAPTER THREE

Structural analysis of ion-exchange membranes.

3.1. Introduction.

Until fairly recently, it was assumed that a large amount of ion-exchange behaviour could be explained in terms of a Donnan equilibrium at the interface between the resin and the solution phases. The application of the Donnan theory to the exchanger as a whole, includes, in its implications, the assumption that the resin structure is homogeneous, i.e. that the cross-linking and space charge density remain virtually constant throughout the exchanger phase.

The Donnan law has found its chief application in explaining the phenomenon of electrolyte exclusion and in predicting the amount of electrolyte absorbed by the exchanger from an external salt solution by use of the well known relation

$$\bar{m}(M + \bar{m}) = m^2 \left(\frac{\gamma_\pm}{\bar{\gamma}_\pm}\right)^2 \qquad (3.1a)$$

where $\bar{m}$ is the concentration of the sorbed electrolyte, M is the concentration of the fixed charges, and m is the concentration of the external solution. $\gamma_\pm$ and $\bar{\gamma}_\pm$ are the activity coefficients in the solution and resin phase respectively, and all the terms are expressed on a molal concentration basis.

For/

For dilute external solutions where the electrolyte exclusion is efficient, this expression reduces to

$$\bar{m} = m^2/M \cdot \left(\frac{\gamma_\pm}{\bar{\gamma}_\pm}\right)^2 \qquad (3.1\beta)$$

If the activity coefficient ratio $\left(\frac{\gamma_\pm}{\bar{\gamma}_\pm}\right)$, is assumed to be constant, - and for low values of the external solution concentration this does not appear unreasonable, - then equation (3.2) may be written as

$$\bar{m} \propto m^2 \quad \text{or} \quad \bar{m} = km^2 \qquad (3.1\gamma)$$

which is the form in which the Donnan law is best known.

Equation (3.1) may also be used to calculate the activity coefficients of the electrolyte in the exchanger if the capacity and electrolyte uptake of the resin are known. It is this application of the Donnan law, using the implied homogeneous gel model for the exchanger, which has produced some interesting and unexpected results.

In 1947, Baumann and Eichhorn [122] carried out a series of experiments to determine the electrolyte uptake of sodium chloride on the exchanger Dowex 50. From these results they calculated the resin activity coefficients and found that as the external solution concentration decreased, so the activity coefficients of the sorbed electrolyte

decreased/

decreased to very low values, quite unlike the behaviour of solution activity coefficients. Further investigations by a number of workers (123) (124) (125) (126) (127) (128) (129) (130) confirmed the findings of Baumann and Eichhorn, some of the authors reporting resin activity coefficients as low as 0.01. (125) Considerable interest has been shown in these anomalously low values and numerous explanations have been suggested. Bauman and Eichhorn themselves, suggested that this abnormal behaviour was due to imperfections in treating a swollen resin as a homogeneous phase. Davies and Yeoman (125) could account for their results if it were assumed that 5% of the resin volume was occupied by voids filled with solution of the same concentration as the external solution. Kraus and Moore (127) attributed the unusually large uptake of hydrochloric acid by their anion-exchangers at low external solution concentrations, to impurities in the resin, notably tertiary and lower amines.

Freeman (131) proposed that the activity coefficients of the sorbed electrolyte at low external concentrations could be linearly related to those at high concentrations by use of two arbitrary constants. The first of these he interpreted as a measure of the amount of electrolyte retained on the surface of the exchanger, the second as a measure of the impurities present in the exchanger and capable/

capable of absorbing electrolyte from the bathing solution. This theory has not met with wide acceptance [132] and it has been pointed out that in order to satisfy the relationship, it must be assumed that the fractional retention, e, is 0.036 for hydrochloric acid and 0.087 for sodium chloride, on the same resin under otherwise indentical conditions. Valid as the criticism of this approach may be, Freeman's theory does point to the two most likely sources of error in the activity coefficient calculations, viz. the retention of solution by the exchanger surface and inhomogeneities in the resin itself.

As mentioned above, much of the early work was plagued by the experimental difficulties of completely separating the resin phase from the equilibrating solution, or of determining the volume of solution retained between the resin beads after centrifugation. When the electrolyte uptake is very low, adherence of even a small amount of solution to the exchanger surface induces considerable error in the determination of the total electrolyte in the exchanger phase. The introduction of ion-exchange membranes facilitated the separation process and the work of Mackie and Meares [81] showed that, even when the error due to surface absorption was considerably reduced by the use of membranes instead/

instead of beads, the uptake, at low concentrations, was still greater than expected from the simple Donnan law.

In 1961 Gleuckauf published a series of papers [2] [38] [133] in which he described a method of determining, unequivocally, the electrolyte uptake of membranes even at very low external solution concentrations. His results further confirmed that at low concentrations the uptake was larger than would be expected for a homogeneous system obeying the simple Donnan law.

It has been observed that the mean activity coefficients of simple electrolytes in aqueous solutions of polyelectrolytes also display low values at low electrolyte concentrations. [134] [135] [136] [137] Here, there is no problem of phase separation and so this phenomenon must be regarded as real and not simply as an artefact of the experimental technique used. Various treatments have been given for polyelectrolyte solutions [138] [139] and a number of attempts have [81] [126] [140] been made to extend these to ion-exchangers. All of these methods require assumptions about the exchanger system and frequently also require estimates of properties such/

such as polymer chain length, number of monomer units between cross links, etc., all of which make this approach less than satisfactory.

There are two ways of explaining the low activity coefficients in the resin phase; one is that these low values are real and are caused by the effect of the macro-ions on the simple sorbed ions, the other that they are a result of treating as homogeneous, a resin which contains regions of quite different cross-linking and charge density. The first of these finds support in the analogies drawn with polyelectrolyte solutions and the low activity coefficients found in them, and in recent theoretical studies of electrical double layer models for ion-exchangers. (141) (142) (143) These theories suffer from the same restrictions as many other ion-exchange theories, that a pore model in assumed, and variations in the properties produced by deviations from the ideal system, are difficult to predict. The results of Raman and PMR spectroscopy are inconclusive, for while they show the absence of covalent bonds, (92) (93) (94) (95) (96) (97) they cannot detect association of the small mobile ions with the large multiply charged molecule, induced by the charge and/

and dielectric effects, and giving rise to abnormally low activity coefficients.

Gustafson[144] considers that the low activity coefficients are real and not due to either faulty experimental technique or inhomogeneity of the resin, but rather to the effect of the macro-ion on the small exchange and sorbed ions. He proposes that at low salt uptake values, the activity coefficient of the co-ions is low, while the activity coefficient of the counter-ions remain virtually constant. This leads to a low value of the mean activity coefficient of the sorbed salt at low external solution concentrations. In aqueous solutions of polyelectrolytes, however, Nagasawa, Izumi and Kagawa [137] found that the counter-ion activity coefficients decreased and the co-ion activity coefficients increased with salt concentration, except at very low salt concentrations where the co-ion activity coefficient showed an decrease.

Marinsky, [145] on the other hand, claims that Gustafson's results at low concentration show that resin heterogeneity contributed to the very low values of $\bar{\gamma}_{\pm}$ obtained. Marinsky [145] [146] has proposed that the activity coefficients of sorbed salt in ion-exchangers can be treated and predicted using the additivity rule which has been found/

found to apply to polyelectrolyte solutions. (136) (137) (147) (148) (149) (150) (151) This treatment predicts that the mean activity coefficient of the sorbed salt decreases with decreasing salt uptake but that the activity coefficients do not drop to the extremely small values obtained in some investigations. (127) (144) These very small experimentally determined values of $\bar{\gamma}_{\pm}$ are attributed to resin heterogeneity.

While it is difficult at present to estimate how valid is the extension of the polyelectrolyte theories in ion-exchange systems, it is undeniable that the ion-exchange resins hereto treated as homogeneous gels, are, in fact, far from homogeneous. There is a considerable weight of evidence which suggests that inhomogeneities in the polymer structure are common, no matter how homogeneous the resin may appear to be. This evidence comes from a number of sources, among which are the direct results of fractionation studies of co-polymers and electron microscopy and the indirect evidence of selectivity and electrolyte uptake experiments.

The work of Mayo and Lewis (152) has shown that copolymerisation of two monomers gives a polymer in which the/

the ratio of the monomers being polymerised into the polymer chain is a function of the fraction of monomer which has already been polymerised. This has not yet been demonstrated for cross-linked polymers but it is reasonable to suppose that to some extent, at least, this must occur there also. The implications of this result for the copolymerisation of, for example, styrene and divinyl benzene to give an ion-exchanger matrix, is very important. It is also important to stress the effect of chain entanglement on the properties of the exchanger. The results of Millar (153) (154) have shown that this phenomenon can have a very great influence on the properties of ion-exchange materials. Different degrees of chain entangelment within the exchanger may lead to a variation in the structure of the exchanger which will have a considerable effect on such properties as the selectivity and electrolyte uptake of the resin.

Although Gordon, (94) (155) using PMR, could find no evidence of inhomogeneity in the exchangers which he studied, electron microscopy has yielded much in the way of evidence for the theories of non-uniformity of structure. Micrographs are difficult to obtain, but those which have been published (156) (157) (162) show a marked degree of heterogeneity in the/

the resin structure.

Further evidence for non-uniformity of fixed site distribution is to be obtained from the results of Reichenberg and MacCauley [158] who, in studies on the selectivity of ion-exchangers as a function of cross-linking, found it necessary to assume that each of the sites within the exchanger could be classified into one of the following three groups:

(1) regions of low cross-linking where fully hydrated ions can approach and little selectivity occurs; (2) regions of medium cross-linking where the size of the fully hydrated ion may be a significant factor and (3) regions of high cross-linking where the energy involved in hydration of ions will be the factor which controls selectivity.

Perhaps the most interesting and comprehensive of the non-uniformity theories is that of Glueckauf, [2] in which he postulates that the abnormally high salt uptake at low concentrations is due to regions of lower than average charge density which nevertheless, still obey the Donnan law. These regions may be voids, regions of low cross-linking, or of low capacity, their nature is irrelevant, and it is only the total fixed charge density of any region which determines/

determines its electrolyte uptake behaviour. This theory has received considerable attention not only as a method of structurally analysing ion-exchange resins, but for its predictions about the transport properties of the exchangers (section 3.5). It is this theory with which this chapter is primarily concerned and the next section deals with it in greater detail.

3.2. Membrane Structure from Electrolyte uptake data. Theory

3.2.1.

Glueckauf's [2] approach is based on the assumption that a Donnan equilibrium holds locally for any small element of the exchanger which has a time-average, local fixed ion molality, M. The electrolyte uptake, $\bar{m}$, for this region can then be related to the external solution concentration, m, by the Donnan equation:

$$\bar{m}^{\nu_2} \cdot \left(\frac{M}{\nu_1} + \bar{m}\right)^{\nu_1} \cdot \bar{\gamma}_{\pm}^{\nu_{12}} = k.(m)^{\nu_2} (m)^{\nu_1} \cdot \gamma_{\pm}^{\nu_{12}} \qquad (3.18)$$

Where ν_1 and ν_2 are the number of counter- and co-ions which make up one molecule of the electrolyte and $\nu_{12} = \nu_1 + \nu_2$; $\gamma_{\pm}$ and $\bar{\gamma}_{\pm}$ are the mean salt activity coefficients in the external solution and the exchanger respectively, and k includes the influence of the volume strain energy and hence the swelling pressure. It can be shown that this term has a value near to unity and does not vary significantly even when the swelling pressure changes by a large amount [160]. It is also assumed that the activity coefficient in the exchanger, $\bar{\gamma}_{\pm}$, is "effectively" proportional to the activity coefficient in the solution $\gamma_{\pm}$, the following justification being used. If the external concentration is 0.01 molal, then a region in/

in the exchanger with M = 5 say, will no doubt have a significantly different value of activity coefficient. However, this region will only take up a very small amount of electrolyte and, therefore, it is immaterial what its activity coefficient is. The activity coefficient is only important if the uptake is of the same order as the external concentration i.e. when $M+\bar{m}$ is similar to $\bar{m}$. Then it is reasonable to assume that $\bar{\gamma}_{\pm}$ is not greatly different from $\gamma_{\pm}$. Using this approximation, the activity coefficients on either side of equation (3.1) can be cancelled leaving only a small factor which can be absorbed into k.

Equation (3.1) may then be written

$$\left(\frac{\bar{m}}{a m}\right)^{\nu_2}\left(\frac{M/\nu_1}{a m}+\frac{\bar{m}}{a m}\right)^{\nu_1} = 1 \qquad (3.2)$$

where $a = k^{1/\nu_{12}}$.

Quite generally then,

$$\frac{\bar{m}}{a m} = f\left(\frac{M/\nu_1}{a m}\right) \qquad (3.3)$$

where the shape of the function is determined by the ratio ν_1/ν_2.

A function ϕ^{m} is then defined, such that a fraction $\phi^{m}(M)$ of the concentration M lies between M and M+dM.

The mean counter-ion concentration M in the exchanger solution is related to the local molality by the expression/

expression

$$M = \frac{c}{z_1 c_3} = \int_{\phi^m=0}^{1} M \, d\phi^m \qquad (3.4)$$

where c is the observed mean capacity of the exchanger and c_3 its water content.

The observed mean electrolyte uptake, Q, and its corresponding mean molality, $\bar{m}$ are given by

$$\bar{m} = \frac{Q}{c_3} = \int_{\phi^m=0}^{1} \bar{m} \, d\phi^m \qquad (3.5)$$

The condition that

$$\int_{M=0}^{M} d\phi^m = 1 \qquad (3.6)$$

must also be satisfied.

A rough indication of the likely form of ϕ^m can be obtained from the following consideration. At low values of M, the uptake $\bar{m}$ is approximately equal to m. If the exchanger is then considered as two parts, one where $M \leqslant m$ and $\bar{m} \cong m$, and the other where $M > m$, and $\bar{m} = 0$. The observed uptake $\bar{m}$ should then be $(\phi^m)_{M=m} = m$. The experimental results of a number of studies have shown that $\bar{m}$ follows a power of m somewhat higher than unity, therefore it follows that ϕ^m must be a fractional power of m=M.

A distribution function is then introduced such that

$$d\phi^m/dM = K_o M^{-z} \quad \text{with } A < M < B$$

and/

and $d\bar{\phi}/dM = 0$ for $M < A$ and $M > B$, (3.7)

where z is a constant between 0 and +1, and A and B are the minimum and maximum values of M in the exchanger, K_o is a constant.

Using equation (3.7) and with $B \gg A$, equation (3.4) gives

$$M = K_o \int_{M=A}^{M=B} M^{(1-z)} dM = \frac{K_o}{2-z} \left(B^{(2-z)} - A^{(2-z)}\right)$$

$$\cong \frac{K_o}{2-z} \cdot B^{(2-z)} \qquad (3.8)$$

while, from (3.5) and (3.6) is obtained the relation

$$1 = \frac{K_o}{1-z}\left[B^{(1-z)} - A^{(1-z)}\right] \cong \frac{K_o}{1-z} \cdot B^{(1-z)} \qquad (3.9)$$

Using the relation $M = C/c_3 z_1$, equation (3.8) and (3.9) yield

$$B \cong \frac{2-z}{1-z} \cdot M \qquad (3.10)$$

and

$$K_o \cong \frac{(1-z)^{(2-z)}}{(2-z)^{(1-z)}(M)^{(1-z)}} \qquad (3.11)$$

Substitution of $d\bar{\phi}$ from equation (3.7) and of $\bar{m}$ from (3.3) into (3.5) gives for the observed uptake of electrolyte

$$\bar{m} = \frac{Q}{c_3} = K_o (am) \int_{M=A}^{M=B} M^{-z} \cdot f\left(\frac{M/v_1}{m}\right) dM \qquad (3.12)$$

where the integration is carried out at constant m.

Introducing $y = M/dv_1 m$, equation (3.12) becomes

$$\bar{m} = K_o (am)^{(2-z)} v_1^{(1-z)} \int_{y_A}^{y_B} y^{-z} \cdot f(y) dy . \qquad (3.13)$$

where/

where $y_A = A/(a.v_I m)$ and $y_B = B/(a.v_I m)$ (3.14)

This integral can be divided into three ranges:

$$\bar{m} = k_o \, v_I^{(1-z)} (am)^{(2-z)} \left[\int_o^{\infty} y^{-z} \cdot f(y)\,dy - \int_o^{y_A} y^{-z} f(y)\,dy - \int_{y_B}^{\infty} y^{-z} f(y)\,dy.\right] \quad (3.15)$$

The value of the first integral is constant and thus independent of m. Hence, in the concentration range where the values of the second and third integrals are small compared to the first, the electrolyte uptake $\bar{m}$ is proportional to a power of m less than 2.

i.e. $Q \approx \bar{m} \approx (m)^{(2-z)}$ (3.16)

In this range equation (3.16) may be written

$$\bar{m} = K.m^{(2-z)} \quad (3.17)$$

which on rearranging gives

$$\bar{m}/m = K.m^{(1-z)} \quad (3.18)$$

where K is a proportionality constant.

Therefore, a plot of log $(\bar{m}/m)$ against log m will be a straight line of gradient (1-z). However, this calculation does not allow for variation in M which can be very significant if a highly swollen exchanger is used in electrolyte solutions of fairly high concentration. Variation in M leads to variation in k_o and hence in K of equation (3.18)

Substituting/

Substituting for k_o in equation (3.15) gives

$$\bar{m} = K_1/M^{(1-z)} . m^{(2-z)} \qquad (3.19)$$

or $(\bar{m}/m) = K_1 \left(\frac{m}{M}\right)^{(1-z)}$

Therefore, for systems with significant variations in M, a plot of log $(\bar{m}/m)$ against log (m/M) is linear with gradient $(1-z)$, and from this plot the value of z may be calculated.

The significance of z is in determining the degree of heterogeneity of the exchanger. If $z = 0$, then the uptake is proportional to m^2 and the Donnan law is obeyed by the exchanger as a whole. This means that the exchanger is completely homogeneous. The greater the value of z, the more inhomogeneous is the membrane.

3.2.2.

The Donnan expression shown in equation (3.1) has been obtained by assuming that the electric potential, $\bar{\phi}$, is constant throughout the resin phase. However, since, on average, the counter-ions are closer to the fixed charges than are the co-ions, they must be at a lower potential than the co-ions, and hence the activity expression should retain the electric potential term, i.e.

$$\ln(a_1 a_2) = \ln(\bar{a}_1 \bar{a}_2) + F(z_1 \bar{\phi}_1 + z_2 \bar{\phi}_2)/RT \qquad (3.20)$$

The difficulty of calculating the values of $\bar{\phi}_1$ and $\bar{\phi}_2$ has been simplified by Tye,[161] who suggested that the exchanger be divided into two regions, one fraction $(1-\beta)$ at an electric potential $\bar{\phi}$, the other fraction (β) at zero electric potential. Using the Boltzman distribution, the concentration of the salt in the exchanger may be shown to be[161]

$$\bar{m} = \beta m - M/2 + \sqrt{[(M^2/4) + (1-\beta)^2 m^2]} \qquad (3.21)$$

A value of β is then chosen to give a good fit of the predicted and observed uptake data over a range of external concentrations.[161] Tye has found that choice of a value of β which gives a good fit at low solution concentrations, also gives a satisfactory fit at higher concentrations.

This/

This theoretical approach has not been widely used in treating experimental data. The results obtained by using it in the present study are given in the next section.

3.3. Results.

Table 3.1.

Electrolyte uptake data.

C60N.

Soln. concentration (molar)	Uptake of NaCl (meqs)	Uptake of water (gm)	Concentration of Na^+ (molal)	Concentration of Cl^- (molal)
0.10	$8.74_{10}-4$	0.1233	2.87	$7.08_{10}-3$
0.50	$1.19_{10}-2$	0.1097	3.33	$1.08_{10}-1$
1.00	$2.98_{10}-2$	0.0958	3.99	$3.12_{10}-1$
2.00	$6.85_{10}-2$	0.0794	5.31	$8.63_{10}-1$

Table 3.2.

Electrolyte uptake data.

C60E.

Soln. concentration (molar)	Uptake of NaCl (meqs)	Uptake of water (gm)	Concentration of Na^+ (Molal)	Concentration of Cl^- (Molal)
0.10	$2.025_{10}-3$	0.1752	2.12	$1.15_{10}-2$
0.50	$2.558_{10}-2$	0.1543	2.55	$1.65_{10}-1$
1.00	$6.23_{10}-2$	0.1344	3.22	$4.64_{10}-1$
2.00	$1.43_{10}-1$	0.1137	4.51	1.26

Table .3.3.

Electrolyte uptake data.

C100N.

Soln. concentration (molar)	Uptake of NaCl (meqs)	Uptake of water (gm)	Concentration of Na+ (molal)	Concentration of Cl- (molal)
0.10	$1.61_{10}-4$	0.0292	5.55	$5.52_{10}-3$
0.50	$1.98_{10}-3$	0.0274	5.98	$7.21_{10}-2$
0.75	$3.58_{10}-3$	0.0265	6.24	$1.35_{10}-1$
1.00	$5.42_{10}-3$	0.0258	6.48	$2.10_{10}-1$
2.00	$1.42_{10}-2$	0.0234	7.52	$6.08_{10}-1$
3.00	$2.30_{10}-2$	0.0209	8.84	1.10
4.00	$3.20_{10}-2$	0.0188	10.31	1.70

Table 3.4

Electrolyte uptake data.

C100E.

Soln. concentration (molar)	Uptake of NaCl (meqs)	Uptake of Water (gm)	Concentration of Na^+ (molal)	Concentration of Cl^- (molal)
0.10	$2.38_{10}-4$	0.0342	4.72	$6.98_{10}-3$
0.50	$2.90_{10}-3$	0.0316	5.20	$9.18_{10}-2$
0.75	$5.20_{10}-3$	0.0300	5.55	$1.74_{10}-1$
1.00	$8.05_{10}-3$	0.0296	5.73	$2.72_{10}-1$
2.00	$2.03_{10}-2$	0.0267	6.80	$7.61_{10}-1$
3.00	$3.08_{10}-2$	0.0225	8.54	1.37
4.00	$4.33_{10}-2$	0.0211	9.65	2.05

Table 3.5.

Processed electrolyte uptake data: C6ON.

m	$\bar{m}$	M	$\bar{m}/m$	m/M	log($\bar{m}$/m)	log(m/M)
0.1005	0.0071	2.863	0.0707	0.0351	-1.1509	-1.4547
0.5062	0.1081	3.218	0.2136	0.1573	-0.6704	-0.8032
1.0222	0.3115	3.685	0.3047	0.2774	-0.5161	-0.5569
2.0859	0.8623	4.447	0.4134	0.4691	-0.3836	-0.3287

Table 3.6.

Processed electrolyte uptake data: C6OE.

m	$\bar{m}$	M	$\bar{m}/m$	m/M	log($\bar{m}$/m)	log(m/M)
0.1005	0.0115	2.114	0.1140	0.0475	-0.9416	-1.3229
0.5062	0.1651	2.395	0.3262	0.2114	-0.4865	-0.6749
1.0222	0.4635	2.749	0.4534	0.3718	-0.3435	-0.4297
2.0859	1.2610	3.250	0.6045	0.6418	-0.2186	-0.1926

Table 3.7.

Processed electrolyte uptake data: C10ON.

m	$\bar{m}$	M	$\bar{m}/m$	m/M	log($\bar{m}$/m)	log(m/M)
0.1005	0.0055	5.540	0.0548	0.0181	-1.261	-1.741
0.5062	0.0721	5.902	0.1424	0.0858	-0.8465	-1.0666
0.7623	0.1351	6.103	0.1772	0.1249	-0.7515	-0.9034
1.0222	0.2100	6.267	0.2054	0.1631	-0.6874	-0.7875
2.0859	0.6070	6.9100	0.2910	0.3019	-0.5361	-0.5203
3.1966	1.1010	7.7360	0.3444	0.4132	-0.4629	-0.3838
4.3607	1.7000	8.6000	0.3898	0.5071	-0.4092	-0.2949

Table 3.8.

Processed electrolyte uptake data: C10OE.

m	$\bar{m}$	M	$\bar{m}/m$	m/M	log($\bar{m}$/m)	log(m/M)
0.1005	0.0070	4.7150	0.0694	0.0213	-1.1590	-1.6714
0.5062	0.0917	5.1868	0.1812	0.0976	-0.7418	-1.0106
0.7623	0.1734	5.3766	0.2275	0.1418	-0.6430	-0.8483
1.0222	0.2721	5.4509	0.2662	0.1875	-0.5748	-0.7271
2.0859	0.7614	6.0396	0.3650	0.3454	-0.4377	-0.4617
3.1966	1.3700	7.1680	0.4286	0.4460	-0.3680	-0.3507
4.3607	2.0520	7.6450	0.4706	0.5704	-0.3274	-0.2438

Table 3.9.

Structural properties of membranes.

Membrane / Constant	C60N	C60E	C100N	C100E
z	0.31	0.35	0.40	0.40
I_o	4.20	3.90	3.70	3.70

Table 3.10.

Structural properties of membranes C60N and C60E.

External concn. molar.	C60N k_o	C60N B	C60N a	C60E k_o	C60E B	C60E a
0.10	0.180	7.03	0.63	0.217	5.40	0.74
0.50	0.162	8.15	0.66	0.193	6.50	0.79
1.00	0.143	9.79	0.66	0.166	8.16	0.80
2.00	0.118	13.01	0.61	0.133	11.46	0.82

Table 3.11.

Structural properties of membranes C100N and C100E.

External concn. molar.	C100N k_o	C100N B	C100N a	C100E k_o	C100E B	C100E a
0.10	0.119	14.78	0.64	0.131	12.58	0.70
0.50	0.115	15.75	0.65	0.124	13.62	0.72
0.75	0.113	16.28	0.65	0.121	14.33	0.72
1.00	0.111	16.70	0.64	0.120	14.58	0.72
2.00	0.105	18.70	0.64	0.113	16.10	0.70
3.00	0.098	20.62	0.63	0.102	19.12	0.70
4.00	0.092	22.95	0.63	0.098	20.25	0.68

Table 3.12.

Fixed ionic group distribution. C60N.

Ext. concn. 0.1M		Ext. concn. 2.0M.	
Range of M molal	$\Delta\phi^{n}$ (%)	Range of M molal	$\Delta\phi^{n}$ (%)
$0 - 10^{-5}$	0.0	$0 - 10^{-5}$	0.0
$10^{-5} - 10^{-4}$	0.02	$10^{-5} - 10^{-4}$	0.02
$10^{-4} - 10^{-3}$	0.10	$10^{-4} - 10^{-3}$	0.08
$10^{-3} - 10^{-2}$	0.60	$10^{-3} - 10^{-2}$	0.39
$10^{-2} - 10^{-1}$	3.58	$10^{-2} - 10^{-1}$	2.32
$10^{-1} - 1.0$	20.10	$10^{-1} - 1.0$	13.19
1.0 - 3.0	29.60	1.0 - 5.0	32.6
3.0 - 5.0	23.50	5.0 - 10.0	31.8
5.0 - B	22.50	10.0 - B	19.6

Table 3.13.

Fixed ionic group distribution. C6OE.

Range of M molal	Ext. soln. 0.1M $\Delta\phi^{\sim}$(%)	Range of M molal	Ext. soln. 2.0M. $\Delta\phi^{\sim}$(%)
0 - 10^{-5}	0.00	0 - 10^{-5}	0.01
10^{-5} - 10^{-4}	0.04	10^{-5} - 10^{-4}	0.03
10^{-4} - 10^{-3}	0.20	10^{-4} - 10^{-3}	0.12
10^{-3} - 10^{-2}	0.86	10^{-3} - 10^{-2}	0.53
10^{-2} - 10^{-1}	3.80	10^{-2} - 10^{-1}	2.91
10^{-1} - 1.0	21.30	10^{-1} - 1.0	15.3
1.0 - 3.0	34.80	1.0 - 5.0	34.9
3.0 - 5.0	26.80	5.0 - 10.0	33.2
5.0 - B	12.20	10.0 - B	13.0

Table 3.14.

Prediction of uptake data by use of Tye theory [161] using uptake data at 0.5M. to give value of β.

	C60N		C60E	
External concn. (molar)	$\bar{m}$ predicted (molal)	$\bar{m}$ observed (molal)	$\bar{m}$ predicted (molal)	$\bar{m}$ observed (molal)
0.10	0.015	0.0071	0.0293	0.0115
0.50	(0.1081)	0.1081	(0.1651)	0.1651
1.00	0.3097	0.3115	0.4236	0.4635
2.00	0.8847	0.8623	1.127	1.261

Table 3.15.

Membrane phase activity coefficients: C60N and C60E.

concentration of ext. soln. (molal)	Mean act. coeff. of NaCl in solution $\gamma_{\pm}$	mean act. coeffic. of NaCl in Membrane, $\bar{\gamma}_{\pm}$ C60N	C60E
0.1005	0.778	0.55	0.50
0.5062	0.681	0.58	0.53
1.0222	0.657	0.60	0.55
2.0859	0.674	0.66	0.59

Table 3.16.

Membrane phase activity coefficients: C100N and C100E.

Concentration of ext. soln. (molal)	mean act. coeff. of NaCl in solution (126) $\gamma_{\pm}$	Mean act. coeff. of NaCl in membrane, $\bar{\gamma}_{\pm}$	
		C100N	C100E
0.1005	0.778	0.45	0.43
0.5062	0.681	0.52	0.50
0.7623	0.663	0.55	0.52
1.0222	0.657	0.58	0.54
2.0859	0.674	0.66	0.62
3.1966	0.730	0.75	0.68
4.3607	0.823	0.86	0.81

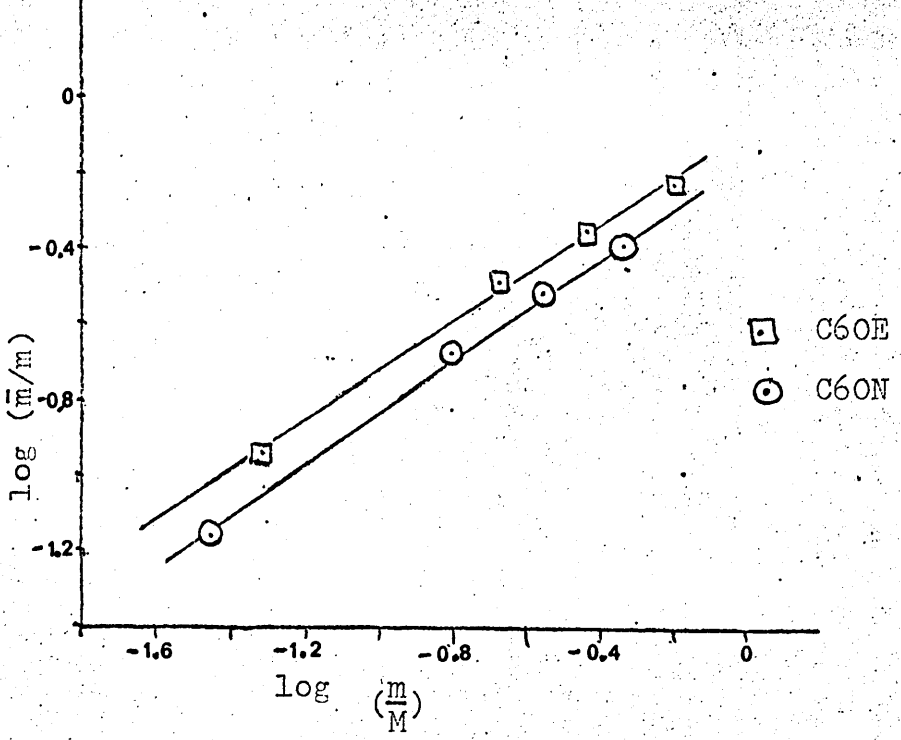

Figure 3.1. Plot of log (m̄/m) versus log (m/M) for the C60 membranes.

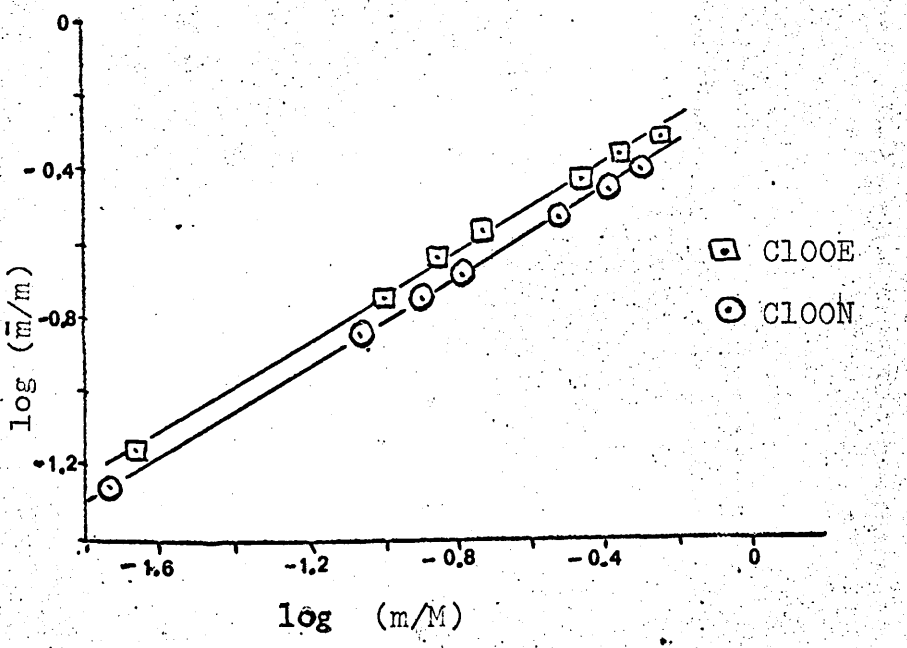

Figure 3.2. Plot of log (m̄/m) versus log (m/M) for the C100 membranes.

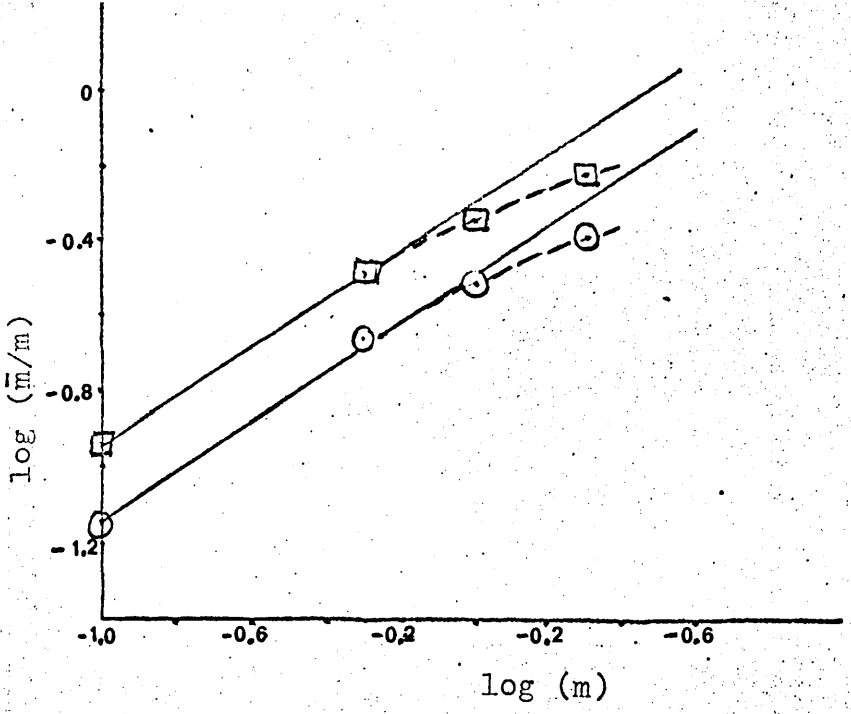

Figure 3.3. Plot of log (m̄/m) versus log m for the C60 membranes.

⊡ C60E ⊙ C60N

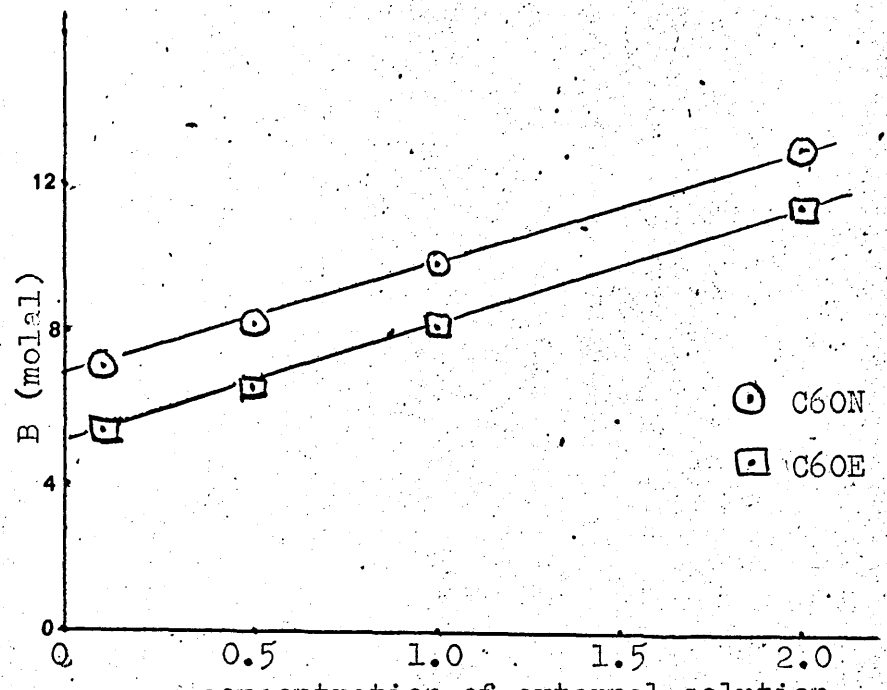

Figure 3.4. Plot of B (max. fixed charge concentration) versus concentration of external solution (C60 membranes).

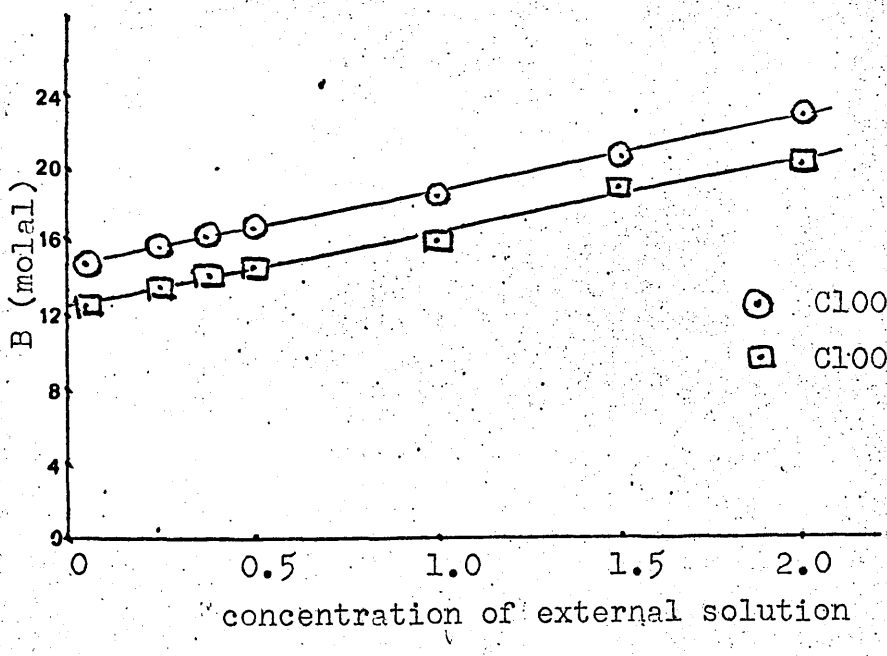

Figure 3.5. Plot of B (max. fixed charge concentration) versus concentration of external solution (C_{100} membranes).

3.4. Discussion

3.4.1. Structural analysis from electrolyte uptake data.

The methods of determining the electrolyte uptake of the C60 and C100 membranes, their attendant difficulties and possible error, have already been discussed in sections 2.3.9. and 2.5.2, and the experimental results are given in tables 3.1 - 3.4.

Applying the simple Donnan law to the exchanger as a whole, and assuming that the structure is perfectly homogeneous, the mean activity coefficients of the sorbed salt have been calculated using the relation (3.1). These results, shown in tables 3.15 and 3.16 display similar trends to those obtained with many other systems, viz. decreasing values of activity coefficients with decreasing solution concentration. Since the lowest concentration studied was 0.1M, it is not possible to determine whether the very small values obtained by a number of authors, would also be obtained in these systems.

The experimental values of the salt uptake have been further analysed by the theoretical methods described in section (3.2) and the results of these calculations are to be found in tables 3.5-3.8. Although the concentration range/

range studied is somewhat limited, the validity of equation (3.15) for these systems is proved by the linearity of the plots shown in figures 3.1 and 3.2. Even at 4M for the C100 membranes, there is little tendency to curvature, indicating that the assumptions about the effective activity coefficients and the neglect of the second and third integrals in equation (3.15) are valid to much higher concentration than might be expected. The effects of neglecting to correct the mean counter-ion molality for changes in the water content of the exchanger, are fairly large as comparison of the corresponding plots in figures 3.1 and 3.3. reveals. At concentrations below 0.1M this correction is probably small, but above 0.1M, and particularly with a highly swollen membrane, it becomes very important.

The gradients of the $\log(\frac{\bar{m}}{m})$ versus $\log(\frac{\bar{m}}{M})$ plots were obtained by least squares analysis, and from them, the values of the exponent z of equation (3.15) were calculated for each of the membranes studied, and are given in table 3.9. It is interesting to compare these values with those obtained for other membranes. Glueckauf [162] gives, for the ACI cation and anion-exchange membranes, a Z- value of 0.63, and for the permaplex A20 membrane a value of 0.74. He/

He also states that similar calculations using the results of other authors, notably Davies and Yeoman, [125] Pepper Reichenberg and Hale, [164] and Mackie and Meares, [81] yield values of z between 0.55 and 0.88. In this context, the values of z obtained in this work for the C60 and C100 membranes are low. This cannot be due to the limited range of concentration studied since, as reference to Glueckauf's plots shows, the results for lower concentrations tend to increase the gradients of the log $(\frac{\bar{m}}{m})$ versus log $(\frac{\bar{m}}{m})$ plots, thereby reducing the values of z.

Arnold and Koch [104] found that for the AMF C60 membrane in the hydrogen form in sulphuric acid, the value of z was 0.5. The hydrogen form of the exchanger is, however, much more highly swollen than the sodium form in solutions of corresponding concentrations and so a strict comparison of these results is not possible.

The z values, to some extent at least, are a measure of the homogeneity of the membrane structure, a truly homogeneous membrane having a z value of zero. It would, therefore, appear that the C60 and C100 membranes are more homogeneous than most membranes previously studied by this method.

It/

It is also interesting to observe the effect of the heat expansion on the membrane structure. In both series of membranes, the thermal treatment causes expansion of the matrix as discussed in section 2.5, and produces a structure capable of absorbing more electrolyte, and, therefore, by inference, one in which the Donnan potential has been reduced. Judging from the z values, the expansion does not seem to have affected the homogeneity of the C100 membranes although the effect on the C60 membrane is to produce a structure in which the heterogeneity of the membrane has increased slightly, probably due to the production of more void regions or by the expansion of existing voids. This difference in the effect of expansion on the two types of membrane may be explained by considering the original structure. The C100 membranes have a much tighter and probably more highly cross-linked structure than the C60 membranes, and it is probable that the effect of this is to increase the rigidity of the structure and prevent the production of further void regions, a process which would probably entail the breaking of covalent cross-linking bonds.

Knowing/

Knowing the value of z, the values of B and k_o are immediately obtainable from equations (3.10) and (3.11). It is important to notice that the values of k_o and B are functions of M and are, therefore, different for each external concentration. The values of k_o and B for each external concentration are given in tables 3.10 and 3.11. The values of B are interesting since they represent the upper limit of the fixed charge concentration for any particular concentration. The B values for each membrane increase linearly with increasing external concentration, as shown in figure 3.4, a consequence of the linear increase in the mean fixed molality M. The curves for the two C60 membranes are parallel, as are those for the C100's. This is a result of the parallel behaviour in water contents exhibited by these pairs of exchangers, (see figure 2.8), and of the similar z values. The B values for the C100's are considerably greater than for the C60's, again demonstrating the tighter structure and lower water content of the former.

Since the concentration range studied is insufficiently large to give any estimate of the true value of A, its value has been assumed to be zero. Glueckauf [2] has shown that/

that if A is small, i.e. less than 10^{-3} molal, then the effect of including it explicitly in the calculations only becomes important at very low external solution concentrations. If the value of A were fairly large, deviations from the straight line plots of figure 3.1 would be observed, due to the effect of the second integral in equation 3.16.

The value of a may be obtained from equation (3.13) and (3.14). In the simplified case this reduces to

$$a = \frac{1}{v_1 \cdot m} \left(\frac{\bar{m} \cdot v_1}{k_o I_o^{\infty}} \right)^{1/(2-z)} \qquad (3.22)$$

The values of a so calculated are shown in tables 3.10 and 3.11.

Once the value of z has been determined, it is possible to calculate the integral

$$I_o^{\infty} = \int_o^{\infty} y^{-z} f(y) dy \qquad (3.23)$$

where $y = M/a v_1 . m$ and $f(y) = \bar{m}/am$ is the positive root of the equation, $f(y) \cdot (f(y) + y)^{v_1/v_2} = 1 \qquad (3.24)$

The values of I_o^{∞} are also given in table 3.9.

Probably the most interesting calculation to be made from the preceding results, is that of the fractional distribution $\Delta\bar{\phi}$ of exchange sites in the membrane. Like the values of k_o and B, the fractional distribution depends on/

on the external concentration. Table 3.12 shows $\Delta\phi^m$ as a function of the range of M for the C60N membrane in equilibrium with 0.1M and 2.0M sodium chloride solutions. Table 3.13 gives the results of a similar calculation for the C60E membrane.

Comparison of the results for the normal and expanded membranes at each concentration shows that the expansion has produced a higher percentage of regions of lower M with a corresponding reduction in the percentage of regions with high fixed charge concentration. The effect of increased external concentration, is to produce a membrane whose physical dimensions and water content are smaller (sections 2.5.1), and hence one with higher values of M. Comparisons of the $\Delta\phi^m$ - M results at 0.1M and 2.0M show that the effect on the very low M regions is small, but that there is a large increase in the number of regions with high values of M.

These results also show that in both membranes, most of the regions have fixed charge molalities which are not very much different from the average value for the whole membrane. This result is a consequence of the small value of z which indicates a fairly homogeneous membrane. The regions with very low values of M are, however, extremely important/

important in determining the electrolyte uptake and have a significant effect on the co-ion diffusion properties of the membrane as shown in section 3.7.

3.4.2. Electron Micrographs.

The electron micrographs shown in figures 3.6 and 3.7 were obtained using the C60N membrane in the thorium form, in order to show up clearly the regions in which the counter-ions are concentrated. These micrographs show that the resin structure is indeed heterogeneous. The regions of high charge density, which show up as dark areas in the photographs, are located in clusters about 400Å in diameter. The sizes of these regions are similar to those obtained by Goldring (156) who studied the AMF membranes using a somewhat different technique, and it seems, therefore, that the structure has not been significantly affected by the processes used to obtain the micrographs. The regions of high fixed charge density are surrounded by lightly stained regions which may represent either voids or areas of low density polyethylene. The results of the co-ion uptake experiments suggest that there cannot be a large number of void regions, in which the electrolyte uptake would be large, and hence it may be concluded that many of the lightly and non-stained regions represent polyethylene. These observations are in keeping with the method of preparation of the membrane, the high counter-ion concentrations being found in

regions/

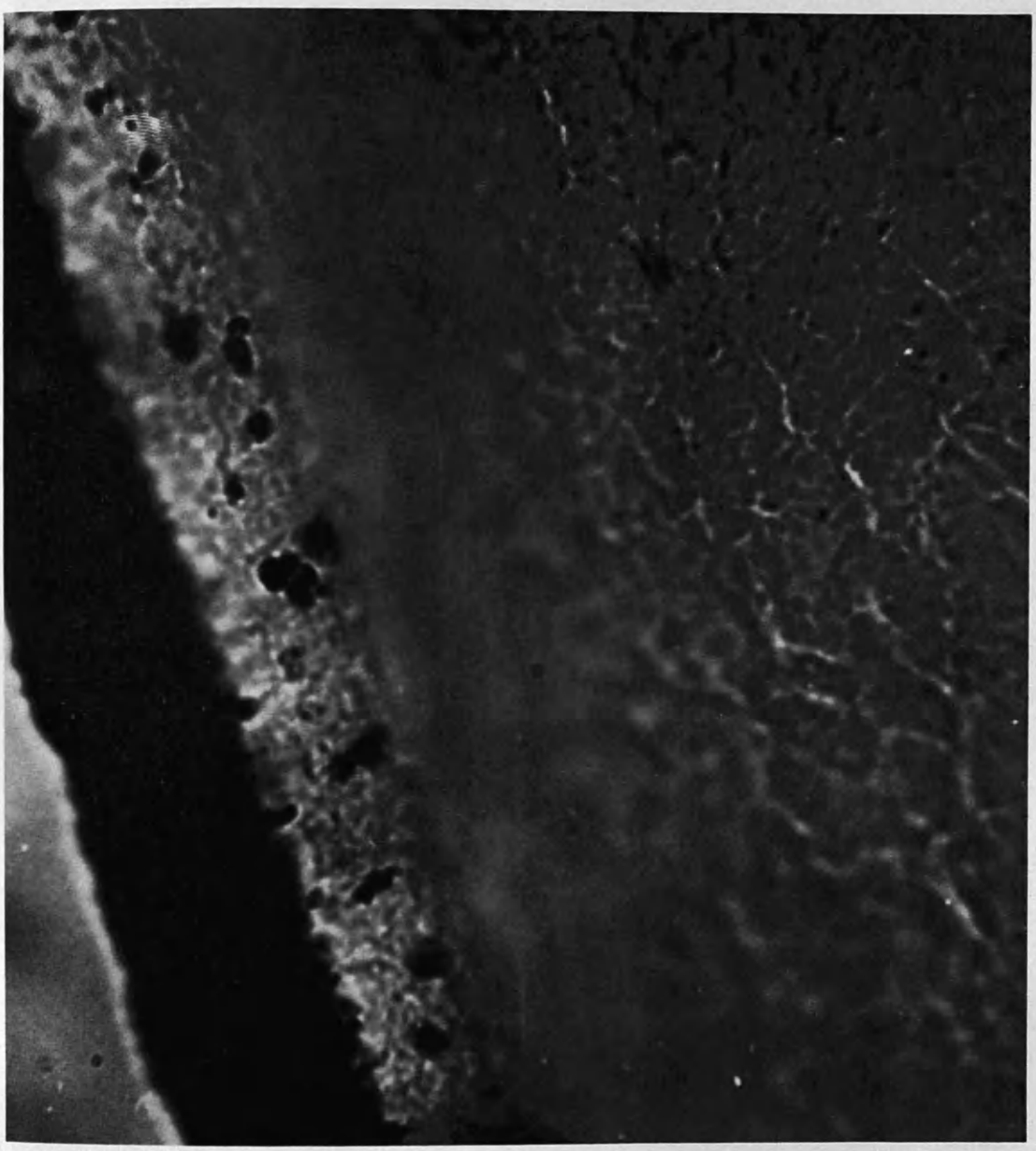

Figure 3.6. Optical ~~Electron~~-micrograph of AMF C60-N membrane. (x 9,000). The edge of the membrane is shown on the left of the picture. The membrane is clearly shown to exhibit heterogeneity.

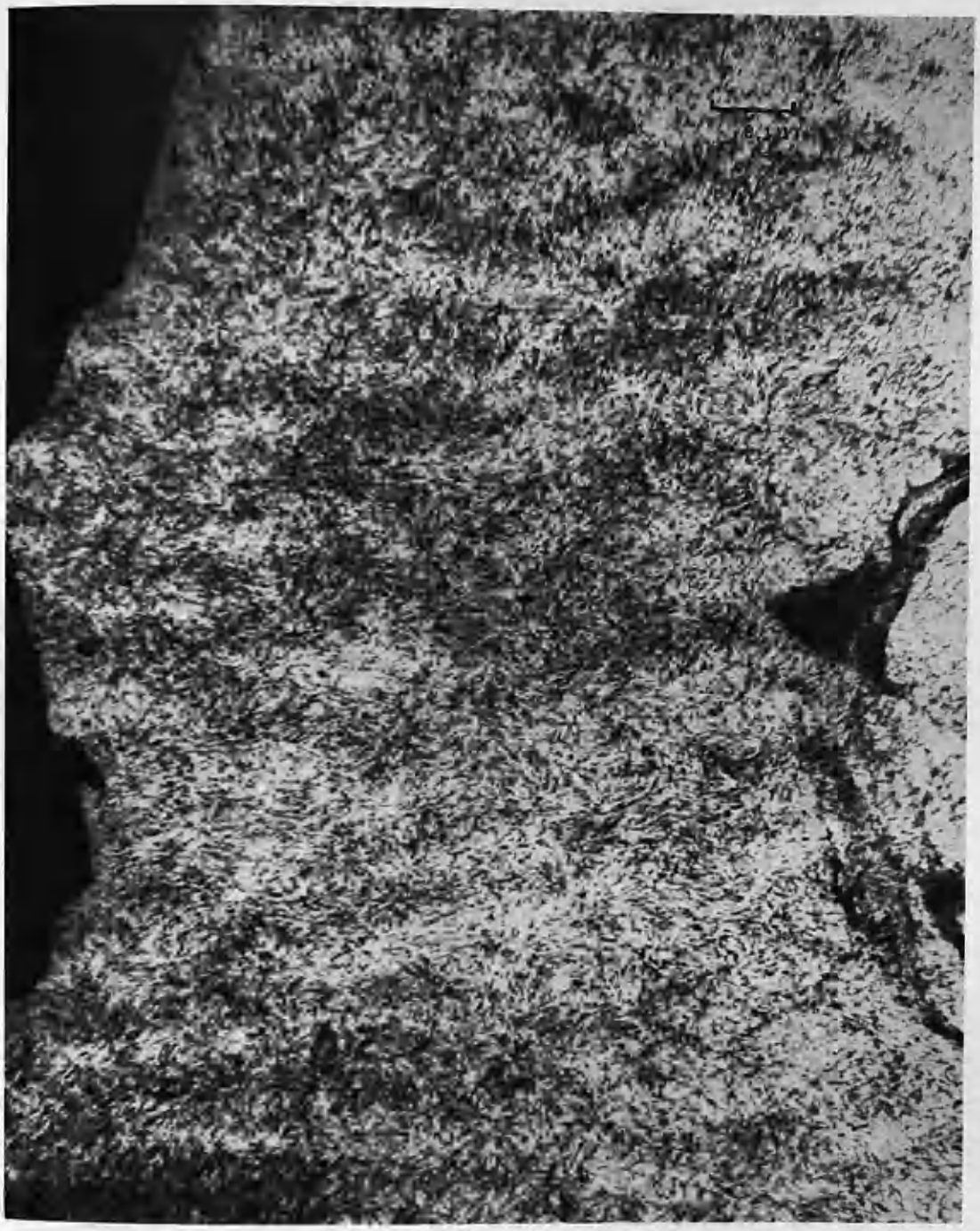

Figure 3.7. Electron-micrograph of AMF C60N membrane. (x 120,000). The lightest tone represents regions of low fixed charge concentration or of polyethylene. (The dark regions on the left are holes in the membrane section, and on the right is a fold produced by the cutting procedure).

regions corresponding to the pre-polymerised styrene.

Comparison of the electron micrographs with others to be found in the literature, [156] [157] [162] suggests that the C60 membrane is probably less heterogeneous than many of the others studied, a fact which lends support to the lower values of z observed for this membrane.

With the simple technique used here, it was impossible to distinguish the normal membrane from the expanded one. This is only to be expected since as the co-ion data suggests, the structure is not significantly altered by expansion.

3.4.3.

The Glueckauf theory defines as the sole cause of the abnormally high uptake observed at low concentrations, the degree of inhomogeneity present in the membrane structure, regardless of how this inhomogeneity arises. This theory removes the need for anomalously low activity coefficients for the sorbed electrolyte and assumes that the activity coefficients in the regions within the exchanger where the uptake is greatest are similar in behaviour to those in free aqueous solutions. On the other hand, the theory published a year earlier, by Tye [161] recognises the lowering of the activity coefficients in the exchanger as a real effect and seeks to find an explanation for it in the inhomogeneity of the charge surrounding the fixed sites. This theory has not met with wide acceptance but it is worth considering as an example of a different approach to the problem of electrolyte uptake.

Table 3.14 shows the values of the uptake predicted by/

by the Tye theory using the β values calculated for each membrane from the 0.5M results. While the agreement is reasonable at high concentrations, the values at 0.1M are considerably in error. If the 0.1M value of β is used then, of course, all the predicted higher concentration values differ substantially from the observed ones. Tye himself, explains the fact that he found the higher concentration values to fit those calculated from the lower concentration β values, by the form of equation (3.21), which is such that the values of $\bar{m}$ at high concentration are not very sensitive to the value of β. It would appear then, that this theory is inadequate to describe the whole range of concentration studied, even though this range is fairly small. Indeed Tye states that at concentrations below 0.1M the theory fails to predict the correct values as determined by Gregor.[123][124] The results of this present study, suggest that this approach is very limited in its application and cannot be regarded as a useful method of predicting electrolyte uptake data.

3.5. Effect of Heterogeneity on membrane permeability - Theory.

The preceding section gives a measure of the distribution of the sites within the exchanger, and this is important in predicting the permeability of the co-ion in the exchanger. However, the absolute value of the co-ion diffusion is governed not only by the site distribution, but by the physical arrangement of these sites into different regions, and the way in which the various regions are linked within the exchanger matrix.

There are two effects of inhomogeneity which may be dealt with separately. In the first place, the effect of the polymer matrix in obstructing the diffusion paths of the ions may be treated using the tortuosity factor discussed in section 2.2.3. Second, the inhomogeneities in the fixed charge distribution affect the permeability, and this effect has been discussed by Glueckauf[2] in the manner outlined below.

The local permeability of any region of the exchanger is given by

$$P = \bar{D}\Delta\bar{c}/\Delta c \qquad (3.25)$$

If the permeability is measured using a radioactive tracer/

tracer technique and the concentration of active species is maintained at zero on one side of the membrane, then equation (3.25) becomes,

$$P = \bar{D}.\frac{\bar{c}}{c} \approx \bar{D}.\frac{\bar{m}}{m} \qquad (3.26)$$

where P is the permeability of the co-ion, $\bar{D}$ its diffusion coefficient, and c and m the local co-ion concentration in molar and molal units respectively and the barred symbols refer to membrane phase. Thus even if $\bar{D}$ were constant, the permeability would vary over several orders of magnitude as the ratio $\bar{m}/m$ varied within the exchanger. The co-ion permeability will depend on which regions in the exchanger are the most continuous.

To obtain the mean value of P for the diffusion process it is necessary to use the Bruggeman equation: (2)(163)

$$\frac{dP}{d\ln(u)} = \frac{3P(P_u - P)}{2P + P_u} \qquad (3.27)$$

where P_u is the permeability associated with the volume fraction between u and (u+du), which is being added to the already treated volume fraction, u, of overall permeability, P. This equation distinguishes between a continuous and a disperse phase. The final result for the mixture weights the mean value in favour of the continuous phase. In equation (3.27), P_u is assumed to be for a region which is less continuous/

continuous than the already treated mixture with overall permeability P. The method used is to choose an arbitrary value for the molality of the most continuous region, M* and calculate the overall permeability P which can then be compared with the observed value. The value of P is dependent not only on the value of M* chosen, but also on the regions which are considered to be the next most continuous. Thus, depending on the direction of the integration of equation (3.27), a different value of P is obtained (see appendix A.13). When agreement between the predicted and measured permeabilities is obtained, then information about the structure of the exchanger may be deduced from the value of M* used, and the direction of the integration procedure. This treatment thus, provides an analytical method for yielding information about the arrangement and interconnection of the various regions in the exchanger, information which can be compared with that obtained from the electron micrographs of the membrane.

3.6. Results.

Table 3.17.

Calculation of most continuous regions.

Ext. soln. concn. (molar)	C6ON M* (molal)	C6ON $\bar{D}_{Cl}$ predicted $\times 10^5$ $cm^2 sec^{-1}$	C6ON $\bar{D}_{Cl}$ observed $\times 10^5$ $cm^2 sec^{-1}$	C6OE M* (molal)	C6OE $\bar{D}_{Cl}$ predicted $\times 10^5$ $cm^2 sec^{-1}$	C6OE $\bar{D}_{Cl}$ observed $\times 10^5$ $cm^2 sec^{-1}$
0.10	< 0.01	1.60	1.63	< 0.01	1.60	1.59
0.50	< 0.01	1.25	1.26	< 0.01	1.50	1.42
1.00	< 0.01	1.26	1.17	< 0.01	1.50	1.45
2.00	~ 0.01	1.0	0.94	~ 0.01	1.20	1.19

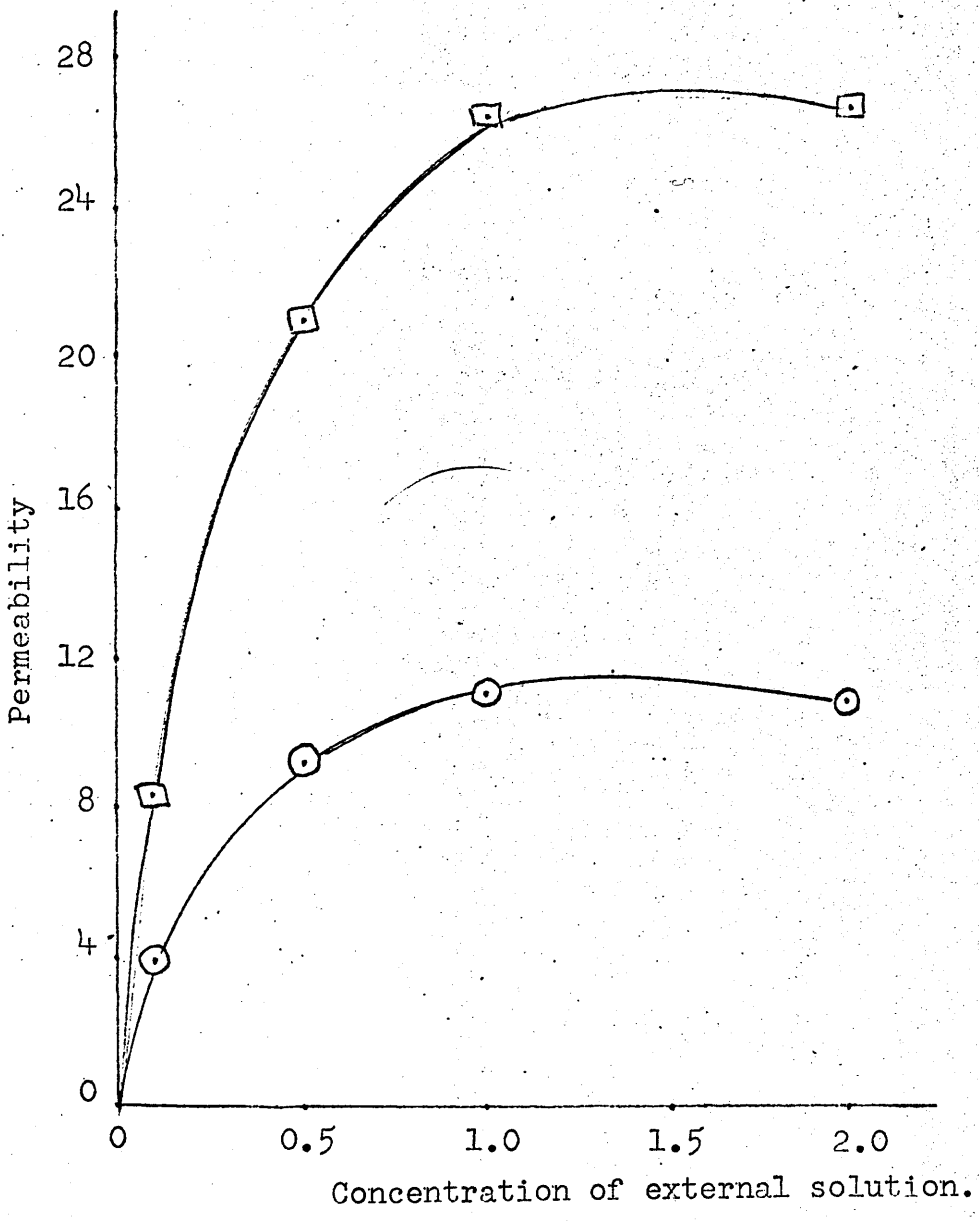

Figure 3.8. Plot of permeability against concentration of external solution (C60 membranes).

⊡ C60E ⊙ C60N

3.7. Discussion.

Table 3.17 shows the values of the observed and calculated co-ion diffusion coefficients, and the values of the molalities of the most continuous regions used in the calculations. In all cases the most continuous regions are those where the fixed charge density is low. The next most continuous regions are those with higher fixed charge density up to the highest fixed charge concentration B, the very low concentration regions being the most disperse. This is the case for both membranes, and, considering the assumptions used in the calculations, there is little difference between them. The results for these membranes is in sharp contrast to that obtained by Glueckauf[162] for the TNO A60 anion-exchange membrane with sodium chloride, where he found the most continuous regions to be those with high fixed charge concentration. Glueckauf supported his results by electron micrographs showing the low concentration regions as 'islands' within the regions of medium and high fixed site concentration. The micrographs obtained in this present study of the AMF C60 membranes, show that the high molality regions are disperse. The regions between them show up as 'transparent'/

'transparent' in the electron beam and may represent regions of low fixed charge density or regions of polyethylene which have not been penetrated by the styrene during the membrane preparation. With the techniques used in this work it was impossible to distinguish between such regions. However, the micrographs do confirm that the high concentration regions are certainly not continuous, but are interconnected by aqueous fissures or voids, or regions of uncharged polyethylene. Further evidence for the difference between the structures of the TNO A60 and the AMF C60 membranes, is to be found in the P-c plots. Glueckauf (162) found this plot for the TNA A 60 membrane to be linear up to almost 2M indicating that the regions with the highest fixed charge concentration are the most continuous and thus govern the rates of through diffusion of the co-ions. This is far from the case for the AMF C 60 membranes, as figure 3.8 shows. It can be seen that, as the external concentration increases, the co-ion diffusion is significantly affected, and, therefore, most of the co-ion concentration - which is in the regions of lower fixed charge density - must be in the regions which are most continuous.

As the concentration of the external solution increases

so/

so the membrane shrinks and the water content of the membrane decreases. Thus, there must be a corresponding increase in the concentration of the fixed charges in all regions, assuming this contraction to be uniform for the whole exchanger. Thus even if the shrinking of the membrane leaves the overall pattern of site distribution unchanged, the molality of the most continuous regions must be increased. The results in table 3.17 show that this increase in M* with increasing external concentration, does indeed occur. If, however, the shrinking has a significant effect on the configuration of the polymer chains, then the most continuous regions may be affected. The magnitude and direction of such a change if indeed it occurred, is impossible to predict from the information available.

3.8 Conclusions.

Although if has been shown in the preceding sections, that the Glueckauf treatment of resin heterogeneity fits the experimental results extremely well, the range of concentration studied is not large, and does not extend to very low values. Therefore, it would be unwise to claim that the observed agreement provides unequivocal proof of the validity of this theoretical approach. The explanation of electrolyte uptake values remains an extremely difficult problem. It appears that, under different conditions, and for different membranes, a large number of widely divergent theories can supply explanations of the observed phenomena, and the problem of finding the correct solution, if indeed, only one exists, is far from solved. The evidence for heterogeneity is very strong and hence the extension of theories of 'homogeneous' polyelectrolyte solutions to ion-exchangers is an oversimplification of the problem and must have limited value, except where there is strong evidence for a homogeneous membrane system. Nevertheless, the existence of low activity coefficients of both counter- and co-ions in polyelectrolyte solutions must be borne in mind/

mind when considering the salt uptake in ion-exchangers. A true solution to the problem probably involves an extension of the polyelectrolyte theory but also including the effects of heterogeneity on the resin properties.

CHAPTER FOUR

Hydrous zirconia as an ion-exchanger.

4.1. Introduction.

As already discussed in chapter 1, there are a large number of inorganic ion-exchange materials, both naturally occurring and synthetic. While these materials have not found such wide use as the synthetic organic resins, many of them have specific properties which make them of great interest, e.g. the zeolites can act as molecular seives, the zirconium phosphate type exchangers have high thermal stability and resistance to radiation, and the hydrous oxides have the property of variable capacity. It is with this last mentioned group that this study is concerned.

The ion-exchange properties of the hydrous oxides can best be described as pseudo-amphoteric. These materials can act as cation-exchangers in solutions of pH above their isoelectric point, and anion-exchangers in solutions of pH below this value. The cation and anion-exchange capacities also vary with the pH of the external solution. [165] Many of these materials are, however, chemically unstable, being attacked by acids and bases. Hydrous zirconium oxide - hydrous zirconia - is the most stable of these compounds being soluble only to the extent of 10^{-7} moles per litre even in 0.1M hydrochloric acid [166], and exhibiting negligible swelling effects in solutions of different pH, as shown/

shown by the constant density of the particles (table 4.1b). Combined with the fact that the isoelectric point of this material is at pH 7, these properties make it a suitable exchanger for a study of the effects of variable capacity on some of the other ion-exchange properties.

4.2. Theory.

4.2. Mechanism of Ion-Exchange on Hydrous Oxides.

Two mechanisms have been postulated for the ion-exchange process in hydrous oxides; (167)

Acid solution Alkaline solution

(1) $M^+ + OH^- \rightleftharpoons M—OH \rightleftharpoons M—O^- + H^+$ (4.1)

(2) $M—OH_2^+ \overset{H^+}{\rightleftharpoons} M—OH \overset{OH^-}{\rightleftharpoons} M—O^- + H_2O$ (4.2)

In order to decide which of these mechanisms best represent the situation it is necessary to consider some of the structural evidence which exists in the literature. For this purpose the case of hydrous zirconia will be taken as a specific example.

Crystalline zirconia has a negligible ion-exchange capacity whereas the amorphous material is capable of attaining a fairly high capacity (166) (168). This evidence suggests that the structure plays a very important part in determining the ion-exchange properties of this material.

Strictly speaking, zirconia is only represented by the formula ZrO_2 after ignition to high temperatures. Normally/

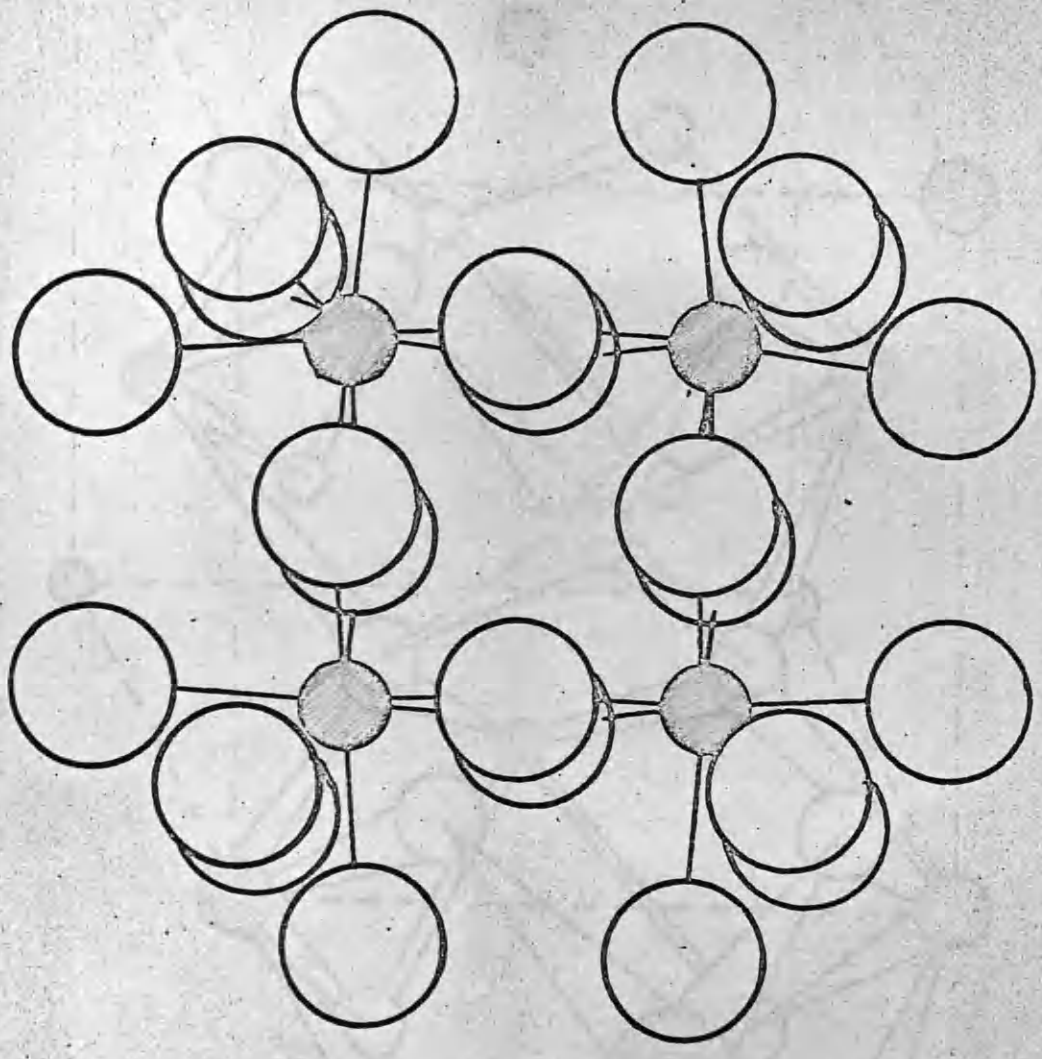

Figure 4.1. Tetrameric structural unit formed in the hydrolysis of zirconyl chloride. Each zirconium atom is shown co-ordinated to four bridging hydroxyl groups and four water molecules. (reference (170)).

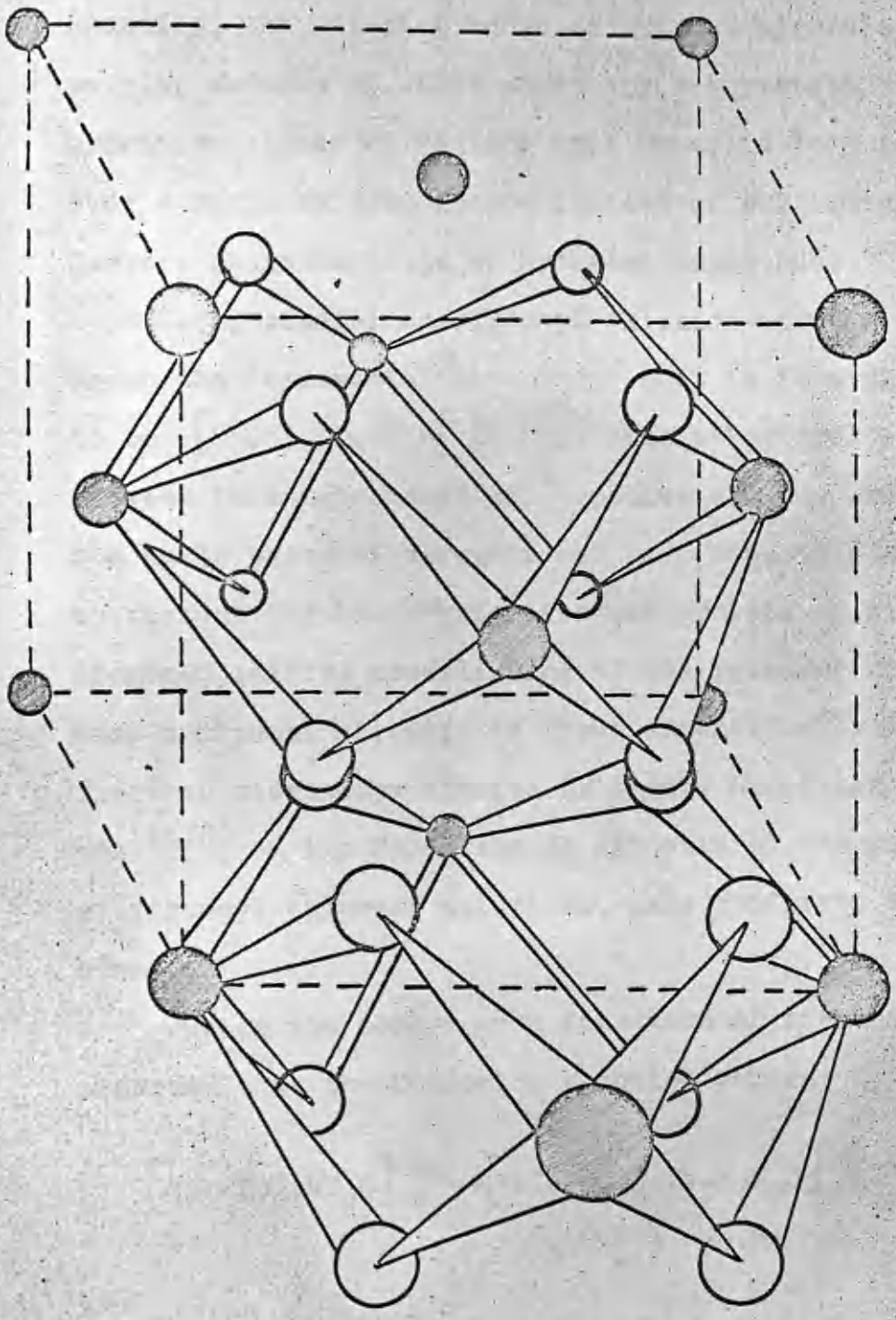

Figure 4.2. Tetrameric units linked by hydroxyl bridges in the manner proposed by Clearfield, (Reference (170)).

Normally, the material known as hydrous zirconia contains varying amounts of water which are not present as water of hydration, since on heating this water is lost continuously over a range of temperature instead of exhibiting dehydration isobars characteristic of hydrated compounds. (166)

X-ray studies on zirconyl chloride octahydrate have shown the fundamental structural unit in this material to be $\left[Zr(OH)_2 .4H_2O\right]_4^{8+}$. The structural similarity between this tetrameric Zr^{IV} species and the ZrO_2 chains in the cubic phase of zirconia was used by Clearfield (169) to account for the crystallisation process of zirconia. He proposed initial crosslinking of the tetramer units to produce amorphous zirconia as shown schemetically in figure 4.1. Electron microscopy studies by Fryer, Hutchison and Paterson (170) on the formation of zirconia by thermal hydrolysis of zirconyl chloride solutions, have confirmed this prediction.

During the homogeneous formation of zirconia it is proposed that the following reaction occurs:

$$\left[Zr(OH)_2.4H_2O\right]_4^{8+} \rightarrow \left[Zr(OH)_{2+n}.(4-n)H_2O\right]_4^{(8-4n)+} + 4n.H^+ \qquad (4.3)$$

At/

At this stage, further hydrolysis and olation occurs, the elimination of water on the tetramers yielding hydroxyl bridges between the individual tetrameric units, as shown in figure 4.2. This reaction produces, finally, a monoclinic crystalline form of zirconia, which, as mentioned above, has negligible ion-exchange capacity.

In contrast to the slow formation described above, precipitation of zirconia by base is rapid and irreversible, thereby preventing the slow crystallisation process. The material so obtained is amorphous and probably contains a large number of non-bridging hydroxyl groups, and co-ordinated water molecules which can act as the fixed sites responsible for the ion-exchange properties of the material. The positive charge associated with the $M\text{-}OH_2^+$ group can then be delocalised to some extent over the neighbouring matrix regions thus conferring greater stability on the material. The variability in the ion-exchange capacity would then be represented by the second of the two mechanisms proposed above, equation (4.2).

4.2. Diffusion Processes.

For many years, diffusion processes have been the subject/

subject to much theoretical and experimental study. Recently, the subject of much of this work has been the diffusion of ions in ion-exchange beads and membranes. Most of these systems can be treated using Fick's laws of diffusion, [47] and the diffusion coefficient of the mobile species so obtained. There has been widespread interest in the results of these studies and many attempts have been made to explain the variation in the values of the diffusion coefficients with variation in the physical properties of the exchangers, e.g. water content, ion-exchange capacity etc.

In order to examine the effect of capacity changes on the properties of an ion-exchanger it is necessary to have a material which combines the property of variable capacity with a rigid structure, negligible swelling and high chemical stability. This is difficult to achieve since changes in the capacity of most exchangers are usually accompanied by changes in other properties such as cross-linking. [5] However, hydrous zirconia has properties as an ion-exchanger which satisfy the above conditions and make it suitable for such a study. In this present study the anion-exchange properties of the system were examined after equilibration with solutions of pH less than 7.

4.2.1./

4.2.1. Kinetics of Ion-Exchange.

(a) Isotope Exchange, in Ion-Exchange Beads.

Ion-exchange is a diffusion process. Diffusion processes are usually described using Fick's first law:

$$J_i = D_i \text{grad } c_i \qquad (4.4.)$$

where J_i is the flux in moles per unit time per unit cross section of the diffusing species i, c_i is its concentration in moles per unit volume and D_i is the diffusion coefficient. In the simplest case where no processes other than diffusion occur, the flux is proportional to the concentration gradient and the diffusion coefficient is thus a constant. This is the case for isotopic diffusion in a system which is in equilibrium except for isotopic distribution.

For the case of ideal particle diffusion control the flux of the isotope A (which is equal and opposite to that of isotope B), in the exchanger is given by (171)

$$J_A = -\bar{D} \text{ grad } \bar{c}_A \qquad (4.5.)$$

The time dependence of the concentration is interrelated with the flux by Fick's second law:

$$\frac{\partial \bar{c}_A}{\partial t} = - \text{div } J_A \qquad (4.6.)$$

where/

where t is the time.

The combination of equations (4.5) and (4.6) for systems with spherical geometry and with a constant diffusion coefficient gives

$$\frac{\partial \bar{c}_A}{\partial t} = \bar{D}\left(\frac{\partial^2 \bar{c}_A}{\partial r^2} + \frac{2}{r}\frac{\partial \bar{c}_A}{\partial r}\right) \qquad (4.7)$$

where r is the radial space coordinate.

This equation must be solved under the appropriate boundary conditions. In the simplest initial condition all A ions are in the ion exchanger at a uniform concentration $\bar{c}_A^o$ and there are no A ions in the solution: i.e.

$$r > r_o,\ t=0\quad \bar{c}_A(r) = 0.$$
$$0 \leq r \leq r_o,\ t=0\quad \bar{c}_A(r) = \bar{c}_A^o = \text{const.} \qquad (4.8)$$

where r_o is the bead radius.

When the concentration of A in the solution remains negligible throughout the process as in a batch experiment where the solution volume is so large that

$$\bar{c}\,\bar{V} \ll c\,V \qquad (4.9)$$

where c is the total concentration of the counter ion, $\bar{V}$ is the volume of the exchanger and V is the volume of the solution, then the 'infinite solution volume' condition can be used without introducing a large error.

With the above conditions applying the infinite solution/

solution volume condition is

$$r = r_o, \quad t > 0 \qquad \bar{c}_A(t) = 0 \qquad (4.10)$$

The solution of equation (4.7) under the conditions of (4.8) gives the function $\bar{c}_A(r,t)$. Integration of this function throughout the bead leads to (171)

$$U(t) = 1 - \frac{\bar{Q}_A}{\bar{Q}_A^0} = 1 - \frac{6}{\pi^2} \cdot \sum_{n=1}^{\infty} \frac{1}{n} \exp\left(- \frac{Dt\pi^2 n^2}{r_o^2}\right) \qquad (4.11)$$

where $\bar{Q}_A$ (t) is the amount of A in the exchanger at time t,

$\bar{Q}_A^0$ is the initial amount of A in the exchanger,

U(t) is the fractional attainment of equilibrium.

The fractional attainment of equilibrium, U(t), is seen to depend only on the magnitude of the dimensionless time parameter $\bar{D}t/r_o^2$. When $\bar{D}t/r_o^2$ is small, equation (4.11) does not converge rapidly. In this case it is sometimes more convenient for practical purposes to use Vermeulen's approximation (171) (172).

$$U(t) = \left[1 - \exp\left(-Dt\pi^2/r_o^2\right)\right]^{1/2} \qquad (4.12)$$

This equation is valid over the whole range $0 < U(t) < 1$, although it is slightly less accurate than equation (4.11).

Equation (4.12) shows that a plot of $\log\left(1 - (U(t))^2\right)$ against time will be a straight line of gradient $-D\pi^2/2.303\, r_o$.

The/

The condition for particle diffusion control for isotopic exchange and non-electrolyte sorption is (173)

$$\frac{\bar{C}_A \bar{D}_A \delta}{C_A D_A r_o} \ll 0.13 \qquad (4.13)$$

In the experiments described in this work particle diffusion control was operative as substitution of the appropriate values can show. Film diffusion control is most likely when the capacity is least. For this case, in the present study, $\bar{C} = 3.7, \bar{D} = 4_{10}-7$, $\delta \cong 10^{-3}, C = 0.2, D = 2_{10}-5$, $r_o = 0.02$, giving a value of $1.7_{10}-2$ for the expression in equation (4.13). This value is less than 0.13 thereby ensuring particle diffusion control.

(b) Ion-exchange membranes.

The method of calculating the diffusion coefficients for the ions in the hydrous zirconia membranes is the same as that used for the organic resins and has been desbribed in section 2.5.3.

4.3. Experimental.

4.3.1. Preparation of Zirconia.

The zirconia particles had previously been prepared by the method outlined below.

To a stirred solution of approx. 0.3M zirconyl chloride was added, dropwise, 3M ammonium hydroxide solution until the precipitation of zirconia was complete and the solution was alkaline. The precipitate was allowed to settle, washed by decantation with distilled water, filtered and washed again before being dried at 40°C for three days. The dry zirconia was then further washed with distilled water which contained a small amount of ammonium hydroxide solution, and finally washed with water until the washings were chloride and acid free. The zirconia was allowed to air dry, again washed to remove acid and allowed to break down. A sieved fraction of 30 - 40 B.S.S. was used in the present study, and was stored in a 98% humidity atmosphere over potassium dichromate solution.

Four batches of zirconia with different anion-exchange capacities were prepared by washing samples of the above material with solutions of hydrochloric acid of concentration 0.1, 0.05, 0.01, and 0.001M respectively, the total chloride/

chloride concentration in each solution being maintained at 0.2M by using sodium chloride as the supporting electrolyte. The chloride ion concentration was maintained at this fairly high constant concentration in order to provide the conditions best studied to give particle diffusion control in the kinetic experiments (see equation 4.13). The conversion to the various capacity forms was carried out by column washing the samples of exchanger with the appropriate solution, for several days, followed by a further period of batch equilibration for several weeks. It had been previously shown (174) that equilibration times of this length were required in order to produce fully equilibrated material. Samples for the kinetic experiments were prepared by further equilibrating the exchanger in solutions of the appropriate concentration containing Cl^{36}. These samples were then filtered, quickly washed with the appropriate Cl^{36} free solution to remove any Cl^{36} which was adhering to the surface, and air dried before being stored over saturated potassium dichromate solution.

4.3.2. Capacity determinations.

Two methods were used, and both are described below:

(a)/

(a) A 0.5 gm. sample of the zirconia was washed with 0.15M nitric acid until no further chloride was released. These solutions were then neutralised with calcium carbonate and titrated for chloride with standard silver nitrate solution using the Mohr method. (171)

(b) A 0.5 gm. sample of the exchanger was washed with a solution of 0.15M nitric acid, the total nitrate ion concentration being made up to 0.5M with sodium nitrate. A sample of this solution was then neutralised with sodium hydroxide and titrated potentiometrically for chloride with silver nitrate solution using silver electrodes (39).

4.3.3. Preparation of zirconia membranes.

Discs of sintered polyethylene were sealed into perspex holders by using chloroform, a perspex solvent, to dissolve the perspex round the edge of the disc, thereby giving a good seal. The discs were then placed in a concentrated zirconyl chloride solution in a desiccator, and the system evacuated using a water pump. This was found to be the best method of filling the pores in the discs, with the solution. After a few hours the discs were removed and dried over 1M ammonium hydroxide solution. This process was repeated/

repeated several times. Thereafter the discs were treated with zirconyl chloride solution then placed in 1M ammonium hydroxide solution. This procedure was also repeated several times until the pores appeared to be completely filled with zirconia. Electrolysis was then carried out using the set up shown below:

Pt electrode: $ZrOCl_2$ solution/membrane/ NaOH solution: Pt
(+) (0.1M) (0.1M) electrode (-)

This procedure precipitated more zirconia in the pores. Rectification and electroosmosis effects were observed.

The discs prepared as described above were then tested for leaks by placing them in a cell with a head of water to check if any water permeated the membrane. Over a period of several hours, no water flow was detected. Together with the evidence of rectification and electroosmosis the membranes were then considered to be leak free.

The membranes were then placed in solutions of hydrochloric acid of concentrations 0.1, 0.01, 0.001, and 0.0001M, the chloride concentration in each case being made up to 0.2M with sodium chloride as the supporting electrolyte. Equilibrations, with frequent changes of solution were carried out for several weeks.

4.3.4. Capacity determination in Zirconia membranes.

The anion-exchange capacity of the hydrous zirconia membranes was determined in a manner similar to the one employed for the capacity determination of the C60 membranes (section 2), except that solutions containing Cl^{36} ion instead of Na^{22} ions were used. The radioactive solutions were of the same concentration as those used for the equilibration processes, and hence, the value of the capacity so determined, included the concentraion of chloride present in the exchanger as sorbed salt.

4.3.5. Electrolyte uptake in Zirconia membranes.

The method used was similar to that used for the capacity determinations (section 4.3.4.), but solutions traced with Na^{22} ions were used. This gives the concentration of the sodium co-ions in the exchanger and since some electrolyte may be present as hydrochloric acid, this value is not identical to the electrolyte uptake. However, only in the case of the membrane equilibrated in 0.1M HCl, 0.1M NaCl solution, is this difference considered significant.

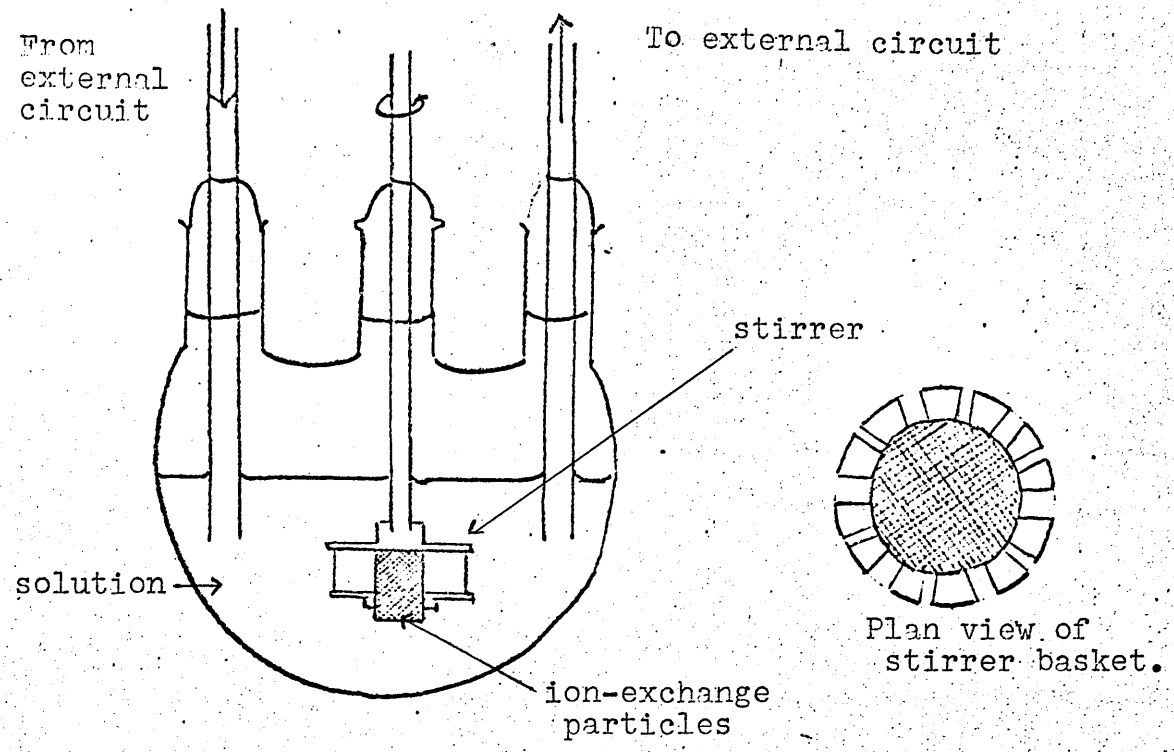

Figure 4.3. Cell for determining counter-ion diffusion coefficients in hydrous zirconia particles.

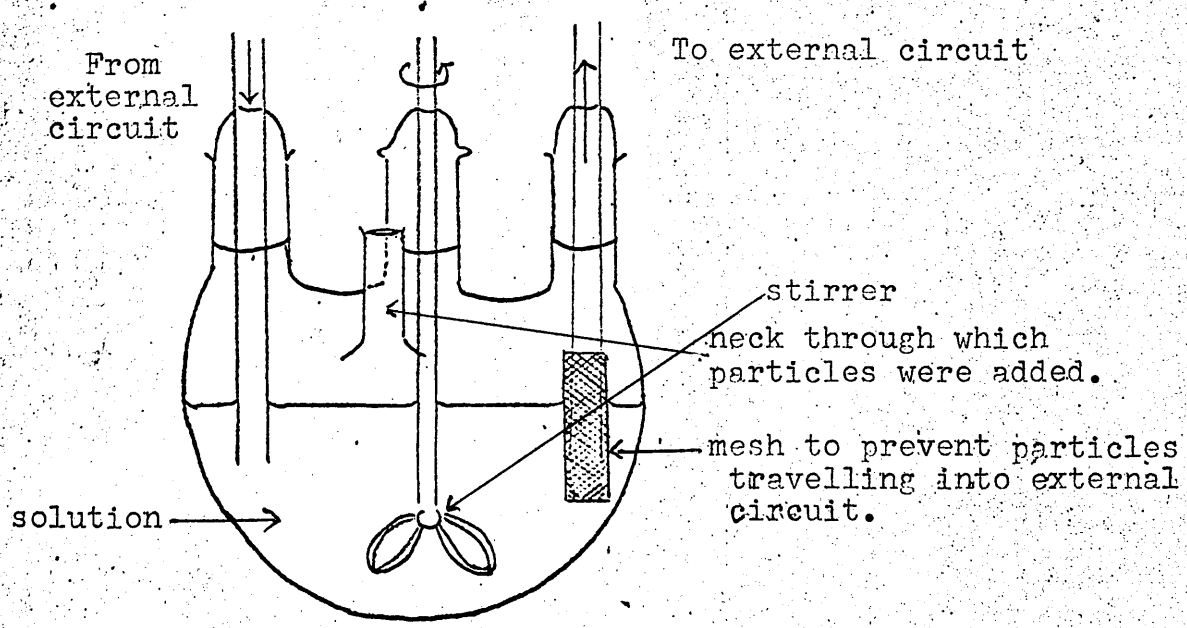

Figure 4.4. Modified cell for determining counter-ion diffusion coefficients in hydrous zirconia particles.

4.3.6. Measurement of Counter-ion Diffusion Coefficients.

(a) Zirconia Particles.

The first method used was similar to one described by Kressman and Kitchener [175]. A weighed amount of the exchanger containing Cl^{36} ions, was placed in a platinum wire cage which constituted the centre part of a centrifugal stirrer (see figure 4.3). The stirrer was started and quickly immersed in approximately 400 ml. of the appropriate electrolyte solution, which was contained in a flask shown in figure 4.3. The solution was pumped through the external circuit by a rotor arm pump at approximately 2 litres per minute. This method, however, proved unsatisfactory since the stirring was insufficiently fast to prevent film diffusion control of the process. A second method was then used, in which the sample was added directly to the electrolyte solution in the flask. The solution was efficiently stirred using a link stirrer as shown in figure 4.4. A fine wire mesh over the outlet tube prevented any exchanger being sucked into the external circuit.

Counting Methods.

Initially, it was hoped to measure the activity in the solution by passing it through a flow meter connected to a pen-recorder./

pen-recorder. The response time of the recorder was, however, too long for accurately recording the rapidly increasing solution activity. The method which was used in all kinetic experiments reported here was to remove samples from the flowing solution and add standard volumes of these samples to phosphor solutions [36] which were then counted in a Packard Tricarb Liquid Scintillation counter. The volume of each sample removed from the solution was approximately 0.1ml and ten such samples were removed in the course of an experiment. The change in volume of the solution due to sampling was less than 1% of the total volume and was neglected.

The volume of solution and the weight of exchanger used were such that the conditions for the infinite solution volume treatment were satisfied, i.e. $\bar{C}\,\bar{V} \ll C\,V$.

The accuracy of the experiments was $\pm$ 5%.

(b) Hydrous Zirconia Membranes.

The method used to measure the chloride ion diffusion coefficients through the zirconia membranes, was identical to that already described for the chloride ions in the AMF C60 membranes. The error in this case was ± 3%.

4.3.7. Conductivity of Hydrous Zirconia Membranes.

For the determination of the conductivity of the hydrous zirconia membranes, the method used was the same as that described in section 2.3.10 for the AMF membranes, the error in the membrane conductivity being ± 1%.

4.4. Results.

Table 4.1a.

Hydrous zirconia particles.

HCl concn. (molar)	Capacity $\bar{C}$ meqs/gm	meqs/ml	$\bar{D}^2/2.303r_o^2$ x10^4	$\bar{D}$ x 10^7	$\bar{D} \times \bar{C}$ x 10^8
0.10	2.11	5.48	20.0	2.14	1.17
0.05	1.94	5.04	22.0	2.36	1.19
0.01	1.72	4.47	26.3	2.81	1.26
0.001	1.41	3.66	38.0	4.07	1.49

Table 4.1b.

Hydrous zirconia particles.

$\bar{C}$ meqs/ml	Density gm/ml.	o λ A	λ^2 A^2	$\bar{D}$ x 10^7 cm^2 sec^{-1}	$\bar{D} / \lambda^2$ sec^{-1} x 10^{-7}
5.48	2.6	6.87	47.0	2.14	4.55
5.04	2.6	6.95	48.2	2.36	4.90
4.47	2.6	7.23	52.1	2.81	5.40
3.66	2.6	7.73	59.8	4.07	6.80

Table 4.2a.

Hydrous zirconia membranes.

Membrane no.	HCl concn. (molar)	Capacity $\bar{C}$ (meqs/ml)	$\bar{D}x\ 10^6$ $cm^2\ sec^{-1}$	$\bar{D} \times \bar{C}_6$ x10	Sp. Cond. $k_{sp} \times 10^3$ $ohm^{-1}\ cm^{-1}$
1	0.10	0.461	-	-	-
5	0.10	0.467	2.28	1.06	9.75
2	0.01	0.463	2.40	1.17	7.50
3	0.001	0.287	3.83	1.10	7.55
3	0.0001	0.226	5.46	1.23	6.95
5	0.0001	0.226	-	-	-

Table 4.2b.

Hydrous zirconia membranes.

$\bar{C}$ meqs/ml	λ (Å)	λ^2 (Å)^2 *	$\bar{D}$	$\bar{D} / \lambda^2$
0.467	11.3	127.5	2.28	1.79×10^8
0.463	11.3	127.5	2.40	1.88×10^8
0.287	13.25	175.5	3.83	2.18×10^8
0.226	14.35	206.0	5.46	2.64×10^8

* calculated assuming a porosity of the polythene of 40%.

Table 4.3.

Rectification effects.*

Applied voltage (volts)	Membrane 2	Membrane 4	Cation/Anion * * membrane sandwich
5.0	1.1	1.6	8.0
10.0	2.3	1.7	6.0
15.0	2.9	2.1	4.6
20.0	3.0	2.8	4.1
25.0	3.5	3.0	3.9
30.0	3.8	3.4	3.4
35.0	4.7	3.6	3.4
40.0	-	3.8	-

* rectification effect = forward current/backward current.

** cation ClO_3 exchanger; anion AlO_4 exchanger.

Table 4.4.

Electrolyte uptake.

Membrane no.	HCl concn. in soln. (molar)	NaCl concn. in soln. (molar)	Cl^- concn. in membrane (meqs/ml)	Na^+ concn. in membrane (meqs/ml)	H^+ concn. in membrane (meqs/ml)
2	0.01	0.19	0.463	0.036	0.002
5*	0.10	0.10	0.467	0.019	0.019

* by inference (see discussion).

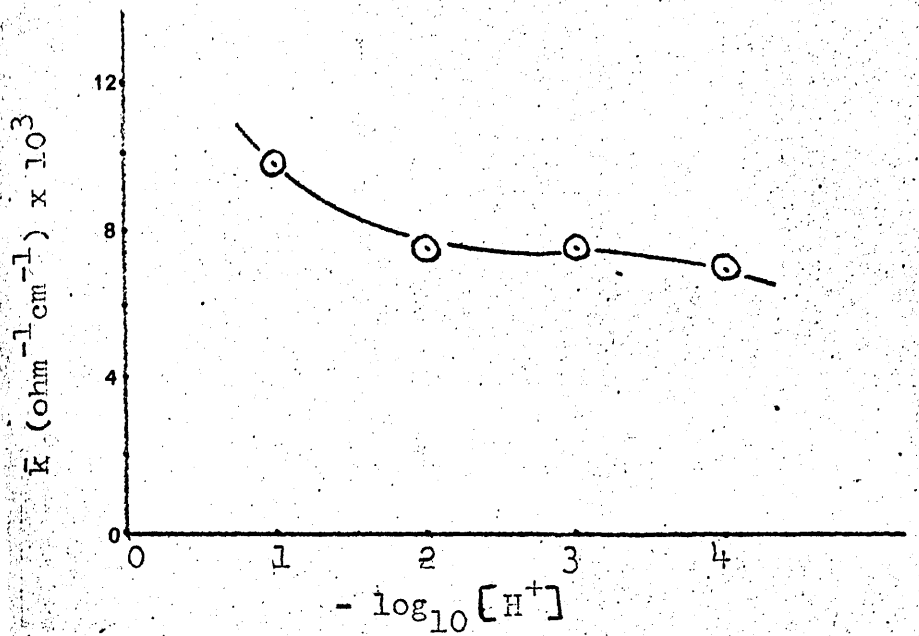

Figure 4.6. Conductivity of hydrous zirconia membranes versus - $\log_{10}$ H^+ in external solution.

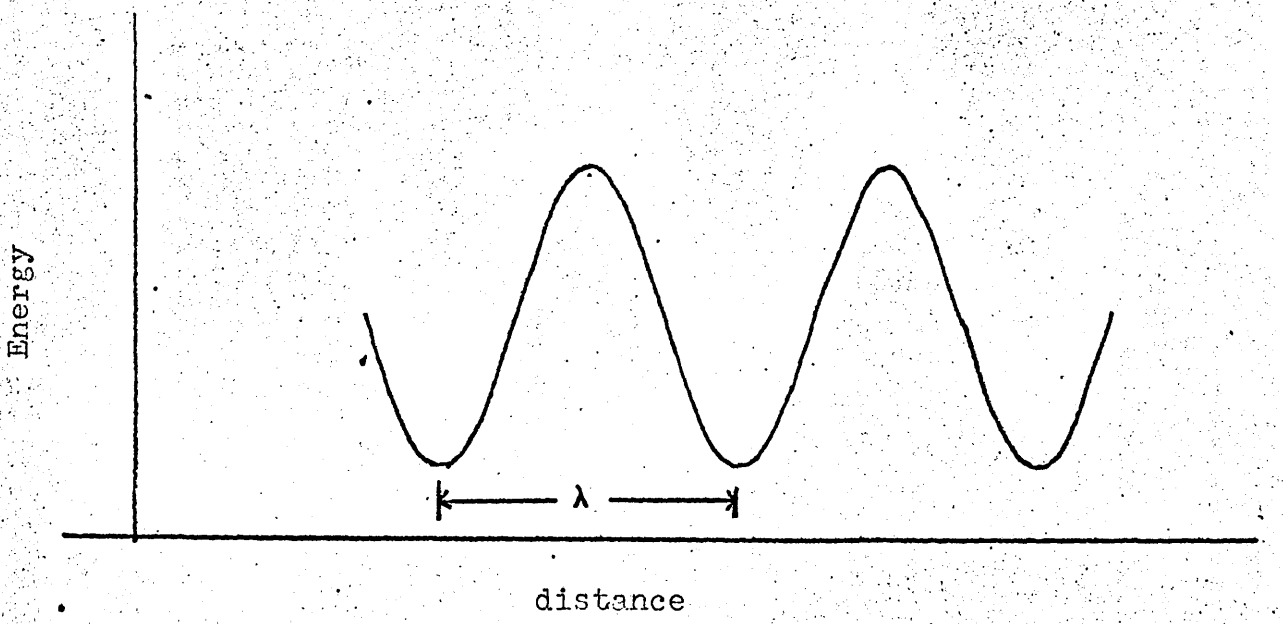

Figure 4.7. Schematic representation of energy profile in an ion-exchanger.

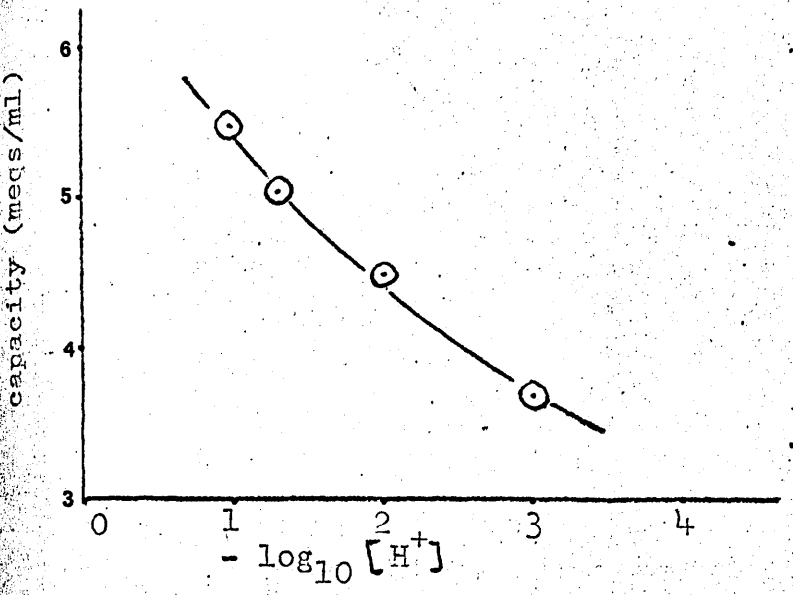

Figure 4.8. Capacity versus - $\log_{10}[H^+]$ in external solution (hydrous zirconia particles).

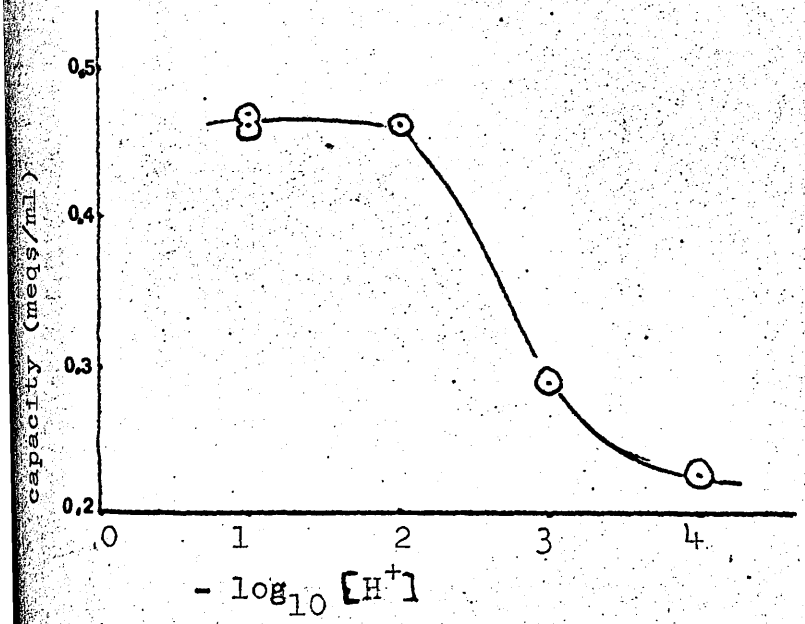

Figure 4.9. Capacity versus - $\log_{10}[H^+]$ in external solution (hydrous zirconia membranes).

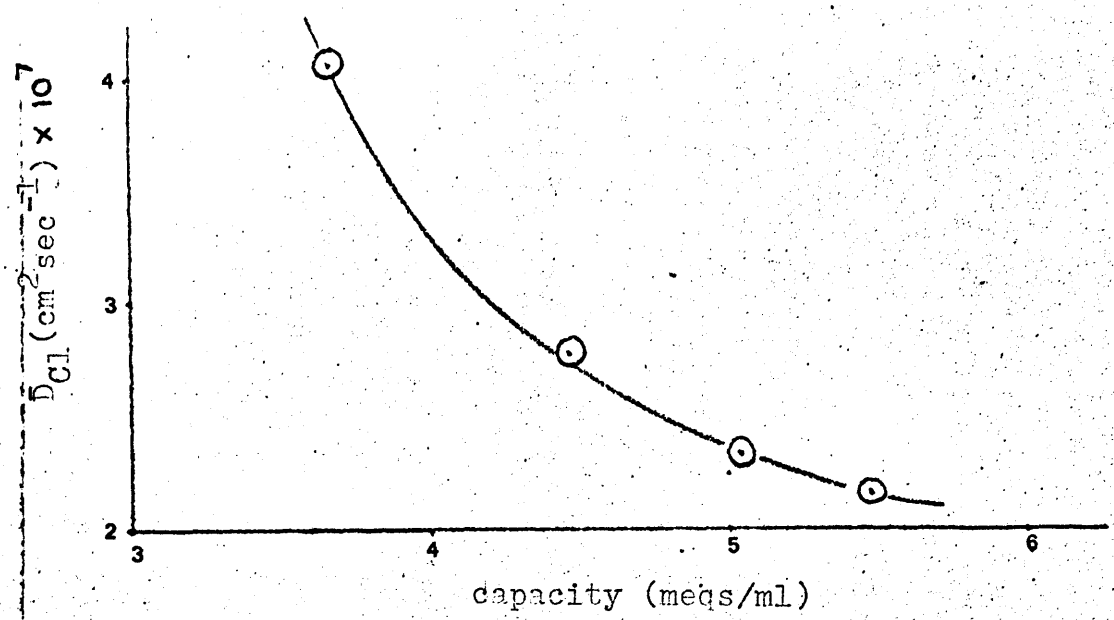

Figure 4.10. Counter-ion diffusion coefficients versus capacity (hydrous zirconia particles)

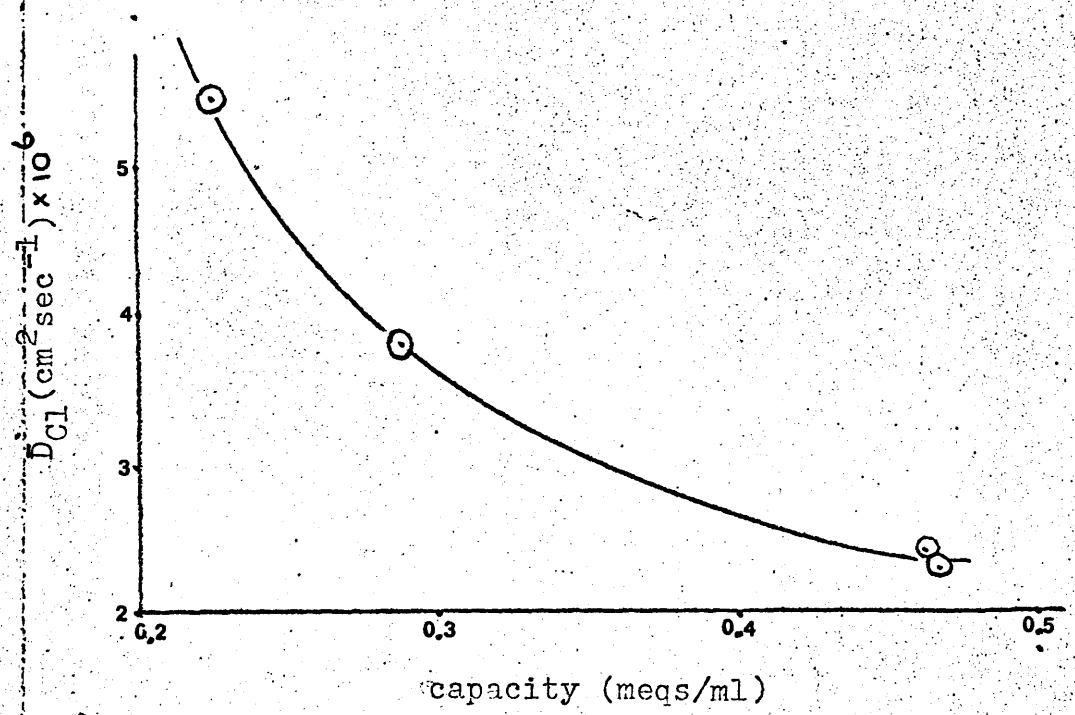

Figure 4.11. Counter-ion diffusion coefficients versus capacity (hydrous zirconia membranes).

4.5. Discussion.

4.5.1.

Tables 4.1a and 4.2a and figures 4.8 and 4.9 show the dependence of the ion-exchange capacity of both the particles and the membranes on the hydrogen ion concentration in the equilibrating solution. Since the methods of preparation of the two materials is so different it is not possible to draw close comparisons between them except to say that the trend observed in both cases is similar - an increase in capacity with an increase in the external hydrogen ion concentration. The process whereby the capacity is achieved is a slow one requiring several weeks. In all cases the particles and membranes were equilibrated with the appropriate solutions for at least eight weeks and frequently for longer periods. There is no doubt, therefore that the results quoted are the equilibrium values of the chloride ion concentration in the exchanger. This value is not a measure of the scientific capacity but includes any chloride ions present in the form of electrolyte uptake. These latter ions are, of course, indistinguishable from the other chloride ions.

4.5.2. Rectification Effects.

During the preparation of the hydrous zirconia membranes rectification effects were observed. The electrolysis set-up has already been described in section 4.3.3. When the electrode in the zirconyl chloride solution was the cathode, the current was high, - approximately 400mamps for an applied voltage of 40 volts, - and Ohm's law was obeyed. However, when the polarity of the electrodes was reversed, the current fell to approximately 3 mamps., while zirconia was being precipitated in the membrane.

To test for rectification in the absence of precipitating solutions the following experiment was set up:

Pt electrode (1) /0.01M HCl/+0.19M NaCl/ zirconia membrane/ 0.01M NaOH/+0.19M NaCl/ Pt electrode (2)

With electrode (1) negative, the observed current was greater than when this electrode was positive. The ratio of this 'forward' to 'backward' current is shown as the rectification factor, for membranes 2 and 4, in Table 4.3.

Because of their pseudo-amphoteric behaviour the zirconia membranes acted as a sandwich of cation and anion-exchange membranes as shown in figure 4.5.

In case (a), sodium chloride is being concentrated in/

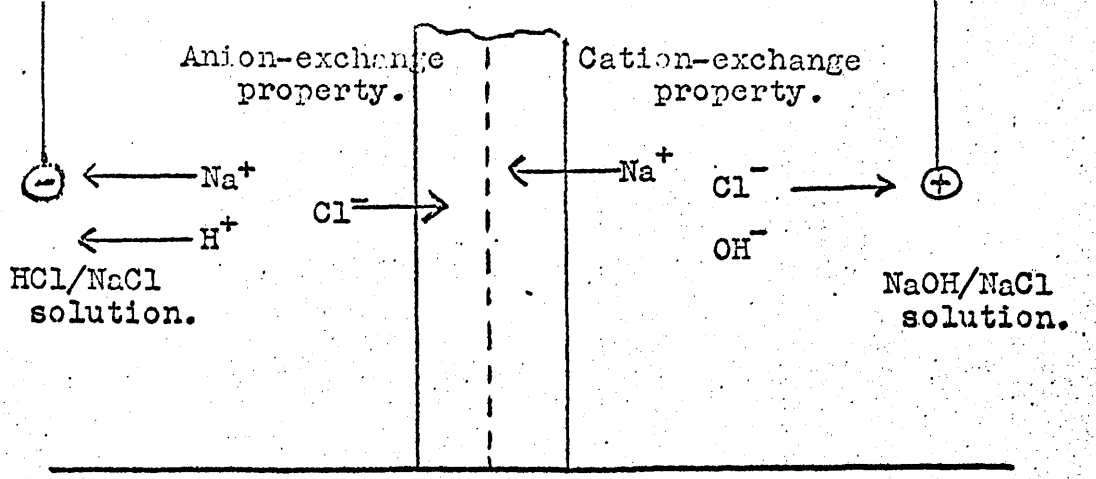

Case (a)

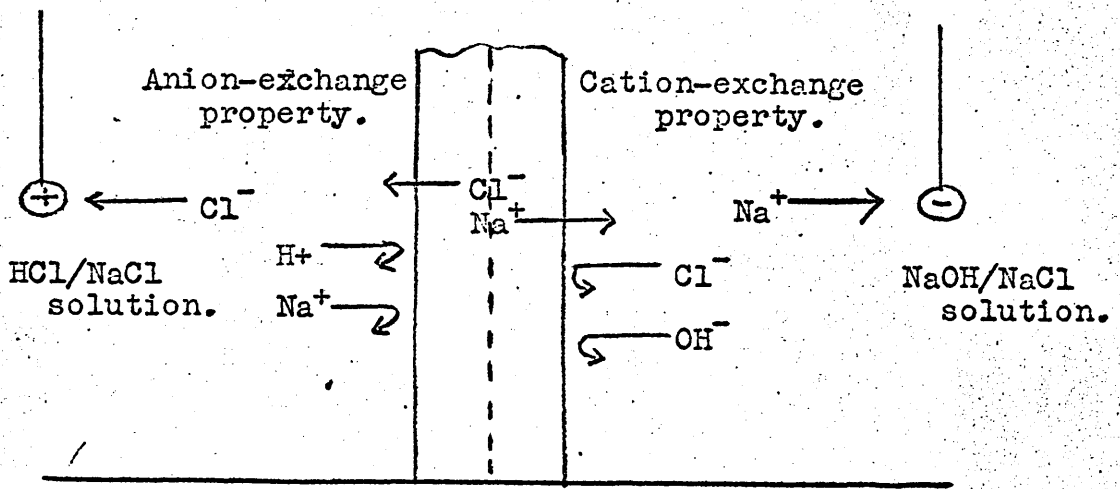

Case (b)

Figure 4.5. Schematic representation of rectification in hydrous zirconia membranes.

in the region in the centre of the exchanger where there is negligible cation- or anion-exchange capacity, and the current in the system is dependent on the rate of diffusion of the sodium and chloride ions into this region.

In case (b) the sodium chloride solution in this central region is being depleted. When all the sodium chloride has been removed by this process, the current will then be dependent on the rate of flow of the chloride and hydroxyl ions through the cation-exchange side and of the sodium and hydrogen ions through the anion-exchange side. This flow will be much lower than the limiting flows in case (a), and thus the current will be lower.

The results obtained with a cation-exchange membrane (AMF C103) - anion-exchange membrane (AMF A104) sandwich are also shown in table 4.3. Rectification effects were also evident here, but the trend in the rectification factor is opposite to that obtained with the zirconia membranes. This may be due to the effect of the not inconsiderable electrolyte uptake observed in the zirconia membranes. The C103 and A104 membranes of the other hand have very low electrolyte uptakes in this concentration range (113) (119) the salt concentration in these membranes being approximately 10^{-3}M./

10^{-3}M. The salt uptake for the zirconia membranes is given in table 4.4. and discussed in section 4.5.3.

4.5.3. Conductivity and Electrolyte Uptake of hydrous zirconia membranes.

Table 4.2a and figures 4.6 show the variations in the conductivity of the membranes with the external solution pH and the capacity of the exchanger. Since the product of the diffusion coefficient of the chloride ions and their concentration in the membranes is approximately constant, (see Table 4.2a), it is reasonable to expect that the conductivity of the membranes should be similar. This is so for the membranes equilibrated in the three lowest concentrations of hydrochloric acid solution. The interesting observation is the high value of the conductivity of the membrane equilibrated in 0.1M hydrochloric acid solution. The explanation of this effect is to be found in the electrolyte uptake of the membranes. Since the capacity of the membranes equilibrated in 0.1 and 0.01M hydrochloric acid solutions are approximately the same and the other properties are similar, the electrolyte uptake in both cases will also be similar. However, in the first case this uptake is/

is approximately half hydrochloric acid, half sodium chloride, whereas in the second case the ratio of hydrochloric acid to sodium chloride in the uptake will be approximately 1:19. If the relative mobilities of the ions in the membrane is similar to those in aqueous solutions, (where U_H/U_{Na} = 7:1.), then this difference in the relative amounts of hydrogen and sodium ions will have a considerable effect on the conductivity. This effect will be increased, the greater the electrolyte uptake.

The uptake of the sodium co-ion in membrane 2 was determined as described in section 4.3.5. It is impossible to determine the hydrogen co-ion uptake directly since the hydrogen ions are involved in the equilibrium which allows the ion-exchange capacity to be varied (section 4.2.). The hydrochloric acid uptake of this membrane is, therefore, assumed to be 1/19 of that for the sodium chloride. The total electrolyte uptake of membrane 5 was assumed to be the same as that of membrane 2, and half of this was attributed to hydrochloric acid and half to sodium chloride. These electrolyte uptake values are shown in Table 4.4.

Assuming the sodium and chloride ions to have similar mobilities in the exchanger and that the hydrogen ions have a/

a mobility of seven times this value, it is possible to explain the observed differences in conductivity of the membranes.

Taking the mobility of the sodium and chloride ions as unity then the mobility of the hydrogen ions is seven. The conductivity is proportional to the sum of the product of the ionic concentrations and their mobilities. Therefore, the conductivity of membrane 5 is proportional to (0.467 x 1) +(0.019 x 1) + (0.019 x 7) = 0.62, whereas the conductivity of membrane 2 is proportional to (0.463 x 1) + (0.036 + 1) + (0.002 x 7) = 0.51.

The ratio of the conductivity of membrane 5 to that of membrane 2 would then be expected to be 1.22. The observed value is 1.3, which is fairly good agreement considering the assumptions which have been made in the calculation.

4.5.4. Diffusion.

Molecular migration in a condensed phase such as an ion exchanger, may be treated as point to point jumps of the elementary particles, and is governed by a rate constant. The nature of the jumps depend on the nature of the diffusing components. By considering a single two component system with molecules that are sufficiently alike so that the whole may be considered to form a more or less perfect lattice and applying absolute rate theory to it, it is possible to arrive at an expression analogous to Fick's first law, of diffusion. (100) (101) (102) Figure 4.7 is a schematic potential diagram for the system. If c_i is the concentration in moles per cubic centimetre, at the ith. position then the amount of material in a volume of unit cross section and length λ is λc_i (λ is the distance between equilibrium minima). If k represents the number of times per second that a molecule jumps and Q is the steady state amount of i passing per second through a square centimetre of surface, then

$$Q = k \lambda c_i - k \lambda c_{i+1} \qquad (4.14)$$

The concentration gradient between the ith. and the (i + 1)th position/

position is

$$\frac{dc}{dx} = \frac{c_{i+1} - c_i}{\lambda} \qquad (4.15)$$

Thus,

$$Q = k\lambda(c_i - c_{i+1})$$

$$= +k\lambda^2 \frac{(c_i - c_{i+1})}{\lambda}$$

$$= -k\lambda^2 \frac{dc}{dx} \qquad (4.16)$$

This is equivalent to Fick's first law

$$Q = -D \frac{dc}{dx} \quad \text{with } D = k.\lambda^2. \qquad (4.17)$$

In an ion exchanger, the positions of the equilibrium minima are the fixed sites. The diffusion coefficient of ions in an ion exchanger should, therefore, be proportional to the distance between the fixed charges. Thus, in a variable capacity exchanger whose other properties remain unchanged, the counter-ion diffusion coefficient should decrease with increasing capacity.

The membranes are by the nature of their preparation, heterogeneous, and it is uncertain to what extent the particles may also exhibit inhomogeneity. It is, therefore, difficult/

difficult to calculate a value of λ, the distance between positions of minimum potential energy for the counter-ions, i.e. the fixed sites on the exchanger matrix or the mobile co-ions. Some estimate of λ may be obtained by assuming a perfectly homogeneous zirconia system and calculating it on the basis of a cubic lattice model. Based on porosity data, a value of 40% of the total volume was used as the volume of zirconia in the membranes. The values of λ so calculated for the particles and membranes are shown in tables 4.1b and 4.2b.

It would be naive to expect the diffusion coefficients of the chloride ions to be proportional to the values of λ^2 so calculated. As shown in tables 4.1b and 4.2b, the chloride ion diffusion coefficients do increase with increasing λ but the proportionality is close to λ^3 than to λ^2, i.e.the diffusion coefficients are inversely proportional to the capacity of the exchangers. In the case of the membranes this last mentioned observation could be explained by the fact that the membranes were leaky. There is, however, a large amount of evidence against this suggestion. The fact that the results obtained from the particles show similar trends suggests that this phenomenon is real. The conductivity/

conductivity of membrane 3 in 0.001M hydrochloric acid + 0.199M sodium chloride solution is 10% higher than that in 0.0001M hydrochloric acid 0.1999M sodium chloride solution although the conductivities of these two solutions are very nearly identical. If this membrane had been leaky the conductivities would have been a function of the solution conductivities and so would have been very similar if not identical. The fact that rectification effects were observed is also strongly in favour of leak-free membranes. Electro-osmotic transport of water was also observed during the preparation of all the membranes. Finally, after preparation and before every experiment, each membrane was placed in a cell and subjected to a pressure head of a few inches of solution. No solution was observed to flow through the membrane even after many hours. All of this evidence supports the proposal that the membranes present a leak-free system.

The ability of these tests to discriminate between a leaky and a sound membrane was shown as follows. A membrane which was known to be slightly leaky, gave a measured diffusion flux approximately 2-3 times higher than the true value measured with the same membrane without leaks. This leaky membrane allowed permeation of solution when

subjected/

subjected to a pressure of a few inches of solution, and no rectification effects were obtained. This confirmed that the above tests were adequate to determine whether a membrane was leak-free.

As can be seen from tables 4.2a and 4.2b, the experiments were not all carried out on the same membrane, and it is, therefore, important to consider how reproducible the results are from membrane to membrane. All the membranes were prepared under identical conditions and table 4.2a shows that membranes equilibrated in the same solutions had capacities identical within the experimental error. This confirms that the properties are reproducible from membrane to membrane, and hence the results can be accurately compared. For the particles the results are of course strictly comparable since all the zirconia particles used in this work came from the one batch of material.

Eyring's application of absolute rate theory to the diffusion process (100) (101) (102) predicts that the diffusion coefficients should increase with the distance between the fixed sites on the exchanger matrix (or between the/

the fixed sites and the mobile co-ions if the electrolyte uptake is significant). The results of this study confirm this prediction, and also show that the diffusion coefficients for a given capacity, and hence a given value of λ, are independent of how this capacity is maintained. In membrane 5 there is a considerable concentration of hydrogen co-ions which can act as jumping sites while in membrane 2 the same co-ion concentration is composed mainly of sodium ions. The diffusion coefficient of the chloride counter-ions is unaffected by this change.

Boyd, Soldano and Bonner [5] carried out a series of experiments on a series of sulphonated polystyrene-divinyl benzene type cation exchangers which were prepared with different capacities. The method of preparation was to subject a given type of exchanger to acid hydrolysis at 180-220°C for different periods of time, in order to obtain a series of materials based on the one exchanger matrix but with different capacities. However, there is good evidence in the authors' report to suggest that this process also affected the cross-linking of the exchanger as well as the capacity, so that the results are not a function of only

one/

one variable. The diffusion coefficients of a number of ions were measured and similar trends were obtained in all cases. The counter-ion diffusion coefficients were found to increase initially with decreasing capacity, but passed through a maximum value with further capacity decrease. These results do not follow the trend expected from the Eyring theory. However, as the authors point out, further data should be obtained from variable capacity exchangers prepared by a method which does not affect the other properties of the exchanger.

The results obtained in this work on hydrous zirconia seem to fit this requirement and although the correlation between diffusion coefficients and λ^2 is not observed, the trend of the diffusion coefficients suggests that the absolute rate theory approach has validity in this type of system.

Appendix A.1.

Kedem and Essig [24] have proved that the relation

$$\frac{r_{oo} - r_{ik}}{r_{ii} - r_{ik}} = \rho_i \quad , \text{ is satisfied for constant } \rho_i.$$

It may be shown that this relation also applies when ρ_i varies throughout the membrane thickness.

Using the equations of Keden and Essig, it may be shown that,

$$(r_{oo} - r_{ik})\, J - (r_{22} - r_{ik})J_2 = RT \frac{\partial \ln \rho_2}{\partial x} \qquad \text{(A.1.1a)}$$

$$(r_{oo} - r_{ik})\, J - (r_{33} - r_{ik})J_3 = RT \frac{\partial \ln \rho_3}{\partial x} \qquad \text{(A.1.1b)}$$

$$(r_{oo} - r_{ik})\, J - (r_{11} - r_{ik})J_1 = RT \frac{\partial \ln \rho_1}{\partial x} \qquad \text{(A.1.1c)}$$

But,
$$\frac{\partial \ln \rho_i}{\partial x} = \frac{c}{c_i} \frac{\partial \left(\frac{c_i}{c}\right)}{\partial x} = \frac{1}{c_i} \frac{\partial c_i}{\partial x} \qquad \text{(A.1.2)}$$

Therefore,

$$c_2(r_{oo} - r_{ik})\, J - c_2 (r_{22} - r_{ik})J_2 = RT \frac{\partial c_2}{\partial x} \qquad \text{(A.1.3a)}$$

$$c_3(r_{oo} - r_{ik})J - c_3 (r_{33} - r_{ik})J_3 = RT \frac{\partial c_3}{\partial x} \qquad \text{(A.1.3b)}$$

$$c_1 (r_{oo} - r_{ik})J - c_1 (r_{11} - r_{ik})J_1 = RT \frac{\partial c_1}{\partial x} \qquad \text{(A.1.3c)}$$

$$c_1 + c_2 + c_3 = C \qquad \text{(A.1.4)}$$

Therefore,/

Therefore,

$$\frac{\partial c_1}{\partial x} + \frac{\partial c_2}{\partial x} + \frac{\partial c_3}{\partial x} = 0. \qquad \text{(A.1.5)}$$

and $J_1 + J_2 + J_3 = J$ (A.1.6)

Therefore, adding (A.1.3 a-c) and substituting equations (A.1.5) and (A.16), gives

$$c(r_{oo} - r_{ik})J = c_2(r_{22} - r_{ik})J_2 + c_3(r_{33} - r_{ik})J_3 + c_1(r_{11} - c_{ik})J_1 \qquad \text{(A.1.7)}$$

The following relations also apply,

$$c_2(r_{22} - r_{ik}) = - c_1 r_{21} - c_3 r_{32} - c_2 r_{ik} - \sum_{j=4}^{n} c_j r_{2j}$$

$$c_3(r_{33} - r_{ik}) = - c_1 r_{31} - c_3 r_{ik} - c_2 r_{32} - \sum_{j=4}^{n} c_j r_{3j} \qquad \text{(A.1.8b)}$$

$$c_1(r_{11} - r_{ik}) = - c_1 r_{ik} - c_3 r_{13} - c_2 r_{12} - \sum_{j=4}^{n} c_j r_{1j} \qquad \text{(A.1.8.c)}$$

Since $r_{ij} = r_{12} = r_{21} = r_{31} = r_{13} = r_{23} = r_{32}$

(A.1.8a - c) are identical.

Therefore, (A.1.7) becomes

$$c(r_{oo} - r_{ik})J = A(J_1 + J_2 + J_3) \qquad \text{(A.1.9)}$$

and/

and $A = c_i(r_{oo} - r_{ik})$. (A.1.10).

Therefore, in general,

$$\rho_i = \frac{c_i}{c} = \frac{r_{oo} - r_{ik}}{r_{ii} - r_{ik}} \qquad \text{(A.1.11)}$$

Appendix A.2.

EMF of a concentration cell.

The cell for measuring the emf of a concentration cell containing an ion-exchange membrane is shown schematically in figure A.2.1. The solution on the sides ' and " are aqueous solutions of the same electrolyte, but of different concentrations, and the electrodes are reversible to the anion of the system. Under these conditions the emf of the whole cell is given by,

$$\Sigma = (E_1) + (E_2) + (E_m) + (E_3) + (E_4) \qquad (A.2.1.)$$

where,

$$\begin{aligned} E_1 &= -RT/F \ln (a_2') \\ E_2 &= -RT/F \ln(\bar{a}_2'/a_2') \\ E_m &= \text{diffusion potential of membrane.} \\ E_3 &= -RT/F \ln(a_2''/\bar{a}_2'') \qquad (A.2.2.) \\ E_4 &= -RT/F \ln(1/a_2'') \end{aligned}$$

From equation (2.67), the diffusion potential, E_m, is given by,

$$E_m = 1/F \left(\frac{\bar{t}_1}{z_1} X_1 + \frac{\bar{t}_2}{z_2} X_2 + \bar{t}_3 X_3 \right)$$

$$= -(RT/F) \left\{ \frac{\bar{t}_1}{z_1} \ln(\bar{a}_1''/\bar{a}_1') + \frac{\bar{t}_2}{z_2} \ln(\bar{a}_2''/\bar{a}_2') + \bar{t}_3 \ln(\bar{a}_3''/\bar{a}_3') \right\}$$

which/

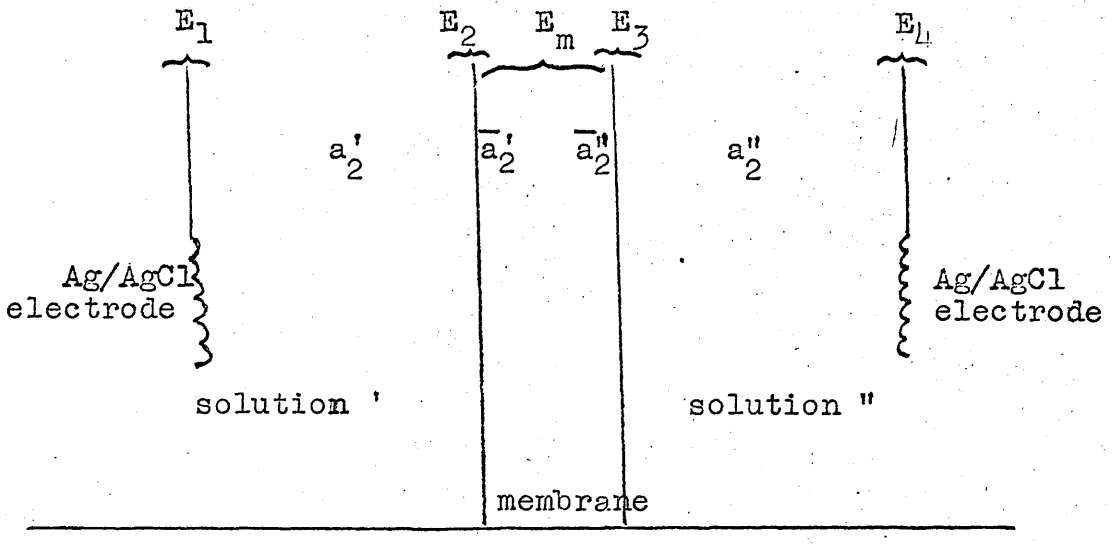

Figure A.2.1. Schematic representation of e.m.f. across a concentration cell containing an ion-exchange membrane.

which, on substituting $\bar{t}_2 = 1 - \bar{t}_1$, putting $z_1=+1$, $z_2=-1$, (for a 1:1 electrolyte) and rearranging, gives,

$$E_m = -(RT/F)\left\{\bar{t}_1 \ln(\bar{a}''_1 a''_2/\bar{a}'_1 a'_2) + \bar{t}_3 \ln(\bar{a}''_3/\bar{a}'_3) - \ln(\bar{a}''_2/\bar{a}'_2)\right\}$$

$$E_m = -2\bar{t}_1(RT/F) \ln(\bar{a}''_{\pm}/\bar{a}'_{\pm}) - (RT/F)\,\bar{t}_3 \ln(a''_3/a'_3) - (RT/F) \ln(\bar{a}''_2/a'_2). \qquad \text{(A.2.3.)}$$

(since $\bar{a}''_1\bar{a}''_2 = (\bar{a}''_{\pm})^2$ and $\bar{a}'_1\bar{a}'_2 = (\bar{a}'_{\pm})^2$)

Since each face of the membrane is assumed to be in equilibrium with the adjacent solution,

$$\bar{a}'_{\pm} = a'_{\pm}, \qquad \bar{a}''_{\pm} = a''_{\pm} \qquad \text{(A.2.4.)}$$

and

$$\bar{a}'_3 = a'_3, \qquad \bar{a}''_3 = a''_3 \qquad \text{(A.2.5.)}$$

Therefore,

$$E_m = -2\bar{t}_1 (RT/F) \ln(a''_{\pm}/a'_{\pm}) - \bar{t}_3(RT/F) \ln(a''_3/a'_3) - (RT/F) \ln(a''_2/a'_2) \qquad \text{(A.2.6.)}$$

The emf of the cell is given by,

$$E = - (RT/F)\ln(a'_2) - (RT/F)\ln(\bar{a}'_2/a'_2) - 2\bar{t}_1(RT/F)\ln(a''_{\pm}/a'_{\pm}) - \bar{t}_3(RT/F)\ln(a''_3/a'_3) - (RT/F)\ln(\bar{a}''_2/\bar{a}'_2) - (RT/F)\ln(\bar{a}''_2/\bar{a}''_2) - (RT/F)\ln(1/a''_2)$$

$$E = -(RT/F) \ln\left(\frac{a'_2\,\bar{a}'_2\,a''_2\,\bar{a}''_2}{a''_2\,a'_2\,\bar{a}''_2\,\bar{a}'_2}\right) - 2\bar{t}_1(RT/F)\ln(a''_{\pm}/a'_{\pm}) - \bar{t}_3(RT/F)\ln(a''_3/a'_3)$$

$$E = -2\bar{t}_1(RT/F)\ln(a''_{\pm}/a'_{\pm}) - \bar{t}_3(RT/F)\ln(a''_3/a'_3) \qquad \text{(A.2.7.)}$$

Appendix A.3.

Under a electrolyte concentration gradient, the salt flow through a membrane is given by,

$$J_s = (1/v_1)(l_{11}X_1 + l_{12}X_2 + l_{13}X_3)$$
$$= (1/v_1)(l_{11}(-d\tilde{\mu}_1/dx) + l_{12}(-d\tilde{\mu}_2/dx) + l_{13}(-d\mu_3/dx) \quad (A.3.1)$$

Expanding $(-d\tilde{\mu}_i/dx)$ in terms of $(-d\mu_i/dx)$ and $(d\phi/dx)$ yields, on rearranging,

$$J_s = (1/v_1)(l_{11}(-d\mu_1/dx) + l_{12}(-d\mu_2/dx) + l_{13}(-d\mu_3/dx))$$
$$+ (1/v_1)(z_1l_{11} + z_2l_{12}).F(-d\Phi/dx) \quad (A.3.2.)$$

Using equation (A.145) for $F(-d\Phi/dx)$ and equations (2.61), gives,

$$J_3 = (1/v_1)((l_{11} - \frac{t_1^2 a}{z_1^2})(-d\mu_1/dx) + (l_{12} - \frac{t_1t_2a}{z_1z_2}).$$
$$(-d\mu_2/dx) + (l_{13} - \frac{t_1t_3a}{z_1})(-d\mu_3/dx)).$$

It may easily be proved that for a 1:1 electrolyte,

$$(l_{11} - \frac{t_1^2 a}{z_1^2}) = (l_{12} - \frac{t_1t_2a}{z_1z_2}) = (\frac{l_{11}l_{22} - l_{12}^2}{a})$$

and since $(-d\mu_{12}/dx) = (-d\mu_1/dx) + (-d\mu_2/dx)$, then

$$J_s = (\frac{l_{11}l_{22} - l_{12}^2}{a})(-d\mu_{12}/dx) + (l_{13} - \frac{t_1t_3a}{z_1})(-d\mu_3/dx).$$

Appendix A.4.

The water flow in a concentration cell is given by,

$$J_3 = l_{13}X_1 + l_{23}X_2 + l_{33}X_3$$

$$= l_{13}(-d\tilde{\mu}_1/dx) + l_{23}(-d\tilde{\mu}_2/dx) + l_{33}(-d\mu_3/dx) \quad (A.4.1)$$

Expanding $(d\tilde{\mu}_i/dx)$ in terms of $(d\mu_i/dx)$ and $(d\Phi/dx)$ gives

$$J_3 = l_{13}(-d\mu_1/dx) + l_{23}(-d\mu_2/dx) + l_{33}(-d\mu_3/dx) + F(-d\Phi/dx)(z_1 l_{13} + z_2 l_{23}) \quad (A.4.2)$$

Substituting for $F(-d\Phi/dx)$ from equation (2.67) and using equations (2.61) gives

$$J_3 = \left(l_{13} - \frac{t_1 t_3 a}{z_1}\right)(-d\mu_1/dx) + \left(l_{23} - \frac{t_2 t_3 a}{z_2}\right)(-d\mu_2/dx) + (l_{33} - t_3^2 a)(-d\mu_3/dx) \quad (A.4.3.)$$

Again it may readily be shown that

$$\left(l_{13} - \frac{t_1 t_3 a}{z_1}\right) = \left(l_{23} - \frac{t_2 t_3 a}{z_2}\right) \quad (A.4.4)$$

Therefore, since $(-d\mu_{12}/dx) = (-d\mu_1/dx) + (-d\mu_2/dx)$,

$$J_3 = \left(l_{13} - \frac{t_1 t_3 a}{z_1}\right)(-d\mu_{12}/dx) + (l_{33} - t_3^2 a)(-d\mu_3/dx) \quad (A.4.5)$$

Appendix A.5.

Capacity determination.

Suppose that the equilibrating solution has a volume V cm^3, a concentration c mmoles/cm^3 and a specific activity x_1 cpm/cm^3. Then the total activity is Vx_1 cpm. and the number of mmoles of the ion under study is cV mmoles.

Suppose the volume of the membrane is $\bar{V}$ cm^3 and the concentration of the counter-ions is $\bar{c}$ mmoles/cm^3 then the number of mmoles of counter-ion in the membrane is $\bar{c}\bar{V}$ mmoles. Therefore, the total number of mmoles of counter-ion is $cV + \bar{c}\bar{V}$.

The fraction of the counter-ion in the solution is $cV/(cV + \bar{c}\bar{V})$.

Therefore, the fraction of total activity in the solution after equilibration is $cV/(cV + \bar{c}\bar{V})$.

Therefore, the total activity inthe solution is then,

$$(cV/(cV + \bar{c}\bar{V})).Vx_1$$

and the specific activity in the solution is $((cV/(cV + \bar{c}\bar{V}).Vx_1)/V$ i.e. $(cV/(cV + \bar{c}\bar{V})x_1$.

But the specific activity of the solution is measured as x_2, therefore,

$$x_2 = (cV/(cV + \bar{c}\bar{V}).x_1$$

giving/

giving

$$\bar{c} = \frac{cV}{\bar{v}} \left(\frac{x_1}{x_2} - 1\right)$$

Thus the capacity of the membrane is obtained.

Appendix A.6.
Edge effect correction to conductivity.

In many measurements of diffusion and conductivity through membranes, the membrane is clamped between the faces of the cell in such a way that only the central part is exposed to the surrounding solution. Normally the diffusion through the overlap region has been neglected. However, if the radius of the total membrane is very much greater than the radius of the diffusion region, then the diffusion through the overlap region may be significant. This phenomenon, called the edge effects, has been treated by Barrer,[41] and a solution to the problem obtained.

Consider a diffusional flow through a membrane of thickness l and radius b, clamped between the faces of a diffusion cell such that flow can only occur through a concentric circle of radius a ($a \ll b$), both at the ingoing face ($z = l$) and the outgoing face ($z = 0$). The type of flow lines for the system are shown in figure A.6.1. If the centre of the outgoing face is chosen as the origin of a cylindrical coordinate system (z,r), with the z co-ordinate normal to the membrane face, then for a constant diffusion coefficient the steady state equation becomes:

$$\frac{\partial^2 c}{\partial r^2} + \frac{1}{r}\frac{\partial c}{\partial r} \quad \frac{\partial^2 c}{\partial z^2} = 0 \qquad \text{(A.6.1)}$$

with/

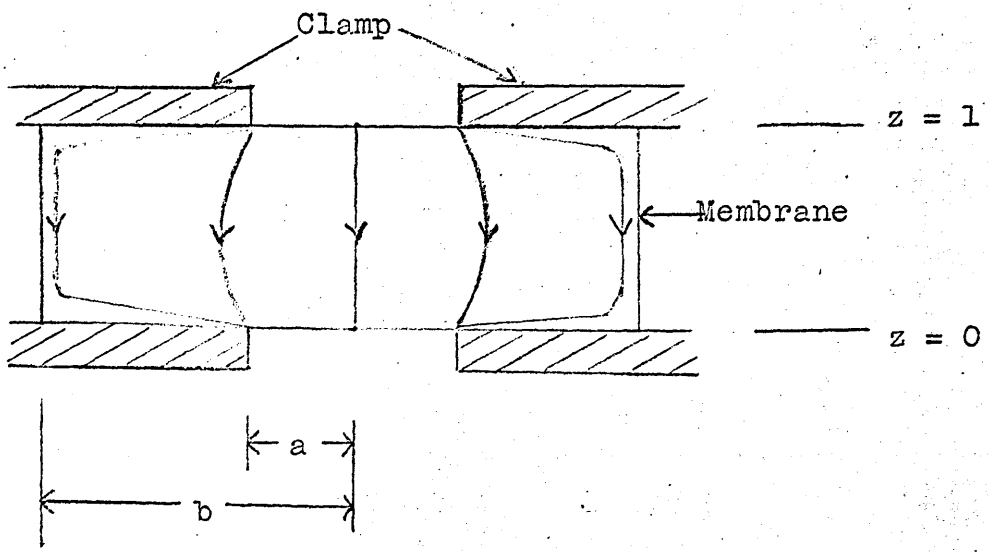

Figure A.6.1. Diffusion with an edge effect.

with the mixed boundary conditions:

(a) $c = c_o$, $0 < r < a$, $z = 1$, $t > 0$ (A.6.2a)

(b) $c = 0$, $0 < r < a$, $z = 0$, $t > 0$ (A.6.2b)

(c) $\partial c/\partial z = 0$, $a < r < b$, $z = 0,1$, $t > 0$ (A.6.2c)

(d) $\partial c/\partial r = 0$, $r = b$, $0 < z < 1$, $t > 0$ (A.6.2.d)

Under these conditions a solution is difficult to obtain, but by replacing conditions (a) and (b) of equation (A.6.2) by conditions of constant flux per unit area, so that the steady state flux per unit area is independent of r over the faces z = 0,1. With fixed flux conditions imposed on faces z = 0, 1 the concentration over each face varies with r, and a solution to equation (A.6.1) can be obtained. This leads to the relationship

$$J/J_o = 1/ (1 + (16/\pi^2 . S_n) \qquad \text{(A.6.3.)}$$

where J is the steady flux in the presence of edge effects, J_o the flux in the absence of edge effects, and

$$S_n = \sum_{q=1}^{\infty} \frac{1 . I_1(q\alpha)}{q^2 I_1(q\beta) .} \cdot (I_1(q\beta)K_1(q\alpha) - K_1(q\beta) I_1(q\alpha)) \qquad \text{(A.6.4.)}$$

where $\alpha = \pi a/1$

$\beta = \pi b/1$

and I_1 and K_1 are Bessel functions.

Barrer has shown that the equation (A.6.3) applies also/

also for conductivity through membranes. Replacing J by kV/R and J_o by kV/R_o where k is a constant, V the applied electric potential and R and R_o the resistance in the presence and absence of edge effects respectively, gives

$$R_o/R = 1/(1 - (16/\pi^2).\ S_n\ ) \qquad (A.6.5.)$$

Since $R_o = 1/\pi a^2\bar{K}$, where $\bar{K}$ is the specific conductivity of the membrane, equation (A.6.5.) may be written,

$$\bar{K} = (1/(\pi a^2 R)) \cdot (1 - (16/\pi^2).\ S_n\ ) \qquad (A.6.6.)$$

from which the true specific conductivity of the membrane may be calculated from the apparent resistance.

Appendix A.7.

Film diffusion correction to diffusion coefficients.

Because of the influence of film diffusion, the apparent diffusion coefficients of the ions in the membranes determined as described in section 2.312, are smaller than the true diffusion coefficients, and a correction must be applied to obtain the true values. A number of such corrections have been suggested by various authors,[51] [52] [53] but the one used in this study is based on that proposed by Scattergood and Lightfoot.[57]

To estimate the true tracer diffusion coefficient $\bar{D}_1$, from the apparent coefficient $\bar{D}_{1A}$ calculated as described in section 2.312, the effect of the boundary layer mass transfer resistance must be taken into account. An estimate of $\bar{D}_1$ can then be obtained if the mass transfer resistance in the solution is assumed to be concentrated in uniform boundary layers on either side of the membrane. The true diffusion coefficient is then given by

$$\bar{D}_1 = \bar{D}_{1A}/(1 - 2\bar{D}_{1A}c_1/(dk_c c_1)) \qquad (A.71)$$

where d is the membrane thickness, and k_c is the local mass transfer coefficient in the solution of concentration c_1, and $\bar{c}_1$ is the concentration of species 1 in the exchanger.

The/

The term k_c corresponds to the D_1/δ term used in the diffusion layer approach [47], where δ is the film thickness.

The value of k_c must be determined from experimental data, and its value is dependent on the viscosity and density of the solution, and the diffusion coefficient of the ion in the solution as well as on the physical dimensions and rate of rotation of the stirrer. If the value of k_c is determined for one set of conditions for which all the other variables are known, then the dependence of k_c on these variables can be calculated and hence the value of k_c obtained for any experimental conditions.

In this study, as in that of Scattergood and Lightfoot, the value of k_c was estimated from limiting current measurements using the cell set up as described in section 2.3.11. k_c can be obtained from the limiting current as follows:

$$k_c = I^{\infty} / F(c_1)b$$

where I^{∞} is the limiting current density, F is Faraday's constant, and $(c_1)_b$ is the concentration of ion 1 in the bulk solution.

The general equation relating this mass transfer coefficient to the other variables of the system, is

$$\frac{(k_c)_m B}{D} = A(NL^2 \rho / \eta)^q \cdot (\eta/\rho D)^{1/3} \quad \text{A.7.2)}$$

where the subscript m on k_c denotes the area mean value,

B/

B is the cathode diameter, D the solute diffusivity, N is the impeller rate of rotation, L the impeller diameter, η the solution viscosity, ρ the solution density and A and q are constants of the system.

From a plot of log ($(k_c)_m B/D$) against log N, the values of A and q can be obtained. The value of k_c for any solution and stirring speed can then be obtained from equation (A.7.2). Substitution of this value of k_c in equation (A.7.1) enables the correction for film diffusion to be applied to the tracer diffusion coefficient and the true value obtained. The magnitude of the correction depends on the flow rate of the species through the membrane, being fairly large for those with high permeabilities, e.g. counter-ions, and low for those species whose permeability is small e.g. co-ions.

Appendix A.8.

Correction to diffusional flow due to volume changes in the system.

Consider a solution of volume V cm^3 and specific activity x cpm/cm^3. The total activity is then, Vx cpm.

Suppose that activity is being added to this solution at a rate of θ cpm/sec and that samples are removed for counting at times t_1, t_2 .....t . Suppose also that n cm^3 are removed in each sample and a cm^3 of inactive solution are used to replace this volume removed.

First sample.

Specific activity of solution = x cpm/cm^3.

Volume of solution removed = n cm^3.

Therefore, total activity removed = xn cpm.

Activity remaining = x(V-n)cmp in (V-n) cm^3

a cm^3 of inactive solution now added.

Activity = x(V-n) cpm in (V-n+a) cm^3.

Specific activity = x(V-n)/(V-n+a).

Second sample.

Specific activity = $$= \frac{x(V-n) + t_1\theta}{(V-n+a)}$$

$$= x + \frac{t_1\theta - ax}{(V-n+a)}$$

$$= x + t_1\theta \text{ -corr(2)}$$

i.e./

i.e. the measured activity is equal to the true activity less a correction, corr(2), where the correction is given by,

$$\text{corr}(2) = \frac{ax}{V}\left(\frac{1 + n-a}{V-n+a}\right) - \frac{t_1\theta}{V} \cdot \left(\frac{n - a}{V-n+a}\right)$$

Suppose this specific activity is called x_1 i.e. $x_1 = x + t_1\theta - \text{corr}(2)$.

After addition of a cm^3 of inactive solution,

Total activity $= x_1 (V-2n+a)$

Specific activity $= x_1 (V-2n+a)/(V-2n-2a)$

Third sample.

$$\text{Specific activity} = \frac{(x_1)(V-2n+a) + t_2\theta}{(V-2n+2a)}$$

A calculation similar to the one for sample 2, gives the measured specific activity of the third sample as

$$x + \frac{t_1\theta}{V} + \frac{t_2\theta}{V} - \text{corr}(2) - \frac{x_1}{V}\left(1 + \frac{2(n-a)}{(V-2n+2a)}\right) + \frac{t_2\theta \cdot 2(n-a)}{(V-2n+2a)}$$

i.e. true activity - corr(2) - corr(3).

The general formula is given by

$$\text{corr}(i) = \left[\theta xn \times (i-1)/V-(i-1)xn\right] \times (x_i - x_{i-1}) + \text{corr}(i-1).$$

where x_i is the measured specific activity of the i^{th} sample.

The/

The values, x_i, are experimentally determined and therefore the measured increase in activity in unit time is obtainable. From this, θ for each time interval is calculated and averaged for all the time intervals. This average value of θ is then used to calculate the true activity at each sample time.

Appendix A.9.

Correction to transport numbers for uptake of chlorine-36 by the electrodes.

In the experiments to determine the transport numbers of the co-ions in the membranes, Ag/AgCl electrodes were used in the solutions of sodium chloride containing Cl^{36}. In the back-flow experiments, i.e. with the flow of chloride against the electric current, the electrode in the solution containing a high activity of Cl^{36} was the anode, so that AgCl was being formed on the electrode and the total chloride concentration and hence the Cl^{36} concentration, was being reduced. The duration of the experiment and the current density used were so adjusted that this concentration change was small, approx. 2-3% of the total concentration. Since the Cl^{36} concentration was assumed constant in the calculation, an average value over the duration of the experiment was used without introducing any great error into the result. In the other side of the cell, chloride ions were being released into the solution, but since only the concentration of Cl^{36} ions permeating the membrane was being measured, the effect on the results was negligible. This was not the case, however, when the forward flow was being measured. Here, the anode was situated in the low activity solution and hence Cl^{36} ions were being/

being removed from this solution with a consequent reduction in the counting rate of the samples removed for analysis. The apparent flow rate of Cl^{36} was, therefore, less than the true value. Since the rate of increase of the Cl^{36} concentration in the sampling side was constant, as was the current density, the number of Cl^{36} ions removed from the solution and consequently, the reduction in count rate could be obtained by the following simple method.

Consider a time t seconds after the start of the experiment. The total number of chloride ions removed from the solution onto the electrode in this time is

$$ECl = \frac{I\ t\ N_a}{F} \qquad (A.9.1)$$

where I is the total current in amps, F Faraday's constant and N_a Avogado's number.

During this time an increasing number of these ions will have been Cl^{36} ions, and this rate of increase will be constant. Thus the number of Cl^{36} ions removed from the solution can be expressed as follows:

$$ECl = \frac{N^*}{N^T} \cdot \frac{ItN_a}{F} \qquad (A.9.2)$$

where the value of N^*/N^T is obtained as follows.

From the laws of radioactive decay,

$$kN^* = -dN^*/dt \qquad (A.9.2a)$$

therefore/

therefore $N^* = (1/k)(-dN^*/dt)$ where k is the rate constant for the decay process and $(-dN^*/dt)$ is the rate of decay as measured by the counting rate of the samples. Also N^T is given by VcN_a where V is the volume of the half cell, and c the concentration of chloride ions in the solution. Therefore, equation (A.92) becomes:

Number of chloride -36 ions removed from solution

$$= ECl = \frac{\left(\frac{1}{k}\right)\left(\frac{dN^*}{dt}\right)}{VcNa} \frac{ItNa}{F}$$

$$= \frac{\left(\frac{1}{k}\right)\left(\frac{dN^*}{-dt}\right) It}{VcF} \qquad (A.9.3.)$$

To express this as a count rate equation (A.92a) is used and the reduction in the counts produced during time t by the formation of $AgCl^{36}$ is

$$\frac{k.\left(\frac{1}{k}\right)\left(-\frac{dN^*}{dt}\right) It}{VcF}$$

$$= \frac{\left(\frac{dN^*}{-dt}\right) It}{VcF} \qquad (A.9.4.)$$

This quantity must be added to each sample count rate in order to obtain the true activity in the solution at that time, before calculation of the transport number is executed.

For the 0.1M sodium chloride solutions, this correction is approximately 2% in the case of the highest activity sample,/

sample, producing a 20% correction in the value of t_2. Thus the omission of this correction would lead to a significant error on the co-ion transport number. At the higher concentrations, the correction to the count rate was considerably smaller because of the much higher value of c. The correction to t_2 was only 2-3%, i.e. within the experimental error on the measurement.

Appendix A.10.

Convection in ion-exchange membranes arises from the fact that the numbers of mobile counter- and co-ions are not equal. Hence, when an electric current is passed through the system, the momentum imparted to the water by the counter-ions is not balanced by that imparted by the co-ions. In free aqueous solutions of n:n electrolytes, the number of cations equals the number of anions, and neglecting flow due to hydration spheres of the ions, the water transference produced by the cations is equal and opposite to that produced by the anions, and no net transfer of water occurs. This suggests that, apart from the hydration water, the cations and anions carry with them equal numbers of water molecules. Assuming this is the case in ion-exchange membranes, and also that all the water, apart from water of hydration, is free to be influenced in this way, then the water associated with each ion is given by,

$$\bar{c}_3^*/(\bar{c}_1+\bar{c}_2) \qquad \text{(A.10.1)}$$

where $\bar{c}_3^*$ is the concentration of free water in the exchanger, and is given by,

$$\bar{c}_3^* = \bar{c}_3 - \bar{c}_1 H_1 - \bar{c}_2 H_2 - \bar{c}_4 H_4 \qquad \text{(A.10.2)}$$

where H_1, H_2 and H_4 represent the hydration numbers of the species/

species 1, 2 and 4 respectively.

Therefore, the water transported by the cations is

$$(t_3')^1 = t_1(\bar{c}_3^*/(\bar{c}_1 + \bar{c}_2)) \qquad \text{(A.10.3)}$$

and by the anions is

$$(t_3')^2 = t_2(\bar{c}_3^*/(\bar{c}_1+\bar{c}_2)) \qquad \text{(A.10.4)}$$

Therefore, the net transport of water in the direction of the cation motion is

$$t_3^* = (\bar{c}_3^*/(\bar{c}_1+\bar{c}_2))(t_1-t_2) \qquad \text{(A.10.5)}$$

where t_3^* has been used since this flow neglects the transference of water of hydration. t_3^* is given by the equation

$$t_3^* = t_3 - t_1H_1 + t_2H_2 \qquad \text{(A.10.6)}$$

Spiegler's analysis of leached membrane systems (21) has shown that in most cases the linear velocity of the water is lower than that of the counter-ions, so that a better representation of the system may be

$$t_3^* \propto (\bar{c}_3^*/(\bar{c}_1+\bar{c}_2))(t_1-t_2)$$

or

$$t_3^* = P.(\bar{c}_3^*/(\bar{c}_1+\bar{c}_2))(t_1-t_2) \qquad \text{(A.10.7)}$$

Appendix A.11.

Using the symbolism of Scattergood and Lightfoot [57] the counter-ion diffusion coefficient is given by the relation,

$$D_{11} = 1/(((x_1+x_{1'})/\mathcal{D}_{11'}) + (x_2/\mathcal{D}_{12}) + (x_3/\mathcal{D}_{13}) + (x_4/\mathcal{D}_{14})) \quad (A.11.1)$$

and using the equations given by Spiegler,[21]

$$D_{11} = RT/(\bar{X}_{11'} + \bar{X}_{12} + \bar{X}_{13} + \bar{X}_{14}) = 1/((\bar{X}_{11'}/RT) + (\bar{X}_{12}/RT) + (\bar{X}_{13}/RT) + (\bar{X}_{14}/RT)) \quad (A.11.2)$$

Equating terms in equations (A.11.1) and (A.11.2) yields the relationships,

$$\frac{x_1+x_{1'}}{\mathcal{D}_{11'}} = \frac{\bar{X}_{11}}{RT} \qquad \frac{x_2}{\mathcal{D}_{12}} = \frac{\bar{X}_{12}}{RT}$$

$$\frac{x_3}{\mathcal{D}_{13}} = \frac{\bar{X}_{13}}{RT} \qquad \frac{x_4}{\mathcal{D}_{14}} = \frac{\bar{X}_{14}}{RT} \quad (A.11.3.)$$

In general, therefore,

$$\frac{x_j}{\mathcal{D}_{ij}} = \frac{\bar{X}_{ij}}{RT} \quad \text{or} \quad \bar{X}_{ij} = \frac{RTx_j}{\mathcal{D}_{ij}} \quad (A.11.4)$$

Since $R_{ij} = -\bar{X}_{ij}/c_j$ (A.11.5)

then

$$R_{ij} = RTx_j/c_j\mathcal{D}_{ij} \quad (A.11.6)$$

Appendix A.12

Thermodynamic Forces.

The thermodynamic force acting on a species is the negative gradient of its electrochemical potential, i.e.

$$X_i = -RT\, d\tilde{\mu}_i/dx \qquad (A.12.1)$$

which may be expanded to give

$$X_i = -RT\, d\mu_i/dx + z_i F\, d\Phi/dx$$
$$= -RT\, d\ln(a_i)/dx + z_i F\, d\Phi/dx \qquad (A.12.2)$$

Electric potential only.

In this case $d\ln(a_i)/dx = 0$ and hence the thermodynamic force is given by

$$X_i = z_i F\, d\Phi/dx$$

For the membrane system this becomes,

$$X_1 = z_1 F\, d\Phi/dx$$
$$X_2 = z_2 F\, d\Phi/dx \qquad (A.12.3)$$
$$X_3 = 0$$
$$d\Phi/dx = I/\bar{\kappa},$$

and if the flow per Faraday is used in the equation, i.e. if $J_i = z_i t_i$, then the forces become,

$$X_1^{el} = z_1 F^2/\bar{\kappa} \qquad (A.12.4a)$$
$$X_2^{el} = z_2 F^2/\bar{\kappa} \qquad (A.12.4b)$$
$$X_3^{el} = 0 \qquad (A.12.4c)$$

Chemical potential gradient only.

In/

In this case $d\phi/dx \neq 0$, and the force acting on species i is given by,

$$X_i = -RT\, d\tilde{\mu}_i/dx \qquad (A.12.5)$$

For the membrane, therefore the forces become,

$$X_1 = -RT\, d\tilde{\mu}_1/dx = -RT\, d\ln(a_1)/dx + z_1 F d\phi/dx \qquad (A.12.5a)$$

$$X_2 = -RT\, d\tilde{\mu}_2/dx = -RT\, d\ln(a_2)/dx + z_2 F d\phi/dx \qquad (A.12.5b)$$

$$X_3 = -RT\, d\mu_3/dx = -RT\, d\ln(a_3)/dx \qquad (A.12.5c)$$

Since single ionic activities are unknown, other expressions have to be used.

It may readily be shown that the force on species 2 is given by

$$X_2 = -z_2 F \Xi \qquad (A.12.6)$$

where Ξ is the e.m.f. of the cell measured with electrodes reversible to the co-ion.

Also,

$$X_s = X_{12} = X_1 + X_2 = -RT(d\ln a_1/dx + d\ln a_2/dx) \qquad (A.12.7)$$

and

$$X_s = -RT\, d\ln(a_s)/dx \qquad (A.12.8)$$

X_1 may therefore, be obtained in one of two ways;

(a) From X_{12} and X_2. This, however, involves obtaining X_1 as the difference of two large numbers.

(b) From equation (2.65) using the values of X_2 and X_3 given by the equations (A.12b) and (A.12c) above. This method/

method is much more accurate than method (a).

However, allowing for the error associated with each of these calculations the values of X_1 calculated by both methods have been found to be in satisfactory agreement.

Appendix A.13.

Calculation of co-ion permeability from electrolyte uptake data (2)

The equation used to calculate the overall permeability from the permeability of each local region is

$$\frac{dP}{d\ln u} = \frac{3P(P_u - P)}{2P + P_u} \qquad (A.2.1.)$$

The starting value of P for this equation is obtained from the equation

$$P^* = D^* \cdot \frac{m}{\bar{m}} = D^* a f^* \qquad (A.2.2.)$$

where * indicated that the property considered is for the most continuous region.

The fraction of the exchanger having fixed charge concentration less than or equal to M* is given by

$$\phi^*_m = \int_0^{M^*} F(M)dM \qquad (A.2.3.)$$

where $F(M) = k_o M^{-z}$.

y^* and f^* are obtained from the equations

$$y^* = M^* / \nu_1 z_1 a m \qquad (A.2.4)$$

$$f^*(f^* + y^*)^{\nu_1/\nu_2} = 1. \qquad (A.2.5)$$

In considering a membrane in which the most continuous regions are the aqueous fissures and with increasing dispersness as M increases, the integration of equation (A.2.3) must/

must be carried out first from $\tilde{\phi} = \tilde{\phi}^*$ to $\tilde{\phi} = 0$ then from $\tilde{\phi} = \tilde{\phi}^*$ to $\tilde{\phi} = 1$. Thus setting

$$u = \tilde{\phi} - \tilde{\phi}^* \text{ and starting with } u = 0 \ (\approx 10^{-5})$$

and $P = P^*$ then integrating up to $\tilde{\phi} = 0$ gives P^{**} for the volume elements $\tilde{\phi} = 0$ to $\tilde{\phi} = \tilde{\phi}^*$. For the second part of the integration from $\tilde{\phi}$ to $\tilde{\phi}^*$ to $\tilde{\phi} = 1$, the treated volume $u = \tilde{\phi}$ is used, the integration starting at $\tilde{\phi} = \tilde{\phi}^*$ and $P = P^{**}$ and ending with $u = 1$ at which point P has the final value P for the exchanger as a whole.

For a membrane whose regions of fixed charge density from M* to B are more continuous than those from M* to A, the order of integration is reversed. (A and B have the same meanings as in chapter 3).

The computer program used to carry out the integration of equation (A.2.3) under the above conditions, is given in appendix A.15.

Appendix A.14.

Under the condition of zero current,

$$I = F(z_1 J_1 + z_2 J_2) \qquad (A.14.1)$$

Expanding J_1 and J_2 equation (A.14.1) becomes

$$I = F(z_1 l_{11} X_1 + z_1 l_{12} X_2 + z_1 l_{13} X_3 + z_2 l_{12} X_1 + z_2 l_{22} X_2 + z_2 l_{23} X_3) = 0.$$

or rearranging,

$$(z_1 l_{11} + z_2 l_{12}) X_1 + (z_1 l_{12} + z_2 l_{22}) X_2 + (z_1 l_{13} + z_2 l_{23}) X_3 = 0 \qquad (A.14.2)$$

Comparison with equations (2.61) shows that this is equivalent to

$$\left(\frac{t_1}{z_1} \cdot X_1\right) + \left(\frac{t_2}{z_2} \cdot X_2\right) + \left(\frac{t_3}{} \cdot X_3\right) = 0$$

i.e. $(t_1/z_1)X_1 + (t_2/z_2)X_2 + (t_3) \cdot X_3 = 0.$ (A.14.3)

Now since $X_i = (-d\tilde{\mu}_i/dx) = (-d\mu/dx) + z_i F(-d\phi/dx)$ equation (A.14.3) becomes

$$(t_1/z_1)((-d\mu_1/dx) + z_1 F(-d\phi/dx)) + (t_2/z_2)(-d\mu_2/dx) + z_2 F(-d\phi/dx)) + t_3 (-d\mu_3/dx) = 0 \qquad (A.14.4)$$

which, since $t_1 + t_2 = 1$, becomes,

$$(t_1/z_1)(d\mu_1/dx) + (t_2/z_2)(d\mu_2/dx) + t_3(d\mu_3/dx) = F(-d\phi/dx). \qquad (A.14.5)$$

PROGRAM 1.

FIXED SITE DISTRIBUTION.

```
begin
      real  ko,z,B,M,phi,fa,int;

      integer for;

      procedure   intstep(y,f,x,h,aux);

      value h;
      real y,f,x,h;

      procedure  aux;

      begin

            real q,w;
            aux(f,x);
            q:=h×f;
            y:=y+0.5×q;
            x:=x+0.5×h;
            aux(f,x);
            w:=0.292893218813×(h×f-q);
            y:=y+w;
            q:=2.0×w + 0.707106781187×q;
            aux(f,x);
            w:=1.707106781187×(h×f-q);
            y:=y+w;
            q:=2.0×w - 0.707106781187×q;
            x:=x+0.5×h;
            aux(f,x);
            y:=y+0.333333333333×(0.5×h×f#q);
      end intstep;


      procedure deriva(fa,M);
      value M;
      real M,fa;
      begin
            fa:= ko×M↑(-z);
      end deriva;
```

```
        open(20);    open(70);

again:      copytext(20,70,[;]);

        for:= format([d.ddв-nd]);

        ko:= read(20);
        z:=read(20);
        B:= read(20);
        int:= read(20);

        phi:= 0.0;
        M:= 0.0;

        writetext(70,[RANGE*OF*M*********PHI]);

        newline(70,2);

        for M:=M while M<B do
        begin
              intstep(phi,fa,M,int,deriva);
              write(70,for,M );
              space(70,10);
              write(70,for,phi);
              newline(70,2);
        end;

        if in basic symbol (20) = 142 then goto again;
        close(20);      close(70);

end→
```

PROGRAM 2.

RUNGE KUTTA INTEGRATION.

```
begin real u, z, f, v;
      integer n, j, i, m, p, s;

      procedure intstep(y, f, x, h,aux);
       value  h;
       real y, f, x, h;
       procedure aux;
        begin real q, w;
       aux(f,x);
       q:=h × f;
       y:=y+0.5×q;
       x:=x+0.5×h;
       aux(f, x);
       w:=0.292893218813×(h×f-q);
       y:=y+w;
       q:=2.0×w+0.707106781187×q;
       aux(f,x);
       w:=1.707106781187×(h×f-q);
       y:=y+w;
       q:=2.0×w-0.707106781187×q;
       x:=x+0.5×h;
       aux(f,x);
       y:=y+0.333333333333×(0.5×h×f-q);
       end intstep;

      procedure deriv(f,v);
       value v;
       real v,f;
        begin  real exa, exb;
        exa:=exp(v);
        exb:=exp(-v×z);
        f:=0.5×exa×exb×(-exa+sqrt(exa↑2+4.0))
       end deriv;

open(20);  open(70);
copytext(20, 70, [;]);
again: n:=read(20);  m:=read(20);
begin array y[0:n], x[0:n,1:m], I[1:m];
y[0]:=read(20);
fori:=1step1until m do begin
I[i]:=read(20);
x[0,i]:=read(20)   end;
s:=1;

for j := 1 step 1 until m do begin
```

```
z:=I[j];
  u:=x[0,j];
  v:=ln(y[0]);
  p:=0;

start: p:=p+1;
       intstep(u,f,v,0.034655,deriv);
       if p≠20 then goto start else begin
         y[s]:=exp(v);
         x[s,j]:=u;
         s:=s+1;
         p:=0;
       if s=n +1then s:=1 else goto start   end   end;

writetext(70,[[2c3s]y[11s]I]);
for i := 1 step 1 until m-1 do
 writetext(70,[[12s]I]);
writetext(70,[[c8s]]);
for i := 1 step 1 until m do
 write(70, format([8sd.ddd]), I[i]);
writetext(70,[[2c]]);

for i := 0 step 1 until n do  begin
write(70, format([d.dddd10-nd]), y[i]);
for j := 1 step 1 until m-1 do
write(70, format([3sd.dddd10-nd]), x[i,j]);
write(70, format([3sd.dddd10-ndc]), x[i,m])   end   end;

p:=read(20);
if p=2 then goto again;
close(20);  close(70)   end  →→
```

PROGRAM 3.

CALCULATION OF THE MOST CONTINUOUS REGIONS IN ION-EXCHANGE MEMBRANES.

```
begin
      real D,ko,z,nug,zg,ms,mup,Io,Mcon,M,alpha,yn,fn,P,phi,
           x,xhold,int,k,f,fa;

      integer for;

      procedure   intstep(y,f,x,h,aux);

      value h;
      real y,f,x,h;

      procedure  aux;

      begin

            real q,w;
            aux(f,x);
            q:=h×f;
            y:=y+0.5×q;
            x:=x+0.5×h;
            aux(f,x);
            w:=0.292893218813×(h×f-q);
            y:=y+w;
            q:=2.0×w + 0.707106781187×q;
            aux(f,x);
            w:=1.707106781187×(h×f-q);
            y:=y+w;
            q:=2.0×w - 0.707106781187×q;
            x:=x+0.5×h;
            aux(f,x);
            y:=y+0.333333333333×(0.5×h×f-q);
      end intstep;


      procedure deriv(f,x);
      value x;
      real x,f;
      begin
            f:=3.0×P×(k×exp(x/(1.00-z))-P)/(2.0×P+k×exp(x/(1.0-z))
      end deriv;
```

```
        procedure    deriva(fa,M);
        value M;
        real M,fa;
        begin
              fa:=koxM↑(-z);
        end    deriva;


        open(20);       open(70);

again:  copytext(20,70,[;]);

        for:=format([d.ddb-ndc]);

            D:=read(20);
            ko:=read(20);
            z:=read(20);
            nug:=read(20);
            zg:=rea(20));
            ms:=rea(20));
            mup:=read(20);
            Io:=read(20);
            Mcon:=read(20);
            int:=read(20);


            alpha:=(nugxmup/(koxIo))↑(1.0/(2.0-z))/(nugxms);
            yn:=Mcon/(nugxzgxalphaxms);
            fn:=0.5x(-yn+sqrt(yn↑2.0+4.0));
            k:=Dxalpha↑(1.0-z)xIox(1.0-z)↑(1.0/(1.0-z))/
            (ko↑(z/(1.0-z))x(nugxms)↑z);
            P:=DxalphaxfnJ
            phi:=0.0;

            M:=0.0;

            for M:=M while M<Mcon do
            intstep(phi,fa,M,int,deriva);

            writetext(70,[MOLALITY*OF*MOST*CONTINUOUS*REGION*=**]);
            write(70,for,Mcon);

            writetext(70,[VALUE*OF*PHI*FOR*THIS*REGION*=**]);
            write(70,for,phi);

            x:=ln(phi);       xhold:=x;
```

```
            if in basic symbol (20) = 142 then
            begin
                 for x:=x while x<0.0do
                 intstep(P,f,x,0.1,deriv)
            end    else
            begin
                 for  x:=x while x> 5.0 do
                 intstep(P,f,x,-0.1,deriv)
            end;

            if in basic symbol (20) =142 then goto simple;
            if in basic symbol (20) =142 then
            begin
                 for xhold:=xhold while xhold> -5.0 do
            intstep(P,f,xhold,-0.1,deriv)
            end      else
            begin
                 for xhold:=xhold while xhold < 0.0 do
                 intstep(P,f,xhold,0.1,deriv)
            end;


simple:     writetext(70,[PERMEABILITY*COEFF*=**]);
            write(70,for,P);

            newline(70,2);
            writetext(70,[DIFFUSION*COEFF*=**]);
            write(70,for,Pxmup/ms);

            if in basic symbol (20) = 142 then goto again;

      close(20);      close(70);

end→
```

PROGRAM 4.

LEAST SQUARES ANALYSIS.

```
begin  comment  This programme works out m and c for the equation
                y = mx + c by least squares from n pairs of x and
                y and gives the mean error in y,m,and c,plus the
                individual deviations in y;

integer  n,f, i, p;
real  sx, sy, sxy, sx2, sy2, m, c, d,dy,dm;

 f:= format([-d.ddddm-nd]);
open(20);
open(70);

start:  copy text (20, 70, [;]);

comment  n is the number of points;

n:= read(20);


begin  array  x, y, e [1:n];
sx := sy := sxy := sx2 := sy2 := 0.0;
for i:=1 step 1 until n do
begin  x[i]:= read(20);
       y[i]:= read(20)     end;

for i:=1 step 1 until n do
begin sx:= sx + x[i];
      sy:= sy + y[i];
      sxy:=sxy + x[i] × y[i];
      sy2 := sy2 + y[i]↑2;
      sx2:= sx2 + x[i]↑2    end;

d:= n × sx2 - sx↑2;
m:= (n × sxy -sx × sy)/d;
c:= (sx2 × sy - sx × sxy)/d;
dy:= sy2 + n×c↑2 + m↑2×sx2 - 2×(c×sy + m×sxy - m×c×sx);
dm:= sqrt(n×dy/(n-2)/d);
d:= sqrt(dy×sx2/(n-2)/d);


for i:= 1 step 1 until n do  e[i] := y[i] - m × x[i] - c;

write text (70, [[4c] gradient*=*]);
```

```
write (70,f,abs( m ));
writetext(70,[[3s]STANDARD*DEVIATION*IN*GRADIENT*=**]);
write(70,f,dm);
write text (70, [[2c] c*=*]);
write (70,f,c);
writetext(70,[[3s]STANDARD*ERROR*IN*C*=**]);
write(70,f,d);

write text (70, [[2c] rms*error*in*y*=**]);
write (70,f,sqrt(dy/(n-2)));
write text (70, [[3c6s] y*obs[8s] y*calc [7s] deviation [2c]]);

for i := 1 step 1 until n do
begin  write (70, format ([2s-d.ddddm-nd]), y[i]);
       write (70, format ([3s-d.ddddm-nd]), m × x[i] + c);
       write (70, format ([3s-d.ddddm-ndc]), e[i])          end;

comment  if another set of data is to follow punch 2 otherwise 0;

p := read (20);
if p = 2 then goto start;
close (70);
close (20)
end  end  →
```

PROGRAM 5.

LINEAR TITRATION PLOTS.

```
begin comment  This programme calculates a Gran plot (r=1) and
               applies a least squares procedure to the
               experimental data .  r=2 for modified Gran plot;
      real fo, k, es, vo, v,ve,d, t, conc, sx, sy, sx2, sy2,
           sxy, m, c, r, kw, pm;
      integer  i, n, p, q, F1, F2, F3;
               open(20);   open(70);
               F1:= format([ -d.ddddb-nd]);
               F2 :=format([ 3s -d.ddddb-nd]);
               F3 :=format([ 3s -d.ddddb-ndc]);
again:         copytext(20, 70, [;]);
           r:=read(20);
            n:=read(20);
           k:=read(20);
           es:=read(20);
           vo:=read(20);
           v:=read(20);
           t:=read(20);
           q:=read(20);
if r=2 then begin kw:=read(20); pm:=read(20)  end;
           vo:=vo + v;
begin   array  e, x, y, f[1:n];
               sx:=sy:=sxy:=sx2:=sy2:=0.0;
for i:= 1 step 1 until n do
          begin  x[i]:=read(20);
                 y[i]:=read(20);
        if r=1 and q=1 then f[i]:=  (vo+ x[i])×10↑((es-y[i])/k);
        if r=1 and q=2 then f[i]:=(vo+x[i])×10↑((y[i]-es)/k) ;
        if r=2 and q=1 then f[i]:=  (vo+x[i])×(10↑((es-y[i])/
        k-pm) -kw×10↑((y[i]-es)/k+pm)) ;
        if r=2 and q=2 then f[i]:=(vo+x[i])×(kw×10↑((y[i]-es)/
        k+pm)-10↑((es-y[i])/k-pm))  end;
      for i:=1 step 1 until n do
      begin    sx:=sx+x[i];
               sy:=sy+f[i];
               sxy:=sxy+x[i]×f[i];
               sy2:=sy2 + f[i]↑2;
               sx2:=sx2+ x[i]↑2   end;
               d:=n×sx2 - sx↑2;
               m:=(n×sxy- sx×sy)/d;
               c:=(sx2×sy -sx×sxy)/d;
               d:=sqrt(abs((sy2 - sy×c - sxy×m)/(n-2)));
      for i:= 1 step 1 until n do e[i]:=f[i] -m×x[i] - c;
      writetext (70, [[4c]  m*=*]);
write(70, F1, m);
writetext(70, [[3s] c*=*]);
write(70, F1, c);
writetext(70, [[3s] rms*error*=*]);
write(70, F1, d);
writetext(70, [[3c9s] v[8s] f*obs[8s] f*calc[7s] deviation[2c]]);
```

```
        for i:= 1 step 1 until n do
                  begin   write(70, F2, x[i]);
                          write(70, F2, f[i]);
                          write(70, F2, mxx[i] + c);
                          write(70, F3, e[i]) end;
try:          fo:=read(20);
              ve:=(fo-c)/m;
              p:= read(20);
              conc:= if p=3 then vext/v else  vxt/ve;
              writetext(70, [[2c3s]ve*=*]);
              write(70, F1, ve);
              writetext(70, [[3s] conc*=*]);
              write(70, F1, conc);
   p:=read(20);
   if p = 1 then goto try;
   if p = 2 then goto again;
         close(70);  close(20);
end end→
```

PROGRAM 6.

EDGE EFFECT CORRECTION TO MEMBRANE CONDUCTIVITY.

```
begin
      comment this program calculates the true resistance of
       a membrane allowing for edge effects
      and then calculates the specific conductivity;
      real  E, x, sn, res, reso, a,b,l,lim,sr,sc,vara,varb,m1,m2,
            n1,n2,b1,b2,bf0,bf1,term, series,unit,lima,K1x,mult,
            multx;
      integer r,n,q,f1,p,u,v,uu,w,i;
      switch sw:=L1,L2;


      open(20);  open(70);

      f1:= format([3s+d.dddn-nd]);
      E:= read(20);
      a:= read(20);
      lim:= read(20);
      lima:= read(20);
      mult:= read(20);
      multx:= read(20);

new membrane: copy text(20,70, [;;]);
      write text (70, [[2c5s]mult[8s]qxvara[7s]qxvarb[9s]
      m1[11s]n1[11s]m2[11s]n2[10s]term[9s]sn]);
      b:= read(20);
      l:= read(20);
      vara:= 22xa/(7xl);
      varb:= 22xb/(7xl);
      sn:=0.0;
      q:= 0;
return: q:=q+1;
      x:=qxvara;
      new line(70,2);
      write (70,f1,mult);   write(70,f1,x);
      p:=1;  if x> 160.0 then goto print;
       goto proc;
L1:   m1:=bf1;
      n1:=K1x;
x:=qxvarb;
     write(70,f1,x);   write(70,f1,m1);   write(70,f1,n1);
     p:=2;  if x > 100.0 then goto omit;
```

```
        goto proc;
L2:     m2:=bf1;
        n2:=K1x;
        write(70,f1,m2);    write(70,f1,n2);

omit:       if x > 100.0  then
        begin
            m2:=0.0;
            n2:=0.0;
            write(70,f1,m2);    write(70,f1,n2);
            term:=m1/q↑2 × n1 × multx;
        end
        else

        term:= m1/(q↑2×m2) × (m2×n1 - n2×m1) × multx;
        write (70,f1,term);
        sn:=sn+term;    write(70,f1,sn);
        if abs(term) > abs(sn×10-4) then goto return;
in:     res:= read(20);
        if sn< 0.0 then  sn:= -sn;
        reso:=res/(1.0 - 16.0 / (3.14159)↑2 × sn);
        sr:= reso × 3.14159 × a↑2 / l;
        sc:= l × (1.0 - 16.0 × sn / (3.14159)↑2 )/ (3.14159 × a↑2× res);

        goto out;

proc:   v:=-1;
        b1:=0.0;   b2:= mult;
        cycle:   v:=v+1;   w:=2×v+2;
        b1:= x/ w × b2;
        b2:= x/w × b1;
          if b2>1.0×36  then goto fail;
        if b1>lim then goto cycle;
        begin
            array beta[0:w];
            beta[0]:=mult;

            u:=-1;
            repeat: u:= u+1;
            uu:=2×u;

            beta[uu+1]:= x/(uu+2) × beta[uu];
            beta[uu+2]:= x/ (uu+2) × beta[uu+1];
            if u<v then goto repeat;
            bf0:=bf1 :=0.0;
            for r:=0step1 until u do
            begin
                    bf0:=bf0 + beta[2×r];
                    bf1:=bf1 + beta[2 ×r+1];
               end;
```

```
        comment this section calculates the value of the Bessel
        function K1x;
calc:       i:=0;  r:=-1;
        unit:=1.0;  series:=1.0;
        rep:  r:=r+2;  i:=i+1;
        unit:=unitx(4-r↑2)/(ix8xx);
        if unit>seriesxlima then
        series:=series +unit
        else goto value;  goto rep;
        value:  K1x:= -sqrt(3.14159/(2xx)) × exp(-x) × series;
        end;
        goto sw[p];
out:    write text (70, [[2c] value*of*the*true*resistance*=*]);
        write (70,f1,reso);
        write text (70, [[2c] value*of*the*specific*resistance*=*]);
        write(70,f1,sr);
        write text (70, [[2c] value*of*specific*conductivity*=*]);
        write (70, f1,sc);
        goto readn;
fail:       write text (70, [[2c] value*of*b2*outside*limit]);
            goto readn;
print:      write text (70, [[2c] value*of* x*greater*than*160.0]);
        write text (70, [[2c] value*of*sn*=* ]);   write (70, f1,sn);
        goto in;
readn:
        n:= read(20);
        if n=2 then goto new membrane;
end:    close(20); close(70);
end→
```

PROGRAM 7.

CALCULATION OF TRACER DIFFUSION COEFFICIENTS.

```
begin comment Self diffusion program

      integer n,r,f;
      f:=format([sss-d.ddddn-nd]);
      open(20);     open(70);
start:copytext(20,70,[;]);
      n:=read(20);
     if in basic symbol(20)=142 then r:=read(20) else r:=1;
     begin integer i,qq,h;
           real sx,sy,sxy,sx2,sy2,m,c,d,dy,dm,vo,a,nn,avinc,
                t12,t;
           array x,y,yy,yc,e,corr[1:n],inc[2:n],s[1:9],base[1:r+1],
                 old[1:r];
           boolean array duff[1:n];
           boolean ba,bb,bc,bd;
           ba:=bb:=false;
           for i:=1 step 1 until n do
           begin    x[i]:=read(20);
                   yy[i]:=read(20);
                 duff[i]:=false;
           end;
           vo:=read(20);
           nn:=read(20);
            a:=read(20);
           if in basic symbol(20)=152 then bb:=true;
           bc:=if r=1 then false else true;
           for i:=1 step 1 until 9 do s[i]:=read(20);
           if bc then for i:=1 step 1 until r do old[i]:=read(20);
           if in basic symbol(20)=12 then ba:=true;
           if a=0.0 then writetext(70,[[4c]SIMPLE*WITHDRAWAL*SAMPLING
                                       [2c]]) else
           writetext(70,[[4c]WITHDRAWAL/ADDITION*SAMPLING[2c]]);
           if bb then
           begin t12:=read(20);
                   t:=read(20);
                 for i:=1 step 1 until n do yy[i]:=yy[i]/exp(-0.693/
                 t12x(i-1)xt)end;
total:     for i:=1 step 1 until n do y[i]:=yy[i];
           writetext(70,[[2c]*INTERVAL[10s]INC[2c]]);
           sx:=sx2:=0.0;    qq:=0;
           for i:=2 step 1 until n do if not(duff[i] or duff[i-1]
           ) then
           begin if notbc then inc[i]:=(y[i]x(vo-(i-1)x(nn-a))-
                 y[i-1]x(vo-(i-1)x(nn-a)-a))/(x[i]-x[i-1])/vo
                 else inc[i]:=(y[i]x(vo-(i+r-1)x(nn-a))-y[i-1]
                 x(vo-(i+r-1)x(nn-a)-a))/(x[i]-x[i-1])/vo;
```

```
                write(70,format([ssdd]),i-1);      out basic
                 symbol(70,161);  write(70,format([dd]),i);
                space(70,6);
                write(70,f,inc[i]);      newline(70,1);
                sx:=sx+inc[i];
                qq:=qq+1;
            end;
            avinc:=sx/qq;
            for i:=2 step 1 until n do sx2:=sx2+(if not(duff[i]
            or duff[i-1]) then (avinc-inc[i])↑2 else 0.0);
            dm:=sqrt(sx2/(qq-1));
            writetext(70,[[c]AVERAGE*INC*=]);   write(70,f,avinc);
            writetext(70,[[c]STANDARD*DEVIATION*IN*INC*=]);
            write(70,f,dm);
correct:    corr[1]:=0.0;
            if a≠0.0 then goto inout;
out:        if bc then goto retro;
            for i:=2 step 1 until n do corr[i]:=-avinc×nn×(i-1)
            /(vo-(i-1)×nn)×(x[i]-x[i-1])+corr[i-1];
            goto merge;
inout:      for i:=2 step 1 until n do corr[i]:=axy[i-1]/
            vo×(1+(i-1)×(nn-a)/(vo-(i-1)×(nn-a)))
            -avinc×(x[i]-x[i-1])×(i-1)×(nn-a)/(vo-(i-1)×(nn-a))+
            corr[i-1];
            goto merge;
retro:      base[1]:=0.0;
            for i:=2 step 1 until r do  base[i]:=-avinc×nn×(i-1)/
            (vo-(i-1)×nn)×(old[i]-old[i-1])+base[i-1];
            corr[1]:=-avinc×nn×r/(vo-r×nn)×(x[1]-old[r])+base[r];
            for i:=2 step 1 until n do corr[i]:=-avinc×nn×(i+r-1)/
            (vo-(i+r-1)×nn)×(x[i]-x[i-1])+corr[i-1];
merge:      for i:=1 step 1 until n do y[i]:=y[i]+corr[i];
leastsq:    sx:=sy:=sxy:=sx2:=sy2:=0.0;      h:=0;
            for i:=1 step 1 until n do
            begin if not duff[i] then
                  begin sx:=sx+x[i];
                        sy:=sy+y[i];
                       sxy:=sxy+x[i]×y[i];
                       sy2:=sy2+y[i]↑2;
                       sx2:=sx2+x[i]↑2;
                         h:=h+1;
                  end
            end;
            d:=h×sx2-sx↑2;
            m:=(h×sxy-sx×sy)/d;
            c:=(sx2×sy-sx×sxy)/d;
            for i:=1 step 1 until n do if not duff[i] then
             yc[i]:=m×x[i]+c;
           dy:=sy2+h×c↑2+m↑2×sx2-2×(c×sy+m×sxy-m×c×sx);
           dm:=sqrt(h×dy/(h-2)/d);
            d:=sqrt(dy×sx2/(h-2)/d);
            for i:=1 step 1 until n do if not duff[i] then
             e[i]:=y[i]-yc[i];
            writetext(70,[[4c]M*=]);      write(70,f,m);
```

```
                writetext(70,[[3s]STANDARD*DEVIATION*IN*M*=]);
                write(70,f,dm);
                writetext(70,[[2c]C*=]);
                write(70,f,c);
                writetext(70,[[3s]STANDARD*ERROR*IN*C*=]);
                write(70,f,d);
                writetext(70,[[2c]RMS*ERROR*IN*Y*=]);
                write(70,f,sqrt(dy/(h-2)));
                writetext(70,[[3c5s]Y*INIT[9s]CORR[10s]Y*OBS[8s]
                Y*CALC[7s]DEVIATION[2c]]);
                for i:=1 step 1 until n do if not duff[i] then
                begin write(70,f,  yy[i]);
                      write(70,f,corr[i]);
                      write(70,f,   y[i]);
                      write(70,f,  yc[i]);
                      write(70,f,   e[i]);      newline(70,1);
                end;
                d:=mxvoxs[1]xs[2]/(s[3]xs[4]xs[5]x60);
                writetext(70,[[2c]DIFFUSION*COEFF*D1A*=**]);
                write(70,f,d);
                if notba then
                begin writetext(70,[[2c]HOLD*UP*TIME*(MIN)*=**]);
                write(70,f,-c/m);
                      writetext(70,[[2c]HOLD*UP*TIME*DIFF*COEFF*=**]);
                write(70,f,-s[2]↑2xm/(cx360));
                end;
                dm:=0.0591x(s[9]x4.84xs[7]/s[8])↑0.57x(s[8]xs[6]↑2/s[7]
                )↑(1/3);
                writetext(70,[[4c]SCATTERGOOD/LIGHTFOOT*CORRECTION[2c]M
                          MASS*TRANSFER*COEFF*=**]);
                write(70,f,dm);
                writetext(70,[[2c]DIFFUSION*COEFF*D1*=**]);
                write(70,f,d/(1-(2xdxs[3]/(s[2]xdmxs[1]))));
again:          if in basic symbol(20)=12 then goto newdata;
                bd:=readboolean(20);
                if in basic symbol(20)=152 then for i:=read(20) while
                in basic symbol(20)≠13 do duff[i]:=true;
                if bd then writetext(70,[[6c]TOTAL*]) else writetext
                (70,[[6c]LEAST*SQUARE*]);
                writetext(70,[RECALCULATION*OMITTING*POINTS]);
                for i:=1 step 1 until n do if duff[i] then
                write(70,format([snd]),i);
                newline(70,2);
                if bd then goto total else goto leastsq;
newdata:        if in basic symbol(20)=142 then goto start;
                close(20);   close(70)

        end
end→
```

PROGRAM 8.

SOLUTION OF SIMULTANEOUS EQUATIONS.

```
begin integer i,j,k,l,m,ma,mb,mc,am,n,ka,r,p,f1,s,repc,rept;
      real    e,ans,bans,b,in,q,a,var;

      open (20);          open(70);
      f1:= format([+d.ddddb+nd]);
      e:=ln(10.0);

again:      copytext (20,70,[;]);
            m:=read (20);
            ma:= m-1;
                        mc:= m+1;

            begin array c,d,cre[1:m,1:m],detr[1:mc],t,tre[1:m],
                        x[1:m];
                for i:=1 step 1 until m do
                begin for j:= 1 step 1 until m do
                      cre[i,j]:= read(20);
                      tre[i]  := read(20)
                end;
                goto jump;

alter:      copytext(20,70,[;]);

            repc:=read(20);
            for s:=1 step 1 until repc do
            begin i:=read(20);
                  j:=read(20);
               cre[i,j]:= read(20);
            end;

            rept:= read(20);
            for s:=1 step 1 until rept do
            begin  i:= read(20);
                tre[i]:= read(20);
            end;

jump:       for i:=1 step 1 until m do
            begin  for j:=1 step 1 until m do
                   c[i,j]:= cre[i,j];
                   t[i]  := tre[i];
            end;

              ans:= 0.0;
```

```
for i:=1  step 1 until m do ans :=ans+(ifc[i,i]>0.0 then
                                  ln(c[i,i])/e
                                else if c[i,i] =0.0 then 0.0
                                else ln(abs(c[i,i]))/e);

      am:=m;
           ans:=ans/am;
           bans:= 10.0↑ ans;
           for i:=1 step 1 until m do
           begin t[i]:=t[i]/bans;
                 for j:=1 step 1 until m do
                 c[i,j]:= c[i,j]/bans;
           end;

for j:=1 step 1 until  mc do
begin      for i:=1 step 1 until m do
           for k:= 1 step 1 until m do
           d[k,i]:=c[k,i];
           b:=1.0;
           mb:=j-1;
           if mb≠0 then for k:=1 step 1 until m do
             d[k,mb]:=t[k];
           for k:=1 step 1 until ma do
               begin  ka:=k+1;
                      if d[k,k]=0.0 then goto P86;

                 P80: b:=d[k,k]×b;
                    q:=d[k,k];
                    for l:=k step 1 until m do  d[k,l]:=d[k,l]/q;
                    for l:=ka step 1 until m do
                      begin  a:=d[l,k];
                             for n:=k step 1 until m do
                             d[l,n]:= d[l,n]-d[k,n]×a;
                      end;
                   for l:=ka step 1 until m do d[k,l]:=0.0;
                   goto out;
               P86:    for i := ka step 1 until  m do
                       if d[k,i]≠0.0 then
                       begin  b:= -b;
                              for l:=k step 1 until m do
                                begin  in:= d[l,k];
                                       d[l,k]:=d[l,i];
                                       d[l,i] := in;
                                end;
                              goto P80;
                      end;
                       detr[j]:=0.0;
                       goto fin;          out:
               end;
               detr[j]:=d[m,m]×b;       fin:
end;
```

```
for j:=2 step 1 until mc do x[j-1]:=detr[j]/detr[1];
      p:= read(20);
      var:= read(20);
            if in basic symbol (20) = 142 then


            begin
            for i:= 1 step 1 until p do
                  begin
                        copy text(20,70,[;;]);
                        write(70,f1,x[i]);
                  end;        goto choice;
            end;
                  for i:= 1 step 1 until p do
                        begin
                              for j:= 1 step 1 until p do
                              begin  space(70,6);
                              out basic symbol (70,var);
                                    write(70,format([nd]),i);
                                    write(70,format([nd]),j);
                                    space(70,5);
                              end;     newline(70,2);

                        end;

            r:= 0;
            for i:= 1 step 1 until p do
            for j:= i step 1 until p do
            begin   r:= r + 1;
                    c[i,j]:= x[r];
                    c[j,i]:= c[i,j];
             end;

            for i:= 1 step 1 until p do
            begin   for j:= 1 step 1 until p do
                    begin   space(70,3);
                            write(70,f1,c[i,j]);
                    end;
                    newline(70,2);
            end;
choice:     if in basic symbol (20) = 142 then goto alter;
            if in basic symbol (20) = 142 then goto again;
            close(20);   close(70);

end
end→
```

BIBLIOGRAPHY.

(1) F. Helfferich, "Ion Exchange", McGraw-Hill, New York, 1962, p.13.

(2) E. Glueckauf, Proc. Roy. Soc. (London), A 268, 350 (1962)

(3) R. Arnold, Aust. J. Chem., 21, 521, (1968).

(4) J. Klinowski and M. Leszko, Roczniki Chem., 42, 123 (1968).

(5) G. E. Boyd, B. A. Soldano and O. D. Bonner, J. Phys. Chem., 58, 456 (1954).

(6) Ref. (1), p.268.

(7) D. Mackay and P. Meares, Trans. Faraday Soc., 55, 1221 (1959).

(8) F. F. Reuss, Mem. Soc. Natur. Mose., 2, 327 (1809).

(9) D. G. Miller, J. Phys. Chem., 70, 2639 (1966).

(10) A. Katchalsky and P. Curran, "Non Equilibrium Thermodynamics in Biophysics", Harvard Univ. Press., U.S.A., 1965, p.79.

(11) Ref. 10. p.80.

(12) Ref. 10. p.79.

(13) L. Onsager, Phys. Rev., 37, 405 (1931).

(14) L. Onsager, Phys. Rev., 38, 2265 (1931).

(15) J. G. Kirkwood, in "Ion Transport Across Membranes", Academic Press, New York, 1954, p.119.

(16) D. G. Miller, Chem. Rev. 60, 15 (1960).

(17) Ref. 10, p.88.

(18) Ref. 10, p.91.

(19) A. J. Staverman, Trans. Faraday Soc., 48, 176 (1952).

(20) P. B. Lorenz, J. Phys. Chem., 56, 775 (1952).

(21) K. S. Spiegler, Trans. Faraday Soc., 54, 1408 (1958).

(22) W. Dorst, A. J. Staverman and R. Caramazza, Rec. Trav. Chim., 83, 1329 (1964).

(23) W. Dorst and A. J.Staverman, Rec. Trav. Chim., 86, 61 (1967).

(24) O. Kedem and A. Essig, J. Gen. Physiol. 48, 1047 (1965).

(25) D. C. Mikulecky and S. R. Caplan, J. Phys. Chem., 70, 3049 (1966).

(26) P. J. Dunlop, J. Phys. Chem., 68, 26 (1964).

(27) R. W. Laity, J. Phys. Chem., 67, 671 (1963).

(28) O. Kedem, in A. Kleinzellar and A. Kotyk, (eds.), "Membrane Transport and Metabolism", Acad. Press, New York, (1960).

(29) S. Ljunggren, Trans. Roy. Inst. Technol., Stockholm, 172, 1 (1961).

(30) D. G. Miller, J. Phys. Chem, 71, 616 (1967).

(31) J. S. Mackie and P. Meares, Proc. Roy. Soc., (London), A232, 498 (1955).

(32) A. O. Jakubovic, G. J. Hills and J. A. Kitchener, J. chim. phys., 55, 263 (1958).

(33) A. O. Jakubovic, G. J. Hills and J. A. Kitchener, Trans. Faraday Soc., 55, 1570 (1959).

(34) A. E. Lagos and J. A. Kitchener, Trans. Faraday Soc., 56, 1245 (1960).

(35) D. D. Perrin, W. L. F. Armarego and D. R. Perrin, "Purification of Laboratory Chemicals", Pergamon, (1966).

(36) G. A. Bray, Anal. Biochem., 1, 279 (1960).

(37) American Machine and Foundry Co., Springdale, Conn. U.S.A., private communication.

(38) E. Glueckauf and R. E. Watts, Proc. Roy. Soc., (London), A268, 339 (1962).

(39) C. MacCallum and D. Midgley, to be published.

(40) "Test Manual for Permselective Membranes," U.S. Office of Saline Water Research, Report No.77, Jan. 1964, P.B. 181575.

(41) R. M. Barrer, J. A. Barrie and M. G. Rogers, Trans. Faraday Soc., 58, 2473 (1962).

(42) K. S. Spiegler, in "Ion Exchange Technology", F. C. Nacod and J. Shubert, (eds.), New York, (1956), p.118.

(43) J. W. Lorimer, Discussions Faraday Soc., 21, 198 (1956).

(44) P. Meares and H. H. Ussing, Trans. Faraday Soc., 55, 244 (1959).

(45) H. P. Gregor, R. Kramer, A. Lalik, V. Holmstrom and T. Saber, Membrane Evaluation Program, New York, Brooklyn Polytechnic, (1961).

(46) P. Meares, Trans. Faraday Soc., 55, 1970 (1959).

(47) Ref. (1) p.315.

(48) R. Schlögl and F. Helfferich, Z. Elektrochem., 56, 644 (1952).

(49) Ref. (1) p.347.

(50) Ref. 1, p.348.

(51) D. Mackay and P. Meares, Kolloid Z, 167, 31 (1959).

(52) M. A. Peterson and H. P. Gregor, J. Electrochem Soc., 106, 1051 (1959).

(53) S. B.Tuwiner, "Diffusion and Membrane Technology", A.C.S. Monograph No.156, Reinhold Publishing Corp., New York; 1962.

(54) R. J.Stewart and W. F. Graydon, J. Phys. Chem., 60, 750 (1956).

(55) A. M. Peers, Discussions Faraday Soc., 21, 124 (1956).

(56) B. Z. Ginzburg and A. Katchalsky, J. Gen. Physiol., 47, 403 (1963).

(57) E.M. Scattergood and E.N. Lightfoot, Trans. Faraday Soc., 64, 1135 (1968).

(58) Wayne Kerr B331 Conductivity Bridge Manual.

(59) F. Bergsma and A. J. Staverman, Discussions Faraday Soc., 21, 61 (1956).

(60) M. Black and K. S. Spiegler, J. Electrochem. Soc., 110, 577 (1963).

(61) H. P. Gregor and D. M. Wetstone, Discussion Faraday Soc., 21, 162 (1956).

(62) G. J. Hills, P. W. M. Jacobs and N. Lakshminarayanaiah, Proc. Roy. Soc., (London), A262, 257, (1961).

(63) G. J. Hills, J. A. Kitchener and P. J. Ovenden, Trans. Faraday Soc., 51, 719 (1955).

(64) J. W. Lorimer, E. I. Boterenbrood and J. J. Hermans, Discussions Faraday Soc., 21, 141 (1956).

(65) Y. Oda and T. Yawataya, Bull. Chem. Soc. Japan, 29, 673 (1956).

(66) Y. Oda and T. Yawataya, Bull. Chem. Soc. Japan, 30, 213 (1957).

(67) N. W. Rosenberg, J. H. B. George and W. D. Potter, J. Electro Chem. Soc., 104, 111 (1957).

(68) A.G. Winger, R. Ferguson and R. Kunin, J. Phys. Chem., 60, 556 (1956).

(69) N. Lakshminarayanaiah, Chem. Rev., 65, 491 (1965).

(70) T. R. E. Kressman and F. L. Tye, Trans. Faraday Soc., 55, 1441 (1959).

(71) D. J. Lewis and T. L. Tye, J. Appl. Chem., 9, 279 (1959).

(72) T. R. E. Kressman and T. L. Tye, Discussions Faraday Soc., 21, 185 (1956).

(73) N. Lakshminarayanaiah and V. Subrahmanyan, J. Polymer Sci. A2, 4491 (1964).

(74) V. Subrahmanyan and N. Lakshminarayanaiah, Current Sci. 31, 146 (1962).

(75) H. P. Gregor and M. A. Peterson, J. Phys. Chem., 68, 2201 (1964).

(76) D. K. Hale and D. J. McCauley, Trans. Faraday Soc., 57, 135 (1961).

(77) H. Kramer and P. Meares, Biophys. J., 9, 1006 (1969).

(78) P. Meares, D. G. Dawson, A. H. Sutton and J. T. Thain, Ber Bunsenges. Physik. Chem., 71, 765 (1967).

(79) T. M. Ellison and H. G. Spencer, J. Polymer Sci., B1, 707 (1963).

(80) D. G. J. Ives and G. J. Janz, (ed.) "Reference Electrodes, Theory and Practice", Academic Press, 1961, p.205.

(81) J. M. Mackie and P. Meares, Proc. Roy. Soc. (London), A232, 485 (1955).

(82) J. M. Mackie and P. Meares, Proc. Roy. Soc. (London), A232, 510 (1955).

(83) P. Meares, J. chim. phys., 55, 273 (1958).

(84) W. J. McHardy, P. Meares and J. T. Thain, J. Electro-Chem. Soc., 116, 920 (1969).

(85) R. Schlögl, Z. Elektrochem., 57, 195 (1953).

(86) N. Ishibashi, T. Seiyama, and W. Sakai, J. Electro Chem. Soc. Japan., 23, 182 (1955); Chem. Abstr., 49, 14524 (1955).

(87) D. Richman, and H. C. Thomas, J. Phys. Chem., 60, 237 (1956).

(88) C. McCallum, private communication.

(89) M. Tetenbaum and H. P. Gregor, J. Phys. Chem., 58, 1156 (1954).

(90) J. H. Wang and S. Miller, J. Am. Chem. Soc., 74, 1611 (1952).

(91) J. H. Wang, J. Am. Chem. Soc., 74, 1612 (1952).

(92) S. Lapanje and S. A. Rice, J. Am. Chem. Soc., 83, 496 (1961).

(93) L. Kotin and M. Nagasawa, J. Am. Chem. Soc., 83, 1026 (1961).

(94) J. E. Gordon, Chem. and Ind. (London), 267, (1962).

(95) R. H. Dinius, M. T. Emerson and G. R. Choppin, J. Phys. Chem., 67, 1178 (1963).

(96) R. H. Dinius and G. R. Choppin, J. Phys. Chem., 68, 425 (1964).

(97) D. Reichenberg and I. J. Laurenson, Trans. Faraday Soc., 59, 141 (1963).

(98) U. P. Strauss and Y. P. Leung, J. Am. Chem. Soc., 87, 1476 (1965).

(99) K. S. Spiegler, reported in . Ref. 1, p. 308.

(100) H. Eyring and E. M. Eyring, "Modern Chemical Kinetics", Reinhold Publishing Corp., New York, (1963).

(101) R. B. Parlin and H. Eyring, in "Ion Transport across Membranes", H. T. Clarke (ed.), Acad. Press, New York, (1954).

(102) B. J.Zwolinski, H. Eyring and C. E. Reese, J. Phys. Chem., 53, 1426 (1949).

(103) K. S. Spigler and M. R. J. Wyllie, in "Physical Techniques in Biological Research", G. Oster and A. Pollister (ed.), Academic Press, Inc., New York, 1956, p.301.

(104) R. Arnold and D. F. A. Koch, Aust. J. Chem., 19, 1299 (1966).

(105) W. J. McHardy, P. Meares, A. H. Sutton and J. F. Thain, J. Colloid and Interface Sci., 29, 116 (1969).

(106) B. Zapior, M. Leszko and J. Klinowski, Zeszyty Naukowe Universytetu Jagiellonskiego, 145, (1967).

(107) N. Lakshminarayanaiah, Desalination, 3, 97 (1967).

(108) A. S. Tombalkian, H. J. Barton and W. F. Graydon, J. Phys. Chem., 66, 1006 (1962).

(109) V. Subrahmanyan and N. Lakshminarayanaiah, Bull. Chem. Soc. Japan, 34, (1961).

(110) N. Lakshminarayanaiah, Proc. Indian Acad. Sci., A55, 200 (1962).

(111) N. Lakshminarayanaiah and V. Subrahmanyan, J. Phys. Chem., 72, 1253 (1968).

(112) V. Subrahmanyan and N. Lakshminarayanaiah, Current Sci., 29, 307 (1960).

(113) E. M. Scattergood, Ph.D. Thesis, University of Wisconsin, (1966).

(114) T. R. E. Kressman, P. A. Stanbridge, F. L. Tye and A. G. Wilson, Trans. Faraday Soc., 59, 2133 (1963).

(115) Ref. 1, p.355.

(116) F. Helfferich, Discussions Faraday Soc., 21, 83 (1956).

(117) R. Schlögl, Z. Elektrochem., 57 195 (1953).

(118) R. Paterson and H. Ferguson, to be published.

(119) E. Christiansen, Ph.D. Thesis, University of Wisconsin, (1968).

(120) H. S. Harned and B. B. Owen, "The Physical Chemistry of Electrolytic Solutions" 3rd Ed., Reinhold Publishing Corp., New York, 1958, p.562.

(121) O. Kedem and S. R. Caplan, Trans. Faraday Soc., 61, 1897 (1965).

(122) W. C. Bauman and J. Eichhorn, J. Am. Chem. Soc., 69, 2830 (1947).

(123) H. P. Gregor, F. Gutoff and J. I. Bregman, J. Colloid Sci., 6, 245 (1951).

(124) H. P. Gregor and M. H. Gottlieb, J. Am. Chem. Soc., 75, 3539 (1953).

(125) C. W. Davies and G. D. Yeoman, Trans. Faraday Soc., 49, 968 (1953).

(126) N. Lakshminaranayaiah, J. Electrochem. Soc., 116, 338 (1969).

(127) K. A. Kraus and G. E. Moore, J. Am. Chem. Soc., 75, 1457 (1953).

(128) M. H. Gottlieb and H. P. Gregor, J. Am. Chem. Soc., 76, 4639 (1954).

(129) F. Nelson and K. A. Kraus, J. Am. Chem. Soc., 80, 4154 (1958).

(130) J. Danon, J. Phys. Chem., 65, 2039 (1961).

(131) D. H.Freeman, J. Phys.Chem., 64, 1048 (1960).

(132) D. H. Freeman, V. C. Patel and T. M. Buchanan, J. Phys. Chem., 69, 1477 (1965).

(133) E. Gleuckauf and R. E. Watts, Nature, 191, 904 (1961).

(134) A. Katchalsky and S. Lifson, J. Polymer Sci., 11, 409 (1953).

(135) U.P. Strauss and P. Ander, J. Am. Chem. Soc., 80, 6494 (1958).

(136) Z. Alexandrowicz, J. Polymer Sci., 56, 115 (1962).

(137) M. Nagasawa, M. Izumi and I. Kagawa, J. Polymer Sci., 37, 375 (1959).

(138) A. Katchalsky and I. Michaeli, J. Polymer Sci., 15, 69 (1955).

(139) S. A. Rice and F. E. Harris, Z. Physik Chem. (Frankfurt), 8, 207 (1956).

(140) I. Michaeli and A. Katchalsky, J. Polymer Sci., 23, 683 (1957).

(141) M. G. T. Shone, Trans. Faraday Soc., 58, 805 (1962).

(142) L. Dresner and K. A. Kraus, J. Phys. Chem., 67, 990 (1963).

(143) L. Dresner, J. Phys. Chem., 67, 2333 (1963).

(144) R. L. Gustafson, J. Phys. Chem., 67, 2549 (1963).

(145) J. A. Marinsky, "Ion Exchange" vol. 1, J.A. Marinsky, (ed.), Edward Arnold, London, 1966, chapter 9.

(146) P. Chu and J. A. Marinsky, J. Phys. Chem., 71, 4352 (1967).

(147) M. Nagasawa, A. Takahashi, M. Izumi and I. Kagawa, J. Polymer Sci., 38, 213 (1959).

(148) Z. Alexandrowicz, J. Polymer Sci., 43, 337 (1960).

(149) R. A. Mock and C. A. Marshall, J. Polymer Sci., 13, 263 (1954).

(150) A. Katchalsky, R. Cooper, J. Upadhyay and A. Wassermann, J. Chem. Soc., 1961, 5198.

(151) F. T. Wall and M. I. Eitel, J. Am. Chem. Soc., 79, 1556 (1957).

(152) F. R. Mayo and F. M. Lewis, J. Am. Chem. Soc., 66, 1954 (1944).

(153) J. R. Millar, J. Chem. Soc., 1960, 1311.

(154) J. R. Millar, D. G. Smith, and W. E. Marr, J. Chem. Soc., 1962, 1789.

(155) J. E. Gordon, J. Phys. Chem., 66, 1150 (1962).

(156) L. S. Goldring, Abstr., 142nd. Meeting Am. Chem. Soc., Atlantic City, N.J., 1962.

(157) N. Grubhofer, Makromol. Chem., 30, 96 (1959).

(158) D. Reichenberg and D. J. McCauley, J. Chem. Soc., 1955, 2741.

(159) R. A. Robinson and R. H. Stokes, "Electrolyte Solutions", Butterworths, 2nd edition, 1965,

(160) Ref. 1, p.143.

(161) F. L. Tye, J. Chem. Soc., 1961, 4784.

(162) J. M. Crabtree and E. Glueckauf, Trans. Faraday Soc., 59, 2639 (1963).

(163) D. A. G. Bruggerman, Ann. Phys., Lpz., 24, 636 (1935).

(164) K. W. Pepper, D. Reichenberg and D. K. Hale, J. Chem. Soc., 1952, 3129.

(165) Ref. 1, p.14.

(166) R. Patterson, Ph.D. Thesis, University of Glasgow, (1962).

(167) C. B. Amphlett, "Inorganic Ion Exchangers", Elsevier Publishing Co., (London), (1964).

(168) K. A. Kraus, H.O. Phillips, T. A. Carlson and J. S. Johnson, Intern. Conf. on Peaceful Uses of Atomic Energy, Geneva, 28, 3 (1958).

(169) A. Clearfield, Rev. Pure and Appl. Chem., 14, 91 (1964)

(170) J. R. Fryer, J. L. Hutchison and R. Paterson, in press.

(171) Ref. 1, p.259.

(172) T. Vermeulen, Ind. Eng. Chem., 45, 1664 (1953).

(173) Ref. 1, p.290.

(174) C. R. Gardner, B.Sc. Thesis, University of Glasgow, (1966).

(175) Vogel. "A Textbook of Quantitative Inorganic Analysis" 3rd edition, Longman Green and Co. Ltd., (London), 1961.

(176) T. R. E. Kressman and J. A. Kitchener, Discussions Faraday Soc., 7, 90 (1949).

(177) Y. Oda and T. Yawata, Bull. Chem. Soc. Japan, 28, 263 (1955).

(178) Juda, J. Marinsky and N. W. Rosenberg, Ann. Rev. Phys. Chem., 4, 373 (1953).

(179) C. W. Carr, R. McClintock and K. Sollner, J. Electrochem. Soc., 109, 251 (1962).